WELCOME TO IBIC14

Stephen Smith, SLAC National Accelerator Lab, Menlo Park, CA, USA

The 3rd International Beam Instrumentation Conference (IBIC 2014) in Monterey's Portola Hotel is dedicated to exploring the physics and engineering challenges of beam diagnostics and measurement techniques for charged particle beams. The International Beam Instrumentation Conferences, first held in Tsukuba (2012) and Oxford (2013) are the successors of the former Beam Instrumentation Workshops (BIW) held from 1989 through 2012 and the Diagnostics and Instrumentation for Particle Accelerators Conference series (DIPAC) held from 1993 through 2011.

We have scheduled two tutorial sessions, 12 invited talks, 20 contributed oral talks, 180 posters, and a tour of SLAC facilities that will be presented during the 4 day scientific program. Twenty-one exhibitors are ready to connect with you to share information on their latest products and services.

On behalf of SLAC, the program committee, the local organizing committee, Stanford Conference Services and the Portola Hotel, it is my pleasure to welcome you to IBIC14!

ISBN 978-3-95450-141-0

NON-DESTRUCTIVE VERTICAL HALO MONITOR ON THE ESRF'S 6GeV ELECTRON BEAM

B.K. Scheidt, ESRF, Grenoble, France

Abstract

The population density along the electron's beam vertical profile at far distance from the central core (i.e. the far-away tails or "Halo") is now quantitatively measurable by the use of bending magnet X-rays. An available beam-port is equipped with two specific adapted absorbers, an Aluminium UHV window, an X-ray light blocker, an X-ray imager, and a few motorizations. The simple and inexpensive set-up (resembling much that of an X-ray pinhole camera system for emittance measurements in Light Sources, but much shorter in length) allows to record images of the electron density profile over the 0.5 to 6mm distance range from the core. Results, obtained under various manipulations on the electron beam to vary either Touchek or residual Gas scattering and thereby the Halo levels, will be presented, to fully demonstrate that this Halo monitor is exploring those realms of the beam where other diagnostics can not reach ...

NON-DESTRUCTIVE MEASUREMENTS OF VERTICAL BEAM HALO

The European Synchrotron Radiation Facility runs a 6GeV electron beam at nominally 200mA and with a vertical emittance typically below 10pm.rad. The typical (natural) lifetime of the beam is above 50hrs, and the ESRF presently only uses 'slow' top-ups at intervals up to 12hrs. The small vertical emittance implies that the vertical size of the electron beam is in a range of roughly 13 to 50um [fwhm] depending on the local vertical Beta value which varies from >45m in some dipole sections to <3m in the straight sections reserved for Insertion Devices. [1]

However, it is known that a non-negligible beam population exists at many millimetres vertical distance from the beam-centre. [2, 3]

This is easily verified by using a vertical scraper and measuring the signal from a down-stream Beam Loss Detector (BLD). The progressive insertion of such a scraper jaw at 10mm above the beam-centre shows the so induced electron beam-losses thanks to the high sensitivity of such BLD. But this method is destructive to the beam and not useable for assessing the Halo population while serving normal users operation.

A prototype of a non-destructive Halo monitor based on imaging the X-rays from an available bending magnet beam-port was successfully operated to demonstrate the principle and the strait forwardness of a practical implementation. [4]

Since the above mentioned prototype device shared this beam-port with other (incompatible) usages we decided to build a dedicated Halo monitor on one of the still un-occupied bending magnet beam-ports, and to optimize both the associated X-ray absorbers and the distances between the main components in this new set-up that are illustrated in Fig.1 and Fig.2.

Long-distance X-rays Projection with Specific Central Absorbers to Attenuate Those Coming from the Intense Beam Core

The ESRF dipoles (0.86T, Ec=20KeV) provide an angular X-ray fan of 6.25degrees that is absorbed mainly in the crotch-absorber indicated at point 1 in Fig.1. Such crotch-absorber lets through about 15mrad of horizontal beam fan from its bending magnet, and normally this beam goes through a Front-End first and then further down-stream to a User's beam-line.

But in our case for this Halo beam-port there is neither Front-End nor beam-line, instead a second horizontal absorber (2) limits the horizontal fan of the X-rays to about 1.6mrad. About 10cm further down-stream is the third absorber (3), positioned vertically such that it takes fully the X-rays beam. However, its upper edge is only 0.7mm above the vertical heart of the beam.

The X-rays that are emitted from electrons that are >0.7mm above the centre of the electron beam will pass over this vertical absorber, and their first (and only) obstacle is a 2mm thick Aluminium window (5cm behind the vertical absorber) before hitting a scintillator screen. This scintillator screen is part of a sensitive X-ray imager that includes focussing optics and CMOS camera and covers a field of view 6.9x5.2mm (hor. x vert.).[5]

The total path length of X-rays is about 4.2m from their source-point in the dipole to the screen.

The X-rays emitted from the centre of the electron beam will hit that 28mm thick Copper vertical absorber. This small absorber is water cooled and evacuates about 240W of heat-load coming from the 1.6mrad wide X-ray beam fan. It protects the Aluminium window behind it that is not cooled.

The 28mm thickness of the Copper absorber is enough to fully take the heat-load but totally insufficient to stop all the X-rays. Therefore a 7mm thick Tungsten blade is positioned behind the window to further attenuate these X-rays coming from the core of the electron beam. This 7mm thickness was chosen so that the intensity of the traversing X-rays (28mm Cu, 2mm Al and 7mm W), coming from the central beam-core, will produce a light signal on the imager system of roughly comparable intensity to that of the Halo signal (created by X-Rays traversing only 2mm Al).

ISBN 978-3-95450-141-0

DESIGN AND INITIAL COMMISSIONING OF BEAM DIAGNOSTICS FOR THE KEK COMPACT ERL

R. Takai#, T. Obina, H. Sagehashi, Y. Tanimoto, T. Honda, T. Nogami, M. Tobiyama,
KEK, 1-1 Oho, Tsukuba, Ibaraki 305-0801, Japan

Abstract

A compact energy-recovery linac (cERL) was constructed at KEK as a test accelerator for the ERL-based light source. Standard beam monitors such as beam position monitors (BPMs), screen monitors (SCMs), and beam loss monitors (BLMs) have been developed for the cERL and used in its commissioning. For the main BPMs, we adopted the stripline type, the time response of which is improved by using a glass-sealed feedthrough. The SCMs are equipped with two types of screens and an RF shield for wake-field suppression. Optical fibers with photomultiplier tubes (PMTs), covering the entire cERL circumference, are used as the BLM. CsI scintillators with large-cathode PMTs are also prepared for detecting local beam loss. The design and some initial commissioning results of these standard monitors are described in this paper.

INTRODUCTION

The energy-recovery linac (ERL) has recently received significant attention as one of the promising candidates for next-generation light sources [1]. The Compact ERL (cERL), which is a test accelerator aimed at demonstrating the key technologies for the ERL-based light source, was constructed at KEK, and the complete system was commissioned in December 2013. The commissioning proceeded without troubles, and we successfully accelerated 6.5-μA CW beams to energies reaching 20 MeV; the beams recirculated without major loss, and they were guided to the beam dump after energy recovery in only two months [2]. In such an early phase of commissioning, standard beam diagnostics such as the monitoring of beam position, beam profile, and beam loss plays a central role. In this paper, we describe the design of our standard beam monitors that have contributed to the efficient cERL commissioning, and we report the initial commissioning results.

The beam monitors used for the cERL are listed in Table 1, and Fig. 1 shows their schematic layout. Four sets of fiber loss monitors cover the entire cERL circumference. Because the CsI-scintillator-based beam loss monitors described later are still under development, they are not listed in Table 1. Four current transformers (CTs) and a DCCT are currently not used, because of the low beam current. The beam current is measured by using not only the three movable Faraday cups (FCs) listed in Table 1 but also two beam dumps: injector and main dumps. In addition to these monitors, a slit scanner and a deflecting cavity are installed along the diagnostic line following the injector for the emittance and bunch-length measurements, respectively [3].

Table 1: List of cERL Beam Monitors

Monitor Type	Objective	#
BPM (Stripline/Button)	Position, Charge	45
SCM (Ce:YAG/OTR)	Position, Profile	30
BLM (Fiber&PMT)	Loss	4
CT	Charge	4
DCCT	Current	1
Movable FC	Charge	3

BEAM POSITION MONITOR

A beam position monitor (BPM) is a very useful tool especially for monitoring high-intensity ERL beams because it can non-destructively measure the beam centroid displacement in the transverse plane. The cERL has 45 BPMs, which are roughly classified into five types according to the duct structure and electrode type. This section describes the design of the BPM duct in the straight section, which contains the largest number of

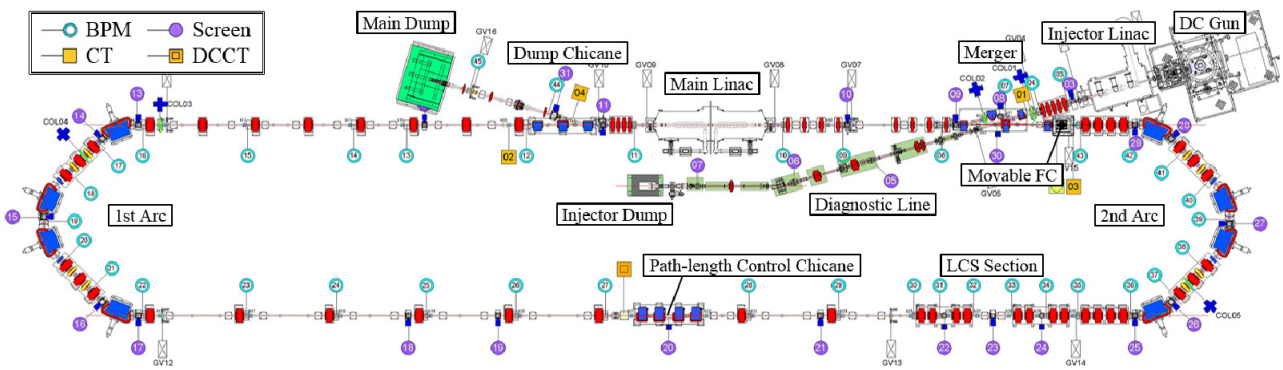

Figure 1: Layout of cERL beam monitors.

#ryota.takai@kek.jp

ISBN 978-3-95450-141-0

LONGITUDINAL LASER WIRE AT SNS

A. Zhukov, A. Aleksandrov, Y. Liu
Oak Ridge National Laboratory, Oak Ridge, TN 37830, USA

Abstract

This paper describes a longitudinal H- beam profile scanner that utilizes laser light to detach convoy electrons and an MCP to collect and measure these electrons. The scanner is located in MEBT with H- energy of 2.5MeV and an RF frequency 402.5MHz. The picosecond pulsed laser runs at 80.5MHz in sync with the accelerator RF. The laser beam is delivered to the beam line through a 30m optical fiber. The pulse width after the fiber transmission measures about 10ps. Scanning the laser phase effectively allows measurements to move along ion bunch longitudinal position. We are able to reliably measure production beam bunch length with this method. The biggest problem we have encountered is background signal from electrons being stripped by vacuum. Several techniques of signal detection are discussed.

INTRODUCTION

The Spallation Neutron Source accelerator complex consists of an H- linac where a one mS long train of ~1us mini-pulses is accelerated to 1GeV to be injected into a storage ring. The mini-pulses are accumulated in the ring and extracted to hit a mercury target as an intense ~700nS long pulse. Every mini-pulse is bunched at a 402.5MHz frequency. The SNS accelerator runs at 60Hz with average current of ~1.6mA resulting in over 1MW of beam power on target. Such a machine requires low loss operation, thus careful matching of longitudinal and transverse planes becomes important. The SNS uses several diagnostics devices and techniques for longitudinal profile measurements [1] including classical wire based Bunch Shape Monitor [2] and Laser Bunch Shape Monitor (LBSM) installed in MEBT. Also a method for measuring longitudinal Twiss parameters with Beam Position Monitors (BPM) was recently developed [3]. The LBSM is the only beam dynamics model independent device that allows non-invasive measurements while the accelerator is running at full power in neutron production mode.

THEORY OF OPERATION

A mode-locked laser running at 80.5MHz – in sync with the 5th sub-harmonic of 402.5MHz – detaches the electrons from the 2.5MeV negative hydrogen ions in the MEBT. The detached electrons are deflected by a magnet to be collected by an MCP as shown in Fig.1. While changing the laser phase we effectively move longitudinally along the ion beam and strip the ions that have a corresponding beam phase only. Using the 5th sub-harmonic results in 72° of scanned laser phase for a full sweep of 360° of ion beam phase.

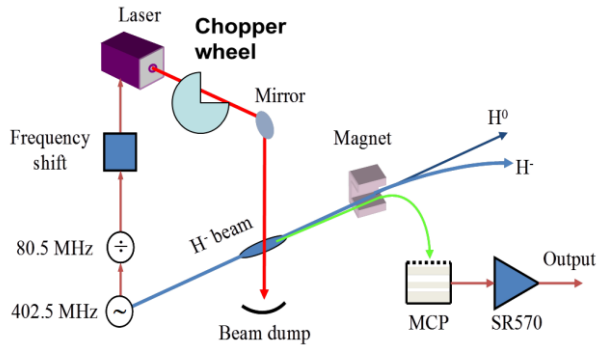

Figure 1: A layout of the Laser Bunch Shape Monitor.

In order to use this technique we need to precisely measure the laser phase vs. the base 402.5MHz carrier. We developed two approaches: frequency offset and phase shift.

Frequency Offset

If we change laser pulse repetition frequency by a tiny Δf on the order of 1kHz it will result in a phase drift with the period of ~1ms. Since the ion pulse length is 1ms it will experience all possible values of laser phase along its length. This will effectively plot longitudinal bunch distribution against time along the macro-pulse where 200us (1ms/5) corresponds to 360° of ion beam phase. Figure 2 shows the bunch profiles for different Δf.

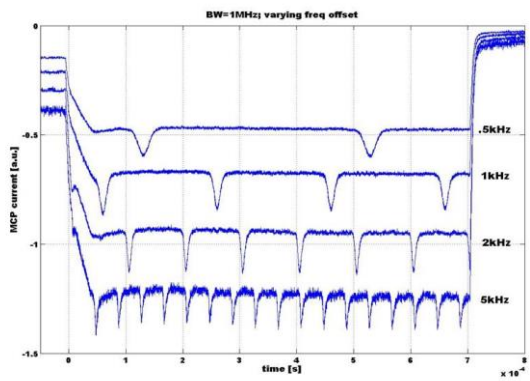

Figure 2: Bunch profile measurements with different frequency offsets in the frequency offset mode.

This method allows measuring bunch profile instantly by capturing one ion beam macro-pulse. It is very convenient because no additional equipment is needed and a scope waveform shows the bunch profile. It also doesn't require any precise measurement of Δf and actually even locking to 402.5MHz is not necessary.

Unfortunately this approach only works for long ion beam pulses. It is impossible to run full-length pulses

ISBN 978-3-95450-141-0

NSLS2 DIAGNOSTIC SYSTEMS COMMISSIONING AND MEASUREMENTS*

W. Cheng#, Bel Bacha, Danny Padrazo, Joe Mead, Marshall Maggipinto, Kiman Ha, Yong Hu, Huijuan Xu, Om Singh, NSLS-II, Brookhaven National Laboratory, Upton, NY 11973

Abstract

As the newest and most advanced third generation light source, NSLS2 commissioning has started recently. A total of 50mA stored beam was achieved in the storage ring. Most of the diagnostic systems have been commissioned with beam and proved to be critical to the success of machine commissioning. This paper will present beam commissioning results of various diagnostic systems in the NSLS2 injector and storage ring, including profile monitors, current monitors and position monitors. We will discuss some preliminary machine measurements as well, like beam current and lifetime, tune, beam stability, filling pattern etc.

INTRODUCTION

NSLS2 is an advanced third generation light source recent constructed at Brookhaven National Laboratory. It includes a 200MeV S-band LINAC, 200MeV to 3GeV Booster, LINAC to Booster (LtB) transfer line, Booster to storage ring (BtS) transfer line and 3GeV storage ring.

Injector commissioning was carried out from Nov 2013 to Feb 2014. 3GeV ramped beam was established in the Booster on last day of 2013. The injector is capable to deliver high charge in multi-bunch mode, as well single bunch beam to the storage ring. So far the storage ring had finished two phases of commissioning. The phase 1 beam commissioning, from Mar 26 to May 12, was using PETRA 7-cell normal conducting cavity. Small gap damping wiggler chambers were installed in three long straight sections. For the phase 1 commissioning, 25mA stored beam was achieved after fixing issues like hanging springs in the vacuum chamber. Many of the storage ring diagnostic systems had seen beam and commissioning during this period. Super-conducting RF cavity was installed during the shutdown together with several other in-vacuum undulators and beamline front end, and beam commissioning was resumed from Jun 30 to Jul 14, 50mA stored beam was achieved with super-conducting RF cavity. To eliminate the effect of insertion devices, all damping wigglers and IVUs were fully open. Beam commissioning will be continued in coming months to close the insertion devices and send X-rays down to beamlines.

Figure 1 shows the storage current and lifetime when 50mA beam was achieved. The stored average current was measured by in-flange type DCCT which is commercially available [1]. Filling pattern monitor system was used to measure the bunch to bunch current, BPM buttons SUM signal was send to high speed digitizer or oscilloscope. Figure 1 bottom snapshot gives the oscilloscope filling pattern at around 50mA, when one long bunch train was filled. Green trace (Ch2) is storage ring revolution clock while yellow trace (Ch1) is four button SUM signal from dedicated BPM.

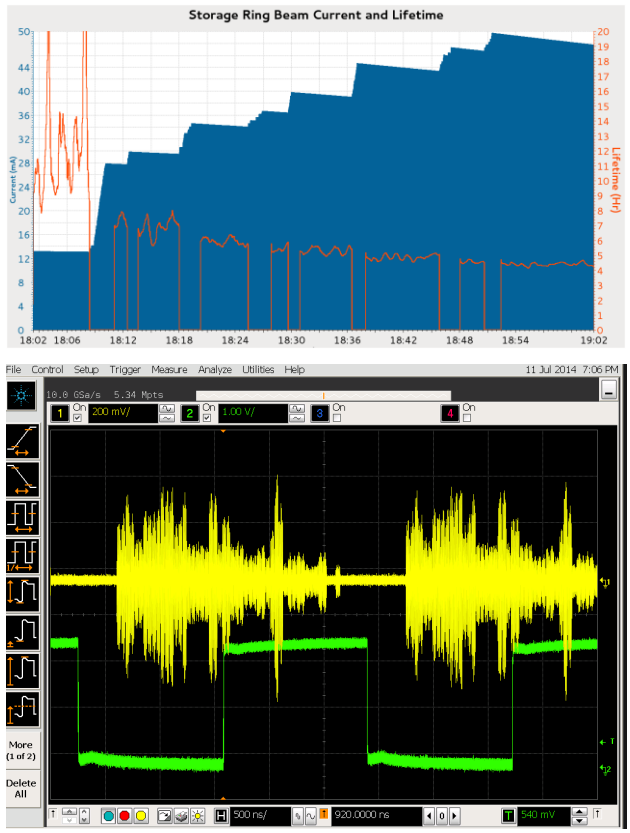

Figure 1: (top) storage ring DCCT measured current and lifetime history plot when fill up to 50mA; (bottom) filling pattern at around 50mA.

Table 1 lists major parameters of NSLS2 storage ring. There are 30 double bend achromatic (DBA) cells in the ring with bare emittance of 2 nm.rad. Horizontal emittance decreases to < 1 nm.rad with three damping wigglers.

* This material is based upon work supported by the U.S. Department of Energy, Office of Science, Brookhaven National Laboratory under Contract No. DE-AC02-98CH10886.

#chengwx@bnl.gov

ISBN 978-3-95450-141-0

A PICOSECOND SAMPLING ELECTRONIC "KAPTURE" FOR TERAHERTZ SYNCHROTRON RADIATION

M. Caselle, M. Brosi, S. Chilingaryan, T. Dritschler, N. Hiller, V. Judin, A. Kopmann, A.-S. Müller, J. Raasch, L. Rota, L. Petzold, N. J. Smale, J., L. Steinmann, M. Vogelgesang, S. Wuensch, M. Siegel, M. Weber, KIT, Karlsruhe, Germany

Abstract

The ANKA storage ring generates brilliant coherent synchrotron radiation (CSR) in the THz range due to a dedicated low-a_c-optics with reduced bunch length. At higher electron currents the radiation is not stable but is emitted in powerful bursts caused by micro-bunching instabilities. This intense THz radiation is very attractive for users. However, the experimental conditions cannot be easily reproduced due to those power fluctuations. To study the bursting CSR in multi-bunch operation an ultra-fast and high-accuracy data acquisition system for recording of individual ultra-short coherent pulses has been developed. The Karlsruhe Pulse Taking Ultra-fast Readout Electronics (KAPTURE) is able to monitor all buckets turn-by-turn in streaming mode.

KAPTURE provides real-time sampling of the pulse with a minimum sampling time of 3 ps and a total time jitter of less than 1.7 ps. The KAPTURE system, the synchrotron operation modes and beam test results are presented in this paper.

INTRODUCTION

At the synchrotron light source ANKA, up to 184 electron bunches can be filled with a distance between two adjacent bunches of 2 ns corresponding to the 500 MHz frequency of the accelerating RF system.

Since a few years, special user operation with reduced bunch length in the order of a few picoseconds has been available to research communities. In this mode, coherent synchrotron radiation is generated for electro-magnetic waves with a wavelength in the order of or longer than the electron bunch length. Due to this, one usually observes a strong amplification of the radiation spectrum in the THz band. Moreover, above a certain current threshold, a coherent modulation of the longitudinal particle distribution (microbunching) occurs due to CSR impedance [1]. This particle dynamic effect changes the characteristics of the CSR tremendously. The microbunching structures fulfil a coherence condition for shorter wavelengths. This leads to an instantaneous increase of the radiated THz power. Observation in the time domain shows bursts of radiations which occur with different periodicities depending on the bunch current. The characteristics of the bursting patterns are unique for different sets of accelerator parameters [2].

The KAPTURE (KArlsruhe Pulse Taking and Ultrafast Readout Electronics) system opens up a possibility to monitor the THz radiation of all bunches in the ring over a principally unlimited number of turns, realising a new type of measurement at ANKA. In this paper we present the KAPTURE system, the synchrotron applications and the measurements of CSR at the ANKA synchrotron light source.

KAPTURE SYSTEM

The KAPTURE system records individual pulses continuously with a sub-millivolt resolution and a relative timing resolution between two consecutive pulses in the order of picoseconds. KAPTURE is a flexible system and can be easily configured for the requirements of others synchrotron facilities.

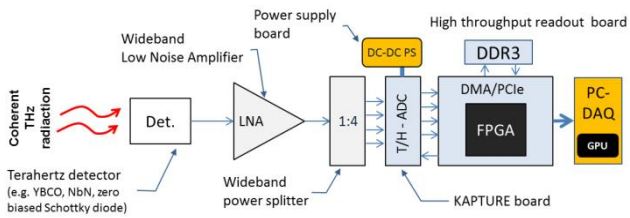

Figure 1: KAPTURE system for the detection of coherent THz radiation generated at ANKA.

The KAPTURE system is shown in Fig. 1. It consists of a Low Noise Amplifier (LNA), a power splitter, a picosecond pulse sampling stage called "KAPTURE board", a high throughput readout board and a high-end Graphics Processing Unit (GPU). The signal from the detector is fed into a LNA and then divided in four identical pulses by a wideband power splitter. The KAPTURE board acquires each pulse with 4 sample points at a programmable sampling time between 3 and 100 ps. The basic concept of the picosecond KAPTURE board and the architecture have been reported previously [3,4]. The high throughput readout board uses a new bus master DMA architecture connected to PCI Express logic [5] to transfer the digital samples from the KAPTURE board to a high-end GPU server. For continuous data acquisition a bandwidth of 24 Gb/s (12 bits @ 2 ns * 4 digital samples) is necessary. The DMA architecture has been developed to meet this requirement with a high data throughput of up to 32 Gb/s. The GPU computing node is used for real-time reconstruction of the pulse from the 4 digital samples. Afterwards, the peak amplitude of each pulse and the time between two consecutive pulses/buckets with a picosecond time resolution are calculated. The GPU node performs also an on-line Fast Fourier Transform (FFT) for the frequency analysis of the CSR fluctuations.

ISBN 978-3-95450-141-0

REFERENCE DISTRIBUTION AND SYNCHRONIZATION SYSTEM FOR SwissFEL: CONCEPT AND FIRST RESULTS

S. Hunziker#, V. Arsov, F. Buechi, M. Kaiser, A. Romann, V. Schlott,
Paul Scherrer Institut, CH-5232 Villigen PSI, Switzerland
P. Orel, S. Zorzut, Instrumentation Technologies d.d., SI-5250 Solkan, Slovenia

Abstract

The development of the SwissFEL [1] reference distribution and synchronization system is driven by demanding stability specs of LLRF-, beam arrival time monitors (BAM) and laser systems on one and cost issues, high reliability/availability and flexibility on the other hand. Key requirements for the reference signals are <10fs$_{rms}$ jitter well as down to 10fs$_{pp}$ temporal drift stability (goal) for the most critical clients (BAM, pulsed lasers). The system essentially consists of a phase locked optical master oscillator (OMO) with an optical power amplifier/splitter, from which mutually phase locked optical reference pulses as well as RF reference signals are derived. Optical pulses will be transmitted to pulsed laser and BAM clients over stabilized fiber-optic links whereas the RF signals are transmitted over newly developed stabilized cw fiber-optic links. Both s- and c-band reference signals use s-band links, whereupon the C band receiver incorporates an additional ultra-low jitter/drift frequency doubler. Furthermore, ultra-low noise analog laser PLLs have been built. We are presenting concepts and first results of sub-10fs$_{rms}$ jitter and 20fs$_{pp}$ long term drift cw links, tested in the SwissFEL Injector Test Facility (SITF).

REFERENCE DISTRIBUTION CONCEPT

Generation of Mutually Stable Reference Signals

High mutual short as well as long-term stability is required between all clients of the reference distribution system. On the other hand the SwissFEL RF system uses three different RF frequencies ($f_{s\ band}$ = 2998.800MHz, $f_{C\ band}$ = 5712.000MHz and $f_{X\ band}$ = 11'995.200MHz = 4x2998.800MHz). The S and X band frequencies are very close to the European standards, whereas 5712.000MHz is a US C band frequency. $f_{C\ band} \neq 2xf_{S\ band}$, which complicates fs-stable electrical reference generation, i.e. mutual stability between C band, S band, X band and various pulsed lasers and BAMs. The European standard S band frequency has been slightly detuned to the above mentioned value in order to find an as high as possible common subharmonic base frequency (f_b = 142.800MHz).

The idea of the SwissFEL reference system is to start with this base frequency and derive laser reference pulses as well as RF reference frequencies from it. It has been shown that a mode locked laser OMO ($f_{rep} = f_b$ = 142.800MHz), synchronized to a stable microwave source, can provide reference signals with extremely high temporal stability, pulses as well as RF harmonics, where the latter can be extracted from the OMO's pulse train (Fig. 2) or are delivered by a microwave oscillator synchronized to the latter [2]. Carefully deriving all reference signals from the OMO laser pulses yields high mutual stability.

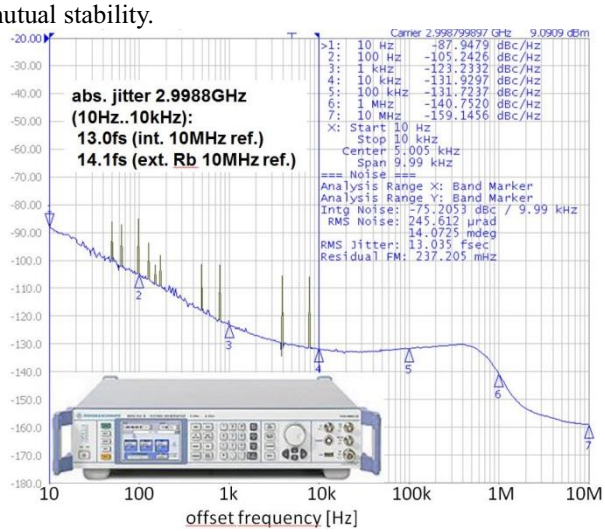

Figure 1: Measured phase noise spectrum timing jitter of the SwissFEL RF MO (Rohde + Schwarz SMA 100A.) Locking with a 10MHz Rb frequency standard (SRS FS725) slightly increases jitter from 13.0 fs to 14.1fs.

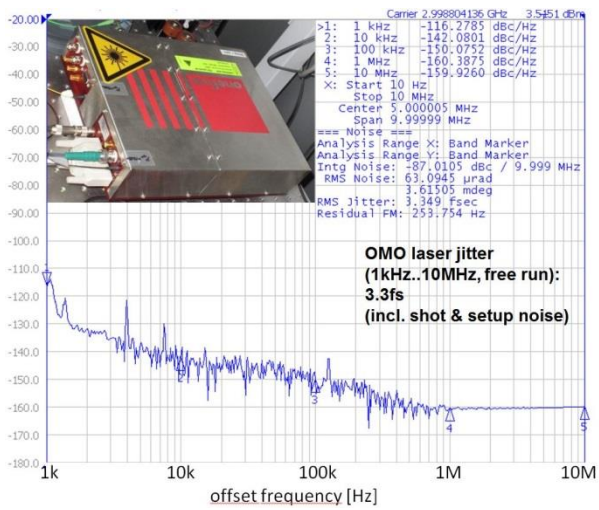

Figure 2: Measured phase noise spectrum and timing jitter of the free running SwissFEL OMO laser (Onefive Origami 15, 1560nm, 142.8MHz repetition rate; Discovery DSC50 photodiode).

Figure 3 shows a schematic overview of the system. The OMO laser is locked on the 10th harmonic to the RF master oscillator (RF MO, Fig. 1), which is itself locked

ISBN 978-3-95450-141-0

COMPARISON OF FEEDBACK CONTROLLER FOR LINK STABILIZING UNITS OF THE LASER BASED SYNCHRONIZATION SYSTEM USED AT THE EUROPEAN XFEL

M. Heuer, S. Pfeiffer, H. Schlarb, DESY, Hamburg, Germany
G. Lichtenberg, HAW, Hamburg, Germany

Abstract

The European X-ray Free Electron Laser will allow scientists to perform experiments with an atomic scale resolution. To perform time resolved experiments at the end of the facility it is essential to provide a highly stable clock signal to all subsystems. The accuracy of this signal is extremely important since it defines limitations of precise measurement devices. A laser based synchronization system is used for the synchronization with an error in a sub-femtosecond range. These light pulses are carried by an optical fiber and exposed to external disturbances which changes the optical length of the fiber. For that reason the fiber is actively stabilized using a controller implemented on the new MicroTCA Platform. Due to the high computation resources of this platform it is possible to attack the time delay behavior of the link system with well known model based control approaches. This contribution shows how to design a model based controller for such a system and compares the control performance of the previously used PID controller with advanced control algorithms at the currently installed laboratory setup.

INTRODUCTION

The European X-ray Free-Electron Laser (XFEL), is currently under construction at the Deutsches Elektronen Synchrotron (DESY) in Hamburg, Germany. This device with a length of 3.5 km will generate extremely intense and short X-ray laser light pulses with a duration of a few femtoseconds. Technical specifications of the facility can be found in [1]. The intense and ultra-short X-ray laser pulses are generated by an electron bunch which is feed through an undulator. They will provide scientists from all over the world the possibility to take a closer look into tiny structures on an atomic scale with a repetition rate of up to 4.5 MHz. This provides the ability to e.g. film the folding and formation of complex biomolecules [2]. One of the main challenges is to distribute a timing signal with a frequency error of less than 10 fs for all devices within the free-electron laser to achieve the required precision. In [3] a laser based synchronization system was proposed for that purpose, it is used for FLASH, and will be implemented for XFEL [4].

This paper is organized as follows: The first section gives an overview of the Laser based Synchronization system (LbSynch) and explains the Links Stabilization Unit (LSU). The second chapter introduces at set of possible control strategies and the dead time compensation. The experimental results and a comparison between the controller is given in section three. The paper closes with a short outlook how to improve the performance further.

Laser Based Synchronization System

Figure 1 shows a simplified version of the laser based synchronization system with the beamline.The injector laser triggers a detachment of electrons at the cathode of the gun, which generates an electron bunch. This bunch is than accelerated by 101 superconducting modules (I0 and I39H, A1.M1-4, ..., A25.M1-4). At the end of the beamline the bunch is lead through the undulator, which forces the electron bunches on a sinusoidal trajectory. This causes the so-called Self-Amplified Spontaneous Emission (SASE) process, which generates the high energy X-ray pulse. Other important devices within the beamline are e.g. the Bunch Arrival time Monitors (BAM) [5], which are used to measure the relative time of the electron bunch crossing a certain position w.r.t. the timing pulse of synchronization system.

To provide a clock signal to these devices the laser based synchronization system is used. It consists of two parts, the Master Laser Oscillator (MLO) generates the laser pulse train at a frequency of 216.66 MHz. This is the timing signal of the system, which is distributed through fibers to the different end station in the facility. This fiber is exposed to temperature and humidity changes as well as vibrations, which results in small changes of its optical length. To stabilize this length, the second part of this system, the so-called Link Stabilizing Unit (LSU) is used.

The lower right part of Fig. 1 shows the control scheme of a LSU. If a pulse enters the LSU, one small fraction of the laser pulse is branched off and the main part goes through a piezo stretcher into the fiber and further to the device in the accelerator. A piezo stretcher allows to slightly change the length of the fiber, hence it is used as an actuator in this scheme. At the device the pulse is partly reflected by an Faraday Rotating Mirror (FRM) and travels back the way to the LSU. This returning pulse and the fraction of the subsequent pulse pass an Optical Cross Correlator (OXC) two times. Each time a new pulse of the shape of the correlation of both incoming pulses is generated. Inside the OXC both polarizations have a different velocity and therefore both new correlation pulses are different. A balanced detector can measure the timing difference between both incoming pulses by measuring the intensity difference of the correlation pulses. If the pulses within the pulse train are equidistant and the signal of the balanced detector is zero, the length of the attached fiber is a multiple of the MLO repetition rate. With this scheme it is possible to suppress the error of the timing signal induced by length changes of the fiber caused by stress, temperature and/or humidity changes acting on the fiber.

ISBN 978-3-95450-141-0

RHIC-STYLE IPMs IN THE BROOKHAVEN AGS*

R. Connolly, C. Dawson, J. Fite, H. Huang, S. Jao, W. Meng,
R. Michnoff, P. Sampson, S. Tepikian, Brookhaven National Lab, Upton, NY, USA

Abstract

Beam profiles in the two storage rings of the Relativistic Heavy-Ion Collider (RHIC) at Brookhaven National Lab (BNL) are measured with ionization profile monitors (IPMs). An IPM measures the spacial distribution of electrons produced in the beam line by beam ionization of background gas. During the 2012 shutdown we installed a RHIC IPM in the Alternating-Gradient Synchrotron (AGS) to measure horizontal profiles and tested it during the 2013 run. This test was successful and during the 2013 shutdown a vertical IPM was built. This paper describes the new AGS IPMs and shows detector data.

INTRODUCTION

The Relativistic Heavy-Ion Collider (RHIC) at Brookhaven National Lab is a pair of concentric synchrotrons in which counter-rotating beams intersect at six points [1]. Beams of ions from protons (E_{max}=250 GeV) to fully-stripped uranium (E_{max}=100 GeV/nucleon) are accelerated and stored for several hours. There are detectors at two of the six intersection points for physics experiments with colliding beams.

Beam is injected into RHIC from a network of five accelerators. There are three primary accelerators: a tandem Van de Graaff, a 200-MeV H^- linac, and the new Electron-beam Ionization Source (EBIS). One of these three accelerators injects beam into the booster synchrotron, which injects into the AGS which injects RHIC.

Ionization profile monitors (IPMs) have been developed at BNL to measure transverse beam profiles in RHIC [2]. An IPM measures the distribution of electrons in the beam line resulting from residual gas ionization during a bunch passage. The electrons are swept transversely from the beam line and collected on 64 strip anodes oriented parallel to the beam axis.

In 2012 we installed a RHIC IPM into the AGS for horizontal profile measurements. The commissioning tests in the 2013 run were successful so for the 2014 run we built and installed a vertical IPM. The vertical AGS IPM is different from the horizontal to accommodate the required large horizontal aperture of the AGS. Also we added electrical coils on the permanent-magnet dipole detector magnets for beta-function measurements.

*Work performed by employees of Brookhaven Science Associates, LLC under Contract No. DE-AC02-98CH10886 with the U.S. Department of Energy

DETECTOR

Figure 1 is a schematic of the detector and electronics in the accelerator tunnel, fig. 2 is a photo of the detector, and fig. 3 shows the beam installation. An electric field to accelerate the signal electrons toward the collector is generated in the 100mmx150mm rectangular beam pipe by biasing the top electrode at -6kV. The electrons are forced to travel perpendicularly to the measurement plane by a permanent dipole magnetic with field of 1.4kG. A second, reversed, magnet corrects the AGS beam trajectory.

A signal-gating grid is located between the beam and the collector. This is normally biased at the sweep voltage of -6kV to prevent the signal electrons from passing. To make measurements the grid is pulled to ground by a Behlke transistor switch to allow the signal electrons to pass through to the input of a microchannel plate (MCP) which amplifies the electron flux by 10^4 to 10^7. Because each channel of an MCP has a dead time of 1ms after firing, the MCP can become dynamically depleted if the input electron flux is left on continuusly. Periodically the signal electrons are gated off, with the MCP bias on, so the plate can recharge.

The amplified electron flux falls on an anode circuit board with 64 channels spaced 0.53mm apart. Each channel is connected via vacuum feedthrough to an amplifier mounted on the beam pipe, fig 3. Each amplifier output drives a shielded twisted-pair transmission line to a 50MSPS VME digitizer channel.

A screen-covered rectangular opening in the grounded half of the beam pipe decouples the electron gate from the beam. The collector board with attached MCP is located in a Faraday enclosure with an opening for the electrons covered by a grounded stainless steel honeycomb grid which attenuates rf by 80dB.

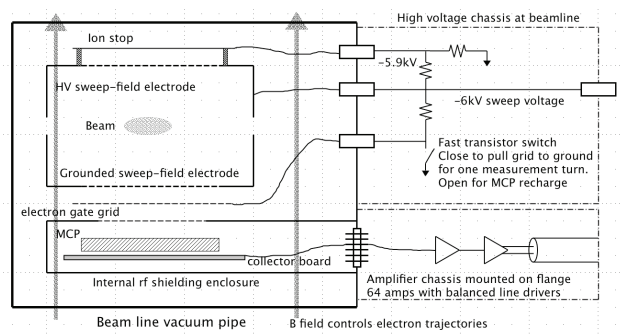

Figure 1: Schematic of detector and electronics located at the beam line.

ISBN 978-3-95450-141-0

NSLSII PHOTON BEAM POSITION MONITOR ELECTRONICS TESTING AND RESULTS

A. DellaPenna, Om Singh, Kurt Vetter, Joseph Mead, Marshall Maggipinto

Brookhaven National Laboratory, Upton, NY 11973, USA

Abstract

Simulated and real beam data has been taken using the new NSLSII Photon BPM electronics. The electrometer design can measure currents as low as 10's of nanoamps and has an ability to measure a current as high as 300mA. The 4 channel design allows for internal calibration and has both a Negative and Positive bias ability. Preliminary bench testing results has shown excellent resolution.

INTRODUCTION

At NSLSII we have installed a 4 blade design X-ray beam position chamber. The focus of this paper will be on the electronics and tests performed in the lab and with beam using diamond detectors installed @ NSLS beamlines. The design requirements of the electronics were to measure beam currents from 500nA to 1mA. With the Blade Chamber design, signals levels we could expect, were to be in this range. The electronics also required both a positive and negative Bias. The blade current transfer function reveals that without bias we would see ~ 0.5ua for every 1ma of stored beam. This number would double with a bias present. A block diagram is shown in Fig 1. The electronics were designed with the same idea of a AFE (Analog Front End) and a DFE(Digital Front End). As shown in - Fig. 2. This allowed the design to move forward quicker, utilizing what was done with the NSLSII RF BPM. The initial testing used the exact same DFE as the RF BPM electronics, but have since evolved and a new DFE was designed using the ZYNQ FPGA. The electronics PC boards also used the same chassis as the RF BPM.

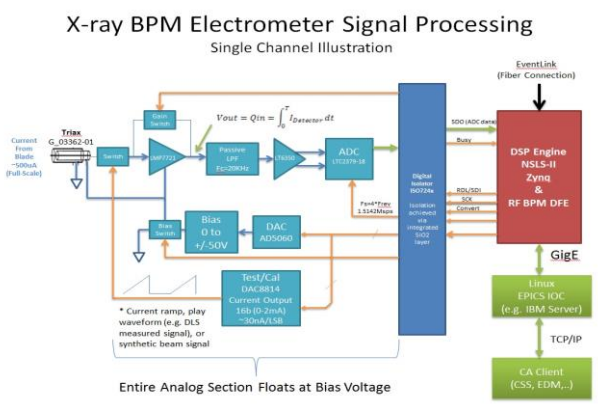

Figure 1: Block diagram of AFE/DFE.

ANALOG ELECTRONICS

The Analog Front End (AFE) was designed as a 4 channel electrometer. The first stage of the design required converting the current into a voltage. The lowest bias current amplifier in the industry was selected as the transimpedance front end. Because of the wide dynamic range mentioned previously 5 gain stages were developed. For the most sensitive gain stage, a range of 10's of nanoamps to 1uA was developed. The other gain stages are 1uA – 10uA, 10uA – 100uA, 100uA -1.2mA and a high gain stage 1mA – 250mA. The switching of the gain stage is done with a very low resistive CMOS switch. A reset switch was also included to discharge the signal before taking a fresh measurement. A simple two pole anti aliasing filter was also included before the digitizer. The digitizer chosen, was a 18bit 1.6Mhz serial device however, a new 20bit version has come out, which has the same footprint and would only require a small software change. Because a Bias was also required we decided to float our entire receiver section. This involved isolators for all signals coming in and out of the receiver. The bias was limited to less than 50V for safety reasons. We ensure that the voltage cannot exceed this by two means. One, our Bias supply control signal is set by a DAC. The reference for this DAC was limited to limit the output to 43V. A 43V Zener diode was also added to provide additional protection. The Xbpm chamber also has a provision for an additional "Electrode". Because of this, the design was modified to allow a bias to also be present on that plate as well. The board also has a provision for on board calibration using a 4 channel 14bit current DAC which allows for testing currents from 100nA to 1.5mA.

Figure 2: AFE and DFE connected together.

To determine what our signal might look like from the blades, a trip to the Diamond Light Source (DLS) was

RHIC INJECTION TRANSPORT BEAM EMITTANCE MEASUREMENTS*

J. Huang#, Duke University, Durham, North Carolina 27708, USA
D.M. Gassner, M. Minty, S. Tepikian, P. Thieberger, N. Tsoupas, C. Zimmer
Brookhaven National Laboratory, Upton, New York 11973, USA

Abstract

The Alternating Gradient Synchrotron (AGS)-to-Relativistic Heavy Ion Collider (RHIC) transfer line, abbreviated AtR, is an integral component for the transfer of proton and heavy ion bunches from the AGS to RHIC. In this study, using 23.8 GeV proton beams, we focused on factors that may affect the accuracy of emittance measurements that provide information on the quality of the beam injected into RHIC. The method of emittance measurement uses fluorescent screens in the AtR. The factors that may affect the measurement are: background noise, calibration, resolution, and dispersive corrections. Ideal video Offset (black level, brightness) and Gain (contrast) settings were determined for consistent initial conditions in the Flag Profile Monitor (FPM) application. Using this information, we also updated spatial calibrations for the FPM using corresponding fiducial markings and sketches. Resolution error was determined using the Modulation Transfer Function amplitude. To measure the contribution of the beam's dispersion, we conducted a scan of beam position and size at relevant Beam Position Monitors (BPMs) and Video Profile Monitors (VPMs, or "flags") by varying the extraction energy with a scan of the RF frequency in the AGS. The combined effects of these factors resulted in slight variations in emittance values, with further analysis suggesting potential discrepancies in the current model of the beam line's focusing properties. In the process of testing various contributing factors, a system of checks has been established for future studies, providing an efficient, standardized, and reproducible procedure that might encourage greater reliance on the transfer line's emittance and beam parameter measurements.

INTRODUCTION

The beam emittance measurements that were performed in various sections along the 580 m long AtR transfer line rely on a series of profile monitors equipped with mostly CCD cameras [1] to help determine the values of the beam parameters prior to injection into RHIC. Two sections of the AtR transfer line are being used to make beam emittance and beam parameter measurements between the machines that are of particular importance given that lower emittance allows for more frequent collisions, in turn producing a desirably higher luminosity.

The beam emittance and beam parameters' measurements are derived from measurements of the horizontal and vertical beam sizes at three separate locations together with the known strengths of the magnets in the AtR [2, 3].

By testing the sensitivity of emittance on factors such as calibrations, resolution, dispersion, and noise under uniform conditions, a straightforward method of measurement that can be applied to future studies was established.

OFFLINE EMITTANCE ANALYSIS

During the RHIC run we collected beam profile data from a variety of flags in the AtR line that were measured under different conditions. This beam profile information was logged for later use because a majority of our analysis was performed offline after the run cycle ended. In order to calculate and test the dependence of emittance to different parameters, we used the logged data and a script file that reads the saved input files and outputs the measurements in the form of the standard deviation (sigma) of the beam profiles. Given that emittance has a dependency on horizontal and vertical sigma values, we tested each potential factor by applying its impact, measured as a ratio or multiplier, to sigma. After editing a file of sigma's to adjust for the factor of interest, we ran the emittance script to determine the corrected measurements and re-evaluate the emittance.

INITIAL CONDITIONS

The beam emittance and beam parameter measurements in the AtR transfer line rely on VPMs which are plunged in and removed from the beam pipe through the FPM controls application which is an interface that allows users to alter configuration settings while viewing immediate results in one of four equally capable frame grabbers, or viewing windows. While inserted, the beam hits and illuminates the phosphor (Gd_2O_2S:Tb) screen; the image data is displayed and automatically logged. The 12 flags are distributed along the transfer line and separated into four sections named the U, W, X, and Y lines. Based on location, flags of interest for this study are UF3, UF4, UF5, WF1, WF2, and WF3 of the U and W-lines, corresponding to the transfer line between the AGS up to the switching magnet that deflects beams into either of the two RHIC accelerators.

The goal of our work was to test factors that affect emittance measurements as a means to produce an efficient method of acquiring accurate data during future run cycles. Before delving into these properties, however, ideal and uniform initial conditions were necessary. The FPM application offers a user-controlled environment for optimizing measurement conditions by way of optional background subtraction, intensity adjustment, and Range of Interest (ROI) selection. Previous research has elaborated on the potentially harmful effects of imperfect background subtraction and on the advantages of the ROI

*Work supported by the auspices of the US Department of Energy
julia.y.huang@duke.edu

ISBN 978-3-95450-141-0

INSTRUMENTATION FOR THE PROPOSED LOW ENERGY RHIC ELECTRON COOLING PROJECT WITH ENERGY RECOVERY*

D. M. Gassner #, A. Fedotov, R. Hulsart, D. Kayran, V. Litvinenko, R. Michnoff, T. Miller, M. Minty, I. Pinayev, M. Wilinski, BNL, Upton, NY 11973, USA

Abstract

There is a strong interest in running RHIC at low ion beam energies of 7.7-20 GeV/nucleon [1]; this is much lower than the typical operations with 100 GeV/nucleon. The primary motivation for this effort is to explore the existence and location of the critical point on the QCD phase diagram. Electron cooling can increase the average integrated luminosity and increase the length of the stored lifetime. A cooling system is being designed that will provide a 30 – 50 mA electron beam with adequate quality and an energy range of 1.6 – 5 MeV. The cooling facility is planned to be inside the RHIC tunnel. The injector will include a 704 MHz SRF gun, a 704 MHz 5-cell SRF cavity followed by a normal conducting 2.1 GHz cavity. Electrons from the injector will be transported to the Yellow RHIC ring to allow electron-ion co-propagation for ~20 m, then a 180 degree U-turn electron transport so the same electron beam can similarly cool the Blue ion beam. After the cooling process with electron beam energies of 1.6 to 2 MeV, the electrons will be transported directly to a dump. When cooling with higher energy electrons between 2 and 5 MeV, after the cooling process, they will be routed through the acceleration cavity again to allow energy recovery and less power deposited in the dump. Special consideration is given to ensure overlap of electron and ion beams in the cooling section and achieving the requirements needed for cooling. The instrumentation systems described will include current transformers, beam position monitors, profile monitors, an emittance slit station, recombination and beam loss monitors.

INTRODUCTION

The Low Energy RHIC electron Cooling (LEReC) project is presently in its design stage and scheduled to begin commissioning components in 2017, with operations planned for 2018-19. The electron and ion parameters are shown in Table 1 and 2. This will be the first bunched beam electron cooler and the first electron cooler in a collider. The goal is to achieve an efficient cooling system for Au+Au collision beams at 7.7, 11.5 and 20 GeV/u in the center of mass corresponding to electron energies of 1.6, 2.7 and 5.0 MeV. An effective cooling process would allow us to cool the beams beyond their natural emittances and also to either overcome or to significantly mitigate limitations caused by intrabeam scattering and other effects. It also would provide for longer and more efficient stores, which would result in significantly higher integrated luminosity.

Cooling of ion and hadron beams at low energy is also of critical importance for the productivity of present and future Nuclear Physics Colliders, such as RHIC, eRHIC and ELIC.

Table 1: Electron Beam Parameters

Electron Parameters	
Electron Beam Energy	1.6-5 MeV
Electron Bunch Charge	100-300 pC
Electron Average Current	30-50 mA
RMS Norm Emittance	≤ 2.5 mm mrad
Bunch Rep Rate	704 MHz
Bunch Train Rate	9.1 MHz
RMS Energy Spread	$\leq 5 \times 10^{-4}$
RMS Bunch Length	100 ps
RMS Trans beam size	2-4 mm
Max power with ER	100 kW

Table 2: RHIC Ion Beam Parameters

Ions with gamma = 4.1	
Particles per Bunch	0.75×10^{9}
Peak Current	240mA
RMS Norm Emittance	2.5 mm mrad
Rep Rate	75.9 kHz
RMS Energy Spread	$\leq 5 \times 10^{-4}$
RMS Bunch Length	3.2m
RMS Trans beam size	4.3 mm
Space charge tune shift	0.02

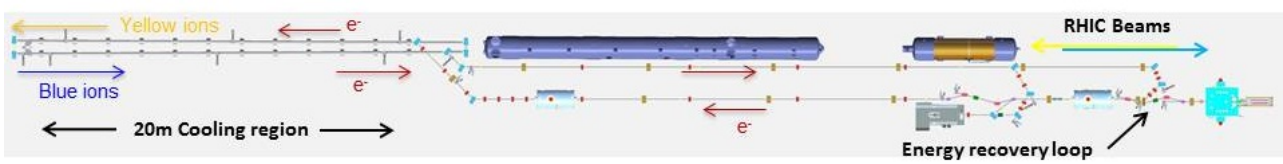

Figure 1: LEReC beam line layout for electron cooling with energy recovery. The Blue and Yellow adjacent 20 m ion cooling beam lines shown at left are located in a RHIC region without superconducting magnets.

* This material is based upon work supported by the U.S. Department of Energy, Office of Science, Brookhaven National Laboratory under Contract No. DE-AC02-98CH10886.

gassner@bnl.gov

ISBN 978-3-95450-141-0

CONSTRUCTION AND OPERATIONAL PERFORMANCE OF A HORIZONTALLY ADJUSTABLE BEAM PROFILE MONITOR AT NSLS-II*

B. Kosciuk#, A. Blednykh, S. Seletskiy, Brookhaven National Laboratory, Upton, NY 11973, USA

Abstract

The NSLS-II Synchrotron Light Source is a 3 GeV electron storage ring currently in the early stages of commissioning at Brookhaven National Laboratory. In order to observe the electron beam cross section in the injection region of the storage ring, a specially designed, horizontally adjustable beam profile monitor was installed at the downstream end of the injection septum. It allows the profile of the injected, bumped or single turn beam to be viewed and measured. In this presentation, we discuss the final design, construction challenges, and operational performance of this novel device.

DESIGN REQUIREMENTS

The primary design requirements for the NSLS-II beam profile monitor [1] or "flag" are as follows. Insert a scintillator screen into the beam path at three different horizontal positions within the vacuum chamber, allowing the beam cross section and rough position to be captured. The chamber length and internal aperture are defined by the space between the upstream septum chamber and downstream kicker chamber. In this case the overall chamber length is 357mm with 150mm CF (Conflat) flanges. The upstream and downstream internal apertures are different and require a tapered transition over the chamber length.

In order to capture the beam at three different locations, the horizontal screen position needs to be precisely controlled to a resolution of 250µm. It is also desirable to have the screen position infinitely adjustable as opposed to just three discreet positions. A position read back device is also required to verify horizontal position.

Due to space constraints in the injection region, the choice was made to incorporate two sets of RF BPM (radio frequency beam position monitor) button assemblies into the flag chamber. One set of BPMs located 24.25mm from chamber center is intended to measure position of the injected beam while the other set located 15mm from chamber center is intended to measure bumped beam position.

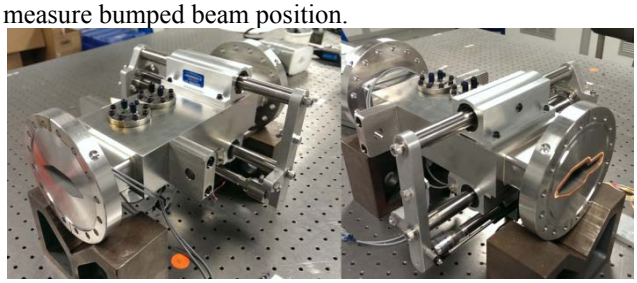

Figure 1: NSLS-II SR Flag in final assembly configuration.

*Work supported by … DOE Contract No: DE-AC02-98CH10886
#bkosciuk@bnl.gov

CHAMBER CONSTRUCTION

The construction of the flag chamber was by far the most challenging aspect of this design. The final design consists of a three piece stainless steel assembly with two brazed joints. The body of the chamber is a rectangular stainless steel "slab" 57mm x 120mm in cross section. The internal aperture is rectangular and is 25mm x 80mm on the upstream side and tapers to 25mm x 76mm over the 230mm length. The internal aperture was precisely cut via a wire EDM (electro discharge machining) process. Ports were machined into the top, bottom and side of the slab to accept the BPMs and bellows assembly. These ports are designed to be used with HelicoFlex® Delta-type UHV (ultra high vacuum) seals and require a specially prepared surface to mate with. The surface finish requirement for these seals is 16 micro inch with a circular lay. Delta-type seals are used extensively in the NSLS-II storage ring with great success.

To simplify the chamber assembly, both the upstream and downstream flanges are a one piece fabrication, each is machined from a slug of 304 stainless steel. This eliminated the need for welding Conflat flanges after the brazing was complete. The upstream aperture has a complex internal geometry, tapering from an asymmetric shape corresponding that of the downstream aperture of the septum chamber to a rectangular aperture that matches the central chamber. Machined into the face of the upstream flange is a dovetailed groove designed to accept a slant coil RF spring, the purpose of which is to shorten any cavities where high order modes can exist. The downstream flange tapers from a rectangular shape to the standard NSLS-II 25mm x 76mm hexagonal aperture. The apertures of both flanges were also cut using EDM. Fiducial targets were machined into the circumference of both flanges for in-situ survey and alignment after installation in the storage ring.

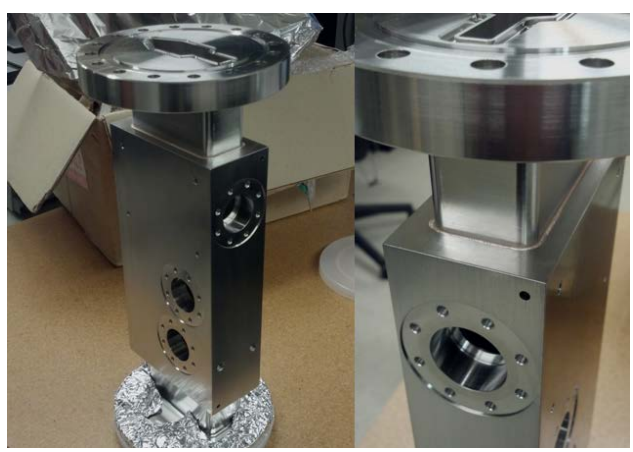

Figure 2: Successfully brazed flag chamber.

ISBN 978-3-95450-141-0

BEAM PROFILE MEASUREMENTS IN THE RHIC ELECTRON LENS USING A PINHOLE DETECTOR AND YAG SCREEN*

T. Miller†, M. Costanzo, W. Fischer, B. Frak, D. M. Gassner, X. Gu, A. Pikin,
C-AD, BNL, Upton, NY, 11973, U.S.A.

Abstract

The electron lenses installed in RHIC are equipped with two independent transverse beam-profiling systems, namely the Pinhole Detector and YAG screen. A small Faraday cup, with a 0.2mm pinhole mask, intercepts the electron beam while a pre-programmed routine automatically raster scans the beam across the detector face. The collected charge is integrated, digitized and stored in an image type data file that represents the electron beam density. This plungeable detector shares space in the vacuum chamber with a plunging YAG:Ce crystal coated with aluminium. A view port at the downstream extremity of the collector allows a GigE camera, fitted with a zoom lens, to image the crystal and digitize the profile of a beam pulse. Custom beam profiling software has been written to import both beam image files (pinhole and YAG) and fully characterize the transverse beam profile. The results of these profile measurements are presented here along with a description of the system and operational features.

INTRODUCTION

In order monitor the quality of the electron beam in the electron lens used to compensate for the effects of head-on Beam-Beam interactions in the collider [1], two parallel methods of beam profile measurement were developed and tested on a test bench [2] toward the end of 2011. Final designs were made and these systems were installed during the shutdown beginning in the summer of 2012 on the electron lens prepared for the RHIC blue beam [3]. Installation of both the electron lenses, one for blue and one for yellow RHIC beams, continued throughout the rest of 2012. The two beam profile measurement instrumentation systems were tested, along with applications for single-bunch beam-beam compensation, during the 2013 polarized-proton run in RHIC [4].

Table 1: Beam Parameters During Measurement

Parameter	YAG	PinHole
Beam Energy	6 keV	6 keV
Beam Current	70 mA	210 mA
Pulse Width	1 μs	12.5 μs
Rep Rate	1 Hz	10 Hz
Resolution	~40 pixels/mm	~8.5pts/mm

In this paper we present the final design and function of the YAG and pinhole scan system and the results of the profiles measured using the two methods. Table 1 summarizes the electron beam parameters, reduced from normal operation during the two profile measurements.

YAG SCREEN IMAGING

A mono-crystalline Cerium doped YAG crystal is used as the scintillating screen. Measuring 30mm diameter and 0.1mm thick, it is coated with a 100μm layer of evaporated aluminium to drain accumulated charge. The mechanical arrangement used on the test bench, presented earlier [5], was repeated in the installation in RHIC. The Gigabit Ethernet camera was upgraded from a Manta G201B to a G145B. The 21% larger sensor has 1.4 megapixels (MP) instead of 2 MP and thus provides increased sensitivity due to the larger pixel size on its SonyICX285 2/3 image sensor. The camera is used in its external trigger mode and is synchronized to the pulsed electron beam by the timing system.

Although two lenses were compared during tests on the test bench [5], the Sigma 70-200mm f/4-5.6 APO DG Macro lens with C-mount adapter was chosen. Its large aperture mates well with the high sensitivity of the camera. The drawback of this commercially available low cost lens is its fragile plastic body and lack of locking mechanism. The focus adjustment was very sensitive as the depth of field was very shallow with the aperture wide open. Sitting 86cm downstream of the YAG crystal, the zoom lens was adjusted to fill the camera's view with the 20mm useable area of the YAG screen. At this zoom, the focus adjustment was at its limit, suggesting an imperfect but sufficient setup of the optical system. The resulting resolution of the 20mm screen projected onto the camera's sensor was measured to be 39.4 pixels/mm. Fig. 1 shows the result of the high-resolution image of the

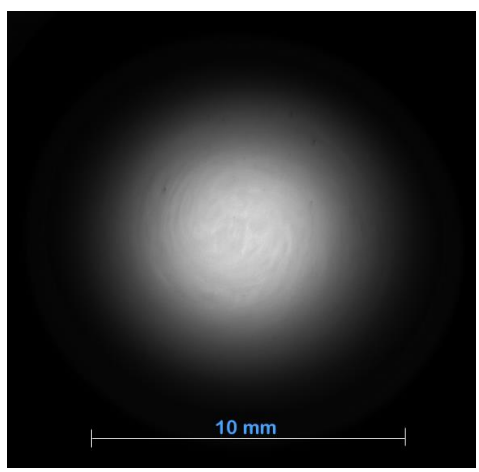

Figure 1: YAG screen profile of the electron beam.

*Work supported by Brookhaven Science Associates, LLC under Contract No. DE-AC02-98CH10886 with the U.S. DOE
†tmiller@bnl.gov

ABSOLUTE BEAM EMITTANCE MEASUREMENTS AT RHIC USING IONIZATION PROFILE MONITORS*

M. Minty#, R. Connolly, C. Liu, T. Summers, S. Tepikian, BNL, Upton, NY, USA

Abstract

In this report we present studies of and measurements from the RHIC ionization profile monitors (IPMs). Improved accuracy in the emittance measurements has been achieved by (1) continual design enhancements over the years, (2) application of channel-by-channel offset corrections and gain calibrations in the beam profile measurements and (3) use of measured beta functions at the locations of the IPMs. The removal of systematic errors in the emittance measurements was confirmed by the convergence of all four planes of measurement (horizontal and vertical planes of both the Blue and Yellow beams) to a common value during beam operation with stochastic cooling. Consistency with independent measurements (luminosity-based using zero degree counters) at the colliding beam experiments STAR and PHENIX was demonstrated.

INTRODUCTION

In the past, comparisons between emittance measurements from ionization profile monitors, Vernier scans (using as input measured rates from zero degree counters, ZDCs), the polarimeters and the Schottky detectors evidenced significant variations of up to 100%. In this report we present studies of the RHIC ionization profile monitors (IPMs). After identifying and correcting for systematic instrumental errors in the beam size measurements, we present experimental results showing that the remaining dominant error in beam emittance measurements was imprecise knowledge of the local beta functions. After application of measured beta functions, thanks to full 3-D stochastic cooling we demonstrate that precise measurements of the absolute emittances result. Also, consistency between the emittances measured by the IPMs and the ZDCs was demonstrated.

BRIEF HISTORY OF THE RHIC IPMS

The design of the RHIC IPMs has evolved over time with continuous improvements. The first prototype was built and tested in 1996 [1] with first measurements in RHIC in 1999 [2, 3]. In 2002 two changes were made motivated by experiences with beam: shielding was added upstream of the detectors to prevent signal contributions from upstream beam losses and the electrodes were made longer to avoid electron clouds from migrating into the region of the detector [4]. In 2005 fast signal gating was added to avoid depletion of the multichannel plate (MCP) detector and better isolation of the detector from the electromagnetic fields of the beam was implemented [4]. As the beam intensities increased, this latter effect was further suppressed with a new design in 2007 which placed all electronics inside a Faraday cage outside of the path of the beam's image current [5]. The prototype for this new design [5] was implemented for the Yellow Ring vertical plane (YV) in 2008. In 2010 the new design [5] was implemented for both the Blue and Yellow Ring horizontal planes (BH, YH) and these IPMs were moved to locations where the beam sizes were larger. The new IPM design [5] was implemented in the last remaining plane, Blue Ring vertical (BV), in 2013.

* Work supported by Brookhaven Science Associates, LLC under Contract No. DE-AC02-98CH10886 with the U.S. Department of Energy

minty@bnl.gov

INSTRUMENTAL SYSTEMATIC ERRORS

During the FY11 RHIC run [6], it was found that when the beams were brought into collision at a new third experiment (AnDY), the vertical beam size measurements from the IPMs changed considerably. To investigate further, measurements were taken while scanning the beam across the area of the detector. The measurements revealed significant damage to the multi-channel plate detectors (MCP) due to depletion [7] however with corrections applied, the position sensitivity still remained (since the beam sizes at full energy were small compared to the region of the MCP depletion). Other issues concerned variations between measurements, which were not small compared to expectation based on the statistical properties (i.e. ionization cross sections) of the measurements, and channel-to-channel variations within a single measurement.

CHANNEL-BY-CHANNEL OFFSET CORRECTION AND GAIN CALIBRATIONS

A conceptual view of the IPM and photographs are shown in Fig. 1. The signals from the MCP (bottom left) are processed through 64 channels as seen on the anode board (bottom right) and transferred to amplifiers through 64 ceramic-beaded wires (bottom left). Using the previously acquired data (beam size measurements as a function of beam centroid position), the channel offsets were determined by measurements with beam passing across the MCPs but not above the specific channels of interest. After applying the offset corrections to all the measured profiles and removing bad channels, the gain calibrations were obtained using the following automated procedure. For each IPM:

(1) Fit each of the (20 to 30 or so) profiles in the calibration scan with a Gaussian and compute the chi-squared, χ^2.

A COMPACT IN-AIR X-RAY DETECTOR FOR VERTICAL BEAM SIZE MEASUREMENT AT ALBA

A. A. Nosych, U. Iriso, ALBA CELLS, Barcelona, Spain

Abstract

An in-air x-ray detector (IXD) was developed for ALBA to study the residual x-rays after traversing copper crotch absorbers. The device prototype is placed in-air after such an absorber, mounted flush with the vacuum pipe. The remaining x-rays (above 120 keV) generate a visible footprint if they impinge upon a sensitive enough scintillator. After unsuccessful testing different screens, we are using a Cerium doped PreLude420 (LuYSiO:Ce) screen, whose the image is observed with a simple optics system mounted on a commercial CCD camera. This measurement allows evaluating the vertical electron beam size with exposure times in the order of 1 second. Similar instruments are used at ESRF and ANKA storage rings. This paper presents the results of the first measurements with IXD (March-July 2014), and describes its potential to be used as a full diagnostics tool for the 3 GeV storage ring of ALBA.

INTRODUCTION

At ALBA, as it is widely used in most 3rd generation synchrotron light sources, the emittance in both planes is measured with the usual pinhole method [1]. However, this only provides a local measurement of the vertical emittance, thus a local measurement of the ver/hor coupling. In order to infer the global coupling, readily available measurements of the vertical beam size are desirable.

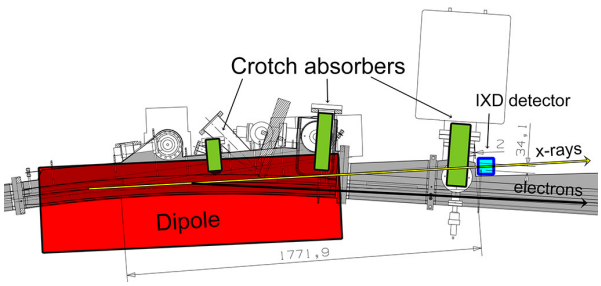

Figure 1: Tunnel section layout, showing a bending magnet with water cooled absorbers and paths of the electron and photon beams.

In-air X-ray Detectors (IXD), developed first at ESRF [2] and ANKA [3], are cheap and simple devices that can provide such measurements. They use the "left-over" hard x-rays produced by the dipoles and going through the absorbers to obtain an image of the synchrotron radiation fan, from where the vertical beam size can be inferred.

At ALBA, the unused excess of x-rays generated by 32 1.4 Tesla dipoles are damped by water cooled absorbers, which are mounted by sets of three into each dipole (Fig. 1). The absorbers are thick large-toothed copper jaws, half-open to form a crotch geometry (Fig. 2), with a minimum thickness of 35 mm and are aimed at complicating the path of x-rays traversing through. Only a fraction of low intensity higher-energy flux can penetrate the absorbers; however, if detected, it can serve as an alternative diagnostics tool for real-time monitoring of vertical beam size and emittance.

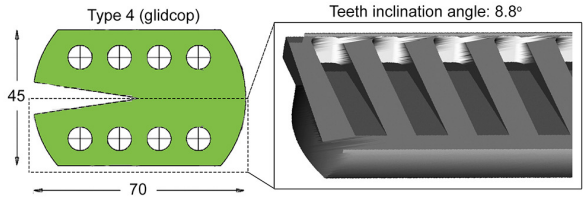

Figure 2: Transverse cross-section of the crotch absorber and a model of its lower jaw.

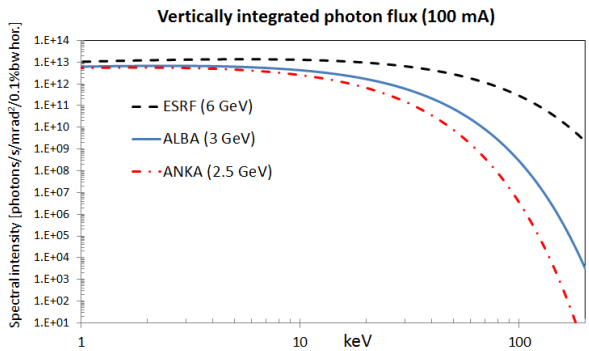

Figure 3: Vertically integrated x-ray spectrum emitted by bending magnets for machines using iXD detectors.

At ESRF and ANKA the combination of beam energy and absorber thickness offer favorable conditions for these detectors: the 6 GeV ESRF has 40 mm absorbers, and 2.5 GeV ANKA has 8 mm absorbers. ALBA is the first 3 GeV 3rd generation synchrotron light source where this technology is applied, which has become possible after choosing the appropriate scintillating material.

The total photon emission, summed over all vertical angles, emitted when an electron beam of energy E crosses a dipole is:

$$N = 2.46 \times 10^{13} E I_b \int_{\frac{\epsilon}{\epsilon_c}}^{\infty} K_{5/3}(u)\, du \qquad (1)$$

in units of photons/second/h-mrad/0.1%BW, where I_b is the electron beam current and $u = \epsilon/\epsilon_C$ is the ratio between the photon energy ϵ and the machine critical energy ϵ_C. For reference, Figure 3 compares this flux to other synchrotron light machines for fixed intensity $I_b = 100$ mA, while Fig. 4

ISBN 978-3-95450-141-0

WIRE SCANNER INSTALLATION INTO THE MICROTCA ENVIRONMENT FOR THE EUROPEAN XFEL

T. Lensch*, A. Delfs, V. Gharibyan, I. Krouptchenkov, D. Nölle, M. Pelzer, H. Tiessen, M. Werner, K. Wittenburg, DESY†, Hamburg, Germany

Abstract

The European XFEL (E-XFEL) is a 4th generation synchrotron radiation source currently under construction in Hamburg. The 17.5 GeV superconducting accelerator will provide photons simultaneously to several user stations [1]. For the transverse beam profile measurement in the high energy sections Wire Scanners are used as an essential part of the accelerator diagnostic system, providing the tool to measure small beam size in an almost nondestructive manner. The scanners will be operated in a fast mode, starting from a trigger the wire will be accelerated to 1 m/s and hitting about 100 bunches out of the long bunch train of E-XFEL within a single macropulse. Slow scans with single bunches are also possible. In the first stage 12 stations are planned to be equipped with Wire Scanners where each station consists of two motion units (horizontal and vertical plane). The new concept uses linear servo motors for the motion of the wires and a new mechanical design has been developed at DESY [2].

This paper describes the electronics developments for the motion part of these Wire Scanners and the integration into the MicroTCA environment.

MOTIVATION

At DESY wire scanners have been used for diagnostic purposes for many years in HERA or Flash, operated with the control systems TINE and DOOCS. Rotating motors or pneumatic cylinders had been used as drive units [3]. The goal was to build the E-XFEL wire scanner as an improved system based on these experience. The new system has to be based on MicroTCA (MTCA.4) in order to be well integrated into the controls hard- and software as well as the timing infrastructure.

OVERVIEW

It is planned to start the commissioning of the E-XFEL with 12 wire scanner stations and about 60 screen monitors. Each station consists of a set of two motion units (horizontal and vertical plane). These wire scanner stations are placed in groups of three stations with well designed phase advance before the collimation system and before each of the 3 SASE undulators, allowing to measure emittance and twiss parameters without changing the magent settings. Additional 15 positions can easily be equipped later with wire scanners if this turns out to be useful.

* timmy.lensch@desy.de
† Deutsches Elektronen Synchrotron

Mechanics and Motor

For the E-XFEL wire scanners the mechanics of the motion unit was developed from scratch. A lot of experience from FLASH and HERA wire scanners went into the design to ease service and thus improve the availability. As a driver for the wire scanner forks linear motors from LinMot [4] were chosen. A catch unit had been added into the design to keep the fork mechanically out of the beam area during times of no scans. The catch unit has to be opened electrically to be able to move the fork into the beam. An end switch inside indicates, when the fork is in parking position and locked. Furthermore magnetic springs guarantee moving the fork back to this out-position in case of failure. Figure 1 shows the mechanical setup of the wire scanner prototype with almost complete cabling and safety housing. Table 1 gives some basic specifications of the device [5].

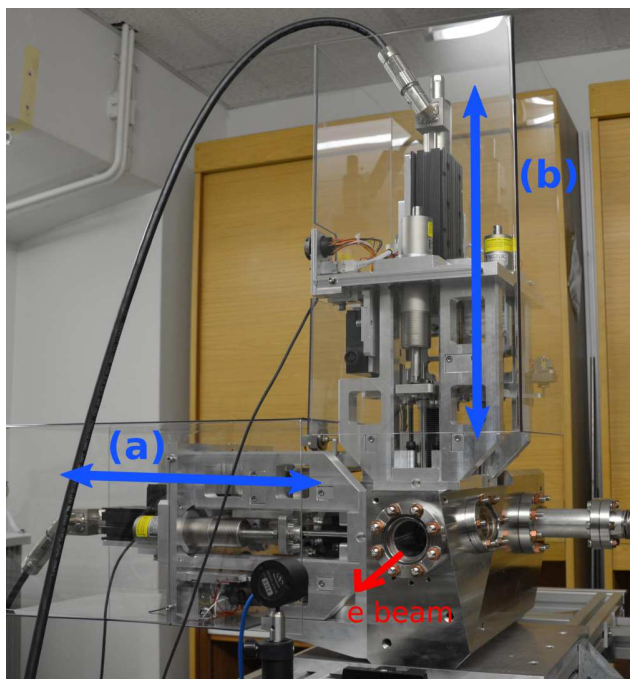

Figure 1: Mechanical Prototype station with horizontal (a) and vertical (b) motion unit.

Wire Scanner Forks

The wire scanner forks are made of titanium to improve the weight im comparison to steel by an comparable rigidity. From experience with former fork designs a lot of detailed improvements were made to ease wire assembly and adjustment. Five wires are installed in total to be able to use different wire thicknesses and to have spare wires. Three

ISBN 978-3-95450-141-0

VERTICAL BEAM SIZE MEASUREMENT AT CESRTA USING DIFFRACTION RADIATION

L. Bobb, JAI, Egham, Surrey, UK; DLS, Oxfordshire, UK
T. Aumeyr, P. Karataev, JAI, Egham, Surrey; Royal Holloway, University of London, Surrey, UK
E. Bravin, T. Lefevre, S. Mazzoni, H. Schmickler, CERN, Geneva, Switzerland
M. Billing, J. Conway, Cornell University, CLASSE, Ithaca, NY, USA

Abstract

Over recent years the first Diffraction Radiation (DR) beam size monitor has been tested on a circular machine. At CesrTA, Cornell University, USA, the sensitivity and limitations of the DR monitor for vertical beam size measurement has been investigated. DR emitted from 1 and 0.5 mm target apertures was observed at 400 and 600 nm wavelengths. In addition, interference between the DR signals emitted by the target and mask has been observed. In this report, we present the recent observations and discuss areas for improvement.

INTRODUCTION

Diffraction Radiation (DR) describes photons which are emitted when a charged particle passes through a target aperture. In this case the charged particle does not intersect the boundary of the medium but interacts with the medium via its electric field. The field of the charged particle excites atomic electrons of the medium. Polarisation currents are produced which are accompanied by the emission of electromagnetic waves called diffraction radiation [1].

The DR spectral angular distribution can be calculated using Eq. 1 where the wave number is defined as $k = 2\pi/\lambda$ and $E_{x,y}$ are the polarisation components of the radiation integrated over the target surface. The total field of the radiation is dependent on the incident charged particle field [1, 2].

$$\frac{d^2W}{d\omega d\Omega} = 4\pi^2 k^2 \left(|E_x|^2 + \left|E_y\right|^2\right) \tag{1}$$

The far-field zone defined by the far-field condition in Eq. 2 where L is the distance from the target to detector, γ is the Lorentz factor and λ is the DR wavelength [3] is the region at which the angular distribution of DR is observed. The prewave zone is the region near the target where the far-field condition is not satisfied.

$$L \gg \frac{\gamma^2 \lambda}{2\pi} \tag{2}$$

As shown in Fig. 1, DR is emitted in two directions. Forward Diffraction Radiation (FDR) is emitted in the direction of the charged particle trajectory. Backward Diffraction Radiation (BDR) is emitted in the direction of specular reflection relative to the incident charged particle trajectory and the target tilt angle θ_0. For high energy beams the emission of DR is considered to be non-invasive. The energy loss of the charged particles to DR is much less than the energy of the fast moving charged particle. For this reason the particle velocity can be treated as constant to a good accuracy [1] and DR, particularly BDR, can be used for non-invasive beam diagnostics.

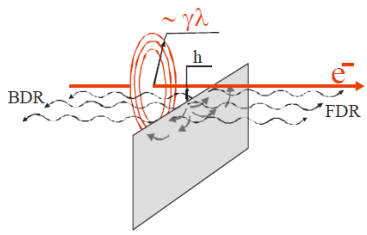

Figure 1: Schematic of DR emission from a particle moving in the vicinity of a medium where $\gamma\lambda$ is the effective electric field radius and h is the impact parameter [2].

EXPERIMENT SET-UP

The DR monitor is located in the L3 straight section of CesrTA (see Fig. 2). The X-ray beam size monitor (xBSM) [5] located at the CHESS synchrotron radiation (SR) station is used to measure the vertical beam size σ_y. The visible beam size monitor (vBSM) [6] located in L3 approximately 10 m upstream of the DR target is used to measure the horizontal beam size σ_x [7, 8].

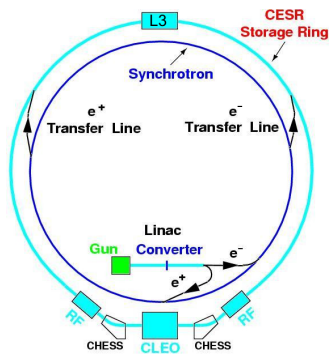

Figure 2: Layout of CesrTA [4].

An overview of the DR tank is shown in Fig. 3. Inside the tank the target is attached to a mechanism with two degrees of freedom: translation IN/OUT and rotation about this axis. DR escapes from the DR tank via a viewport at the top which is connected to the optical system.

In Fig. 4 a schematic and photograph of the optical system are shown. The optical system is a dual purpose system providing direct imaging of the target surface using the achromat

ISBN 978-3-95450-141-0

STATUS OF AND FUTURE PLANS FOR THE CERN LINAC4 EMITTANCE METER BASED ON LASER ELECTRON-DETACHMENT AND A DIAMOND STRIP-DETECTOR

T. Hofmann*, E. Bravin, U. Raich, F. Roncarolo, F. Zocca, CERN, Geneva, Switzerland
S. Gibson, K.O. Kruchinin, A. Bosco, G. Boorman
John Adams Institute at Royal Holloway, University of London, Egham, United Kingdom
E. Griesmayer, CIVIDEC Instrumentation, Vienna, Austria

Abstract

LINAC4 has started its staged commissioning at CERN. After completion it will accelerate high brightness H^- beams to 160 MeV. To measure the transverse profile and emittance of the beam, a non-destructive method based on electron photo-detachment is proposed, using a pulsed, fibre-coupled laser to strip electrons from the H^- ions. The laser can be focused and scanned through the H^- beam, acting like a conventional slit. A downstream dipole separates the neutral H^0 beamlet, created by the laser interaction, from the main H^- beam, so that it can be measured by a diamond strip-detector. Combining the H^0 beamlet profiles with the laser position allows the transverse emittance to be reconstructed. A prototype of this instrument was tested while commissioning the LINAC4 at 3 and 12 MeV. In this paper we shall describe the experimental setup, challenges and results of the measurements, and also address the characteristics and performance of the diamond strip-detector subsystem. In addition, the proposal for a permanent system at 160 MeV, including an electron detector for a direct profile measurement, will be presented.

INTRODUCTION

In the context of the High-Luminosity upgrade of the LHC (HL-LHC), CERN needs to upgrade its LHC injector chain, to deliver higher brightness beams. LINAC4 will replace the ageing LINAC2, the first injector in the chain, aiming to accelerate H^- ions from 45 keV at the source front-end to 160 MeV at the injection into the PS-Booster (PSB). Using a H^- beam makes injection via the charge-exchange scheme into the PSB possible [1]. With the brightness of the PSB proton beam is expected to double with respect to the present configuration based on protons injected at 50 MeV from LINAC2.

The transverse emittance has to be measured precisely at the machine's top-energy of 160 MeV. It is not possible to do so with a conventional slit & grid method as at this energy the H^- ions will travel through any possible slit material. Other methods, such as three-profile measurement, can be heavily influenced by space-charge effects while the secondary emission monitors typically used for this cannot handle the nominal LINAC4 pulse length of 400 µs.

To overcome these problems, a non-destructive method based on laserwire technology was proposed [2]. A pulsed laser with a peak power of about 1 kW can be focused to a diameter of less than 200 µm in the interaction region with the H^- beam. Since the outer electron of the H^- is very weakly boundeded to the atom, it can easily be stripped by a low energy photon [3]. Having neutralized a slice of the H^- beam, the H^0 move straight forward to a detector while the H^- are deflected by a bending magnet between the laser and the H^0 detector. By scanning the laser beam across the H^- beam, the H^0 profiles measured can be used to reconstruct the transverse emittance. Figure 1 shows the prototype setup that has been developed for tests during the LINAC4 commissioning at 3 and 12 MeV.

EXPECTED SIGNAL AND BACKGROUND

The H^0 background is expected to be dominated by H^- stripping upstream due to collisions with residual gas atoms particularly where the laser H^- interaction region is not preceded by a dipole magnet. This has been simulated in order to estimate the signal to background ratio at the H^0 detector. The simulation results are shown in Table 1 for different beam energies (3 and 12 MeV during commissioning and 160 MeV for the final system). The signal values are calculated assuming a laser pulse with an energy of 67 µJ when crossing the center of the H^- beam and a diamond strip detector with an area of 18 mm x 3.5 mm, used to integrate the arriving H^0 . The signal variation for different energies comes from the different time of flight of the H^- in the laser light (the slower the H^- the larger the stripping for similar stripping cross-sections) and the varying H^- beam sizes at different energies. The reduction of the background for increasing energy follows from the lower expected rest gas concentration. More details can be found in [2].

Table 1: Comparison of Simulation Results for Signal and Background in Different Commissioning Stages

H^- Beam Energy [MeV]	3	12	160
Laser Stripped [H^0 / ns]	1549	408	2400
Background [H^0 / ns]	105	69	67
SNR	**14.7**	**5.9**	**35.8**

* thomas.hofmann@cern.ch

ISBN 978-3-95450-141-0

CERN-SPS WIRE SCANNER IMPEDANCE AND WIRE HEATING STUDIES

E. Piselli, O. E. Berrig, F. Caspers, B. Dehning, J. Emery, M. Hamani, J. Kuczerowski, B. Salvant, R. Sautier, R. Veness, C. Vuitton, C. Zannini,
CERN, Geneva, Switzerland

Abstract

This article describes a study performed on one of the CERN-SPS vertical rotational wire scanners in order to investigate the breakage of the wire, which occurred on several occasions during operation in 2012. The thermionic emission current of the wire was measured to evaluate temperature changes, and was observed to rise significantly as the wire approached the ultimate LHC beam in the SPS, indicating the possibility of strong coupling between the beam's electromagnetic field and the wire. Different laboratory measurements, complemented by CST Microwave Studio simulations, have therefore been performed to try and understand the RF modes responsible for this heating. These results are presented here, along with the subsequent modifications adopted on all of the operational SPS wire scanners.

INTRODUCTION

Beam Wire Scanners (BWS) are instruments used for precise transvere profile measurements in the LHC and its injector chain.

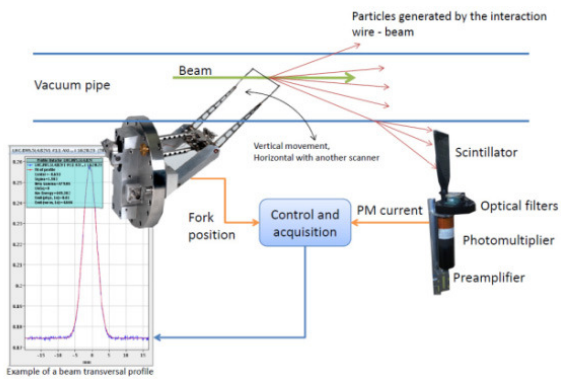

Figure 1: BWS working principle.

During the scan, a thin carbon wire is moved through the beam, with the interaction of beam and wire generating a cascade of secondary particles. For a high energy primary beam these secondary particles are energetic enough to exit the vacuum chamber and can be detected by a scintillator/photomultiplier assembly. With appropriate settings the amplitude of the light produced by the scintillator is proportional to the intercepted beam intensity (Fig. 1).

As the scitillator/photomultiplier signal is fast compared to the revolution frequency, synchronising the acquisition of the wire position and the measured light intensity allows the transverse beam profile to be reconstructed as the wire moves across the beam over multiple turns.

The CERN-SPS is equipped with 6 rotating BWS fitted with a carbon wire of 30µm diameter and which can scan at a maximum speed of 6 ms^{-1}.

SPS WIRE BREAKAGE MECHANISMS

The CERN-SPS rotational wire-scanners are used on a regular basis by machine operators to perform beam size measurements to verify and optimise the beam emittance.

During the run in 2012, there were many more abnormal wire breakages during the use of these scanners compared to previous years. Table 1 summarize these failures. Since the SPS machine was being pushed to provide high intensity beams for LHC, the first suspected cause of these events was due to these higher intensites, as had previously been observed in the high intensity run of 2002 [1]. During this 2002 run, there were observations of a large current induced in the wire, leading to wire breakage, when the scanning fork was in its parking position. This was finally explained by radio-frequency (RF) modes developing in the scanner tanks with the wire acting as an antenna. This was though to be solved by the addition of ferrites to the scanner tanks to damp these modes.

Table 1: BWS SPS Wire Failures During in 2012

Scanner	Beam induced failures	Mechanical failures
416.H	0	0
416.V	2	0
519.H	1	2
519.V	1	0

To try and understand the failures of 2012, the evolution of the wire current of one of the first breakage event observed was plotted as function of the time. Fig. 2 shows four consecutive wire-scans for vertical scanner 416, one before, one during and 2 after wire failure. The first two clearly indicate a current increase in the wire as the wire approaches and then crosses the beam (at 0.008 s as can be seen on the corresponding profile measurements). A current as high as 12 mA is observed when the wire has passed the beam and is close to its IN position. The wire breakage occurs during the second wire-scan (shown in blue). It can be seen that the

METHODS FOR MEASURING THE TRANSVERSE BEAM PROFILE IN THE ESS HIGH INTENSITY BEAM

C. Roose*†, I. Dolenc Kittelmann, A. Jansson
European Spallation Source AB (ESS), Lund, Sweden

Abstract

The European Spallation Source (ESS), currently under construction, consists of a partly superconducting linac which will deliver a 2 GeV, 5 MW proton beam to a rotating tungsten target. Beam transverse profile monitors are required in order to insure that the lattice parameters are set and the beam emittance is matched. Due to the high intensity of the beam and the constraint to perform non-disturbing measurements, non-invasive techniques have to be developed. The non-invasive profile monitors chosen for the ESS are based on the interaction of the beam with the residual gas. Two different devices are developed, one utilises the fluorescence process, the other one the ionisation process. The paper presents their latest preliminary developments.

INTRODUCTION

The ESS [1] is a multi-disciplinary research centre based on the world's most powerful neutron source. With an average flux of 1.6×10^{15} neutron cm^{-2} s^{-1} and a peak flux of 40×10^{15} neutron cm^{-2} s^{-1}, ESS will be around 30 times brighter than today's leading facilities. The spallation will occur by bombarding a tungsten target with protons accelerated by a linac up to 2 GeV with an average power of 5 MW. The ESS accelerator, illustrated in Fig. 1, consists of:

- an ECR source which will produce 75 keV protons,
- a warm linac part consisting of a Low Energy Beam Transport line (LEBT), a Radio Frequency Quadrupole (RFQ), a Medium Energy Beam Transport line (MEBT) and a Drift Tube Linac section (DTL), which will accelerate the protons up to 90 MeV,
- a cold linac part, made of a spokes section and elliptical cavities (called Medium β and High β) which will accelerate the protons up to 2 GeV,
- a High Energy Beam Transport line (HEBT) and an upgrade part which transports the beam to the target.

The linac will create a pulsed beam with an average pulse current of 62.5 mA, pulse duration of 2.82 ms and repetition rate of 14 Hz.

In beam diagnostics, it is important to measure the beam transverse profile in order to insure that the lattice parameters are set properly and the beam emittance is matched. Two different kinds of devices are currently been designed [2, 3] for the ESS linac, an invasive and a non-invasive one, which will both be located in the same module. The invasive device will be a wire scanner [4] and will be used during the commissioning at low beam current and short pulse. However the invasive system would get damaged by the beam at its full power, therefore the non-invasive profile monitors are being developed as well in order to provide the profile information without disturbing the beam during normal operation.

NON-INVASIVE TRANSVERSE PROFILE MONITORS

The ESS Non-invasive transverse Profile Monitors (NPMs) [5] are based on the interaction processes between the proton beam and the vacuum chamber residual gas, primarily composed of H_2 (65-80%) and the rest being a mixture of CO, CO_2, CH_4, Ar and H_2O. They exploit the secondary excited/ionised particles produced by these interactions to reproduce the transverse profile. For the ESS linac, two designs are being developed. The main parameters influencing the design are the residual gas pressure in the vacuum chamber, the excitation/ionisation cross sections between the primary proton beam and the hydrogen molecules and the space allocated for the devices.

In the warm linac and HEBT, Beam Induced Fluorescence monitors (BIFs) will be used. While the cold linac will host Ionization Profile Monitors (IPMs). The position and the number of the NPMs along the whole linac are showed in Fig. 1. Both technologies are already well developed by others facilities [6–9] however they have to be adapted to the ESS main constraints i.e. the beam intensity, the H_2 residual gas and the radiation level.

BEAM INDUCED FLUORESCENCE PROFILE MONITOR

In the warm linac, the main constraint is the 10 cm available space for the NPM. The BIF monitor [10], based on the fluorescence emission of the excited residual gas, is a good choice to that issue as both horizontal and vertical profile measurements can be performed at the same place. Furthermore, its optical design is quite simple and can be easily changed, since all the device components, except for the beam pipe viewport, are outside the beam pipe.

For this monitor, the major worries are the light yield level and the optical design. If the first question will be partially answered below, the second has still to be addressed as it is strongly depended on the ambient radiation levels which still have to be studied.

Fluorescence Light Yield

As previously said, the residual gas present in the beam pipe is expected to be composed of 65-80 % of H_2. In the warm linac and the upgrade part, the pressure is expected

* charlotte.roose@esss.se
† Marie Curie Fellow oPAC Project

ISBN 978-3-95450-141-0

DESIGN OF A PROFILE MONITOR WITH 12 INCHES OF ACTUATION FOR FRIB*

S. Rodriguez#, G. Kiupel, I. Nesterenko, D. Sattler FRIB, Michigan, USA

Abstract

Actuated diagnostics present additional challenges that static diagnostics devices do not such as alignment, stability, and incorporating an appropriate drive mechanism. These challenges become even more apparent as the actuaded length increases. At the Facility for Rare Isotope Beams (FRIB) we plan on using a number of actuated diagnostics devices including a Profile Monitor (AKA: Wire Scanner) with 12 inches of actuation. The Profile Monitor uses tungsten wires to traverse the beam pipe aperture to measure the beam intensity with respect to it's location in the X-Y plane. This paper will detail the design of the 12 inch Profile Monitor and how it is able to overcome the stability, alignment, and drive issues that come with the 12 inches of actuation.

INTRODUCTION

The FRIB beam line has three folding segments where the beam pipe increases to up to 6 inches in diameter. This profile monitor design scans the whole aperture while maintaining the fork outside the aperture at all times. Due to cross-talk between sense wires, these wires are typically separated such that only one wire is inside the beam pipe aperture at a time. Having a fork in this configuration scanning a 6 inch aperture would result in over 16 inches of stroke which is why the task has been separated into two separate profile monitors; one would scan the horizontal "X-axis" and the other would scan the vertical "Y-axis" as well as an additional axis 45° from the vertical axis. This paper focuses on the latter which results in a minimum stroke requirement of 11.39 inches.

*This material is based upon work supported by the U.S. Department of Energy Office of Science under Cooperative Agreement DE-SC0000661, the State of Michigan and Michigan State University. Michigan State University designs and establishes FRIB as a DOE Office of Science National User Facility in support of the mission of the Office of Nuclear Physics.

#rodrigus@frib.msu.edu

†Presently at Facility for Rare Isotope Beams, Michigan State University.

‡Presently at Department of Physics, University of Chicago.

DESIGN

FRIB first explored the idea of using an off-the-shelf mechanical feedthrough and it was low in cost. Upon testing a purchased unit, it was apparent that the actuator would wobble during its motion. This wobble is unacceptable to FRIB which is why a custom design was pursued.

Overall Design

The design of the Profile Monitor attempts to maintain all key components axially aligned so that the motion of actuation is as linear as possible. *Figure 1* shows the overall design of the profile monitor. Although shown in a horizontal position, this device gets mounted in a vertical orientation onto a 10-inch port of a vacuum vessel.

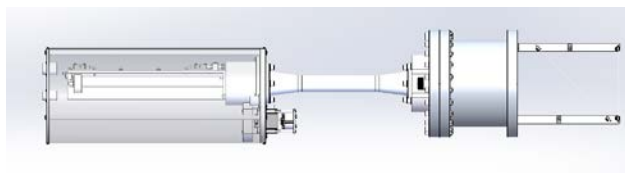

Figure 1: Overall Design.

The nipple in the front serves as a housing for the fork to retract into. This keeps the size of the vacuum vessel smaller as the flange to center distance is reduced. As it can be seen on *Figure 2*, many of the components have a piloting feature to maintain alignment.

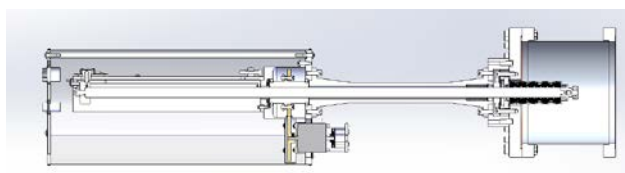

Figure 2: Section view of the profile monitor.

Fork

As previously mentioned, this fork utilizes two wires to scan the vertical axis and an axis at a 45° angle from the vertical axis. *Figure 3* shows the design of the fork.

Assuming that the first wire is tangent to the aperture of the beam pipe, and the second wire must fully traverse this 6-inch aperture, the total minimum stroke results in 11.39-inches.

ISBN 978-3-95450-141-0

DIAGNOSING NSLS-II: A NEW ADVANCED SYNCHROTRON LIGHT SOURCE*

Yong Hu#, Huijuan Xu, Om Singh, Leo Bob Dalesio, BNL, NSLS-II, NY 11973, U.S.A.

Abstract

NSLS-II, the successor to NSLS (National Synchrotron Light Source) at Brookhaven National Lab, is scheduled to be open to users worldwide by 2015 as a world-class advanced synchrotron light source because of its unique features: its half-mile-circumference (792 m) Storage Ring provides the highest beam intensity (500 mA) at medium-energy (3 GeV) with sub-nm-rad horizontal emittance (down to 0.5 nm-rad) and diffraction-limited vertical emittance at a wavelength of 1 Å (<8 pm-rad). As the eyes of NSLS-II accelerators to observe fascinating particle beams, beam diagnostics and controls systems are designed to monitor and diagnose the electron beam quality so that NSLS-II could be tuned up to reach its highest performance. The design and implementation of NSLS-II diagnostics and controls are described. Preliminary commissioning results of NSLS-II accelerators, including Linac, Booster, and Storage Ring, are presented.

INTRODUCTION

The construction of NSLS-II (NSLS-2) began in Mar. 2009. Three years later, preliminary Linac commissioning started in Mar. 2012. The Injector, which includes Linac, Booster and transfer-lines in between, has been successfully commissioned by Feb. 2014. The Storage Ring commissioning is on going and in good progress -- 50 mA stored beam was achieved in July 2014. When the whole machine is fully commissioned and tuned up, NSLS-II will be the most advanced third-generation light source in terms of the following parameters:

1) The lowest horizontal emittance at 0.5nm-rad;
2) The smallest beam size at ~3um;
3) The highest beam current (intensity) at 500mA;
4) The highest photon spectral brightness due to the lowest emittance, the smallest beam size, and the highest beam current as stated above.

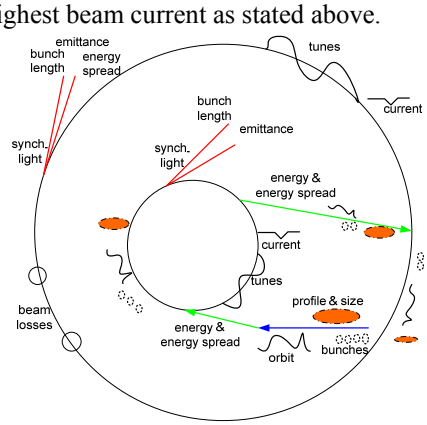

Figure 1: Beam Parameters Measured at NSLS-II.

Machine commissioning and tuning up is all about diagnosing. To achieve the exceptional performance of NSLS-II, beam diagnostics and control systems are designed to monitor and diagnose the electron beam of NSLS-II accelerator complex. Diagnosing NSLS-II means measuring a variety of beam parameters (~10 types), including beam charge/current, filling pattern, beam position/orbit, beam size/profile, energy spread, tunes, emittance, bunch length, beam losses, etc., via a variety of beam monitors (~16 types, ~370 total device counts as shown in Table 1 below) distributed around the whole machine. Figure 1 briefly shows how the NSLS-II accelerators are diagnosed, i.e. what kind of beam parameters is measured from Linac to Storage Ring.

Effective diagnosing of NSLS-II accelerator depends on the effective combinations of a variety of beam monitors, control and data acquisitions (DAQ), and high level physics applications. Figure 2 shows how beam instrumentation, controls, and physics work together to diagnose the NSLS-II machine.

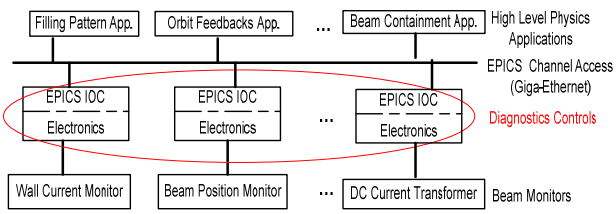

Figure 2: NSLS-II diagnostics and control architecture.

BEAM MONITORS AND SUBSYSTEMS

NSLS-II accelerators consist of one Injector and one Storage Ring (SR). According to the functionality as well as geographical distribution, the Injector is divided into 4 sub-accelerators: Linac, Linac to Booster (LtB) transfer line (including 2 beam dumps), Booster, Booster to Storage ring (BtS) transfer line (including 1 beam dump). Table 1 gives a summary of the beam monitors distributed over the whole machine.

From system functionality and application point of view, the variety of beam monitors as shown in Table 1 could be classified into a few subsystems such as beam position monitor (BPM), filling pattern (Wall Current Monitor, Fast Current Transformer), beam intensity (Integrating Current Transformer, DC Current Transformer), loss control and monitoring (Beam Loss Monitor, Scraper), beam profile (Screen, Visible Light Monitor, Streak camera), tunes, etc., as shown in Figure3.

*Work supported by DOE contract No: DE-AC02-98CH10886
#yhu@bnl.gov

ISBN 978-3-95450-141-0

SIMULTANEOUS OPERATION OF TWO UNDULATOR BEAMLINES AT FLASH

S. Ackermann*, V. Ayvazyan, B. Faatz, E. Hass, K. Klose, S. Pfeiffer, M. Scholz, S. Schreiber
Deutsches Elektronen-Synchrotron (DESY), Hamburg, Germany

Abstract

In the last few years, first tests have been performed to show that two FLASH undulator lines can deliver FEL radiation simultaneously to users with a large variety of parameters, such as radiation wavelength, pulse duration, intra-bunch spacing etc. In order to achieve this, FLASH has the possibility to have two injector lasers on the cathode of the gun with different parameters, and the accelerator can vary gradient and phase within one RF-pulse to guarantee optimal performance for both beamlines. In this contribution, we show the flexibility which can be achieved with this system.

INTRODUCTION

FLASH, the free-electron laser at DESY in Germany has been in operation as a user facility since summer 2005 [1]. Since then, the request for beamtime has been growing steadily over the years, with a factor of 4 overbooking in the recent user periods. A description of the FLASH facility can be found in Ref. [2].

In order to meet the increased demand, a study started in 2006 to look at the feasibility to add an undulator line to the existing accelerator. In order to double the beamtime, both users would need the 10 Hz repetition rate. A fast kicker in combination with a DC septum is used to deflect the beam into the second undulator line. In addition, the large variety in beam parameters should be possible at both beamlines independently in order to ensure a maximum flexibility in planning of the beamtime. For this reason, it was decided to use two cathode lasers, each with its own bunch train. A variable delay between the two lasers within the RF pulse of gun and modules ensures that the two users get their own set of parameters. In addition, the start time of kicker pulse is shifted with the start time of the laser pulse and the RF-phase and amplitude of gun and each of the modules can be tuned for optimal conditions for both users.

The layout of the facility including the new beamline is described in Ref. [2] and shown in Fig. 1. In addition to a new undulator line with variable gap undulators, a new experimental hall has been built which has space for an additional 5 to 7 experimental stations. In Table 1, the parameters expected for FLASH2 are shown. They are similar to those for FLASH with the exception of the energy spread, which is increased due to coherent synchrotron radiation and the large separation angle of 12° [3, 4].

That the RF-system is able to handle the flexibility needed to compress the beam independently for FLASH1 and FLASH2 has already been presented earlier [5]. Also the fast kicker system has been tested and is behaving according to specifications. What we want to present in this paper is that we are able to get two independent bunch trains to radiate with different charges and a variable delay in time.

Table 1: Expected Parameters for FLASH2

Electron Beam	**Value**
Energy Range	0.5 – 1.25 GeV
Peak Current	2.5 kA
Bunch Charge	0.02 - 1 nC
Normalized Emittance	1.4 mm mrad
Energy Spread	0.5 MeV
Average β-function	6 m
Rep. rate	10 Hz
Bunch separation	1-25 µs
Undulator	**Value**
Period	31.4 mm
K	0.5 - 2
Segment length	2.5 m
Number of segments	12
Photon Beam SASE	**Value**
Wavelength range (fundamental)	4 - 60 nm
Average single pulse energy	1 - 500 µJ
Pulse duration (FWHM)	10 - 200 fs
Peak power (from av.)	1 - 5 GW
Spectral width (FWHM)	≈ 0.5 - 2 %
Peak Brilliance	10^{28} - 10^{31} B

SIMULTANEOUS OPERATION OF FLASH1 AND FLASH2.

User demands vary in almost all respects. A significant increase in beam time can only be achieved, if the parameters between the two undulator lines can be varied independently. For the wavelength, this is clear and straightforward. For other parameters, such as the bunch length, this is not so trivial. Figure 2 shows, how the bunch length was varied by varying the charge. The measurements were performed with a standard diagnostics implemented in FLASH1 and foreseen for FLASH2 [6, 7].

The next tests show the possibility to produce SASE for different parameters. For these tests, only RF parameters were changed within the RF-pulse and orbit was adjusted behind the FLASH2 extraction point. Because the FLASH2 beam line was under construction, the tests presented in this section were all performed at FLASH1. This means, that a certain freedom, which one normally has for lasing with two pulse trains, such as adjustment of orbit and optics in the part of the machine which the beamlines do not have in common, is not available for these tests.

* sven.ackermann@desy.de

ISBN 978-3-95450-141-0

SIMULATION AND FIRST RESULTS OF THE ELBE SRF GUN II

P. Lu, H. Vennekate, HZDR & TU Dresden, Germany
A. Arnold, U. Lehnert, P. Murcek, J. Teichert, R. Xiang, HZDR, Germany

Abstract

Recently a new SRF gun has been installed at HZDR, which is named of ELBE SRF Gun II. Stable operation at 8 MV/m RF Gradient has been achieved. The energy and energy spread have been measured for different laser phases. And the results are compared with the beam simulations in this publication. The minimum energy spread is 10 keV at a laser phase of 50°, this is true for both simulation and measurement. In addition, the phase space has been measured and compared to simulation. The determined transverse emittance is in the order of 0.4 µm.

At present the bunch charge is less than 1 pC generated by a bare cooper cathode, which has been installed for first tests of the SRF cavity. In future, the installed UV laser is planned to be operated in either the 13 MHz mode or the 500 kHz mode. The bunch charge will be respectively 77 pC or 1 nC. A simulation based study is in progress, aiming to look for the according "high bunch charge" parameters of the gun and an optimization of the beam transport to the ELBE accelerator.

The code packages ASTRA and elegant are combined in a Labview interface to perform the simulation studies. A 1D model, including space charge effect, is applied to the electron emission and the low energy beam transport in ASTRA. From the exit of the gun cavity, elegant takes charge of the beam transport simulation in the ELBE accelerator. The requirement for the SRF gun to realize 1 nC operation mode is discussed.

INTRODUCTION

ELBE SRF Gun II

The ELBE (Electron Linac with high Brilliance and low Emittance) SRF Gun II [1]has been set up at Helmholtz-Zentrum Dresden-Rossendorf (HZDR) in May 2014. This SRF Gun is an improved version of the ELBE SRF Gun I [2] with a fine grain 3½-cell Nb cavity for realizing higher beam energy up to 9 MeV , and a superconducting solenoid for an improvement in emittance compensation [3]. Figure 1 shows the section view of the gun cryostat.

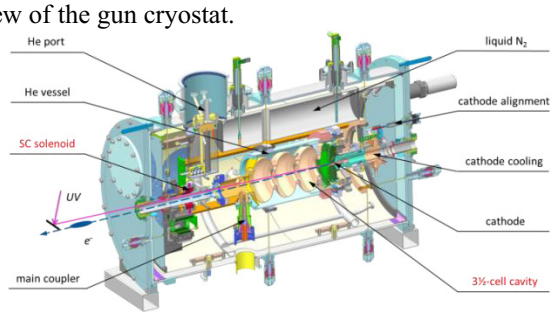

Figure 1: construction of the ELBE SRF Gun II.

The standard material for the gun cathodes is Cs_2Te[4], which has been used in the ELBE SRF Gun I. In this paper all measurement results are from a copper cathode, which has been installed for the current commissioning phase. New Cs_2Te cathodes are under preparation and will replace the copper cathode in the near future.

Compared to the old cavity, the new Niobium SRF cavity generates higher fields at the cathode position in the half-cell. This feature reduces the range of the space charge effect dominated region for low energy bunches near the cathode. Furthermore, the reduced power dissipation on the cavity wall is another improvement, which allows higher gradients in the superconducting cavity at similar helium consumption.

A 258 nm UV laser is used to excite electrons from the cathode cooled by liquid Nitrogen. The laser parameters have serious impacts on the gun's behavior. The synchronization between the laser and the RF generation, characterized by the laser phase, influences both the energy gain of the beam and the emittance. The initial structure of the extracted bunch is directly determined by the laser pulse shape itself. A uniformly distributed, large laser spot is expected to exploit the quantum efficiency of the cathode. Meanwhile for a certain bunch charge, a larger laser spot results in a reduced space charge effect. This direct dependency of the beam quality on the laser spot size could be reproduced by the simulations.

Beam Transport

Electron bunches from the ELBE SRF Gun II are supposed to be transported through a dogleg beam line and into the linac beam line of the ELBE, which is primarily designed for a thermionic gun. Therefore, it is necessary to simulate the entire beam transport to get the optimized parameters for this particular setup.

The longitudinal phase space can be manipulated by two accelerator modules and two chicanes. The beam should be focused longitudinally at the final target position and kept defocused in transport to reduce the space charge effect. Since the longitudinal elements also have a significant influence on the transverse beam parameters, they have to be optimized first. Proceeding on the basis of fixed cavity phases and chicane bending angles, transverse elements like a super conducting solenoid and in total 35 quadrupoles can be used to achieve the desired transverse phase space.

The bunch emission from the cathode and the acceleration in the gun are simulated with ASTRA, and further beam transport is computed using elegant[5]. The Coherent Synchrotron Radiation (CSR) effect[6] in the bending magnets, as well as the following short drifts, and the Longitudinal Space Charge (LSC) effect[7] in other

ISBN 978-3-95450-141-0

BEAM DIAGNOSTICS AND TIMING MONITORING FOR SUPERKEKB INJECTOR LINAC

F. Miyahara#, K. Furukawa, R. Ichimiya, N. Iida, M. Ikeno, H. Kaji, M. Satoh, M. Shoji, T. Suwada, M. Tanaka, Y. Yano, KEK, Tsukuba, Ibaraki, Japan
T. Okazaki, EJIT, Tsuchiura, Ibaraki, Japan

Abstract

The KEK e^+/e^- linac has multiple operation modes for the electron beam injection into three rings, the SuperKEKB HER (High Energy Ring), PF (Photon Factory) Ring and PF-AR, and the positron beam injection into the damping ring (DR) and the SuperKEKB LER (Low Energy Ring). The operation modes can be switched every 20 millisecond, repetition rate of 50 Hz, with arbitrary order. The beam parameters such as charges, energies are different for each of the rings. Moreover, the bunch charges of the electron beam for HER, 5nC, is 5 times higher and the transverse emittance of ~10 mm mrad is 30 times lower than those of the KEKB injector.

Thus, the development for the BPM readout system with a wide dynamic range, the installation of optical fiber detectors with a good S/N ratio for the wire scanners and bunch-length monitor have been performed. For stable operation of the linac, many timing signals have to be monitored as well. To that end we have developed 32-bit multi-hit time-to-digital converters (TDCs) with 1-ns resolution. The first beam tests of those systems are reported.

COMPONENTS OF THE LINAC

The SuperKEKB injector linac is under development to achieve the required performance [1]. The layout of the linac with energy evolution from downstream of the 180-degree arc for each operation modes is shown in Fig. 1. The linac consists of eight sectors (A – C, 1 – 5). Each sector has eight accelerating units except for sector A, 1, and 4. The black square represents an accelerating unit which provides an average energy gain of 160 MeV. In sector A, a new photocathode RF gun designed to obtain high charge (5 nC) and low emittance (10 mm mrad) electron beam [2-3] is set on beginning of the sector. The linac also has a conventional thermionic gun which is dedicated to PF/AR in sector 3. Thus, electron source for PR/AR rings can be exchange. A magnetic chicane to give an energy chirp for bunch compression in the arc section and a diagnostic beamline are located on downstream of the RF gun.

A new positron source which consists of a tungsten target with a 2-mm diameter beamline-centered hole for electron, a beam spoiler, a flux-concentrator and six large-aperture S-band (LAS) accelerating structures inside DC solenoids have been installed in sector 1 [4,5]. In case of beam injection to PF or HER, the electron beam goes through the hole of the target. To obtain positron beam, an electron/positron separator chicane has been installed at downstream of the last LAS accelerating structure. To reduce the geometric emittance down to 41(horizontal)/2(vertical) nm, the positron beam injected to the damping [6] is stored 40 ms, the store time depends on the injection rate, then return to the linac. Thus, trigger timing of upstream (sector A – 2) and downstream (sector 3 - 5) for the RF system and the BPMs will be controlled independently [7].

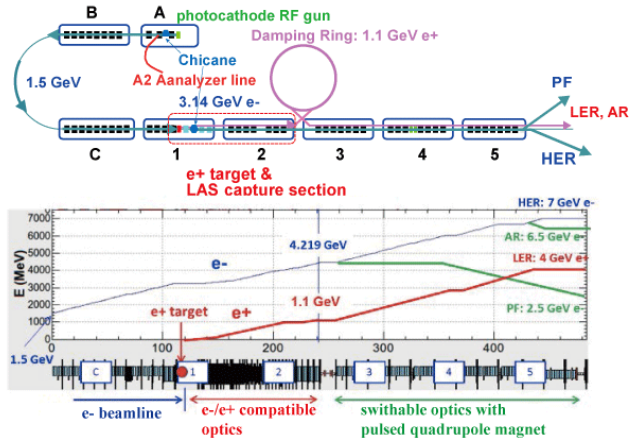

Figure 1: Schematic layout of the linac and energy-evolution patterns for each operation mode.

MONITORING SYSTEM

The beam positions and charges are monitored by stripline BPM. There are more than 90 BPMs and 23 oscilloscopes for fast BPM data acquisition (DAQ) system [8]. The position resolution of the BPM system is about 50 μm. To achieve emittance preservation of high bunch charges of 5 nC electron beam, the alignment error of 0.1 mm for each section and a dedicated orbit correction are required. These specifications require less than 10 μm position resolution for the BPM, but current DAQ system does not satisfy it. Then, we have been developed a VME-based readout system. The position resolution of 3 μm was achieved that was measured on the basis of 3-BPM method in the linac [9]. To measure the beam size and emittance, Al_2O_3 ceramic screen (30 μm thick) is set in the vacuum chamber at the chicane downstream of the gun, 4 sets of four successive wire

#fusashi.miyahara@kek.jp

ISBN 978-3-95450-141-0

DIAGNOSTICS OF THE TPS BOOSTER SYNCHROTRON FOR BEAM COMMISSIONING

C. H. Huang, C. Y. Liao, Y.S. Cheng, Demi Lee, P. C. Chiu, C. Y. Wu, S. Y. Hsu, K. H. Hu, Jenny Chen, C. H. Kuo, K. T. Hsu
NSRRC, Hsinchu 30076, Taiwan

Abstract

Booster synchrotron for the Taiwan photon source project is in commissioning. Diagnostics which consist of screen monitors, intensity monitors, beam position monitors, tune monitors, visible light synchrotron radiation monitors and radiation-sensing field-effect transistors are integrated with accelerator control system. Integration and functionality check were done recently. Details of these diagnostics and preliminary test results will be summarized in this report.

INTRODUTION

Taiwan Photon Source (TPS) is a low emittance, third-generation light source in NSRRC [1]. It consists of a 150 MeV S-band linac, linac to booster transfer line, 0.15 to 3 GeV booster ring, booster to storage ring transfer line, and 3 GeV storage ring. The booster has 6 FODO cells which include 7 BD dipoles with 1.6 m long and 2 BH dipoles with 0.8 m long in each cell. Its circumference is 496.8 meters and it is concentric with the storage ring in the same tunnel. The radio frequency is 500 MHz with 828 harmonic numbers. The ramping repetition rate is 3 Hz which is locked with the frequency of the power system. Preliminary commissioning of the booster synchrotron is being proceeded and it shares some windows for installation and system-integrated test from mid-August 2014. Diagnostics which equips in booster to help the beam commission will be described in the report, and preliminary results will be summarized as well.

DIAGNOSTIC DEVICES IN THE BOOSTER

There are seven screen monitors in the booster ring to monitor the beam profile and beam position, shown in Fig. 1. The average beam current is measured with a Bergoz's new parametric current transformer (NPCT) and the pulse current is observed by a fast current transformer (FCT). Sixty beam position monitors (BPMs) can be used to measure beam position and rough beam intensity along the longitudinal position. For the tune monitor, the beam is shaken by stripline electrodes or a magnetic shaker using narrow band white noise; the beam motion signal is picked up by BPMs. Two visible light synchrotron radiation monitors (SRMs) are used to measure the synchrotron radiation profile. They are set up in the opposite side of the booster with a camera inside the tunnel and one outside the tunnel. In order to investigate applicable of radiation-sensing field-effect transistors (RadFETs) for measuring the local beam loss, several RadFETs are installed at the injection area of the booster ring.

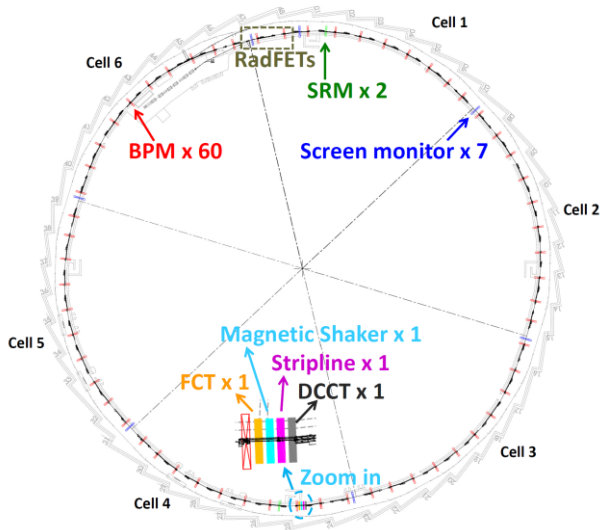

Figure 1: The layout of the diagnostic devices in the booster ring.

SCREEN MONITOR

Seven screen monitors are designed in the beginning of six cells of the booster and behind the 1st DB dipole of the 1st cell for booster commissioning. The screen monitor assembly consists of a hollow tube, a Yag:Ce screen with 25 mm in diameter and 0.5 mm in thickness. The YAG:Ce screen is mounted at 45° angle in one side to intercept the beam. A vacuum-sealed window is in the other end of the tube to extract the light. A CCD camera is mounted at a supporting tube with LEDs installed beside the CCD camera for illumination. A pneumatic device is used to move the whole assembly in or out. All of these devices are controlled remotely including the on/off of the LED. The structure of the screen monitor assembly is shown in Fig. 2. The power over Ethernet (PoE) switches are used to connect the cameras and uplink to the vision system in the input / output controller (IOC) of the experimental physics and industrial control system (EPICS) [2]. The IOC is constructed based on Linux operating system with areaDetector EPICS module and a compiled Matlab analysis program is used as a graphical user interface, shown in Fig. 3. The camera trigger comes from TPS timing system. Exposure time and camera gain are adjustable to meet various beam conditions. This scheme is simpler than the complicated attenuator design.

ISBN 978-3-95450-141-0

OVERVIEW OF BEAM INSTRUMENTATION ACTIVITIES FOR SwissFEL

R. Ischebeck, R. Abela, V. Arsov, R. Baldinger, H. Braun, M. Calvi, R. Ditter, C. Erny, F. Frei, R. Ganter, S. Hunziker, Y. Ivanisaenko, P. Juranić, B. Keil, W. Koprek, R. Kramert, D. Llorente Sancho, F. Löhl, F. Marcellini, G. Marinkovic, B. Monoszlai, G.L. Orlandi, C. Ozkan, L. Patthey, M. Pedrozzi, P. Pollet, M. Radovic, M. Roggli, M. Rohrer, V. Schlott, A. Stepanov, J. Stettler, PSI, Villigen, Switzerland
P. Peier, DESY, Hamburg, Germany
F. Ardana-Lamas, I. Gorgisyan, C.P. Hauri, L. Rivkin, EPFL, Lausanne & PSI, Villigen, Switzerland

Abstract

SwissFEL will provide users with brilliant X-ray pulses in 2017. A comprehensive suite of diagnostics is needed for the initial commissioning, for changes to the operating point, and for feedbacks. The development of instrumentation for SwissFEL is well underway, and solutions have been identified for most diagnostics systems. I will present here an overview of the instrumentation for SwissFEL, and give details on some recent developments.

INTRODUCTION

A comprehensive diagnostics suite has been designed to assist in the commissioning and operation of SwissFEL [1]. The normal-conducting accelerator will run at a repetition rate of 100 Hz, generating two electron bunches separated by 28 ns in each RF pulse. The bunch charge can be adjusted between 10 and 200 pC, depending on the operation mode. A significant effort has been put into designing instrumentation suitable for the low-charge mode, which generates the smallest signals in the pick-ups, but has the tightest tolerance goals.

Instrumentation for SwissFEL has been tested at the SwissFEL Injector Test Facility [2]. Detailed measurements demonstrate the suitability for the SwissFEL design parameters [3].

CHARGE MONITORS

For calibration of the FEL photon pulses, an absolute charge measurement accuracy of 1% is desired. We currently have two possibilities: 1) in-house developed BPMs; 2) Bergoz Turbo-ICT-2 with BCM-RF-2 readout electronics. The BPM is a highly sensitive but not a calibrated device. The charge related signals of the BPM still need to be calibrated. The Turbo-ICT-2 is a calibrated device. It is an upgrade of the Bergoz Turbo-ICT with 2-bunch resolving capability and can accomplish these requirements with negligible beam position and bunch length dependence. It is insensitive to dark current due to its fast readout of the beam induced current (3 ns) at higher bandwidth. The resolution of the Turbo-ICT-2 is comparable to that of the BPM at charges > 10 pC (Fig. 1). Hence, the ICTs can still be mounted with the BPMs in every dispersive section of the machine and used to calibrate the BPMs.

The second option for calibrating the BPMs is the Bergoz ICT with BCM-IHR readout electronics. This is a calibrated device that gives the total charge in an integration window of 5 µs and cannot resolve the two bunches at SwissFEL. It measures the total charge, including the dark current. The single-shot resolution of this device is 20 pC; however, it can be used to calibrate the BPMs by first measuring the dark current and subtracting this value from the total integrated charge, one bunch at a time, to ascertain the charge of a single bunch.

BEAM POSITION MONITORS

SwissFEL will use cavity beam position monitors (BPMs) to align the beam along the linac, and to measure the electron energy in dispersive sections [4]. The proper alignment of the beam is important to reduce emittance growth due to wake fields, and to ensure overlap of the electron bunch with the radiation in the undulators. The BPMs consist of dual-resonator cavities. The dipole cavity determines the position, while the monopole cavity is used as a charge reference measurement. This measured charge value is also used for other monitors that exhibit a strong bunch charge dependence, such as bunch compression monitors.

There will be three types of cavity BPMs in SwissFEL, taking into account vacuum chamber diameters of 38, 16, and 8 mm in the gun, the linac and the undulator lines, respectively. For the cavities designed for a vacuum chamber diameter of 38 and 16 mm, a frequency of 3.3 GHz and a low quality factor of about 40 was chosen to minimize the crosstalk between the two bunches separated by 28 ns. The BPMs with 8 mm diameter will be deployed in the undulator lines, where only single bunches will be present in each RF pulse. For this reason, a higher quality factor will be chosen.

The resolution of the BPMs has been determined by comparing the measurements of several monitors installed in series. The residual of the SwissFEL cavity BPM (BPM16) is 0.8 µm rms for a 0.35 mm beam offset (Fig. 2).

BUNCH ARRIVAL MONITORS

Two bunch arrival monitors (BAMs) have been commissioned in the SwissFEL Injector Test Facility [5]. The first BAM upstream of the bunch compressor (FINXB-DBAM10) was commissioned in 2012. Two pick-ups were used there

ISBN 978-3-95450-141-0

RHIC p-CARBON POLARIMETER TARGET LIFETIME ISSUE*

H. Huang, I.G. Alekseev, E. Aschenauer, G. Atoian, A. Basilevsky, K.O. Eyser, A. Fernando, D. Gassner, D. Kalinkin, J. Kewisch, G. Mahler, Y. Makdisi, S. Nemesure, A. Poblaguev, W. Schmidke, D. Steski, D. Svirida, T. Tsang, K. Yip, A. Zelenski
Brookhaven National Laboratory, Upton, NY 11973, USA

Abstract

RHIC polarized proton operation requires fast and reliable proton polarimeter for polarization monitoring during stores. Polarimeters based on p-Carbon elastic scattering in the Coulomb Nuclear Interference(CNI) region has been used. Two polarimeters are installed in each of the two collider rings and they are capable to provide important polarization profile information. The polarimeter also provides valuable information for polarization loss on the energy ramp. As the intensity increases over years, the carbon target lifetime is getting shorter and target replacement during operation is necessary. Simulations and experiment tests have been done to address the target lifetime issue. This paper summarizes the recent operation and the target test results.

INTRODUCTION

The collision of polarized proton beams at RHIC (at up to $\sqrt{S}$ = 510 GeV energy) provides a unique physics opportunity for studying spin effects in hard processes at high luminosities, including the measurement of the gluon polarization and the quark and anti-quark spin flavor composition.

RHIC is the first polarized proton collider where the Siberian snakes were successfully implemented to maintain polarization during beam acceleration [1]. The fast polarization measurements are critical for the accelerator setup and physics programs during the physics stores. The pC CNI polarimeters in RHIC are based on elastic proton scattering with low momentum transfer in the CNI region and measurement of asymmetry in recoil carbon nuclei production [2]. This process has a large cross-section and sizable analyzing power of a few percents which has weak energy dependence in the 24-255 GeV energy range. A very thin (5-10 µg/cm^2, 5-10 µm wide) carbon ribbon target in the high intensity circulating beam produces high collision rate and a highly efficient DAQ system acquires up to 5×10^6 carbon events /sec. The absolute beam polarization was measured with a polarized H-jet polarimeter which is also based on elastic proton-proton scattering in the CNI region [3]. These calibration measurements have been done at various energies, such as 24 GeV, 31 GeV, 100 GeV, 250 GeV and 255 GeV. The results showed weak energy dependence, especially above 100 GeV. The simultaneous measurements in pC and H-jet polarimeters provide the calibration for pC polarimeter analyzing power. A typical store would result a ±3% statistical error in the polarized jet measurement. The fast pC polarimeter measures polarization profiles in both transverse planes, which are used to derive the polarization at collision points for experiments. The pC polarimeter also measures possible polarization losses during the energy ramp and possible polarization decay during the RHIC store.

POLARIMETER ASSEMBLY

RHIC polarimeters have evolved in past ten years [4]. Two identical polarimeter vacuum chambers are located in the warm RHIC sections which are separated for the two rings and have the separate vacuum systems. Due to the complexity of the chamber and the electronics, it is not practical to bake the chamber. A non-evaporable getter cartridge pump is added to each chamber to provide additional continuous pumping. As a result, the pump down speed is greatly improved, which allows the target replacement during maintenance day. A full intensity physics store can be resumed within 24 hours (vacuum down to 10^{-9} Torr).

It is desirable for the polarimeter to measure both horizontal and vertical beam polarization profiles, which requires separate targets scanning both vertically and horizontally. Since the thin carbon target has a relative short lifetime at the full RHIC beam luminosity, it would be advantageous to mount multiple targets on the driving mechanism (spaced so that the beam sees one ribbon at a time) to extend the time between maintenance periods. Each polarimeter consists of six horizontal targets and six vertical targets. Simulation shows that the expected equilibrium temperature at 255 GeV with full loaded intensity (2.4×10^{13}) for a typical carbon ribbon target would be around 1800°K. It is generally inadvisable to run the fiber at temperatures exceeding 2000°K, which is the onset of thermionic emission, since this would shorten the lifetime of the fiber.

The large aspect ratio of the thin carbon target (2.5 cm long, 10 µm wide and 25-50 nm thick) is essential for polarization measurement. First, it increases heat dissipation rate so that the target can survive the high intensity beam. Second, it reduces multiple scattering for recoil carbon ions and also keep the event rate within the detectors and DAQ capabilities. However, the ultra thin target is very fragile and has limited lifetime. Good targets survive in the RHIC beam for 50-100 measurements at the full beam intensity and 255 GeV. The ultra-thin carbon target production procedure was developed at Indiana University [5] and it is a routine now at BNL [6]. The target positioning accuracy is about ±0.5 mm and limited by the target straightness. The accuracy is required due to limited detector acceptance.

The time-of-flight and recoil carbon energy measurements are required for elastic scattering identification. The silicon-

* Work performed under contract No. DE-AC02-98CH1-886 with the auspices of the DOE of United States

ISBN 978-3-95450-141-0

THE ELECTRON BACKSCATTERING DETECTOR (eBSD), A NEW TOOL FOR THE PRECISE MUTUAL ALIGNMENT OF THE ELECTRON AND ION BEAMS IN ELECTRON LENSES*

P. Thieberger#, F. Z. Altinbas, C. Carlson, C. Chasman, M. Costanzo, C. Degen, A. Drees, W. Fischer, D. Gassner, X. Gu, K. Hamdi, J. Hock, Y. Luo, A. Marusic, T. Miller, M. Minty, C. Montag, A. Pikin, S. White,
Collider Accelerator Department, Brookhaven National Laboratory, Upton, NY, U.S.A.

Abstract

The Relativistic Heavy Ion (RHIC) electron lenses being commissioned to attain higher polarized proton luminosities by partially compensating the beam-beam effect require good alignment of the electron and proton beams. These beams propagating in opposite directions in a 6 T solenoid have an rms width as small as 300 microns and need to overlap each other over an interaction length of about 2 m with relative deviations of less than ~50 microns. A new beam diagnostic tool to achieve and maintain this alignment is based on detecting electrons that are backscattered in close electron-proton encounters. Maximizing the production of these electrons ensures optimum beam overlap. The successful commissioning of these electron backscattering detectors (eBSDs) using 100 GeV/nucleon gold and ^{3}He beams is described. Future developments are discussed that could further improve the sensitivity to small angular deviations.

INTRODUCTION

The partial compensation of the beam-beam effect in RHIC is necessary for mitigating the limit imposed by this effect on the achievable proton-proton beam luminosities. Electron lenses (e-lenses) [1] consisting of low energy (in our case ~6 keV), high intensity (~1 A) magnetized electron beams, can in principle provide the precise non-linear focusing properties necessary to effect such compensations. After developments on a test bench [2], two such e-lenses have now been installed in the RHIC tunnel. In preparation for the 2015 RHIC polarized proton-proton run, commissioning of the RHIC e-lenses has been successfully accomplished [3] with the ion beams available during the 2014 run; namely 100 GeV/nucleon gold and 100 GeV/nucleon helium (^{3}He).

The precise alignment of the electron and ion beams is an important prerequisite for achieving maximum compensation. Over the 2 m interaction region in the ~6 T solenoid, the centers of these ~300 micron rms wide beams need to be separated by less than ~50 microns. The precision achievable with the installed beam position monitoring system [4] isn't quite sufficient for ensuring this result. As described before [5], electron beam electrons backscattered by the relativistic ions or protons (henceforth, ions) can provide the "luminosity" signal required for optimizing and maintaining this alignment.

After briefly reviewing the principle and design of the RHIC electron backscattering detectors (eBSDs), we show results from commissioning the eBSDs with relativistic gold (Au) and helium (^{3}He) beams. We present conclusions about their expected performance with proton beams.

* Work supported by Brookhaven Science Associates under Contract No. DE-AC02-98CH10886 with the U.S. Department of Energy
#pt@bnl.gov

PRINCIPLE OF THE METHOD

The lensing effect of an e-lens on the relativistic ions is due to the macroscopic electric and magnetic fields produced by the Gaussian-shaped electron beam. In other words, it is the collective long-range Coulomb interaction of the electrons with individual ions that affects the trajectory of these ions. The vast majority of the electron trajectories are only slightly affected since their trajectories are confined by a strong magnetic field. There is however a finite probability for ion-electron collisions with impact parameters that are so small as to produce a significant electron scattering angle imparting at the same time considerable momentum and energy to the scattered electrons. Large scattering angles, correlated with high energies, result in energetic electrons spiraling backwards (towards the electron gun) along the magnetic field lines. As described below, some of these backscattered electrons are intercepted and counted by a scintillation detector placed in air, behind a thin vacuum window.

To first order in the fine structure constant, the Coulomb scattering of relativistic electrons by nuclei is described by the Mott formula which in the rest frame of the nucleus is written as [6]:

$$\frac{d\sigma}{d\Omega} = \frac{Z^2}{4}\left(\frac{e^2}{E}\right)^2 \frac{1}{sin^4\left(\frac{\theta}{2}\right)} \times \left[1 - \left(\frac{pc}{E}\right)^2 sin^2\frac{\theta}{2}\right]$$

$$\times \left[1 + \frac{2E\, sin^2(\theta/2)}{M_A c^2}\right]^{-1} \times \left[1 - \frac{q^2 \tan^2(\theta/2)}{2M_A^2}\right]$$

where σ is the cross section, Z the atomic number , M_A the mass of the nucleus, e the elementary charge, E and p the energy and momentum of the electron in the frame of the nucleus, $\boldsymbol{\theta}$ the electron scattering angle in that frame and $\boldsymbol{q}$ the four momentum transfer coefficient. The first term is the classical Rutherford cross section and the last

ISBN 978-3-95450-141-0

PERFORMANCE AND UPGRADE OF THE FAST BEAM CONDITION MONITOR AT CMS

M. Hempel, DESY, Zeuthen, Germany*
B. Pollack, Northwestern University, Evanston, Illinois†
A. Bell, H. M. Henschel, O. Karacheban, W. Lange, W. Lohmann, J. L. Leonard,
M. Penno, S. Schuwalow, R. Walsh, DESY, Zeuthen, Germany
Dominik Przyborowski, University of Science and Technology, Cracow, Poland
David Peter Stickland, Princeton University, Princeton, New Jersey, USA
P. Bartowy, A. E. Dabrowski, R. Loos, V. Ryjov, A. A. Zagozdzinska, CERN, Geneva, Switzerland
K. Afanaciev, NC PHEP BSU, Minsk, Belarus
On behalf of CMS Collaboration

Abstract

The Fast Beam Condition Monitor (BCM1F) is a diamond based particle detector inside CMS. It consisted of 8 single-crystal chemical vapor deposition (sCVD) diamond sensors on both ends of the interaction point, and was used for beam background and luminosity measurements. The system has been operated with an integrated luminosity of 30 fb^{-1}, corresponding to a particle fluence of $8.78 \cdot 10^{-13}$ cm^{-2} (24 GeV proton equivalent). To maintain the performance at a bunch spacing of 25 ns and at the enhanced luminosity after the LHC Long Shutdown LS1, an upgrade to the BCM1F is necessary. The upgraded system features 24 sensors with a two pad metallization, a very fast front-end ASIC built with 130 nm CMOS technology, and new back-end electronics. A prototype of the upgraded BCM1F was studied in the 5GeV electron beam at DESY. Measurements were done on the signal shape as function of time, the charge collection efficiency as a function of voltage, and the amplitude as a function of the position of the impact point of the beam electron on the sensor surface. The preliminary results of this test-beam experiment and the status of the newly upgraded BCM1F will be presented.

BCM1F DURING OPERATION

BCM1F is a particle counter with nanosecond time resolution based on single-crystal chemical vapor deposition (sCVD) diamonds. Due to the linear dependence between detection probability and luminosity as shown in Figure 1, it is possible to use BCM1F as a luminosity monitor as well as a background monitor [1, 2].

During the first LHC running period from 2008-2012 BCM1F delivered online background and luminosity measurements as feedback for the CMS and LHC operation [3,4]. Since the data acquisition for BCM1F is decoupled from the main CMS DAQ, it could measure luminosity even before physics data was taken.

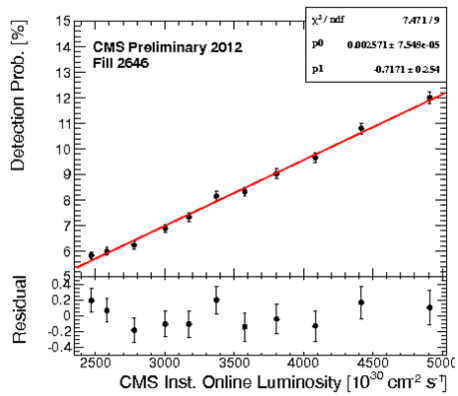

Figure 1: Particle detection probability as a function of luminosity.

MOTIVATION FOR THE BCM1F UPGRADE

The BCM1F modules are located around the beam pipe at a distance of 5 cm from the beam center. A particle fluence of $8.78 \cdot 10^{-13}$ cm^{-2} (24 GeV proton equivalent) at this position led to radiation damage of the laser diodes, which were used in the front-end electronics to convert the diamond sensor signal to an optical signal.

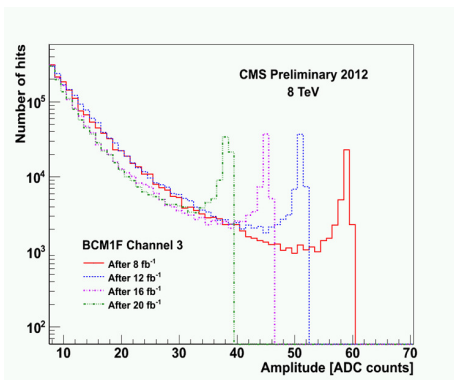

Figure 2: Decrease of the amplification measured by an ADC amplitude spectrum.

* maria.hempel@desy.de
† brian.lee.pollack@cern.ch

ISBN 978-3-95450-141-0

SYNCHRONISATION OF THE LHC BETATRON COUPLING AND PHASE ADVANCE MEASUREMENT SYSTEM

J. Olexa, M. Gasior, CERN, Geneva, Switzerland

Abstract

The new LHC Diode ORbit and OScillation (DOROS) system will provide beam position readings with sub-micrometre resolution and at the same time will be able to perform measurements of local betatron coupling and beam phase advance with micrometre beam excitation. The oscillation sub-system employs gain-controlled RF amplifiers, shared with the orbit system, and followed by dedicated diode detectors to demodulate the beam oscillation signals into the kHz frequency range, subsequently digitized by multi-channel 24-bit ADCs. The digital signals are processed in each front-end with an FPGA and the results of reduced throughput are sent using an Ethernet protocol to a common concentrator, together with the orbit data. The phase advance calculation between multiple Beam Position Monitors (BPMs) requires that all DOROS front-ends have a common phase reference. This paper presents methods used to generate such a reference and to maintain a stable synchronous sampling on all system front-ends. The performance of the DOROS prototype synchronisation is presented based upon laboratory measurements.

INTRODUCTION

The DOROS system has been primarily designed and optimised for processing beam signals from the beam position monitors (BPMs) embedded into the jaws of the new LHC collimators [1]. The system will provide orbit readings used for the automatic positioning of the collimator jaws symmetrically around the beam, which will reduce the time needed to set-up the collimators and potentially improve the collimation efficiency. The Diode ORbit (DOR) system will be complemented by Diode OScillation (DOS) sub-system optimised for processing the beam oscillation signals. The DOS part will provide data that can be used for the measurement of local betatron coupling and the phase advance between the BPMs with micrometre beam excitation.

The simplicity of the DOROS system and its already proven sub-micrometre orbit resolution [2] made it a good candidate to complement the standard LHC BPM system. This system was designed for bunch-by-bunch trajectory measurements and is limited to an orbit resolution at the micrometre level. The DOROS system will therefore be installed on all BPMs close to the LHC interaction points, where a better orbit resolution will help in optimising the collision process. Electrode signals of these BPMs will be passively split and sent to both systems. This way the standard system will provide bunch-by-bunch beam trajectories while the DOROS will measure precisely beam orbits. In addition, the DOS part of the DOROS system will be capable of providing oscillation data with micrometre beam excitation for betatron coupling and phase advance measurements.

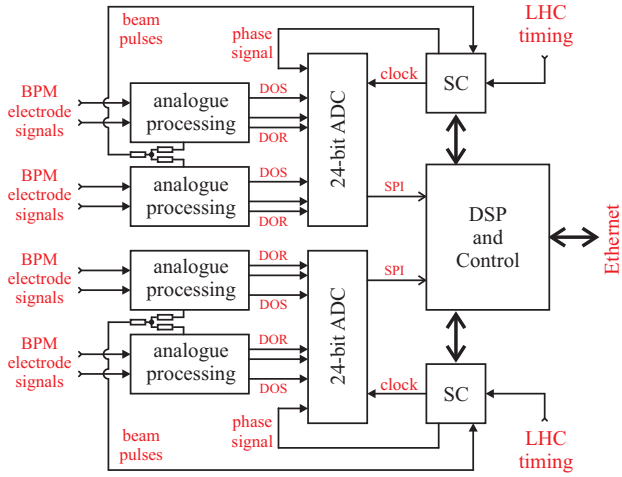

Figure 1: Block diagram of a DOROS front-end. Abbreviations: SC – synchronisation circuits, DOR – diode orbit, DOS – diode oscillation, SPI – serial peripheral interface link.

DOROS SYSTEM

The DOROS front-ends will be built as 1U 19" modules distributed around the LHC. Each front-end is foreseen to process signals from four BPM electrode pairs. Typically it will be up-stream and down-stream BPMs of two collimators or horizontal and vertical electrodes of two stripline BPMs [2]. The block diagram of one DOROS front-end is depicted in in Fig. 1.

The analogue processing channels of each electrode pair provide two low frequency orbit signals (DOR) proportional to the BPM electrode voltages, which are produced by compensated diode detectors [2], and one oscillation signal (DOS), resulting from the difference of the beam oscillation signals demodulated by diode peak detectors. All three signals are low-pass filtered and are digitized by a 24-bit ADC at the rate of the LHC revolution frequency (f_{rev}) of about 11.2 kHz. The subsequent digital signal processing (DSP) of the samples is implemented in an FPGA. The same FPGA provides the system control and timing as well as the Ethernet communication and data transmission to a common DOROS concentrator. The DOROS data transmission uses the same Ethernet protocol and the 25 Hz frame rate as the standard BPM system. The total DOROS data throughput is about 40 KB/s per front-end.

ISBN 978-3-95450-141-0

DUAL TRANSVERSE AND LONGITUDINAL STREAK CAMERA IMAGING AT ELSA*

M. Switka, F. Frommberger, P. Haenisch, M. Schedler and W. Hillert, ELSA, Bonn, Germany

Abstract

The electron pulse stretcher ring ELSA located at Bonn University provides 0.5–3.5 GeV polarized and non-polarized electron beams for external experimental stations. A streak camera system has been installed to capture time resolved images of beam dynamics ranging from nanoseconds to several milliseconds [1]. Particular attention was drawn to the capability of simultaneous imaging of both transverse beam dimensions, hence providing information of all spatial dimensions in one synchroscan or slow sweep measurement. Incoherent and coherent beam instabilities, especially at high stored beam currents, are subject of analysis due to the planned intensity upgrade towards 200 mA for standard operation. The current resolution performance of the imaging system and machine relevant measurements are presented.

INTRODUCTION

As streak cameras convert three dimensional light beam information into a two dimensional image with aspect on longitudinal resolution, the dimension of one transverse plane is always suppressed, either by the streak action or the narrow slit of the input optics. As for certain events interest arises for capturing dynamics in all three dimensions simultaneously, a method for dual transverse imaging at ELSA was introduced and demonstrated in [2]. In order to test the convenience of such a setup, a low-cost version was installed mostly utilizing equipment already available at the lab. Resolution limits were encountered primarily due to the limiting aperture of the optical system and for very short time windows due to limited light intensity. Furthermore, longitudinal instability behaviour was investigated through grow-damp measurements using the bunch-by-bunch feedback system (BBB). Attention was especially drawn to cavity temperature effects and decoherence observation.

BEAM MANIPULATION AND RECOUPLING

The primary lens of ELSA's *M7* optical synchrotron radiation diagnostic beamline focuses the visible synchrotron radiation onto the focal plane of the first lens of a relay line lens pair. The subsequent beam manipulation section in is illustrated in Fig. 1. The parallel light bundle is split by a 50 % beamsplitter, partially bypassing a Dove prism which rotates the beam transversally by 90°. Both light bundles, upright and flat, are recoupled onto the same light path with slight displacement and angular deviation. The second relay lens focuses the beam onto the streak camera's input slit (M_{tot} = 0.044). Hence the two perpendicular electron beam images are projected next to each other. In this setup, two main apertures restrict the resolution of transverse beam dynamics: The 0.15 × 4.41 mm^2 (v × h) large photo cathode limits the imaging of vertical light beam displacements. Secondly, the rectangular mirror downstream from the Dove prism imposes a horizontal aperture for the flat beam and a vertical aperture for the upright beam. Note that the original beam image orientation is upright.

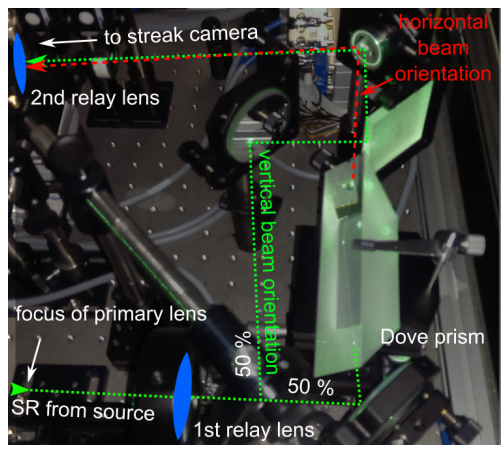

Figure 1: Optical setup for simultaneous imaging of both transverse beam dynamics. One part of the beam is rotated by 90° after exiting the Dove prism.

DUAL TRANSVERSE IMAGING

The streak camera used is the model C10910 by Hamamatsu [3]. Exemplary *slow sweep* measurements for the dual transverse imaging capability are shown in Fig. 2. Parts of

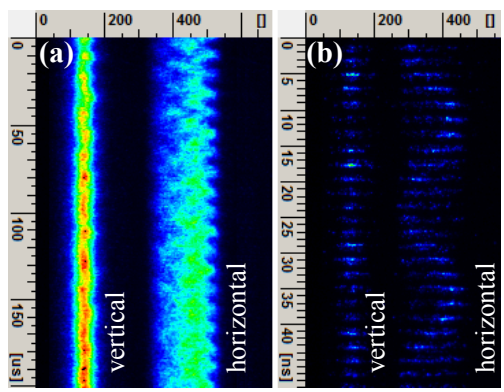

Figure 2: Dual transverse *slow sweep* images. Injection beam dynamics are captured at sufficient SNR (a) and single bunch resolution (b).

the injection process are captured where large horizontal

* Work supported by the DFG within SFB/TRR16.

ISBN 978-3-95450-141-0

ELECTRON BEAM DIAGNOSTICS FOR SHORT PULSE FEL SCHEMES AT CLARA

S. Spampinati#, University of Liverpool and The Cockcroft Institute, Cheshire, U.K
D. Newton, University of Liverpool, Liverpool, U.K

Abstract

CLARA (Compact Linear Accelerator for Research and Applications) [1] is a proposed 250 MeV, 100-400 nm FEL test facility at Daresbury Laboratory. The purpose of CLARA is to test and validate new FEL schemes in areas such as ultra-short pulse generation, temporal coherence and pulse-tailoring. Some of the schemes that can be tested at CLARA depend on a manipulation of the electron beam properties with characteristic scales shorter than the electron beam and require a 30 - 50 μm modulation of the beam energy acquired via the interaction with an infrared laser beam in a short undulator. In this article we describe the electron beam diagnostics required to carry on these experiments.

INTRODUCTION

Some of the most advanced schemes proposed to improve FEL performance depend on a manipulation of the electron beam properties with characteristic scales of several coherence lengths and shorter than the electron beam [2, 3, 4]. We are interested to test, among other schemes, mode locking FEL and femto-slicing for the production of trains of short pulses [5, 6, and 7]. The implementation of these schemes at CLARA requires a 30 - 50 μm modulation of the beam energy acquired via the interaction with an infrared laser beam in a short undulator (modulator). The performance of these FEL schemes depend on this energy modulation. So monitoring the longitudinal phase space of the electron beam is important to perform and to realize these experiments. A deflecting cavity [8] installed in the last part of the FEL line will allow the longitudinal beam distribution to be observed on a screen placed after the dipole leading to the beam dump. Figure 1a shows the FEL line of CLARA, composed of a modulator, a dispersive section, seven radiators and an afterburner section. The afterburner is composed by a series of short undulators and delay chicanes. A possible layout of the diagnostic system placed at the end of the CLARA undulator from the afterburner is shown in Fig. 1b.

In this design, the electron beam is deflected vertically by the deflecting cavity. This deflection maps the electron beam longitudinal coordinate to the vertical coordinate on an intercepting screen after the spectrometer dipole magnet; the dipole converts the particle's energy to the screen horizontal coordinate. Consequently, the electron beam longitudinal phase space is imaged on the screen, and the energy modulation taking place in the modulator can be studied and optimized. Another interesting application of this diagnostic beam line could be the study of the FEL process taking place in the different operation modes of CLARA.

#simone.spampinati@cockcroft.ac.uk

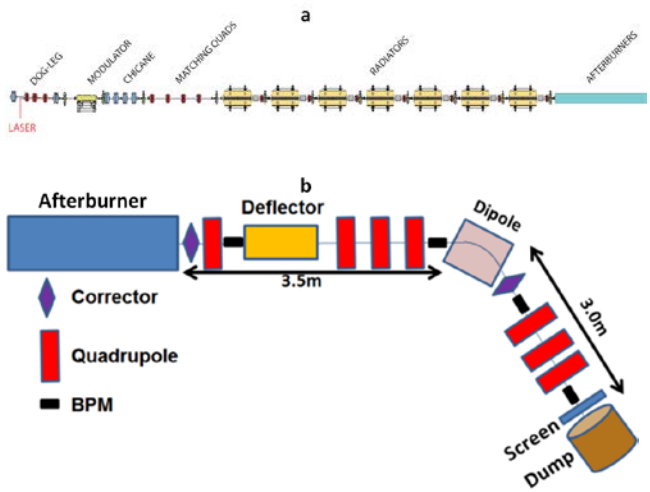

Figure 1: Top: FEl line of CLARA. Bottom: Layout of the phase space diagnostics composed by of a transverse deflector and an energy spectrometer.

OPTICS OPTIMIZATION AND RESOLUTIONS

The vertical beam size at the screen, after deflection, is [9]:

$$\sigma_y = \sqrt{\sigma_{y,0}{}^2 + (S\sigma_Z)^2} \qquad (1)$$

where $\sigma_{y,0}$ is the vertical beam size at the screen location without deflection, σ_z is the longitudinal beam size and S is the calibration factor representing the strength of the beam deflection [9]:

$$S = \frac{e_0 V k}{pc}\sqrt{\beta_{yS}\beta_{yD}}\left|\sin\Delta\Psi\right| \qquad (2)$$

here $k = \frac{2\pi}{\lambda}$ with λ = 10.01cm for an S-band cavity (frequency of 2.998 GHz). V_0 is the deflecting voltage, $\beta_{y,D}$ and $\beta_{y,S}$ are vertical betatron functions at the deflector and the screen, respectively. ΔΨ is the vertical

ISBN 978-3-95450-141-0

NEW MTCA.4-BASED HARDWARE DEVELOPMENTS FOR THE CONTROL OF THE OPTICAL SYNCHRONIZATION SYSTEMS AT DESY*

M. Felber#, M. K. Czwalinna, H. T. Duhme, M. Fenner, C. Gerth, M. Heuer, T. Lamb, U. Mavrič, J. Mueller, P. Peier, H. Schlarb, S. Schulz, B. Steffen, C. Sydlo, M. Titberidze, T. Walter, R. Wedel, F. Zummack, DESY, Hamburg, Germany
J. Szewinski, NCBJ, Świerk, Poland
T. Kozak, P. Prędki, K. Przygoda, TUL-DMCS, Łódź, Poland
E. Janas, ISE-WUT, Warsaw, Poland

Abstract

The optical synchronization group at DESY is operating and continuously enhancing their laser-based synchronization systems for various facilities which need femtosecond-stable timing. These include the free-electron lasers FLASH and the upcoming European XFEL as well as the electron diffraction machine REGAE (Relativistic Electron Gun for Atomic Exploration) and the future plasma acceleration test facilities (LAOLA and FLASHforward). One of the major upgrades under development is the migration of the entire electronic control hardware to the new MTCA.4 platform which was introduced as the new standard for accelerator control in many facilities worldwide. In this paper we present the applied modules and the topology of the new systems. Main advantages are a compact design with higher performance, redundancy, and remote management.

INTRODUCTION TO MTCA.4

MTCA is a novel electronic framework derived from the Advanced Telecommunication Computing Architecture (ATCA) [1]. MTCA.4 was released as an official standard by the PCI Industrial Manufacturers Group (PICMG [2]) in 2011 and is supported by the xTCA for physics group, a network of physics research institutes and electronics manufacturers. Its main improvements over the preceding standards are enhanced rear I/O connectivity and provisions for improved precision timing. MTCA.4 has inherited many of the advantages of ATCA including capabilities for remote monitoring, remote maintenance, hot-swap of components, and the option to duplicate critical components, making the standard highly modular and flexible. It also made the outstanding signal processing performance of ATCA systems more affordable and less demanding in terms of space requirements and energy consumption.

Major accelerator facilities worldwide currently evaluate the deployment of MTCA.4-based Low-Level Radio Frequency (LLRF) systems, either for extensions or upgrades of existing infrastructure or for the initial equipment of new facilities.

*This work has partly been funded by the Helmholtz Validation Fund Project MTCA.4 for Industry (HVF-0016)
#matthias.felber@desy.de

MTCA.4 System Architecture

A picture of an equipped MTCA.4 system is shown in Figure1. Fundamental components are the chassis which is available in different form factors and sizes, the power supply, a crate management controller (MCH), and CPU and hard drive.

For user applications specific analog and digital processing cards are used. From the front Advanced Mezzanine Cards (AMC) are inserted to the crate. There are various connections on the backplane which provide e.g. Gigabit Ethernet and PCI Express links between the slots and the MCH, dedicated clock and trigger distribution lines, and point to point links between the slots for fast real time communication between the cards. Additionally, there is the possibility to insert cards from the rear of the crate, so-called Rear Transition Modules (RTM) which connect to the according AMC board via the Zone 3 connector. This connection provides 60 differential pairs for analog or digital signals, which will be defined in the standard [3]. Often the cards have connectors for additional industrial standard piggy back boards like FPGA Mezzanine Cards (FMC) or IndustryPack (IP) modules.

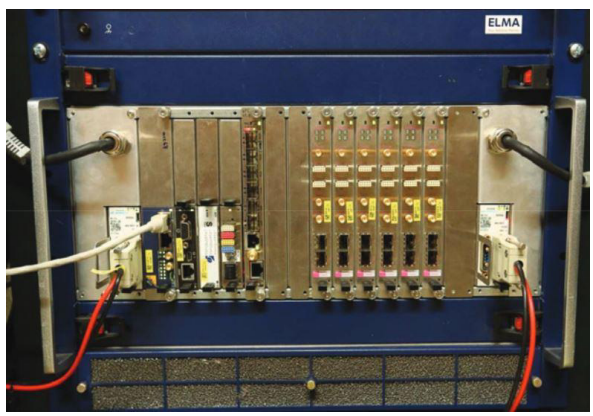

Figure 1: MTCA.4 crate equipped with AMC cards.

MTCA.4 AT DESY

In broad agreement between the involved groups, it was decided to use the MTCA.4 standard for the control electronics of the European XFEL. This involves the LLRF field control [4], timing system, diagnostics like beam position monitors [5] and camera readouts, and the optical synchronization system [6].

ISBN 978-3-95450-141-0

A DOUBLE-PRISM SPECTROMETER FOR THE LONGITUDINAL DIAGNOSIS OF FEMTOSECOND ELECTRON BUNCHES WITH MID-INFRARED TRANSITION RADIATION *

S. Wunderlich†, E. Hass, M. Yan and B. Schmidt, DESY, 22603 Hamburg, Germany

Abstract

Electron bunch lengths in the sub-10 fs regime and charges of a few tens of picocoulombs are parameters required for free-electron lasers [1] and are also a consequence from the intrinsic process in laser-driven plasma wake field acceleration [2]. Since the coherent spectrum of transition radiation of these bunches carries the information on the longitudinal bunch profile in the form factor, the spectroscopy of transition radiation is an attractive method to determine the electron bunch length. A double-prism spectrometer has been developed and demonstrated for the single-stage measurement of mid-infrared transition radiation between 2 µm and 18 µm. The spectrometer facilitates single-shot spectral measurements with high signal-to-noise ratio utilising a line array of mercury cadmium telluride detectors. In this contribution, we present the spectrometer and measurements of electron bunches at the Free-Electron Laser in Hamburg (FLASH) at DESY. The results are compared to established bunch length monitors which are a multi-stage grating spectrometer for transition radiation and a transverse deflecting structure accessing the longitudinal phase space of the electron bunches directly.

DIAGNOSIS OF ELECTRON BUNCHES WITH COHERENT RADIATION

The coherent spectrum of characteristic radiation from relativistic and charged particle bunches carries the information on the three-dimensional current profile encoded in the form factor. In other words, the complex form factor F yields the wavelength-dependent level of coherence in the emission of radiation, like coherent diffraction radiation (CDR), coherent synchrotron radiation (CSR) and coherent transition radiation (CTR). This project focuses on the latter, CTR.

Spectral Intensity of Coherent Radiation

The spectral intensity $U = U(\omega,\Omega)$ of transition radiation (TR) per solid angle Ω and wavelength ω can be described by

$$\frac{\mathrm{d}^2U}{\mathrm{d}\omega\,\mathrm{d}\Omega} \approx \frac{\mathrm{d}^2U_1}{\mathrm{d}\omega\,\mathrm{d}\Omega}\, N^2\, |F(\omega,\Omega)|^2 \qquad (1)$$

with, expressing the nature of coherent emission, the number of radiating particles squared, N^2, and the single-particle contribution U_1 [3]. The modulus of the complex form factor is denoted by $|F\,(\omega,\Omega)|$.

* The project has been supported by the BMBF under contract 05K10GU2 & FS FLASH 301.

† steffen.wunderlich@desy.de

Form Factor

The complex form factor

$$F = F\,(\omega,\Omega) = |F\,(\omega,\Omega)|\exp\,(i\Phi\,(\omega))$$

is the Fourier transform of the three-dimensional normalised charge density $\rho_{3D}(\vec{r})$ in position space and can be expressed, at an observation distance much larger than the electron bunch extension, by

$$F(\omega,\Omega) = F(\vec{k}) = \int_{-\infty}^{\infty} \rho_{3D}(\vec{r})\ \exp(-i\,\vec{k}\,\vec{r})\,\mathrm{d}\vec{r}.$$

A decomposition of $F(\omega,\Omega)$ into transverse and longitudinal components, F_t and F_l, is justified for a negligible coupling of the two planes [4].

The longitudinal form factor $F_l = F_l(\omega)$ now reflects a charge density in the direction of the movement of the high-relativistic particles

$$F_l = \int_{-\infty}^{\infty} \rho_l(t)\ \exp(-i\,\omega\,t)\,\mathrm{d}t \qquad (2)$$

Due to the high-relativistic motion of the particles, the influence of the transverse form factor is strongly suppressed. This allows to approximate $F(\omega,\Omega)$ by $F_l(\omega)$ in Equation (1) for sufficiently small transverse beam sizes [3].

Utilising F for Estimating the Bunch Length

Figure 1 shows examples of form factors on the beam axis of electron bunches with lengths (σ_l) in the femtosecond regime between 0.5 µm (≈ 1.5 fs) and 3 µm (≈ 10 fs). As depicted, the form factor shows a strong modulation with bunch length in the wavelength range between 2 µm and 20 µm. Hence, this range has been chosen for the region of interest of the prism spectrometer described in the following section.

According to Equation (2), the determination of the absolute value and the slope of the modulus of the form factor, $|F_l|$, allows the estimation of the bunch length and moreover, a time-domain current profile. However, the spectral phase $\Phi(\omega)$ of the complex form factor F cannot be acquired by intensity spectroscopy. Underlying several constraints, phase-retrieval processes [5–7] can access a possible temporal current profile and show an impressive accordance with direct time-domain diagnostics like a transverse deflecting structure (TDS) [4].

DOUBLE-PRISM SPECTROMETER

Compared to grating-based spectrometers, prism spectrometers yield bulk absorption in the prisms, but provide

ISBN 978-3-95450-141-0

LONGITUDINAL PHASE SPACE TOMOGRAPHY USING A BOOSTER CAVITY AT THE PHOTO INJECTOR TEST FACILITY AT DESY, ZEUTHEN SITE (PITZ)

D. Malyutin*, M. Gross, I. Isaev, M. Khojoyan, G. Kourkafas, M. Krasilnikov, B. Marchetti, F. Stephan, G. Vashchenko, DESY, 15738 Zeuthen, Germany

Abstract

One of the ways to measure the longitudinal phase space of the electron bunch in a linear accelerator is a tomographic technique based on measurements of the bunch momentum spectra while varying the bunch energy chirp. The energy chirp at PITZ can be controlled by varying the RF phase of the CDS booster – the accelerating structure installed downstream the electron source (RF gun). The resulting momentum distribution can be measured with a dipole spectrometer downstream. As a result, the longitudinal phase space at the entrance of the CDS booster can be reconstructed.

In this paper the tomographic technique for longitudinal phase space measurements is described. Results of measurements at PITZ are presented and discussed.

INTRODUCTION

For successful operation of linac based Free Electron Lasers (FELs) there are quite stringent requirements on the electron beam quality: small transverse emittance, small energy spread and high beam peak current (high brightness) [1]. The measurements of the beam slice energy spread and current profile can be done using a transverse deflecting structure (TDS) [2] or using a tomographic technique [3, 4]. Both methods allow full longitudinal phase space characterization. With the current setup of the Photo Injector Test facility at DESY, Zeuthen site (PITZ), only the tomographic technique can be employed. A TDS, which is already installed in the beamline, is planned to be put into operation at the end of this year.

The PITZ facility was built as an electron source test stand [5] for FELs like FLASH and the European XFEL. The present PITZ beamline layout is shown in Fig. 1. The main components of the PITZ facility are a photocathode laser system, an RF photo-electron gun (first accelerating structure) surrounded by main and a bucking solenoids, a second accelerating structure – Cut Disk Structure (CDS) which is also called booster cavity; and three dipole spectrometers. One spectrometer is located in the low energy section downstream the gun (Low Energy Dispersive Arm – LEDA), a second one in the high energy section downstream the booster (the first High Energy Dispersive Arm – HEDA1), and the third one in the end of the PITZ beamline (the second High Energy Dispersive Arm – HEDA2). Additionally there are three Emittance Measurement Stations (EMSYs) and a transverse deflecting structure (TDS), Fig. 1.

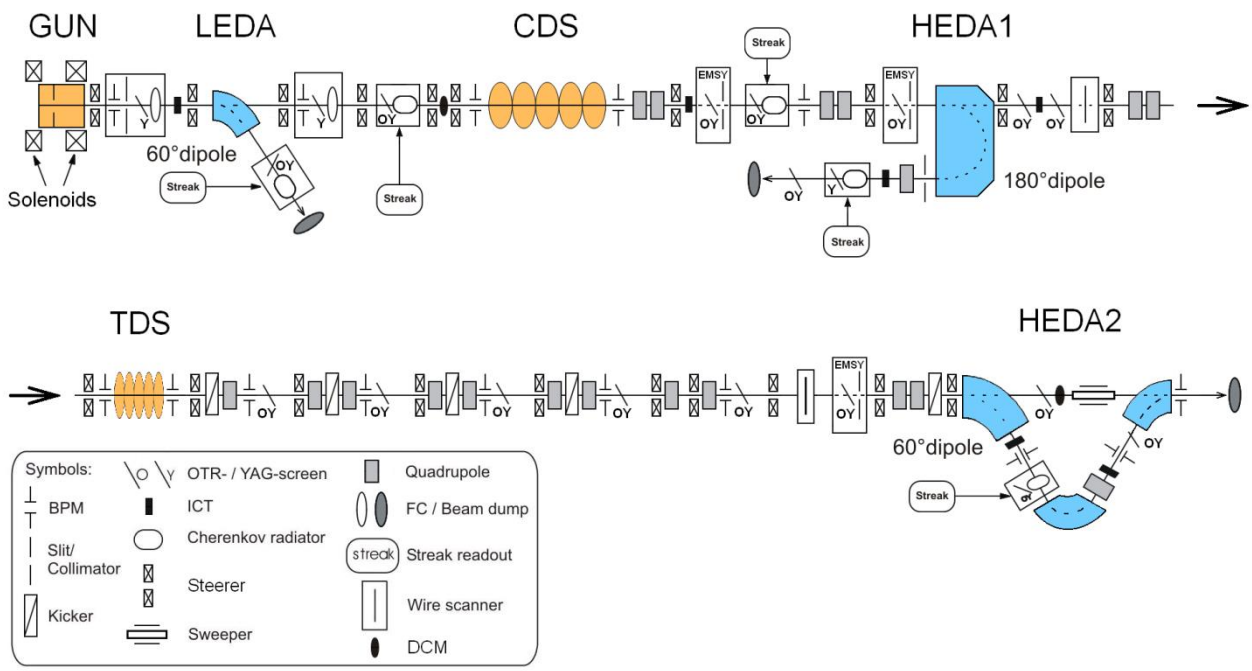

Figure 1: PITZ beamline layout. The beam propagates from left to right.

*dmitriy.malyutin@desy.de

ISBN 978-3-95450-141-0

NEW RESULTS OF FERMI FEL1 EOS DIAGNOSTICS WITH FULL OPTICAL SYNCHRONIZATION

M. Veronese*, E. Allaria, P. Cinquegrana, E. Ferrari, F. Rossi, P. Sigalotti, C.Spezzani,
Elettra-Sincrotrone Trieste, Trieste, Italy

Abstract

The electro optical sampling diagnostics (EOS) of the FERMI FEL has been recently upgraded with a full optical synchronization of its dedicated femtosecond fiber laser to the ultra-stable optical pulsed timing system of FERMI. For this purpose a dual synchronization electronics has been developed and installed. It exploits a mixed error signal derived from both optical to electrical conversion and from second harmonic generation based optical phase detection. For this second part a new optical setup including a cross correlator has been installed. The operation of the EOS has greatly benefited from the upgrade. The arrival time measurements have been compared with the ones from the bunch arrival monitor diagnostics (BAM) showing very good agreement. This new setup has also allowed to improve the bunch profile measurement. Some examples of measurement with ZnTe and GaP are presented. Finally, usability and operator friendliness of the new setup are also discussed.

INTRODUCTION

FERMI is a seeded free electron laser (FEL) operating in the spectral range from VUV to soft x-rays. It is based on a SLAC/BLN/UCLA type RF-gun, and a normal conducting LINAC, currently operated at 1.2 GeV (up to 1.5 GeV). Longitudinal compression is provided by two magnetic chicanes BC1 and BC2 (respectively at 300 MeV and 600 MeV). The FEL has two undulator chains, namely FEL1 [1] and FEL2 [2]. The first, FEL1, is a single cascade HGHG seeded free electron laser designed to provide ultrashort radiation pulses with energies up to hundreds of micro joules per pulse in the wavelength range from 100 nm to 20 nm. The second, FEL2, is a double cascade seeded system designed to reach 4 nm at the shortest wavelength, implementing the fresh bunch technique. Optimization of a seeded FEL is a multi-parameter optimization process. To reach an optimal FEL emission several conditions have to be met. All information pertaining the time of arrival and the temporal profile of the electron bunch are of crucial importance. For this reason an electro optical sampling (EOS) diagnostics station has been installed at the entrance of both the FEL undulators chains. This paper is focused on the FEL1 EOS (see Fig. 1). This device in based on a fiber laser oscillator installed in the tunnel and exploits the spatial encoding scheme. The FEL1 EOS initial operational experience has been described in [3]. We made a major upgrade to the locking of the laser with a full optical synchronization setup and electronics with the aim of improving the time jitter performances of the FEL1 EOS.

* marco.veronese@elettra.eu

EXPERIMENTAL LAYOUT

The layout of FEL1 chain, in the undulator hall, is depicted in Fig. 1. In the figure the electron beam travels from left to right and its trajectory is depicted in black. The seed laser is depicted as a red flash. The modulator undulator (MOD) is in light blue while the dispersive section is in green and radiator (RAD) undulators are in violet. After the last radiator the electron beam is bent towards the main beam dump while the FEL radiation travels towards the experimental hall. The EOS diagnostic station is installed just upstream the modulator and is depicted in yellow in Fig. 1.

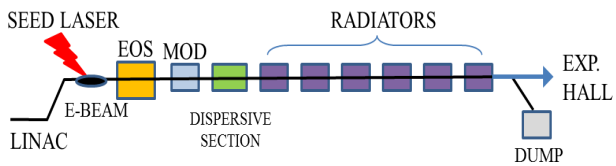

Figure 1: FERMI FEL1 layout.

The upgraded EOS optical layout is depicted in Fig. 2. The laser source is visible in the upper left part of the figure. It is a fiber laser (Menlosystems, TC780) delivering pulses at 780 nm wavelength with 110 fs duration, average power of 55 mW and repetition rate of 78.895 MHz. The pulses pass a delay line needed for fine time delay adjustments. Then the laser beam passes a Glan-Taylor polarizer (P) to improve polarization purity and a motorized zero order $\lambda/2$ waveplate for rotation of the polarization. The laser is focused on the electro optic (EO) crystals surface by a cylindrical lens (L2). The laser angle of incidence on the crystal is of 30 degrees with respect to the electron beam. This angle allows encoding temporal information in the spatial profile of the laser. After passing through the EO crystal the laser exits the vacuum chamber and passes through the polarization analysis optics. This is composed of two motorized waveplates ($\lambda/4$ and $\lambda/2$) and a Wollaston prism. They are adjusted to work in a cross polarizer configuration. The beam is then directed to the intensified charge-coupled device (ICCD) camera. Two lenses are set between the vacuum chamber and the ICCD camera to provide the necessary magnification. The vacuum 3-axis manipulator houses a ZnTe 1 mm thick crystal, a GaP 0.4 mm thick, a GaP 0.1 mm thick, an OTR screen and a YAG:Ce crystal. In the bottom part of Fig. 2 we show the coarse longitudinal alignment system. Coherent optical transition radiation (COTR) is used to set the correct ICCD gate delay. The extraction path for COTR radiation is depicted in violet.

ISBN 978-3-95450-141-0

NEAR-SATURATION SINGLE-PHOTON AVALANCHE DIODE AFTERPULSE AND SENSITIVITY CORRECTION SCHEME FOR THE LHC LONGITUDINAL DENSITY MONITOR

M. Palm*, E. Bravin, S. Mazzoni, CERN, Geneva, Switzerland

Abstract

Single-Photon Avalanche Diodes (SPADs) monitor the longitudinal density of the LHC beams by measuring the temporal distribution of synchrotron radiation. The relative population of nominally empty RF-buckets (satellites or ghosts) with respect to filled bunches is a key figure for the luminosity calibration of the LHC experiments. Since afterpulsing from a main bunch avalanche can be as high as, or higher than, the signal from satellites or ghosts, an accurate correction algorithm is needed. Furthermore, to reduce the integration time, the amount of light sent to the SPAD is enough so that pile-up effects and afterpulsing cannot be neglected. The SPAD sensitivity has also been found to vary at the end of the active quenching phase. We present a method to characterize and correct for SPAD deadtime, afterpulsing and sensitivity variation near saturation, together with laboratory benchmarking.

INTRODUCTION

The LHC RF cavities operate at about 400 MHz (2.5 ns RF buckets), with a distance of at least 10 buckets between nominally filled buckets (main bunches). A fraction of the beam can be found in the nominally empty buckets, where they are called satellite or ghost bunches [1]. The number of particles in satellites and ghost bunches is typically less than four or five orders of magnitude lower than the main bunches. However, they can create background noise at the interaction points and, due to their large number, cause problems for luminosity calibration [1].

The purpose of the LDM is to measure the relative number of particles in the different buckets, via the synchrotron radiation emitted by the beam.

A schematic overview of the LHC LDM system (one per beam) that was installed during Run 1 is shown schematically in Fig. 1: an SPAD registers individual synchrotron radiation photons emitted from an undulator (below 2 TeV) or separation dipole (above 2 TeV). Their arrival times relative to the LHC turn clock are stored with 50 ps resolution, allowing a histogram over the longitudinal beam profile, with sufficient statistics, to be generated in a few minutes. The light intensity on the SPAD sensor can be adjusted by moving individual neutral density (ND) filters in or out of the light path. With little filtering, the average number of *photons* per ghosts is high, but the *counts* per ghost that are within one deadtime of a main bunch is reduced due to the deadtime of the detector. For heavy filtering, the availability of the detector is higher, but the number of photons per ghost

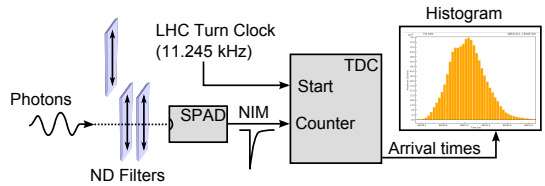

Figure 1: Schematic overview of the LDM system.

lower. The filtering strength should therefore be chosen to maximize the number of counts per ghost. A more detailed description of the system can be found in [1].

An example of part of the beam profile histogram measured by the LDM during Fill 3005 in 2012 is shown in Fig. 2 (integrating over 5 minutes, or 3.3 million turns). Two features must be taken into account when resolving the relative bunch population:

1. Reduced detector availability due to the detector deadtime.
2. Afterpulsing from main bunches, which is comparable to, or greater than, the signal from ghost and satellite bunches.

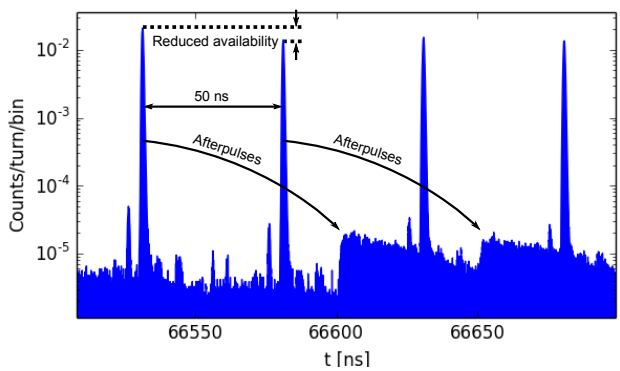

Figure 2: Part of the uncorrected profile histogram from fill 3005 (Beam 1). Main bunch separation is 50 ns. Satellites and ghosts are visible around the main bunches as smaller peaks.

The LDM sensors used in the LHC are of the PDM-series from Micro Photon Devices[1], with Peltier-cooling and integrated active quenching circuits. An identical spare detector was used for the characterization described in this paper, with the key figures summarized in Table 1.

* marcus.palm@cern.ch

[1] http://www.micro-photon-devices.com/

ISBN 978-3-95450-141-0

NOVEL FEMTOSECOND LEVEL SYNCHRONIZATION OF TITANIUM SAPPHIRE LASER AND RELATIVISTIC ELECTRON BEAMS

M. Titberidze*, F. Grüner, A.R. Maier, B. Zeitler, University of Hamburg, CFEL, Hamburg, Germany
M. Felber, K. Flöttmann, T. Lamb, H. Schlarb, C. Sydlo, DESY, Hamburg, Germany
E. Janas, Warsaw University of Technology, Warsaw, Poland

Abstract

Laser driven plasma accelerators are offering high gradient (~10-100 GV/m), high quality (low emittance, short bunch length) electron beams, which can be suitable for future compact, bright and tunable light sources. In the framework of the Laboratory for Laser-and beam-driven plasma Acceleration (LAOLA) collaboration at Deutsches Elektronen-Synchrotron (DESY) the external injection experiment for injecting electron bunches from a conventional RF accelerator into the linear plasma wave is in progress. External injection experiments at REGAE (Relativistic Electron gun for Atomic Exploration) require sub-20fs precision synchronization of laser and electron beams in order to perform a beam scan into the plasma wave by varying the delay between electron beam and laser pulses. In this paper we present a novel optical to microwave synchronization scheme, based on a balanced single output integrated Mach-Zehnder Modulator (MZM). The scheme offers a highly sensitive phase detector between a pulsed 800 nm Ti:Sa. laser and a 3 GHz microwave reference source. It is virtually independent of input laser power fluctuations and it offers femtosecond long-term precision. Together with the principal of operation of this setup, we will present promising preliminary experimental measurements of the new detector stability.

INTRODUCTION

Preparations for external injection experiments at REGAE facility for mapping the plasma wakefield are currently ongoing. At REGAE, electron bunches are generated by impinging commercial ultrafast (25 fs pulse duration) Ti:Sa. laser on a photo-cathode. Generated electrons are accelerated by S-band (resonance frequency f_{RF} = 2.9979 GHz) RF structure. Accelerated electrons reach maximum energy of ~ 5 MeV. Subsequently, electrons are longitudinally compressed down to 10 fs rms by S-band RF buncher using so called "ballistic bunching" technique, more details about REGAE can be found everywhere [1].

In order to deliver ultrashort electron bunches with femtosecond level accuracy for external injection purposes in a linear plasma wave, it is crucial to precisely synchronize photo-injector 83 MHz repetition rate 800 nm center wavelength Ti:Sa. laser oscillator to 2.9979 GHz RF source from Master Oscillator (MO).

Different approaches can be considered for synchronizing femtosecond laser pulses to RF reference signals: One could employ a so called direct conversion scheme which involves a fast photo-diode followed by an RF band-pass filter, used to extract a desired microwave signal from the laser pulse train. The phase difference between the RF reference and the microwave signal generated from the laser can be used to synchronize the latter. Currently, the direct conversion based down converter scheme is in daily operation at REGAE. General layout of the REGAE is shown in Fig. 1. It is clear form the block diagram that our reference source is RF Master Oscillator. Signals from MO are distributed to different sub-systems of the accelerator as well as to photo-injector laser for synchronization purposes.

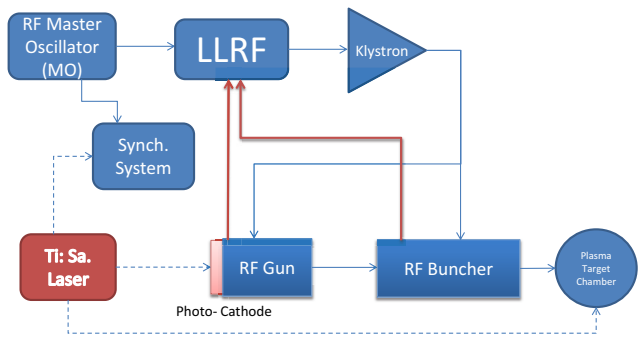

Figure 1: Layout of the RF and laser systems of REGAE.

In general, earlier mentioned direct conversion scheme suffers from AM/PM (amplitude modulation to phase modulation) effects in the photodiode, which can be as high as 1-3 ps/mW [2]. Another Laser to RF locking setup, which is highly accurate and very sensitive, uses an single output integrated electro-optical amplitude modulator (EOM, practically a Mach-Zehnder Intensity Modulator). The phase error between the laser pulse train and the RF reference causes an amplitude modulation of the laser pulse train, which can be detected with a photodiode much more accurately. The original idea of the new synchronization setup based on MZM was first published in 2011 [3] for RF stabilization purposes when the reference was laser itself. The scheme was realized for 1.3 GHz RF and 216 MHz repetition rate (FLASH and European XFEL frequencies) 1550 nm wavelength laser pulses and it showed very promising results ~ 15 fs peak-to-peak drift over 40 hours, the results were improved in 2013 where the experiment showed 3.6 fs peak-to-peak stability over 24 hours [4]. At REGAE, our reference is a 2.9979 GHz RF signal coming from RF Master Oscillator. Therefore, we

* mikheil.titberidze@desy.de

ISBN 978-3-95450-141-0

CW BEAM STABILITY ANALYSIS IN TIME AND FREQUENCY DOMAIN

M. Kuntzsch#, HZDR, Dresden Germany, TU-Dresden, Dresden, Germany
U.Lehnert, R.Schurig, J. Teichert, M.Gensch, S. Kovalev, B. Green, P. Michel, HZDR, Dresden, Germany

Abstract

The continuous wave (CW) mode of operation enables a high bandwidth jitter analysis for different diagnostic devices. The measurement is only limited by the bunch repetition rate and the acquisition time, since the bunch train is not interrupted by a macro pulse. At ELBE various diagnostics capable for continuous data acquisition has been installed and used for an analysis of noise sources. This paper comprises measurements from a bunch arrival time monitor (BAM), results from a fast beam position monitor (BPM) installed in a dispersive section and the power spectra from a coherent transition radiation (CTR) source.

INTRODUCTION

General

The recent update of the ELBE accelerator included the installation of a new beamline section which will be used to compress the electron bunches to a duration of 100 fs at a charge of 1 nC. Two THz sources based on coherent transition or diffraction radiation und and an undulator source making use of the compressed bunches [1]. The bunch shaping is done in multiple stages by using two magnetic chicanes [2]. Along the new beamline path a couple of diagnostic stations have been set up to measure the beam properties. Figure 1 gives an overview on the ELBE accelerator and the recently installed femtosecond-beamline. The schematic shows the location of beam diagnostics used to generate the data presented in this letter.

Diagnostics

The bunch compression monitors (BCM) are measuring the power of diffraction radiation generated by the electron bunches travelling thru a hole in a silicon screen. The amplitude increases when the bunch length is reduced. Fast detectors are used to acquire qualitative bunch by bunch information [3][4].

Bunch arrival time monitors (BAM) are used to measure the timing jitter of the electron bunches with respect to an optical reference. The reference is provided by a low noise laser synchronization system. The laser pulse train is modulated by an electro-optical modulator driven by a high bandwidth beamline pickup. The arrival time information is coded into an amplitude modulation of the laser pulses and analyzed with single bunch resolution [5][6]. BAM and BCM are located between the broadband THz source and the undulator. In this section the bunch compression is optimized for the THz production and the diagnostics experiences the same jitter as the secondary sources.

In order to observe beam energy fluctuations a spectrum analyzer was used to measure the modulation of a fast analog BPM readout based on a logarithmic amplifier [7]. The BPM pickup was installed in the dispersive section right after the THz sources before entering the beam dump. Energy fluctuations are translated into position variations after the dipole magnet. By keeping the trajectory of the beam entering the dipole constant measurement artifacts caused by beam pointing could be minimized.

To measure the impact of beam instabilities on the secondary radiation, the power spectrum of the coherent diffraction radiation has been measured inside the THz laboratory. The measurement has been done with a high dynamic range spectrum analyzer connected to a fast pyro-electric detector radiated by the THz field.

All measurements are limited by the bunch repetition rate and the acquisition time. Noise components faster than half the bunch rate violate the Nyquist theorem and cause aliasing. Mirror frequencies have been identified by comparison to measurements at other repetition rates.

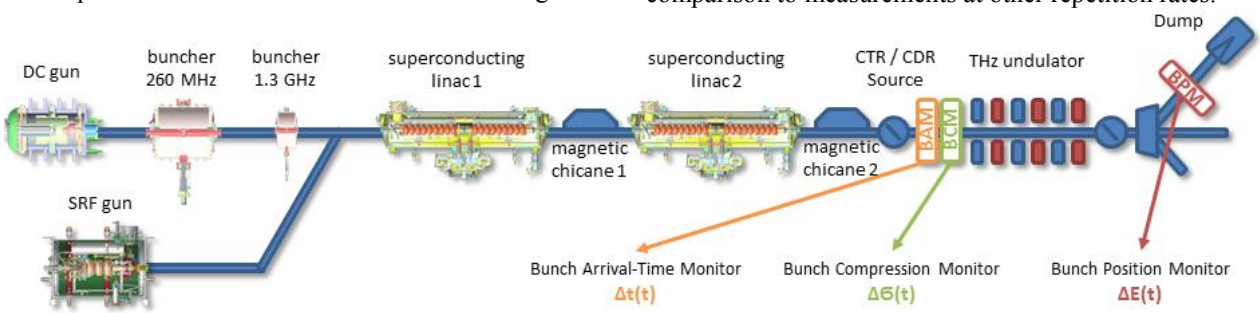

Figure 1: Schematic view on ELBE with two injectors, two superconducting accelerating cavies, magnetic chicanes for bunch compression and the THz sources. The diagnostics used to acquire the data for this contribution are highlighted, like bunch arrival time monitor, bunch compression monitor and energy dependent beam position monitor.

m.kuntzsch@hzdr.de

ISBN 978-3-95450-141-0

SINGLE-SHOT ELECTRO-OPTICAL DIAGNOSTICS AT THE ANKA STORAGE RING*

N. Hiller, A. Borysenko, E. Hertle, V. Judin, B. Kehrer, A.-S. Müller, M.J. Nasse, P. Schönfeldt, M. Schuh, N.J. Smale, J.L. Steinmann, KIT, Karlsruhe, Germany
B. Steffen, P. Peier, DESY, Hamburg, Germany
V. Schlott, PSI, Villigen PSI, Switzerland

Abstract

ANKA is the first storage ring in the world with a near-field single-shot electro-optical (EO) bunch profile monitor. The method of electro-optical spectral decoding (EOSD) uses the Pockels effect to modulate the longitudinal electron bunch profile onto a long, chirped laser pulse passing through an EO crystal. The laser pulse is then analyzed with a single-shot spectrometer and from the spectral modulation, the temporal distribution can be extracted. The setup is tuned to a sub-ps resolution (granularity) and can measure down to bunch lengths of 1.5 ps RMS for bunch charges as low as 30 pC. With this setup it is possible to study longitudinal beam dynamics (e. g., microbunching) occurring during ANKA's low-α_c-operation, an operation mode with longitudinally compressed bunches to generate coherent synchrotron radiation in the THz range. In addition to measuring the longitudinal bunch profile, long-ranging wake-fields trailing the electron bunch can also be studied, hinting bunch-bunch interactions.

INTRODUCTION

During the low-α_c-operation of the ANKA storage ring at the Karlsruhe Institute of Technology, the momentum compaction factor α_c is reduced to compress the bunches longitudinally and thus generate coherent synchrotron radiation (CSR) in the THz range [1]. Previous streak camera measurements have shown a beam current dependent bunch lengthening and deformation effect at ANKA in this special operation mode [2, 3]. In addition, the emitted CSR exhibits a bursting behavior [4–6], which we believe to be caused by dynamic changes of the longitudinal bunch shape (e. g., microbunching). EOSD offers the possibility to measure the longitudinal bunch profile and its arrival time relative to the revolution clock (f_{rev} = 2.7 MHz at ANKA) with a sub-ps time resolution without averaging. First single-shot measurements with the setup have indicated the formation of substructures on the compressed bunches [7], and we have now performed systematic studies of this behavior for different accelerator conditions. Additionally, the EO near-field setup is sensitive to the vertically polarized component of the wake-fields generated by an electron bunch passing the setup. Studying the transverse wake-fields, which are coupled to the longitudinal ones, and comparing them to simulations, helps greatly to improve the simulation model for longitudinal wake-fields [8]. The observed wake-fields range further than our minimum bunch spacing of 2 ns and could influence a following bunch. An increase of CSR has previously been observed at ANKA when the ring impedance was changed by inserting a copper scraper in order to induce strong wake-fields [9].

* This work is funded by the BMBF contract numbers: 05K10VKC, 05K13VKA.

METHOD

Electro-optical bunch length measurement techniques rely on the field-induced Pockels effect to modulate the longitudinal electron bunch profile onto a laser pulse passing through an EO crystal (further reference e. g., [10]). Figure 1 illustrates the working principle of EOSD.

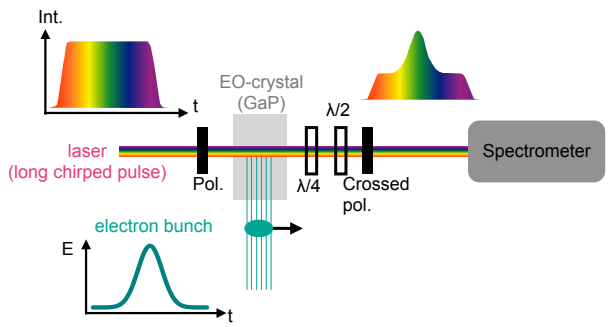

Figure 1: Schematic of EOSD (see text for details).

For the near-field measurements at ANKA, the EO crystal is brought close to the electron beam, so the direct Coulomb field of the bunch causes a modulation of polarization of the initially linearly polarized laser. This can be turned into an intensity modulation with the depicted optical components (quarter- and half-wave plates in combination with a crossed polarizer). Practically, the electric field of the bunch acts as a field-dependent phase retarder for the electric field of the laser pulse with the phase retardation being directly proportional to the field strength. For this to hold true, the crystal axis orientation, the direction of polarization of the Coulomb field and the laser need to be aligned in a specific way. Furthermore, the angles of the wave-plates need to be set in a way that the quarter-wave plate compensates the intrinsic birefringence of the the crystal and the half-wave plate regulates the transmission through the crossed polarizer (see e.g. [11] for a detailed description).
The laser system needs to be in sync with the bunch repetition rate and its delay with respect to the electron bunch

ISBN 978-3-95450-141-0

ALS TIMING SYSTEM UPGRADE*

J. Weber#, C. Lionberger, E. Norum, G. Portmann, C. Serrano, E. Williams, Lawrence Berkeley National Laboratory, Berkeley, CA 94720, USA

Abstract

The Advanced Light Source (ALS) is in the process of upgrading its timing system as a part of the ALS Instrumentation and Controls Upgrade project. The timing system built upon construction of the machine at the beginning of the 1990s is still in operation today, and a replacement of the machine timing system is under way based on a commercially available solution, benefiting from 20 years of improvements in the fields of digital electronics and optical communications. An overview of the new timing system architecture based on a Micro-Research Finland (MRF) solution is given here.

INTRODUCTION

The primary function of the ALS timing system is to synchronize and sequence all systems required to deliver beam from the gun through the injection system to the storage ring. In addition, the timing system synchronizes diagnostics to the beam and provides controls for optimizing injection efficiency and selecting the operating mode.

The existing timing system has a centralized architecture that performs control and logic functions locally and distributes individual signals with coaxial or single-fiber optical cables. The hardware modules are primarily based on discrete ECL and TTL logic and reside in eurocard bins [1]. The remote control interface is provided by three embedded Intelligent Local Controllers (ILCs) [2] that communicate with the logic modules through the custom bin backplanes. The ILCs communicate with the rest of the control system through a multi-drop 2 Mb/s serial link connected to a Multibus I processor which now connects to the newer EPICS-based control system equipment.

The timing system upgrade is part of a larger Instrumentation and Controls Upgrade (ICU) project at the ALS to modernize controls, improve machine performance, and reduce vulnerability to single-point failures and aging equipment. Many of the ILCs have been replaced by a plug-compatible ILC Replacement Module (IRM) [3], but it was not feasible to use this solution for ILCs in systems such as the timing system where their usage is more specialized. The ICU project also includes new systems with timing requirements that could not be met by the existing system without significant changes to the infrastructure. Some of these systems, such as Beam Position Monitors (BPMs) based on the NSLS-II BPM architecture [4], rely on event-based timing, which the existing system does not support.

A survey of similar, more modern accelerator timing systems revealed that the most common commercial solution for event-based timing systems was based on Micro Research Finland (MRF) [5] hardware. In particular, NSLS-II had developed EPICS drivers for the MRF hardware in their timing system [6]. MRF hardware was chosen as the platform for the new ALS timing system to accelerate development by leveraging demonstrated commercial hardware with EPICS drivers.

Since the timing system has many existing clients that are not in the scope of the ICU project, interfaces to existing equipment had to be carefully considered to define the scope of the timing system upgrade. In general, timing logic and distribution infrastructure that could be slaved to a new trigger from the MRF system was retained. In particular, the existing sequencing and trigger generation system for the Linac, the trigger distribution infrastructure for Booster magnets, and the user timing and gating systems for beamlines will be slaved to the new MRF system.

The existing timing system relies on a measurement of the Booster dipole magnetic field to generate raw Booster injection and extraction field triggers, and then synchronizes them to the RF domain and the beam, as described here [7]. The new system uses time-based field triggers, so the field measurement was separated into a new diagnostic system. This system takes the field triggers as inputs and provides a "field" stamp of the measured field at the time of each field trigger, which is available for monitoring in the control system.

An additional challenge with this upgrade is commissioning a complex new system on a multi-user accelerator with minimal impact to experimenters. This constraint requires careful planning to minimize the risk of downtime during installation, testing, and commissioning of new system components. To accommodate this, where possible the project has been broken into several phases so new functions, features, and equipment can be tested in smaller groups. A bench test environment and a parallel machine test system have been set up so development can be demonstrated as fully as possible before migrating to production.

ARCHITECTURE

The ALS event system consists of a central Event Generator (EVG), event distribution using high speed serial transceivers, fiber optic cables, and electro-optical fanouts, and an array of Event Receivers (EVRs) placed as close to existing client signal inputs as feasible, or embedded in the system firmware of new clients. Each EVG and physical EVR resides in a VME crate with an IOC running EPICS connected to the ALS control system

*This work was supported in part by the U.S. Department of Energy under Contract Number DE-AC02-05CH11231.
#jmweber@lbl.gov

ISBN 978-3-95450-141-0

BUNCH ARRIVAL TIME MONITOR FOR PAL-XFEL

J. Hong*, C. Kim, J.-H. Han, H.-R Yang, H.-S Kang, PAL, Pohang, Korea

Abstract

The X-ray Free Electron Laser project in Pohang Accelerator Laboratory (PAL-XFEL) requires high stability of bunch arrival time, and measurement resolution better than a few femtoseconds. The pickups of the electron Bunch Arrival time Monitor (BAM) for PAL-XFEL have been developed and simulated. The BAM pickups are based on an S-band monopole cavity with two coupling loops. The prototype BAM has been fabricated and installed downstream of the accelerating column at the Injector Test Facility (ITF) for PAL-XFEL. In this paper we will present the recent measurement results on the beam test of the BAM as well as a proposed strategy for developing the BAM for PAL-XFEL.

INTRODUCTION

PAL-XFEL requires high stability of bunch arrival time, and measurement resolution of bunch arrival time less than a few femtoseconds. The cavity type (monopole mode) BAM pickup is applied, which allows the detection of the bunch arrival time with a few femtoseconds. The BAM pickups are based on an S-band monopole cavity (LCLS type) with two coupling loop antennas. Figure 1 shows the geometry of the prototype BAM for PAL-XFEL. The prototype BAM

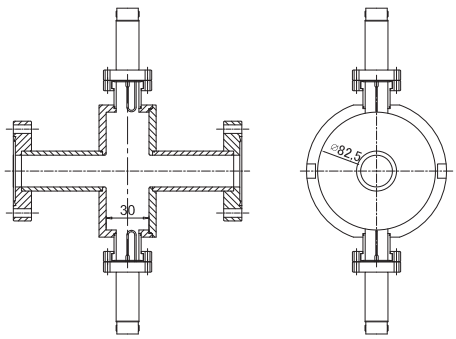

Figure 1: Prototype BAM geometry for PAL-XFEL.

pickup has been developed and installed downstream of the accelerating column at ITF [1] for PAL-XFEL. Figure 2 shows the photograph of the prototype BAM. The prototype BAM was tested for S-parameters and the results were compared to simulations. CST Microwave Studio is used to compute. Table 1 shows the resonance frequencies and their obtained quality factors. For the signal processing, the LLRF system is employed. Because the LLRF PAD is similar to electronics of the BAM. In the LLRF system, the RF signal is downconverted to the Intermediate Frequency (IF) signal while keeping the information of the preserved signal. The IF signal is sampled using by 16 bit Analog to Digital Converter (ADC) at a constant sampling rate of 238 MHz.

* npwinner@postech.ac.kr

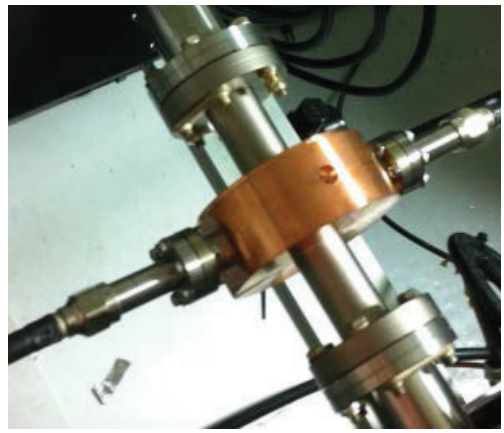

Figure 2: Photograph of the prototype BAM.

Table 1: BAM Pickup Parameters

Parameter	Value	Unit
Operating Frequency	2,823	MHz
Coupling Coefficient	0.1	
Quality Factor	10,000	

More detail on the LLRF system will be found in Ref. [2]. For the RF system, the RF frequency is 2,856 MHz, the LO frequency is 2,826.25 MHz, and then the IF frequency is 29.75 MHz. There frequencies are not well matched to the prototype BAM pickup.

SIGNAL PROCESSING

The schematic diagram of the signal processing is shown in Fig. 3. RF signal is firstly converted to IF signal and then directly digitized. If reference signal, $y_{\mathrm{Ref}}(t)$ and raw BAM signal, $y_{\mathrm{BAM}}(t)$ are:

$$\begin{aligned} y_{\mathrm{Ref}}(t) &= A_{\mathrm{Ref}}(t)\sin(\omega_{\mathrm{Ref}}(t)-\phi_{0,\mathrm{Ref}}), \\ y_{\mathrm{BAM}}(t) &= A_{\mathrm{BAM}}(t)\cos(\omega_{\mathrm{BAM}}(t)-\phi_{0,\mathrm{BAM}}), \end{aligned}$$

then IF signal, $y_{\mathrm{IF}}(t)$ can be written as:

$$y_{\mathrm{IF}}(t) = A_{\mathrm{IF}}(t)\cos(\omega_{\mathrm{IF}}(t)-\phi_{0,\mathrm{IF}}).$$

By using digital modulation the in-phase component, $I_{\mathrm{IF}}(t)$ and the quadrature-phase component, $Q_{\mathrm{IF}}(t)$ of the IF signal can be written as:

$$I_{\mathrm{IF}}(t) = \frac{A_{\mathrm{IF}}(t)}{2}\cos(\phi_{0,\mathrm{IF}}),\ Q_{\mathrm{IF}}(t) = \frac{A_{\mathrm{IF}}(t)}{2}\sin(\phi_{0,\mathrm{IF}}). \quad (1)$$

From Eq. 1, the amplitude, A_{IF} and the phase, $\phi_{0,\mathrm{IF}}$ can be calculated as:

$$A_{\mathrm{IF}}(t) = 2\sqrt{I_{\mathrm{IF}}^2+Q_{\mathrm{IF}}^2},\ \phi_{0,\mathrm{IF}} = \tan^{-1}\frac{Q_{\mathrm{IF}}}{I_{\mathrm{IF}}}.$$

ISBN 978-3-95450-141-0

BUNCH PATTERN MEASUREMENT VIA SINGLE PHOTON COUNTING AT SPEAR3*

Jeff Corbett†, Perry Leong and Linnea Zavala
SLAC National Accelerator Laboratory, Menlo Park, CA, 94025, USA

Abstract

SPEAR3 is a 3GeV storage ring light source with 500mA circulating beam current and a 5 minute top-up cycle. The bunch pattern contains 4 bunch 'trains' and a single timing pulse isolated by ±60ns dark space for laser pump/x-ray probe applications. In order to quantify the bunch pattern and charge purity of the probe pulse, a time-correlated single-photon counting system has been installed (TCSPC). In this paper we report on preliminary results using a photomultiplier tube with a commercial PicoHarp300 TCSPC device to identify bunch charge purity, afterpulse effects and top-up performance.

INTRODUCTION

SPEAR3 is an 18-cell, 234m circumference storage ring light source servicing 16 photon beam lines with up to 30 experimental endstations. The 476MHz RF system produces 372 RF buckets of which typically 280 contain charge bunches distributed in 4 bunch 'trains' separated by 30ns to minimize ion accumulation [1]. A single isolated timing pulse separated by ±60ns is available for time resolved pump/probe experiments using fast-gated detectors [2].

Charge injection into the 500mA electron beam takes place on a fixed 5 minute time interval. During each injection period the 10Hz booster synchrotron injects single-bunch pulses into consecutive SPEAR3 buckets until full current is restored. Each circulating bunch contains 1.4nC, or about 30 injection pulses (3% per shot). With a 9 hour electron beam lifetime, the periodic 1% beam loss is replenished by ~50 charge pulses containing 50pC each. Of significance, the arrival time of injected charge must be sufficiently accurate to avoid charge spill into adjacent buckets. The time separation between buckets is 2.1ns and the beam revolution time is 781ns (1.28MHz).

Historically a control room oscilloscope connected to a dedicated BPM was used to monitor the bunch pattern. More recently a PicoScope [3] was installed to enable remote viewing site wide. Although the 'scope solutions provide rough monitoring of the charge pattern, a more precise system is needed to measure bunch purity of the timing pulse and to study injector performance on a more quantitative basis. Furthermore, to remove unwanted charge, plans are underway to install x-y kicker magnets driven by the bunch-by-bunch feedback system [4].

In this paper we report on preliminary bunch pattern measurements using a Hamamatsu photomultiplier tube in conjunction with the PicoHarp300 TCSPC module [5].

*Work sponsored by US Department of Energy Contract DE-AC03-76SF00515 and Office of Basic Energy Sciences.
†corbett@slac.stanford.edu

The work follows directly from previous authors [6,7,8]. In short, for TCSPC, the PicoHarp300 records the time difference between the 1.28MHz storage ring orbit clock synchronization pulse (SROC) and single photon detection events. Upon integration, the resulting histogram displays the electron bunch pattern with potentially high resolution.

TCSPC DETECTOR CONFIGURATION

The PicoHarp300 was installed in the visible beam diagnostic laboratory at SPEAR3 [9]. At 500mA, the visible beam power is 0.5mW or about 10^{15} photons/sec. In order to reduce the count rate to ~1 count every 10 turns (7.8μs) the beam power incident on the PMT must be attenuated by 10 orders of magnitude. Most of the reduction was achieved by placing a small translatable pick-off mirror in the far beam halo. This arrangement also permits operation of other beam diagnostics in parallel. As shown in Fig. 1, redirected photons then pass through an ND filter and a 10nm bandpass filter inside a double-walled optical isolation box. A series of mirrors and irises serve to reduce background photon counts from ambient room light.

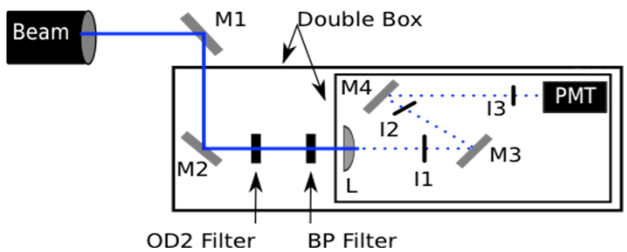

Figure 1: Schematic optical input system. The PMT has a dark count rate of 15 cps.

The PicoHarp300 was selected because it has two independent channels which can read up to 10^6 counts per second with 4ps time resolution [10]. Each channel requires a negative-going input pulse between 0V and -1V, and has a high resolution constant-fraction discriminator followed by time-to-digital conversion electronics (TDC) [10]. The 1.28MHz SROC is connected to Channel 1 as a timing reference (Sync port) after conversion from TTL to NIM in a commercial CAEN module.

Single photon detection was carried out using a Hamamatsu H7360-01 photon counting head [11]. The H7360-01 was selected based on experience with laser/SR cross-correlation bunch length measurements previously made in the diagnostics laboratory [12].

For each detected photon event, the H7360-01 outputs a single TTL pulse which is again converted to NIM and subsequently connected to PicoHarp300 Channel 2 (Signal port). Figure 2 shows the circuit schematic.

ISBN 978-3-95450-141-0

DEVELOPMENT STATUS OF SINAP TIMING SYSTEM

M. Liu*, K. C. Chu, C. X. Yin, L. Y. Zhao, SINAP, Shanghai, China

Abstract

After successful implementation of SINAP timing solution at Pohang Light Source in 2011, we started to upgrade SINAP timing system to version 2. The hardware of SINAP v2 timing system is based on Virtex-6 FPGA chip, and bidirectional event frame transfer is realized in a 2.5Gbps fiber-optic network. In event frame, data transfer functionality substitutes for distributed bus. The structure of timing system is also modified, where a new versatile EVO could be configured as EVG, FANOUT or EVR with optical outputs. Besides standard VME modules, we designed PLC-EVR as well, which is compatible with Yokogawa F3RP61 series. Based on brand new hardware architecture, the jitter performance of SINAP v2 timing system is improved remarkably.

INTRODUCTION

Timing information with high precision is required to synchronize distributed devices and equipments in large accelerator facilities. Based on event timing mechanism, SINAP timing solution provides trigger pulses with programmable polarity, width and delay. Edge aligned clocks with variable fractional factors are integrated in output function as well. [1]

We started to develop SINAP timing system since 2007. The prototype of SINAP timing system was completed and tested at LINAC of SSRF in January 2010. Pohang Light Source adopts the system in its upgrade project, and first beam accumulation was realized in August 2011. [2] [3] Subsequently, we modified system design and improved performance in SINAP v2 timing system. The hardware development is completed so far. And we will implement the system for different project this year.

SYSTEM DESIGN

Thanks to rapid development of high-speed serial communication and FPGA technology, event timing system became the sophisticated solution for timing system in the large-scale accelerator facilities, especially for the 3rd generation light source. The main advantage of event timing system is that the required triggers and clocks could be transmitted in the uniform fiber-optic network. This means wherever the timing system fiber-optic network reaches, triggers and clocks could be provided. [4]

SINAP v1 Timing System

SINAP v1 timing system adopts classic star broadcast topology based on fiber-optic link of 2.5Gbps. Single event clock from 120MHz to 135MHz is supported. All of EVG (event generator), EVR (event receiver) and FANOUT are standard 6U VME modules. All output triggers delay could be adjusted with coarse resolution of event clock period. Optical triggers from front panel of EVR could be additionally adjusted with fine delay resolution of 1/20 event clock period and 5ps. Interrupt function is integrated in EVG and EVR. The event logic and VME local bus is realized in Virtex-4 FPGA chip and CPLD respectively. [5] The system structure is illustrated in Fig. 1.

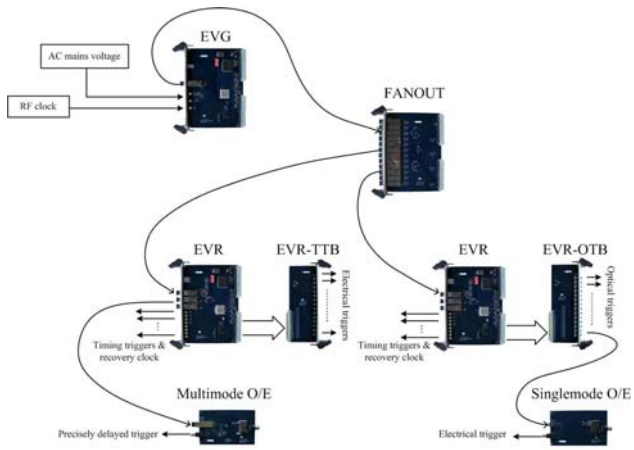

Figure 1: Structure of SINAP v1 timing system.

Software of the system is based on EPICS base 3.14.8.2 and vxWorks 5.5.1. During injection, the positions of all injection event codes stored in Sequence RAM of EVG are changed, but delay values of EVR output keep fixed. When transmission of all event codes is completed, an interrupt is generated in EVG, which makes a new list of event codes added to Sequence RAM. The whole mechanism is easy and efficiency. [6]

SINAP v2 Timing System

SINAP v2 timing system adopts similar topology based on fiber-optic network as well, but communication mode upgrades from simplex to duplex, which means that we could conduct deterministic data transfer and event distribution at the same time.

The frame format in the new version is illustrated in Fig. 2. One byte is for event code and the other byte is for data frame. Conventional distributed bus is abandoned, and all clocks are generated in EVR. Event clock from 60MHz to 135MHz is supported. EVG cascading function is supported. Two or more RF clocks are allowed to exist and synchronize output triggers in one single system consequently. Besides, all output triggers, no matter

*liuming@sinap.ac.cn

ISBN 978-3-95450-141-0

DIAGNOSTICS OF AND WITH LASER-INDUCED ENERGY MODULATION AT THE DELTA STORAGE RING*

S. Khan†, S. Hilbrich, M. Höner, H. Huck, M. Huck,
C. Mai, A. Meyer auf der Heide, R. Molo, H. Rast, P. Ungelenk,
Center for Synchrotron Radiation (DELTA), TU Dortmund University, 44227 Dortmund, Germany

Abstract

DELTA is a 1.5-GeV synchrotron light source operated by the Center for Synchrotron Radiation at the TU Dortmund University. An interaction between electron bunches and femtosecond laser pulses is routinely used to generate ultrashort pulses of coherent synchrotron radiation at harmonics of the laser wavelength (coherent harmonic generation, CHG) as well as short and coherent pulses in the THz regime. The paper describes diagnostics methods to optimize the laser-electron overlap and to characterize the generated VUV and THz pulses. Furthermore, the laser-electron interaction can be employed as a beam diagnostics tool, e.g. to study the longitudinal steady-state bunch profile as well as dynamic properties during RF-phase modulation, which is applied to improve the beam lifetime.

INTRODUCTION

Synchrotron radiation (SR) sources based on electron storage rings [1] are complementary to high-gain free-electron lasers (FELs) [2] in various ways. The extreme peak brilliance of FELs has opened up new scientific opportunities, while the brilliance of SR sources, having increased by several orders of magnitude per decade, is still sufficient for many applications. Since high-gain FELs are based on linear accelerators, they serve only one experiment at a time with a relatively low pulse repetition rate, while SR sources are multi-user facilities producing very stable beams with a pulse rate of up to 500 MHz. The pulse duration of FELs is in the femtosecond regime allowing to study dynamic processes such as chemical reactions, structural and electronic changes in molecules or crystals, or fast magnetic phenomena, while the pulses from SR sources with a duration of 30 to 100 ps (FWHM) are inadequate for this purpose. Presently, four high-gain FELs are in user operation while about 50 SR sources exist worldwide. Reducing the pulse duration of SR sources by about three orders of magnitude would, therefore, increase the research opportunities for a very large user community.

While the electron bunches can be shortened to a few picoseconds by reducing the momentum compaction factor [3, 4], sub-picosecond SR pulses are obtained by extracting radiation from a small longitudinal fraction (a "slice") of long electron bunches [5]. To this end, the electron energy is modulated by the electric field of a femtosecond laser pulse co-propagating with the bunch in an undulator. The modulation has the periodicity of the laser wavelength, an envelope similar to the laser pulse shape, and an amplitude proportional to the square root of the laser pulse energy. Typically, Ti:sapphire laser systems are employed with a wavelength of 800 nm, a pulse energy of a few mJ and a repetition rate in the kHz range, leading to a modulation amplitude of 5-10 times the rms energy spread within a slice of 1/1000 of the bunch length. An undulator used for this purpose is called "modulator". The laser-induced energy modulation may be employed in several ways (Fig. 1):

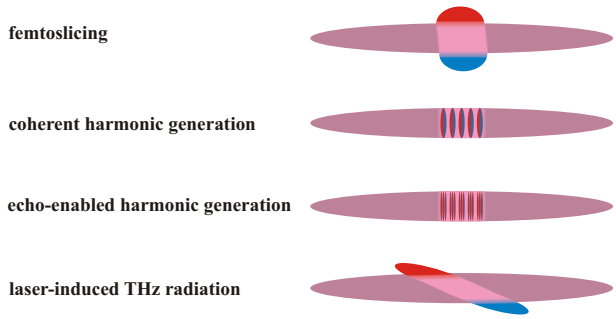

Figure 1: Laser-based methods to generate ultrashort SR pulses (see text). Note that the central "slice" of energy-modulated electrons (red and blue) is typically 1000 times shorter than the whole bunch.

- Off-energy electrons are transversely displaced in magnets such that their short SR pulse from a second undulator (the "radiator") can be separated spatially from the long pulse produced by the other electrons. In this "femtoslicing" scheme [6], the radiator wavelength can be tuned to any value. Even though incoherent SR from a small fraction of the bunch is rather weak and the laser pulse rate is 10^{-5} of the bunch rate, this scheme produces significant scientific results at the ALS in Berkeley/USA [7, 8], BESSY in Berlin/Germany [9, 10], and the SLS in Villigen/Switzerland [11, 12]. Another femtoslicing source is currently under commissioning at SOLEIL in Saint-Aubin/France [13].

- Using a dispersive chicane, the energy modulation may be translated into a periodic density modulation giving rise to coherent radiation at harmonics of the laser wavelength. Since the coherent SR intensity scales with the number of energy-modulated electrons squared [14], it is higher than the incoherent SR intensity from the rest of the bunch, and no spatial separation is required. This scheme, called CHG (coherent harmonic generation) [15], is restricted to harmonics $h < 10$ since

* Work supported by BMBF (05K13PEC), DFG (INST212/236-1), and by the state NRW.
† shaukat.khan@tu-dortmund.de

ISBN 978-3-95450-141-0

TIME DOMAIN PICKUP SIGNAL CHARACTERISATION FOR LOW CHARGE ARRIVAL-TIME MEASUREMENTS AT FLASH*

A. Angelovski†, A. Penirschke, R. Jakoby, Institut für Mikrowellentechnik und Photonik, TU Darmstadt, Germany
M.K. Czwalina, C. Sydlo, H. Schlarb, DESY, Hamburg, Germany
T. Weiland, Institut für Theorie Elektromagnetischer Felder, TU Darmstadt, Germany

Abstract

For the low charge operation mode at the European XFEL, high bandwidth cone-shaped pickups were developed as a part of the Bunch Arrival-time Monitors (BAMs). The simulation showed that the signal parameters of interest, the signal slope and bandwidth are improved by more than a factor of six compared to the state of the art pickups. The pickups are installed at FLASH for verification. In this paper, time domain measurements of the cone-shaped pickups at FLASH are presented. The pickup signal is recorded with a high bandwidth sampling oscilloscope. Two channel measurements are conducted with a single and a combined pickup signal in order to analyse the orbit and charge dependence. The measured time domain pickup signal wave form is compared with the full wave CST PARTICLE STUDIO as well as with the Agilent Advanced Design System (ADS) simulation.

INTRODUCTION

In order to measure the arrival-time of the electron bunches at FLASH, Bunch Arrival-time Monitors (BAMs) are installed as an integral part of the laser-based synchronisation (LbSyn) system [1,2]. A BAM comprises RF pickups, electro-optical and RF front-end and read-out electronics. The beam induced pickup signal modulates the amplitude an external laser pulse train in the Mach-Zender type electro-optical modulator (EOM). The reference timing is determined by the laser pulse sampling the pickup signal at the zero-crossing resulting with a zero amplitude modulation at the output of the EOM. An arrival-time jitter of the electron bunch and thus of the transient signal translates into a laser amplitude modulation. The arrival-time is deduced by comparing the amplitude of the modulated laser pulse to the adjacent ones. The sensitivity of the BAMs depends on the pickup signal slope steepness. This detection scheme provides for a time resolution of the arrival-time measurements of less then 10 fs for bunch charges above 500 pC. For the new European - XFEL a low charge operation mode is planed with bunch charges of 20 pC. As the bunch charge reduces below 200 pC, the time resolution of the BAMs decreases significantly [3]. For improving the time resolution for low charges the bandwidth of the BAMs is increased from the current 10 GHz to 40 GHz. The high bandwidth system provides for a beam induced signal with steeper slope compared to the low bandwidth one.

Cone-shaped Pickups

The cone-shaped pickups were developed in [4] as a part of the 40 GHz BAMs for low bunch charge operation of the European-XFEL. Figure 1 shows the cross-section of the pickups with dimensions.

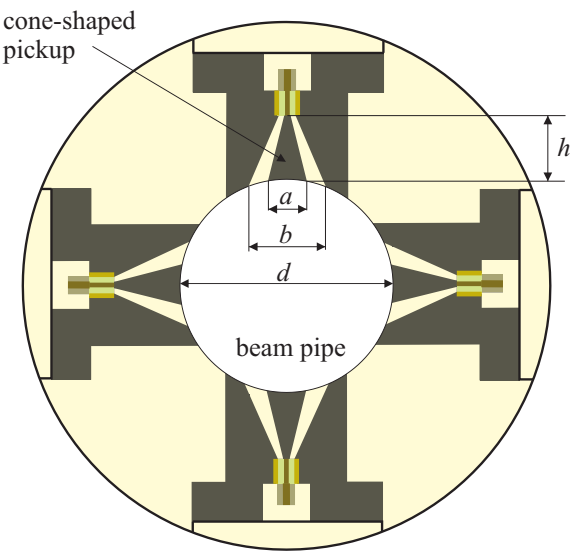

a = 2.42 mm	h = 6 mm
b = 5.60 mm	d = 40.50 mm

Figure 1: Cross section of the cone-shaped pickup with dimensions [4].

The simulated slope steepens at the zero-crossing is 417 mV/ps and it is by a factor of six higher compared to signal slope of the current 10 GHz pickups [4]. The pickups are installed in FLASH for testing and evaluation as part of the BAMs for low charges.

In this paper we present the time domain measurements of the cone-shaped pickups at FLASH. A comparison between the measured wave forms and simulations is performed for validation of the results. The signal slope is evaluated for different bunch charges and orbit displacements.

* Work supported by the German Federal Ministry of Education and Research (BMBF) within Joint Project - FSP 302.
† angelovski@imp.tu-darmstadt.de

ISBN 978-3-95450-141-0

A BUNCH EXTENSION MONITOR FOR THE SPIRAL2 LINAC

J.L. Vignet, R. Revenko, GANIL, Caen, France

Abstract

Measurements of the bunch longitudinal shape of beam particles are crucial for optimization and control of LINAC beam parameters and maximization of its integrated luminosity. The non-interceptive bunch extension monitor for the LINAC of SPIRAL2 facility is being developed at GANIL. Five bunch extension monitors will be installed at the beginning of the LINAC between superconducting cavities. The principle of operation is based on the registration of x-rays induced by ions of accelerator beam interacting with a thin tungsten wire positioned on the beam path. The monitor consists of two parts: a system for wire insertion and positioning, and an x-ray detector based on microchannel plates (MCP). A detector prototype has been developed for three years and was tested using protons and heavy ions beams. The influence of the cryomodule operation on the diagnostic measurement was also studied.

INTRODUCTION

The SPIRAL2 project [1] is based on a multi-beam LINAC driver in order to allow both ISOL and low-energy in-flight techniques to produce RIB. A superconducting light/heavy-ion LINAC capable of accelerating 5 mA deuterons up to 40 MeV and 1 mA heavy ions up to 14.5 MeV/u is used to bombard both thick and thin targets. These beams could be used for the production of intense RIB by several reaction mechanisms (fusion, fission, transfer, etc.) and technical methods (ISOL, IGISOL, recoil spectrometers, etc.). The production of high intensity RIB of neutron-rich nuclei will be based on fission of uranium target induced by neutrons, obtained from a deuteron beam impinging on a graphite converter (up to 10^{14} fissions/s) or by a direct irradiation with a deuteron, ^{3}He or ^{4}He beam.

The accelerating RF of the LINAC [2] is 88.0525 MHz. It means that time distance between two bunches is 11.26 ns. The extension of the phase for bunch (±2σ) is 60˚ or ~1,6ns for bunch length. The LINAC can operate at continuous or pulsed mode with period of macropulse between 100 µs and 1s.

Correct adjustment of the LINAC is necessary for obtaining maximal intensity and luminosity on the target. Adjusting includes synchronization of phase for each acceleration section. For this reason, information about bunch length distribution is needed and will be obtained using a Bunch Extension Monitor (BEM). These diagnostic detectors will be placed inside the warm sections between superconducting acceleration cavities. Each warm section consists of two quadrupoles and diagnostic box placed in between. Five BEM will be mounted into the first five diagnostic boxes at the LINAC entrance where deuteron beam energy will be between 1.46 and 2.29 MeV.

BEM DESCRIPTION

Bunch extension monitor is a non-destructive beam diagnostic detector for estimation of the length of LINAC bunches. The principle of BEM measurement is based on registration of x-rays emitted from a thin tungsten wire due to the interaction with ions beam. All components of BEM should meet UHV requirements since the LINAC will be operated at 10^{-8} mbar. Moreover, all BEM materials must satisfy required purity conditions for preventing cavity pollution.

BEM Working Principle

The photons emitted from the tungsten wire will be produced due to ionization of atoms hit by beam ions. The ions can knock-out electrons from inner shells and produce electron vacancy. Electrons from outer shells fill this vacancy and emit the difference of energy of bound states as characteristic x-ray photons. The energies of emitted characteristic photon are unique for each element and in case of tungsten they are 60 keV and 11 keV for K- and L-shell ionization respectively. A two stage microchannel plates is used to produce photoelectrons and multiplied them. Output signal is transmitted through coaxial cable to the input of a constant fraction discriminator CFD 7174. Signal of accelerator RF comes to another channel of CFD. The two logical signals from CFD output are sent to a time-to-amplitude converter Ortec 566 as “start” and “stop” signals. The output signal from TAC (whose amplitude is proportional to the time difference) is digitized by multichannel analyzer CANBERRA Multiport II. The Schema of BEM electronics operation is presented in Fig. 1.

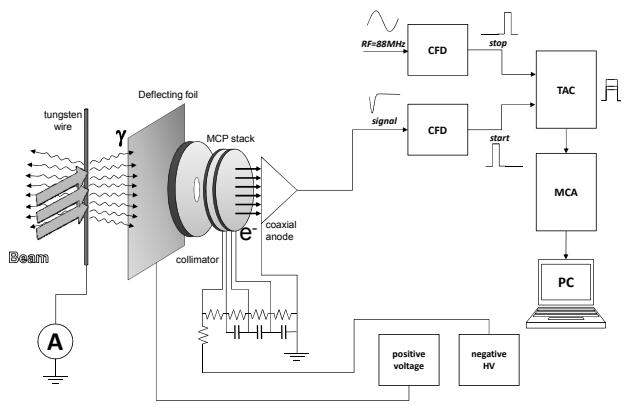

Figure 1: Principal schema of operation of BEM electronics.

X-rays of ^{55}Fe was used to measure the electronic temporal resolution. Output signal from detector prototype was transmitted through a long coaxial cable of 70 meters length and split in two signals. Both signals

ISBN 978-3-95450-141-0

THE BEAM INSTRUMENTATION AND DIAGNOSTIC CHALLENGES FOR LHC OPERATION AT HIGH ENERGY

O. R. Jones, CERN, Geneva, Switzerland

Abstract

This contribution will present the role of beam diagnostics in facing the challenges posed by running the LHC close to its design energy of 7TeV. Machine protection will be ever more critical, with the quench level of the magnets significantly reduced, so relying heavily on the beam loss system, abort gap monitor, interlocks on the beam position and fast beam current change system. Non-invasive profile monitoring also becomes more of a challenge, with standard synchrotron light imaging limited by diffraction and rest gas ionisation monitoring dominated by space charge effects. There is also a requirement to better understand beam instabilities, of which several were observed during Run I, leading to the need for synchronised bunch-by-bunch, turn-by-turn information from many distributed instrumentation systems. All of these challenges will be discussed along with the strategies adopted to overcome them.

INTRODUCTION

The first beam was injected into the LHC during tests in August 2008, with circulating beams established on the 10th September 2008. Nine days later disaster struck as a fault in one of the superconducting circuits led to the release of 600MJ of stored energy during a test of high current powering. It took over a year to recover from the damage caused by this event, with over 30 magnets needing to be repaired or replaced. After intensive investigations the source of this accident was concluded to be due to a faulty splice between the superconducting cables of neighbouring magnets. In addition it was found that for many magnets there was poor electrical and thermal conductivity between the superconducting cable and the copper stabiliser surrounding these joints. In the event of a magnet quench, when the superconductor becomes normal conducting due to overheating, these copper stabilisers take the full current until it can be safely extracted, a process which takes several minutes. Under such circumstances any poor contacts can lead to a thermal runaway, resulting in a similar accident to the one experienced in 2008. Due to these issues it was decided to initially run the LHC at half its design energy of 7TeV. This represents some 6kA in the main circuits, a current which was considered could be safely extracted even with such poor contacts still present in the machine.

The beam was back in the machine for commissioning on the 29th November 2009, with first physics collisions at 3.5TeV per beam occurring on 30th March 2010. This was the start of 3 years of nearly continuous LHC operation, culminating in the discovery of the Higgs boson on the 4th July 2012. During this time the stored beam intensity was gradually increased, with the energy also increased to 4TeV per beam in 2012. A total integrated luminosity of nearly 30fb^{-1} was accumulated over this period (Fig. 1), with the LHC ending the 2012 run reaching peak luminosities of 8×10^{34} cm^{-2}s^{-1}, close to its design value of 10^{34}.

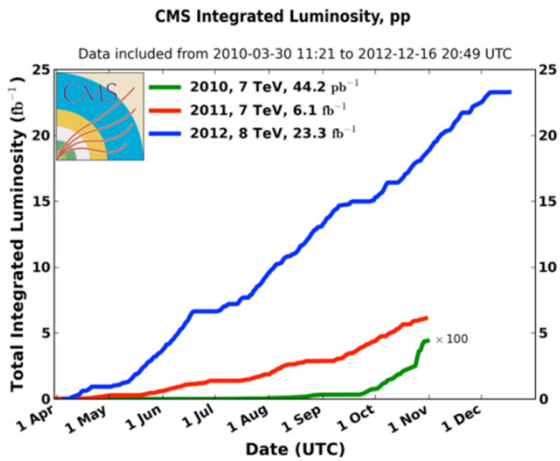

Figure 1: LHC performance during Run I.

In order for the LHC to work at, or close to, its nominal energy of 7TeV, major consolidation of all the superconducting circuits was necessary. Long Shutdown 1 (LS1) started on the 14th February 2013 with the aim of consolidating over 10,000 superconducting splices, reducing the effects of radiation to electronics and carrying out full maintenance on all equipment, including the majority of beam instrumentation systems.

At the time of writing, this consolidation work is complete and the LHC is in the process of being cooled to 1.9K before the start of hardware commissioning. The beam is currently expected back in March 2015, with the LHC foreseen to run at 6.5TeV for the remainder of that year.

The beam instrumentation and diagnostic systems of the LHC [1] worked remarkably well throughout Run I, and played an important part in the rapid commissioning and reliable operation of the machine. However many lessons have been learned and shortcomings identified, the majority of which have been addressed during the long shutdown. Run II of the LHC, at an energy close the design energy of 7TeV, will in addition bring its own challenges, and it is these that will be addressed in this contribution.

ISBN 978-3-95450-141-0

MANAGING ELECTROMAGNETIC INTERFERENCE IN LARGE INSTRUMENTATION SYSTEMS*

M. Gruchalla, EG&G Division of URS, Albuquerque, NM 87110, USA
M. Thuot, Los Alamos National Laboratory (Retired), NM 87545, USA

Abstract

Implementing high-quality measurement systems in large test environments presents a number of unique challenges. And, these challenges are made even more interesting where new instrumentation systems are being implemented in existing legacy environments where there is little opportunity to modify the infrastructure. Often, Electromagnetic Interference (EMI) is encountered. This interference may be simply an annoyance when sufficiently low that data integrity is not severely compromised, but in many cases, perhaps most, EMI is so severe as to totally obscure the signals of interest. Various sources of EMI and common points of entry of are reviewed. Means of mitigation of EMI in the design and implementation of instrumentation systems in legacy environments are presented. Common sources of EMI potentially introduced by the instrumentation systems themselves are examined, and means of design to mitigate such self-induced interference are examined. Real-life examples are provided to demonstrate the EMI issues, and the effect of mitigation. It's all about the current – pretty much!

EMC vs EMI

Virtually everyone involved in instrumentation systems has encountered electronic noise that corrupts data acquisition. Two terms used in instrumentation venues in discussion of electromagnetic effects are Electromagnetic Compatibility ("EMC") and Electromagnetic Interference ("EMI"). Often it is found that these two terms are used somewhat interchangeably. This however is incorrect interpretation of the terms.

EMC is a goal to be achieved. EMI is a corrupting signal compromising competent collection of data signals. Very simply, the goal of EMC is to minimize EMI.

Specifically, the goal of EMC is to "minimize" EMI, but not to totally eliminate the EMI signals. Interfering signals need only be reduced to the level that allows competent collection of the signals of interest. Although it may be feasible to further reduce EMI, there is little to be gained in terms of the data acquisition, and there may be significant increases in cost and time.

EMC is most effectively managed in the initial design of a facility. At this point, such critical elements as grounding structures, placement of high-energy sources, instrumentation placement, high-energy cable parameters, high-energy cable routing, signal-cable parameters, signal-cable routing, conduit systems for carrying high-energy and signal cables, and virtually all other characteristics of the facility may be addressed to attempt to assure that interference is minimized.

However, typically the facility infrastructure is designed to support the mission, and the instrumentation systems simply must live in this environment. And in many cases, perhaps most, instrumentation systems must be implemented in facilities and systems that have been in place for a very long time, e.g., legacy systems.

STANDARDS AND REFERENCES

There are numerous EMC standards. A number of IEEE publications address the EMC topic, and one of the more common references is MIL-STD-461 [1]. In general, two specific types of emissions are considered: Radiated Emissions ("RE") and Conducted Emissions ("CE"). Similarly, two specific types of susceptibility are considered: Radiated Susceptibility ("RS") and Conducted Susceptibility ("CS").

Although standards are necessary and valuable, these simply define emissions allowable from a source, and the required tolerance to emissions of systems exposed to the allowed emissions. Standards tell you what you must do, but do not give you any guidance as to how to do it.

There are also numerous "How To" references providing insight into both control of emissions and minimizing EMI. One of the industry standards is *Noise Reduction Techniques in Electronic Systems* by Ott [2]. However, in many cases, these references are highly theoretical and very general, and it is often found that it is quite difficult to apply the guidance in "your" systems. And, often the guidance provided is more easily implemented in new designs, and more difficult in legacy systems. For example, just how does one implement a "single-point ground" and avoid "ground loops" in a new cable plant installation in a facility where cable plants are as much as a hundred meters long, and perhaps even much longer, and where all the high-energy cables and other potential noise sources are permanently in place?

CLASSIC EMC DESIGN PROCESS

There is no standardized process in applying EMC principles to minimize EMI. Every situation is unique, and must be examined independently based on the specific system elements and the operational requirements. However, the general design approach to assure EMC reviewed in many references is typically the control of the emissions at the source.

* This material is based upon work supported by the U.S. Department of Energy, Office of Science, Los Alamos National Laboratory under Contract No. DE-AC52-06NA25396.

ISBN 978-3-95450-141-0

DIAGNOSTICS FOR HIGH POWER ACCELERATOR MACHINE PROTECTION SYSTEMS*

S. Lidia#, Facility for Rare Isotope Beams, Michigan State University, East Lansing, MI, USA

Abstract

Modern hadron accelerators create and transport beams that carry MW-scale power or store GJ-scale energy. The Machine Protection Systems (MPS) that guard against both catastrophic failures and long-term performance degradation must mitigate errant beam events on time scales as short as several microseconds. Measurement systems must also cope with detection over many orders of magnitude in beam intensity to adequately measure and respond beam halo loss. Other issues, such as radiated signal cross-talk, also confound and complicate delicate measurements. These requirements place enormous demands on the MPS beam diagnostics and beam loss monitors. We will review the current state of MPS diagnostic systems for this class of accelerator, including SNS, ESS, FRIB, LHC, J-PARC, and SPIRAL-II. Specific designs and key performance results will be presented and discussed.

INTRODUCTION

Trends in modern accelerators push at the boundaries of beam energy (LHC, ILC), beam power (Fig. 1) and brightness [1][2]. Accelerator based neutron-generating facilities (SNS, JPARC, PSI, LANSCE) have pushed the frontier of proton beam power to 1 MW, with 5 MW beams in development [ESS]. For heavy ion beams, the frontier will be advanced by more than two orders of magnitude to 400 kW at FRIB [FRIB]. High energy hadron colliders have pushed the frontier of stored proton beam energy from 1-3 MJ (SPS, RHIC, HERA, TEVATRON) to 140 MJ (LHC, design goal 360 MJ).

Key technology development has powered the push at high intensity frontier [1]. Continuing improvements in SRF accelerator and large-scale cryogenics enable efficient, high gradient acceleration and robust operation. Ion source, RFQ, and low energy beam transport produce intense, high charge state, high brightness, CW beams. High power charge strippers and beam collimators accept many kWs of beam power. Rapid-cycling booster synchrotrons accept and accumulate high intensity beams and then accelerate with minimal losses. High power beam targets and radiation resistant magnets operate are necessary to handle the intense thermal and radiation fields generated. Finally, loss detection and machine protection techniques are crucial to prevent damage from prompt, fast events and to monitor and control chronic losses from small ($<10^{-4}$-10^{-6}) fractions of the beam power.

*This material is based upon work supported by the U.S. Department of Energy Office of Science under Cooperative Agreement DE-SC0000661, the State of Michigan and Michigan State University.
#lidia@frib.msu.edu

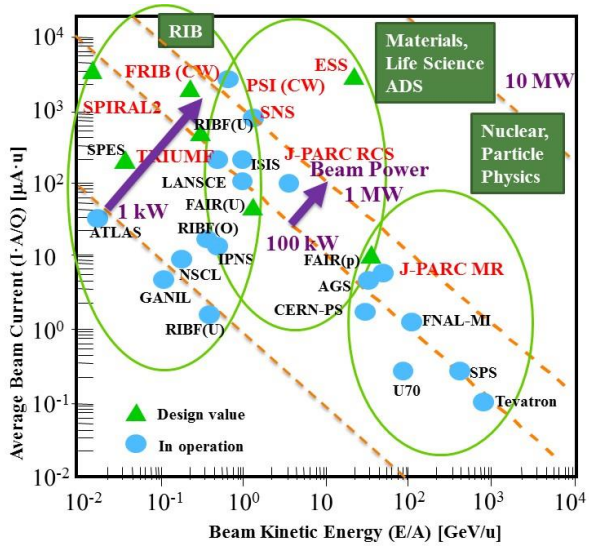

Figure 1: Development of high power hadron accelerators. [1].

MACHINE PROTECTION SYSTEM BASICS

Machine protection systems exist to avoid prompt and long-term damage to the accelerator and experimental instrumentation, to minimize the number of false trips that limit production, and to provide evidence of failures or fault events when interlock systems stop beam operation [3][4].

Machine failures can derive from several sources. Hardware failures can include power supply trips, magnet or cavity quench, RF trips and low-level control loss, loss of vacuum, etc. Control system failures include incorrect calibrations and settings updates, trigger mistiming and timing distribution errors, feedback malfunctions. Operational sources include tuning and steering errors, and administrative controls on beam mode and machine state. Beam instabilities at high current or high brightness can develop quickly and damage components.

The time response for MPS interdiction ranges over many orders of magnitude. Fast protection systems (FPS) serve to protect against prompt damage from beam impacts. Typical FPS response times can vary from several to some hundreds of microseconds, and reflect thermodynamic changes of accelerator materials caused by errant beams. Run permit systems (RPS) operate on a slower time scale, from milliseconds to many seconds, typically, and are used to verify machine state and identify conditions that may lead to unintended damage or long term irradiation effects that limit personnel access. As accelerator facilities may function

ISBN 978-3-95450-141-0

STUDY OF SCINTILLATION STABILITY IN KBR, YAG:CE, CAF_2:EU AND CSI:TL IRRADIATED BY VARIOUS-ENERGY PROTONS *

L. Y. Lin#, D. Leitner, C. Benatti, S. W. Krause, R. Rencsok, S. Nash, W. Wittmer,
NSCL, East Lansing, MI 48824, USA
G. Perdikakis, Central Michigan University, Mt. Pleasant, MI 48859, USA

Abstract

The luminescence of KBr, YAG:Ce, CaF_2:Eu and CsI:Tl scintillators induced with H_2^+ ion beams in the energy range of 600-2150 keV/u has been systematically measured as a function of irradiation time. The measurements showed that the luminescence of CsI:Tl and YAG:Ce remained constant within the 1-hour continuous irradiation. An initial fast drop of the luminescence on CaF_2:Eu was observed but the light output eventually approached a stable state under constant ion bombardment. We also observed that the light output of KBr initially increased and then degraded gradually with further irradiation. The CsI:Tl screen produced the highest scintillation yield and KBr the lowest.

INTRODUCTION

The wide use of scintillator screens in beam profile measurements and pepper-pot emittance systems has motivated a number of studies [1-4] on the scintillation stability under ion irradiation. The scintillation degradation caused by radiation damages can deteriorate the accuracy of beam width and emittance measurements. The degradation of luminescence can be attributed to many factors, some of which are related to the nature of the scintillator materials, the accumulated fluence, and the energy of bombarding particles. In a previous work [5], we have reported that the scintillation yield of single crystal YAG: Ce was significantly degraded under low-energy (28-58 keV) He^+ irradiation. By using the Birks model, we explained that the decrease of the observed light yield in YAG:Ce is the result of a competition between the creation of luminescence photons and displacement damage defects. The model allows to quantitatively explain how the degradation time depends on the bombarding energy in the low radiation energy range. The degradation of scintillation yield is reduced as the beam energy increases under low-energy bombardments.

In this report, our measurements were focused on investigating the scintillation stability of KBr, YAG:Ce, CaF_2:Eu and CsI:Tl single crystals under H_2^+ irradiation at the energies of 600-2150 keV/u. The scintillation materials and their optical properties [6] are listed in Table 1 together with their manufacturers and dimensional sizes. The choice of these materials was based on their availability and common use as diagnostics in low energy accelerators delivering low intensity beams.

Table 1: The Scintillator Materials under Study

Material	CsI:Tl	CaF_2: Eu	YAG: Ce	KBr
Density (g/cm^3)	4.51	3.18	4.55	2.74
Light yield photons/MeV	55,000	24,000	16,700	----
Thickness (mm)	1	1	1	2
Diameter (mm)	19	19	18	19
Manufacturer	SGC	SGC	MII	ICL

SGC: Saint-Gobain Crystals [7]
MII: Marketech International Inc. [8]
ICL: International Crystal Laboratory [9]

EXPERIMENTAL SETUP

The irradiation experiments were performed at the rare isotope ReAccelerator (ReA) facility of the National Superconducting Cyclotron Laboratory (NSCL) in Michigan State University (MSU). A H_2^+ beam from a stable ion beam injector was accelerated by a room temperature RFQ and the SRF linac, and then delivered to the scintillator target chamber installed in the ReA experimental hall, as shown in Fig. 1. The four different scintillator materials were held on a rotating target wheel inside the chamber under vacuum. A CCD camera (PCO

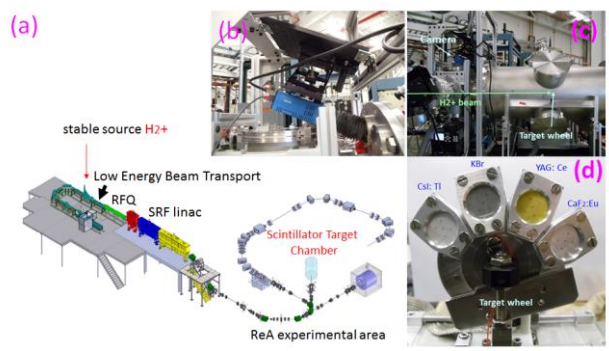

Figure 1: (a) Layout of the beam delivery to the scintillator target chamber in the ReA facility of NSCL. The experimental setup consists of (b) a CCD camera, (c) a target chamber and (d) a target wheel with four different scintillator screens.

*Supported by Michigan State University.
Lingy@frib.msu.edu

ISBN 978-3-95450-141-0

PULSED GREEN LASER WIRE SYSTEM FOR EFFECTIVE INVERSE COMPTON SCATTERING*

Arpit Rawankar#, School of High Energy Accelerator Science, Graduate University for Advanced Studies, Shonan International Village, Hayama, Miura, Kanagawa 240-0193, Japan
Tomoya Akagi, Alexander Aryshev, Yosuke Honda, Nobuhiro Terunuma, Junji Urakawa, High Energy Accelerator Research Organization [KEK], 1-1 Oho, Tsukuba, Ibaraki 305-0801, Japan
Didier Jehanno, Laboratoire de l'Accélérateur Linéaire [LAL], Orsay, France
Kazuyuki Sakaue ,Waseda University, 3-4-1 Okubo, Shinjuku, Tokyo, 169-8555, Japan

Abstract

Laser-Compton scattering has become an important technique for beam diagnostics of the latest accelerators. In order to develop technologies for low emittance beam, an Accelerator Test facility (ATF) was built at KEK. It consists of an electron linac, a damping ring in which beam emittance is reduced and an extraction line. For emittance measurement we developed a new type of beam profile monitor which works on the principle of Compton scattering between electron and laser light. In order to achieve effective collision of photon and electron, very thin size laser is required. Laser wire is one of such a technique to measure a small beam size. With green laser which is converted to second harmonics from IR pulsed laser, minimum beam waist is half of beam waist obtained using IR laser oscillator. Therefore, it is possible to obtain beam waist less than 5 μm (σ value) using green laser pulse, which is required for effective photon-electron collision. First pulsed IR seed laser is amplified with 1.5 meter long PCF based amplifier system. This high power pulsed IR laser is converted to second harmonics with a non-linear crystal. Pulsed green laser is injected inside four mirror resonator to obtain very small beam waist at IP (Interaction Point). Using a pulsed compact laser wire, we can measure 5 μm electron beam in vertical direction. From observed Compton signal profile, bunch length of electron beam is measured as 23.3$\pm$0.7 ps. Electron beam size in vertical plane is measured as 12.6$\pm$1.8 μm and vertical emittance is measured as 24.1 $\pm$ 6.8 pm-rad. Longitudinal bunch length and vertical beam size of electron beam was measured with pulsed laser wire system. We report the development of high power pulsed green generation and compact four mirror resonator parameters for effective Inverse-Compton scattering in this paper.

KEK-ATF DAMPING RING

Figure 1 shows the ATF-DR layout. The electron source is an RF gun with CsTe cathode driven by a mode-locked UV laser. The electron beam is accelerated to 1.28 GeV.

by the linear accelerator with RF cavity of 2856 MHz. After accelerated to 1.28 GeV, the electron beam is injected to the Damping Ring (DR). RF frequency of the DR is 714 MHz and the revolution frequency is 2.16 MHz.

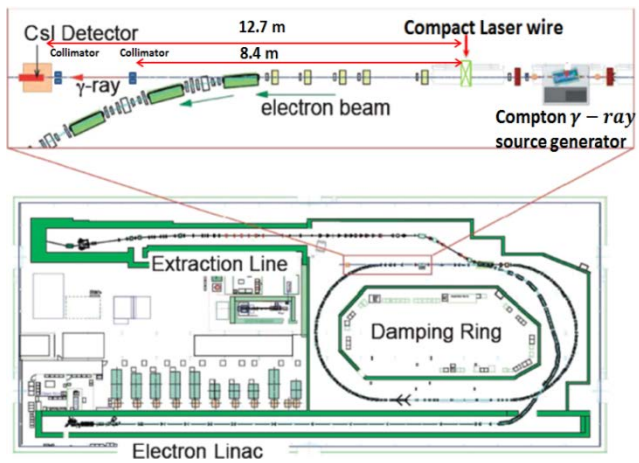

Figure 1: ATF DR layout.

COMPACT FOUR MIRROR CAVITY

The optical cavity assembly consists of four mirrors, mirror holder system and cyilindrical spacers which define length of cavity. In order to have precision control over cavity length, both plane mirror holders were supported by a piezo actuator through a disk type plate spring. Hollow piezo actuators are used for laser beam to pass through them. Four mirror optical cavity is designed for 532 nm wavelength. Distance between concave-concave mirror is kept at 102.8 mm and distance between plane-plane mirror is kept at 103.2 mm. A complex mirror alignment scheme as shown in fig. 2 and fig. 3 is used to keep side by side distance between plane and concave mirror to 29.2 mm [1]. All mirrors are fixed with angle tilt of 8°. The cavity angle of system which indicates laser pulse crossing angle is 16°. All mirrors used in cavity design are of 1 inch diameter. The radius of curvature for two concave mirror is 101.81 mm.

*Work supported by Quantum beam technology project of Japanese Ministry of Education, Culture, Sports, Science and Technology (MEXT)

arpit@post.kek.jp

ISBN 978-3-95450-141-0

TRANSVERSE PROFILE MONITORS FOR SwissFEL

Rasmus Ischebeck, Eduard Prat, Volker Schlott, Vincent Thominet, PSI, Villigen, Switzerland
Minjie Yan, DESY, Hamburg, Germany
Patrick Krejcik, Henrik Loos, SLAC, Menlo Park, CA, USA

Abstract

We have developed a beam profile monitor that allows us to measure two-dimensional electron beam profiles for highly compressed electron bunches. Such bunches have plagued profile measurements in optical transition radiation monitors in the past, because coherent radiation entering the optical system has invalidated the images and even destroyed cameras. The present design makes use of a scintillating crystal, and directs coherent transition radiation away from the optical axis by careful choice of the angle. When observing Snell's law of refraction as well as the Scheimpflug imaging condition, a resolution better than the thickness of the scintillator can be achieved. We will present here measurements performed at the SwissFEL Injector Test Facility and at the Linac Coherent Light Source. The high resolution and excellent sensitivity of this monitor make it ideal for installation in SwissFEL.

REQUIREMENTS ON TRANSVERSE PROFILE MONITORS FOR FREE ELECTRON LASERS

The slice emittance of the electron beam is among the most important parameters when designing a free electron laser, because it has a direct influence on the gain length. Second-generation X-ray FELs such as SACLA [1] or SwissFEL [2] achieve a much more compact footprint by basing their design on a lower energy than what has been implemented in first-generation FELs. This scheme requires a shorter undulator period, possible with in-vacuum undulators, as well as a smaller normalized emittance. The generation of these beams, as well as the diagnostics for the emittance are thus of primary interest. Slice emittance measurements are based on a transverse deflecting radiofrequency cavity, a quadrupole magnet lattice to control the phase advance, and a two-dimensional transverse profile monitor. Measurements of projected emittance can be performed without the deflector, and using a one-dimensional profile measurement, but sources of projected emittance growth may not need to affect the slice emittance, which is central to the FEL process in the undulators.

Developments in photocathode as well as thermionic electron guns have resulted in the generation of smaller and smaller emittances, which result in progressively smaller beam sizes, putting ever tighter requirements on the transverse profile monitors. In addition to increased requirements on resolution, an effect has occurred in recent years, which has hampered transverse profile measurements using optical transition radiation: highly compressed electron bunches have a pronounced longitudinal structure at sub-micrometer length scales, resulting in the coherent emission of optical transition radiation [3–7]. This coherent OTR (COTR) is several orders of magnitude brighter than the incoherent light that is proportional to the particle density.

SwissFEL will use wire scanners [8], as well as two-dimensional profile monitors that image scintillators inserted into the beam. Profile measurements with wire scanners are not affected by coherent emission effects, because the scattering process is based on individual collisions of the electrons with particles in the wire. Similarly, the scintillation process in materials such as cesium doped yttrium aluminum garnet (Ce:YAG) originates from individual excitations of the scintillator by the primary electrons. One has to be careful, however, as coherent transition radiation generated on the scintillator surface, or in-vacuum mirrors, might affect the measurement. This can happen in one of two ways: either it enters the imaging system directly, or it generates radiation with a sufficient photon energy to excite the scintillator.

The first effect can be avoided by delaying the acquisition in the detector until the prompt transition radiation has disappeared. This requires an effective shutter that opens on a nanosecond scale to catch the tail of the scintillation light. Such shutters are implemented by using microchannel plates, a method that increases the complexity of the camera significantly, leads to more frequent service intervals, and most importantly, leads to a loss in image quality through smearing of the image, as well as a non-uniform response. Another method consists of choosing the observation geometry such that the COTR is directed away from the camera. Care has to be taken in this case to not artificially degrade the resolution by imaging radiation from a scintillator with finite thickness. Another issue to take into account is a possible saturation of the scintillator for high-density beams.

RESOLUTION OF PROFILE MEASUREMENTS

The SwissFEL design aims for a normalized slice emittance of 180 to 430 nm. This results in beam sizes down to about 30 µm FWHM at the location of the profile monitors. The resolution of the imaging system was verified according to the ISO 12233 standard. The limiting resolution was found to be better than 8 µm (Figure 1).

The resolution of the optical system is however not the only factor determining the resolution for beam profile measurements. One has to take into account also the broadening inside the scintillator [9], as well as the imaging of a scintillating crystal of finite thickness [10]. The SwissFEL profile monitor takes into account the Snell-Descartes law of refraction [11], as illustrated in Figure 2. The observation angle

ISBN 978-3-95450-141-0

RADIATION SOURCES AND THEIR APPLICATION FOR BEAM PROFILE DIAGNOSTICS

G. Kube
DESY, Hamburg, Germany

Abstract

Radiation generated by high-energy particle beams is widely used for beam diagnostic purposes. Depending on the mechanism of radiation generation, the emitted wavelength range extends from the THz up to the X-ray region, thus allowing to measure beam profiles in the longitudinal and the transverse plane over a wide range. In this talk, basic considerations for radiation based profile measurements will be discussed with special emphasis on the mechanism of radiation generation and the impact on beam diagnostic measurements.

INTRODUCTION

Beam monitors probing the particle electromagnetic field are widely used in accelerator physics. The majority of them is sensitive to the particle near field, i.e. the field which is directly bound to the charged particle, and a usable signal is derived from the interaction of this field with the environment. Examples of this kind of monitors are beam position and beam current monitors. In an other type of monitors, information about the beam properties is generated from the fields which are separated from the charged particle itself. These freely propagating fields can be measured at large distances from the particle as radiation in a wide spectral range, even outside of the accelerator tunnel. Depending on the separation mechanism of the electromagnetic field, the process of radiation generation is named in a different way. Examples considered in the following are synchrotron radiation, transition radiation, diffraction radiation, parametric X–ray radiation, and Smith–Purcell radiation. A comprehensive overview of the radiation generation by ultra–relativistic particles can be found for example in the textbooks [1]– [4], actual topics in radiation physics are discussed at the RREPS conference series [5] or at the conference series *Charged and Neutral Particles Channeling Phenomena*.

All radiation mechanisms mentioned before are either widely applied or investigated in view of an applicability in the field of particle beam diagnostics in different ways. A vast number of information can be extracted from the radiation field, as for example beam energy, energy width and beam divergence, but in the following only beam profile measurements will be considered. In this context, the transverse beam profile diagnostics based on imaging with visible radiation is widespread, the focus will be on their description and the applied concepts (see also Ref. [6]). Besides beam imaging techniques, a measurement of the angular distribution can also be gathered to gain information about the transverse beam profile. Finally, coherent radiation diagnostics is a technique to determine both shape and length of a charged particle bunch by spectral investigation of the coherently emitted radiation.

Starting from imaging with classical light and a discussion about resolution, the radiation generation from ultra–relativistic particles is described in terms of the separation of the pseudo- or virtual photon field associated with the charged particle (Weizsäcker–Williams approximation [7,8]). In this picture, the various radiation processes appear as different ways to separate the virtual photons from the particle, and the formalism of classical imaging can simply be applied to the separated field. Examples are given for particle beam imaging, and the concept of beam size determination from the angular distribution is presented for different radiation sources. Finally, bunch length diagnostics based on coherent Smith–Purcell radiation is presented as an example.

IMAGE FORMATION AND RESOLUTION

In the case of particle diagnostics, the object from which the size has to be determined, i.e. the particle bunch, is not directly accessible because it is moving in a vacuum beam pipe in the accelerator tunnel. In this situation, radiation based diagnostics in general and imaging in particular helps to generate a replica of the object in a more comfortable environment, and the replica size (image) is adjusted to size of measuring device (CCD) with the help of an optical system (lenses). In the subsequent discussion about imaging, only aberration–free optical systems will be considered. Nevertheless, from classical optics it is known that even for imaging with a perfect lens, the image of a point source will never result in a point image because the uncertainty relation imposes a fundamental limit $\Delta x = \lambda/(2\sin\theta)$ with Δx the uncertainty in the location of the emission point, λ the wavelength of observation, and $\sin\theta$ the acceptance angle (numerical aperture) of the imaging lens. To be more precise, the point source image is the result of plane wave diffraction at a circular aperture (lens), and the intensity distribution in the image plane is described by the well known Airy disk (see eg. [9] or textbooks about classical optics). The resolution is usually expressed as the first minimum of the Airy disk

$$\Delta x = 0.61\frac{M\lambda}{\sin\theta} \qquad (1)$$

with the magnification factor M of the optical setup.

A deeper discussion of the resolution requires some basic knowledge of the image formation process. For this purpose a simple optical setup is considered as shown in Fig. 1. The common procedure is to calculate the intensity distribution of a point source in the image plane which is proportional to

ISBN 978-3-95450-141-0

NOVEL EMITTANCE DIAGNOSTICS FOR DIFFRACTION LIMITED LIGHT SOURCES BASED ON X-RAY FRESNEL DIFFRACTOMETRY

M. Masaki#, Y. Shimosaki, S. Takano, M. Takao
Japan Synchrotron Radiation Research Institute (JASRI/SPring-8), Hyogo, Japan

Abstract

A novel emittance diagnostics technique with high sensitivity using X-ray Fresnel diffraction by a single slit has been developed to measure micron-order electron beam sizes at insertion devices (IDs) of photon beamlines. The X-ray Fresnel diffractometry (XFD) is promising for diagnostics especially of a so-called diffraction limited storage ring with ultra-low emittance. The XFD observes a double-lobed diffraction pattern that emerges by optimizing the single slit width. The principle is based on a correlation between the depth of a median dip in the double-lobed pattern and the light source size at the ID. The validity of the new technique was theoretically and experimentally studied. The achievable resolution of the XFD will be also discussed.

INTRODUCTION

In recent years, a diffraction limited storage ring (DLSR) [1] as ring-based future light sources has been extensively and intensively discussed, aiming to drastically boost the average brilliance and the transverse coherence by orders of magnitude compared with existing storage rings. In the DLSR, due to inevitable field errors of strong quadrupole and sextupole magnets, unwanted distortion of lattice functions and local betatron coupling may result in a different light source size at each X-ray photon beamline. One of the most important things for synchrotron light sources is to maximize the light performance at photon beamlines for user experiments. Therefore, measurements of electron beam sizes at the ID source points will be more crucial for securing the absence of degradation of brilliance and transverse coherence of radiation at the beamlines. So far, various techniques have been developed to measure the micron-order vertical beam sizes, for examples, π-polarization imaging method [2], method using a vertical undulator spectra [3], widely used X-ray pinhole cameras (XPCs) e.g. [4], an X-ray imaging method using Fresnel zone plates [5][6] and interferometric techniques [7][8]. However, these methods are not necessarily as readily applicable as they are to emittance diagnostics of all the ID sources of the beamlines. Therefore, development of a new emittance diagnostics technique universally applicable to all the ID beamlines is necessary. We have developed a novel emittance diagnostic method, X-ray Fresnel diffractometry (XFD) [9]. It is capable of resolving a micron-order beam size at the ID source point with high sensitivity and available at typical photon beamlines equipped with a 4-jaw slit and a monochromator.

masaki@spring8.or.jp

PRINCIPLE OF XFD

The XFD observes a double-lobed diffraction pattern that emerges by optimizing a single slit width A under given conditions of distance L from a source point to the slit, distance R from the slit to an observation point, and the observing wavelength λ (Fig. 1). The principle of XFD is based on the correlation between the depth of the median dip in the double-lobed pattern and the light source size; i.e., the dip becomes shallow with growth in the source size. The only requirement for light sources is that the radiation should be a spherical wave with a flux distribution wider than the slit width. Therefore, the XFD is applicable to both most types of ID sources and bending magnet sources.

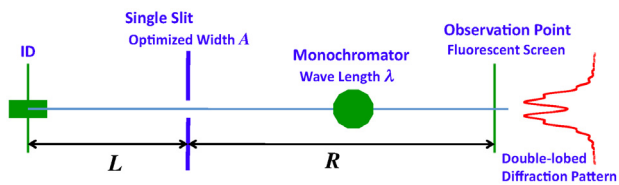

Figure 1: Layout of ID source size measurement using the XFD.

In a one-dimensional case for simplification, a point spread function (PSF) at the observation point is expressed by the following Fresnel integral,

$$I(y,y_e) \propto \left| \int_{-A/2}^{A/2} \sqrt{I_s(y_s - y_e)} \exp\left[i \frac{\pi}{\lambda} \left\{ \frac{1}{L} + \frac{1}{R} \right\} \left\{ (y_s - y_e) - \frac{L(y - y_e)}{L+R} \right\}^2 \right] dy_s \right|^2 \quad (1)$$

where the function $I_s(y_s\text{-}y_e)$ is the radiation flux distribution at the slit, y_e, y_s and y are an electron position at source point, coordinates on the slit and the screen, respectively. An optimized slit width to obtain the double-lobed diffraction pattern is given by a following formula derived from a destructive interference condition of the light at the center (y=0),

$$A \approx \sqrt{7\lambda \frac{LR}{L+R}}. \quad (2)$$

The distance between two lobe peaks, i.e., the pitch P, is expressed as follows from a constructive interference condition of the light,

ISBN 978-3-95450-141-0

MEASUREMENTS OF SMALL VERTICAL BEAMSIZE USING A CODED APERTURE AT DIAMOND LIGHT SOURCE

C. Bloomer, G. Rehm, Diamond Light Source, Oxfordshire, UK
J.W. Flanagan, KEK, Tsukuba, Ibaraki, Japan

Abstract

Diamond Light Source produces a low emittance 3 GeV electron beam which is now regularly operated at 8 pm rad vertical emittance. This corresponds to a vertical beamsize of just 13 µm in the dipole, which is at a high vertical beta location and routinely used for observing the synchrotron radiation using a pinhole camera. Deconvolution of the images from the pinhole camera to maximise resolution is limited by uncertainty regarding the precise shape of the pinhole, resulting in uncertainty on its computed point spread function. Recently a coded aperture has been installed which offers the potential to improve upon the traditional pinhole measurement by offering both higher resolution and increased flux seen through a larger total aperture, however, at the cost of significantly more complex analysis of the recorded images. A comparison of results obtained using the coded aperture and those achieved using the conventional pinhole is presented.

INTRODUCTION

Diamond Light Source (DLS) is a third generation light source, nominally operating with a vertical beam size of 13 µm (0.3 % coupling) through the dipole arcs. Measurements of the transverse beam size are typically made by imaging the synchrotron radiation source point using a pinhole camera. A 25 µm x 25 µm square pinhole, located in air, is used to image the source for storage ring currents from below 1 to 300 mA. X-rays are passed from the vacuum chamber to air through a 1.0 mm aluminium window. They pass through the pinhole located at 3.8 m from the source, to a 200 µm thick LuAG:Ce screen located at 9.1 m from the pinhole. The total path length through air is 9.2 m. The spectrum of the synchrotron radiation is filtered by both the aluminium window and the 9.2 m of air, leading to a peak energy seen at the LuAG:Ce screen of 26 keV. Vertical electron beam size resolutions of better than 1 µm for 1 ms exposure time are achievable [1] [2].

To obtain a beam size measurement with this resolution the pinhole image must be deconvolved with the point spread function (PSF) of the system. At this bandwidth the resolution of the measurement is limited by uncertainty in the PSF, obtained analytically from the pinhole dimensions and scintillator screen properties [1]. Photon flux is sufficiently high that the statistical noise seen on the pinhole camera image for 300 mA stored beam is negligible compared to the errors in the calculated PSF. However, a 1 ms exposure time integrates several electron beam orbits of the DLS storage ring (circulation frequency = 534 kHz). Beam size measurements at turn-by-turn, or even bunch-by-bunch bandwidths require much shorter exposure times, reducing the observed photon flux. For short enough exposure times the statistical counting noise from the small number of photons passing through the pinhole would dominate the measurement errors.

To open up the potential to make beam size measurements of individual bunches with sufficient resolution (better than 1 µm for 13 µm vertical beam size), various alternative 'large aperture' approaches have been proposed. These aim to overcome the limitations in flux seen through the small aperture of a traditional pinhole camera [3].

CODED APERTURE

One such proposal is an adaptation of the coded aperture. This was first introduced as a tool for X-ray astronomy, originally using a collection of randomly distributed pinholes to produce an image that is made up of many overlapping images, unrecognisable as the original object. Figure 1 shows how the coded aperture operates. With knowledge of the location of each of the pinholes it is possible for the complex overlapping pinhole images to be unscrambled (originally described as 'rectification' in early papers, more commonly referred to as 'deconvolution' or 'decoding' in the modern era). This can be carried out either using optical techniques, or digitally using Fourier transforms [4] [5].

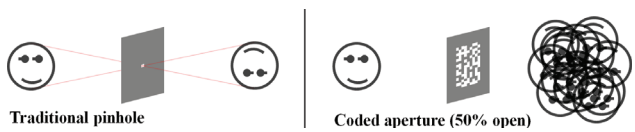

Figure 1: Left: The operation of a traditional pinhole camera. Right: A coded aperture with randomly distributed pinholes, and the resultant overlapping images.

Later, pseudo-random pinhole arrays ('uniformly redundant arrays') were introduced, with pinhole locations chosen such that they exhibit favorable properties for deconvolution [6]. The open aperture of these arrays can be up to 50 % of the total aperture size, giving them the ability to image very low intensity sources, or to image high intensity sources at very high bandwidths.

A vertical beam size monitor using a coded aperture has been proposed and developed for bunch-by-bunch measurements at SuperKEKB and CESR-TA [7] [8]. A 59 element 1-dimensional array produced for use at SuperKEKB has been installed for tests at DLS, intercepting the synchrotron radiation fan at the location of an existing X-ray pinhole (in air). In order to verify the performance of the analysis techniques that have been developed at KEK,

ISBN 978-3-95450-141-0

A QUANTUM GAS JET FOR NON-INVASIVE BEAM PROFILE MEASUREMENT

A. Jeff, CERN, Geneva, Switzerland & University of Liverpool, U.K.
E.B. Holzer, T. Lefèvre, CERN, Geneva, Switzerland.
V. Tzoganis, C. Welsch, H. Zhang, Cockcroft Institute, Daresbury & University of Liverpool, U.K.

Abstract

A novel instrument for accelerator beam diagnostics is being developed by using De Broglie-wave focusing to create an ultra-thin neutral gas jet. Scanning the gas jet across a particle beam while measuring the interaction products, the beam profile can be measured. Such a jet scanner will provide an invaluable diagnostic tool in beams which are too intense for the use of wire scanners, such as the proposed CLIC Drive Beam.

In order to create a sufficiently thin jet, a focusing element working on the de Broglie wavelength of the Helium atom has been designed. Following the principles of the Photon Sieve, we have constructed an Atomic Sieve consisting of 5230 nano-holes etched into a thin film of silicon nitride. When a quasi-monochromatic Helium jet is incident on the sieve, an interference pattern with a single central maximum is created. The stream of Helium atoms passing through this central maximum is much narrower than a conventional gas jet. The first experiences with this device are presented here, along with plans for further tests.

INTRODUCTION

The Compact Linear Collider (CLIC) will use a novel two-beam acceleration scheme to collide electrons and positrons at up to 3TeV [1]. Energy is extracted from a very intense, lower energy Drive Beam (DB) using specially designed RF structures, and transferred to the less intense, high energy colliding beams.

Table 1: Relevant Parameters for the CLIC Drive Beam

Beam Energy	to 2.4 GeV
Beam Current	4.2 A
Pulse Length	140 μs
Bunch Length	13 ps
Bunch Separation	2 ns
Repetition Frequency	50 Hz
Normalised Emittance	150 mm mrad

High intensity beams pose a challenge for beam diagnostics, since all instruments must be non-interceptive. In addition, the short bunch length and separation envisaged for the CLIC DB will generate substantial high-frequency wake fields which can interfere with beam measurements. A number of solutions are being explored, including synchrotron radiation for the high-energy part of the DB. The gas jet monitor described here is a promising option for the lower energy section of the DB accelerator, as well as for other planned high-intensity accelerators.

BEAM GAS IONISATION

Residual gas ionisation is used as a diagnostic tool in many accelerators [2][3]. A charged particle beam ionises a fraction of the residual gas present in the beam pipe. If an electric field is applied across the beam pipe, the ions and the liberated electrons are accelerated away from the beam in opposite directions. A position sensitive detector is used to image either the ions or the electrons, and thus measure the beam profile. Throughout the discussion below we refer for clarity to ion collection; however the conclusions remain valid if the electrons are collected instead.

In order for this technique to be accurate, the position at which the ions are generated must be mapped onto the detector, that is, the ions should fly in a straight line. In reality, however, this is not quite true. Firstly, the ions are created with a certain initial momentum. Secondly, the electromagnetic field of the beam will influence their trajectory. Thus, the profile of ions arriving at the detector will not exactly match the beam profile.

In order to reduce this effect, a magnetic field may be added parallel to the electric field. In this case, the ions follow a helical path which, if the gyroradius is sufficiently small, may be taken to approximate a straight line. In the case of a very intense beam, however, the space charge field may be so strong that a small gyroradius cannot be guaranteed. Numerical methods can be used to correct for this effect [4] but the resolution of the profile is in consequence reduced.

GAS JET MONITOR

Gas jet monitors have been developed at NIRS and J-Parc [5] in order to decrease the measurement time and allow 2-d profile measurements at a single point. A planar gas jet or ‘gas curtain’ crosses the beam pipe. The curtain is tilted at 45° and acts like a screen when combined with an electric field for ion extraction. The pressure of the gas jet is locally much higher than the residual gas pressure, so that sufficient ions for beam profile measurement with a given accuracy are collected in a shorter time. The jet passes through the beam pipe into a collection chamber, so that the beam vacuum is not substantially affected.

ISBN 978-3-95450-141-0

NSLS-II RF BEAM POSITION MONITOR-SYSTEM TEST AND INTEGRATION

Danny Padrazo, Anthony Caracappa , Weixing Cheng , Christopher Danneil, Al Dellapenna , Kiman Ha, Marshall Maggipinto, Joseph Mead, Om Singh, Kurt Vetter
Brookhaven National Laboratory, Upton, NY 11973, USA

Abstract

The NSLS-II Synchrotron Light Source is a state of the art 3GeV electron storage ring currently in the process of commissioning at Brookhaven National Laboratory. The RF Beam Position Monitors (RF BPM) are one of the key diagnostics systems required for a successful and efficient commissioning. There are more than 250 RF BPM installed in the injector and storage ring. Each RF BPM was fully tested, first under laboratory environment, and then after installation utilizing a built in pilot tone signal source. These successful tests provided a solid base for the integrity of the RF BPM system, prior to the start of beam commissioning. This paper will describe tests performed and results of system integration.

INTRODUCTION

Beam stability is a key factor in meeting the specifications for intensity and brightness designed to be delivered by NSLS-II. The multi-bunch stored beam condition for vertical and horizontal resolution, as well as long term stability must be less than 200nm. The NSLS-II BPMs are installed in thermally stabilized racks which are regulated to +/- 0.1 degree C of operating rack temperature, which is essential to meet the stability requirement [1,2]. This paper will detail the implementation of various test procedures designed and performed on each BPM receiver (Fig. 1) pre and post installation.

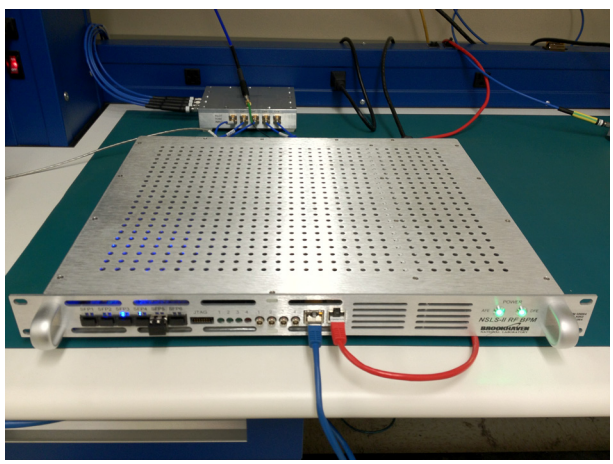

Figure 1: NSLS-II RF BPM production unit.

PILOT TONE COMBINER

An integral part of testing depends on implementation of the on board Pilot Tone Synthesizer, which generates a CW signal that is phase locked to the machine clock and is connected to the Pilot Tone Combiner module (PTCM) – shown in Fig. 2. This module is a custom design consisting of a passive RF board mounted in an aluminum enclosure and resides in the tunnel, near the BPM PUE and is connected via custom SIO2 Semi-Rigid Cables. The PTCM is characterized by comprehensive S-Parameter measurements, where S21 channel to channel variations are removed via automatic calibration routine, which maps the pilot tone to the received beam signal via measured S21[1,2].

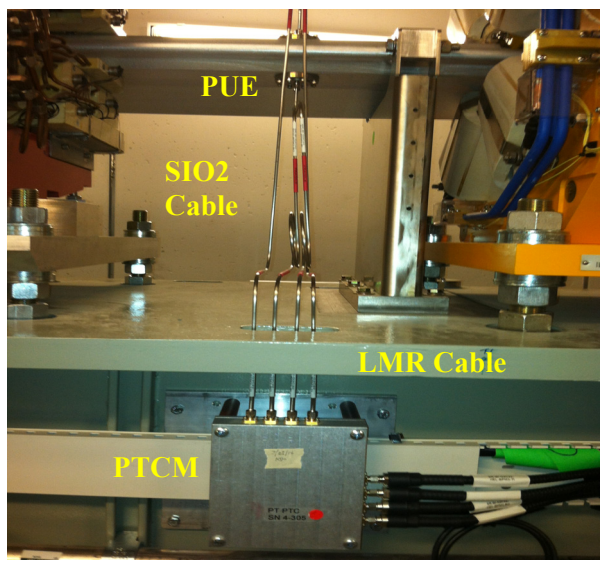

Figure 2: Pilot Tone Combiner Module (PTCM).

PRE/POST-INSTALLATION TESTING

Testing is conducted in a controlled laboratory environment using a custom test setup including VME based event/timing system, data acquisition, and post processing. MATLAB and Python based scripts have been developed to execute routines to test key functions and features of the BPM receiver. Performance tests procedures are first completed on each Analog Front End Board (AFE) using a dedicated receiver chassis populated with a Digital Front End Board (DFE). System testing is accomplished using custom routines developed to capture data for all three

ISBN 978-3-95450-141-0

PROPOSED PULSE STRETCHING OF BPM SIGNALS FOR THE POSITION DETERMINATION OF VERY SHORT AND CLOSELY SPACED BUNCHES*

P. Thieberger#, S. Brooks, C. Hamdi, R. Hulsart, G. Mahler, M. Minty, R. Michnoff and D. Trbojevic
Collider Accelerator Department, Brookhaven National Laboratory, Upton, New York, U.S A.

Abstract

A proposal for a future ultra-relativistic polarized electron-proton collider (eRHIC) is based in part on the transport of multiple electron beams of different energies through two FFAG beam transports around the 3834 m long RHIC tunnel circumference in order to recirculate them through an Energy Recovery Linac (ERL) for their stepwise acceleration and deceleration. For each of these transports, the beams will travel in a common vacuum chamber horizontally separated from each other by a few mm. Determining the position of the individual bunches is challenging due to their very short length (~12 ps rms) and their temporal proximity (less than 4 ns in some cases). Providing pulses adequate for accurate sampling is further complicated by the less-than-ideal response of long coaxial cables. Here we propose two approaches to produce enhanced, i.e. stretched, pulse shapes of limited duration; one based on specially shaped BPM electrodes and the other one on analog integration of more conventional stripline BPM signals. In both cases, signals can be generated which contain relatively flat portions which should be easier to sample with good precision without requiring picoseconds timing accuracy.

INTRODUCTION

A plan is being developed for replacing the Relativistic Heavy Ion Collider (RHIC) by a high energy electron proton collider (eRHIC) [1]. The proton beam would be accelerated and stored in one of the existing RHIC rings while the 16 GeV or 21 GeV electrons would be accelerated and decelerated in multiple passes through an Energy Recovery Linac (ERL) [1, 2]. The present design calls for two electron beam transport arcs, located in the RHIC tunnel, both based on a Fixed-Field Alternating Gradient (FFAG) lattice design [1]. There would thus be several electron trajectories within each of these two FFAG arcs, slightly displaced horizontally and nominally at the same vertical height. Figure 1 shows an example of a short portion of such trajectories through a set of three FAG magnets in the "high energy" FFAG beam transport.

Accurately monitoring the positions of these beams at multiple locations around the arcs is a major challenge because some of these very short bunches (~12 ps rms) are separated in time by less than 4 ns, and because no beam position monitor (BPM) pick up electrodes (PUEs) may overlap the orbit plane due to the intense synchrotron radiation. Various alternative options are being considered to mitigate these difficulties, such as providing so called pilot bunches, well separated in time from the regular bunch sequence and also the possible use of synchrotron radiation generated in or near the visual range to measure orbit positions with optical systems.

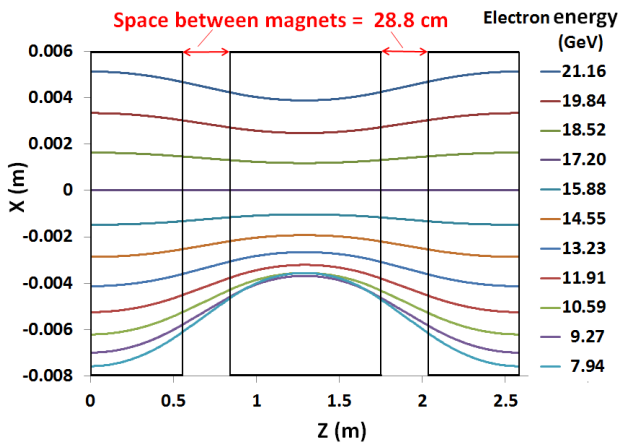

Figure 1: Electron trajectories in one cell of the high energy FFAG beam transport [1].

Here we have started to address these issues by performing Particle Studio [3] simulations for two preliminary designs of possible BPM configurations, one based on a set of conventional "button" pickup electrodes (PUEs) and the other one on a new design of tapered stripline PUEs designed in an attempt to mitigate an additional challenge, namely the result of sample timing errors. This last problem is particularly severe when closely-spaced bunches make it impossible to use conventional filters [4] with long enough time constants so as to provide pulse maxima that are flat enough to be accurately sampled and digitized.

DESCRIPTION OF THE MODELS

The two models used for the Particle Studio simulations are shown in Figs. 2 and 4. In both cases, the left and right tubular parts of the vacuum chamber cross sections will have cooled walls to absorb the power generated by the intense synchrotron radiation.

The tapered striplines shown in Fig. 4 are designed to receive a linearly increasing and decreasing induced charge as the "pancaked shaped" (Lorentz-contracted)

* This material is based upon work supported by the U.S. Department of Energy, Office of Science, Brookhaven National Laboratory under Contract No. DE-AC02-98CH10886.
# PT@BNL.GOV

OVERVIEW OF THE GEOMETRICAL NON-LINEAR EFFECTS OF BUTTON BPMS AND METHODOLOGY FOR THEIR EFFICIENT SUPPRESSION

A. A. Nosych, U. Iriso, A. Olmos, ALBA CELLS, Barcelona, Spain
M. Wendt, CERN, Geneva, Switzerland

Abstract

This paper describes an overview of the geometric non-linear effects common to beam position monitors (BPMs) installed in the accelerators and a methodology to correct for these effects. A typical characteristic curve of a pick-up is linear within a limited range from the BPM origin. At larger offsets the non-linearity of the curve is more pronounced and gets worse if the button diameter is small with respect to the beam pipe diameter. The general real-time linearization methods usually utilize linear correction combined with a simplistic polynomial, which may lead to inaccuracies in their limited application. We have developed a more rigorous methodology to suppress the non-linear effects of the BPMs through electromagnetic (EM) simulations and 2D fitting approximations. The focus is mainly on standard button pick-ups for the electron (ALBA) and proton machines (LHC).

INTRODUCTION

BPMs are among the most important and numerous parts of a diagnostics system of any particle accelerator. Accelerators require constant beam orbit monitoring in order to control the quality of passing beams and allow various feedback systems to improve it. Usually beams travel close to geometrical centers of BPMs on their way, following the optimal "golden" orbit. However, beams are sometimes intentionally steered away from the optimal orbit, whether it is to increase the crossing angle in order to improve luminosity of a collider (LHC), or to study the non-linear magnetic field components of a storage ring (ALBA).

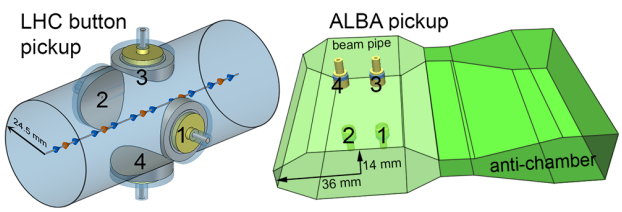

Figure 1: 3D models of a typical LHC curved-button pickup and a standard pickup of ALBA.

Every beam position reading of a BPM is subject to non-linear errors. The non-linear behavior of a BPM pickup is caused by its geometrical design and the resulting errors are more pronounced at larger beam offsets from the BPM origin. In this paper we will describe two standard BPM geometries, one belonging to LHC: a proton collider, and another to ALBA: a synchrotron light source (both geometries are shown in Fig. 1). After discussing the modeling and simulation process we will summarize non-linear effects of the BPMs' characteristic response for different signal treatments, and address results of an efficient non-linearity correction using high-order surface (2D) polynomials.

MODELLING AND MAPPING A BPM

Left in Fig. 1 is a common 4-button (arranged 90^o apart) pickup mounted on a beam pipe of circular cross-section (radius $R_{\mathrm{lhc}} = 24.5$ mm) belonging to the LHC. Right in Fig. 1 is a flat-button BPM used in ALBA, a 3 GeV synchrotron light source, with 2 pairs of buttons located above and below the beam, which travels in a hexagonal beam pipe of 72×28 mm transversely ($R_{\mathrm{alba}} = 36$ mm).

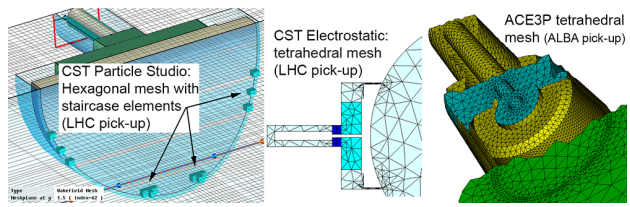

Figure 2: Meshing BPM buttons with hexahedral mesh of CST Particle Studio and tetrahedral meshes of CST Electrostatic and ACE3P.

As usual in light sources, parts of ALBA vacuum chamber include the anti-chamber used for photons. Depending on location in the storage ring, the anti-chamber has different dimensions; one of them is shown in Fig. 1 right. Here the beam pipe loses its symmetry in Y plane; however, we have studied 2 types of anti-chambers attached to the same BPM module, and have not observed any noticeable effect on BPM sensitivity. Hence, in our studies we consider all types of ALBA beam pipes symmetric, omitting the anti-chamber.

To simulate BPM response of the LHC button in time-domain we have initially used CST Particle Studio [1]. We have found that for 3D geometry with small curved elements (e.g. a curved button and a curved vacuum gap around it, Fig. 2 left) the hexahedral mesh of CST PS is not very efficient: in pursuit to approximate curves by orthogonal edges, the mesh cells greatly multiply in numbers (at least 6M mesh cells for this BPM), leading to lengthy simulations: it took 25 minutes on a desktop PC with 2x3.5 GHz CPU and 8 Gb RAM to simulate a single beam transit.

To avoid this time waste we have switched to the Electrostatic solver of CST in "semi-2D" mode [2], using the tetrahedral mesh with more accurate approximation of curved elements. The solver itself does not allow a true 2D input, so we introduce a 1 mm thick "slice" of the BPM with magnetic

ISBN 978-3-95450-141-0

NUMERICAL CALCULATIONS FOR THE FAIR PROTON LINAC BPMS

C. Simon#, V. Bellego CEA-Saclay/DSM/Irfu, Gif sur Yvette, France,
M. Almalki, P. Forck, W. Kaufmann and T. Sieber, GSI, Darmstadt, Germany

Abstract

Fourteen Beam Position Monitors (BPMs) will be installed along the FAIR Proton Linac. These monitors will be used to determine the beam position, the relative beam current and the mean beam energy by time of flight (TOF). A capacitive button type pickup was chosen for its easy mechanical realization and for the short insertion length which is important for the four BPMs locations of the inter-tank sections between the CH-cavities. Depending on the location, the BPM design has to be optimized, taking into account an energy range from 3 MeV to 70 MeV, limited space for installation and a 30 mm or 50 mm beam pipe aperture. This paper reports wake field numerical simulations performed by the code CST PARTICLE STUDIO to design and characterize the BPMs. Response time of monitors are presented and results of calculations for various pickup-geometries are discussed taking into account different beam velocities.

INTRODUCTION

The FAIR Project [1] (Facility for Antiprotons and Ions Research), built at GSI Darmstadt, requires a Proton Linac [2] which has to provide the primary proton beam for the production of antiprotons. This Linac will operate at a frequency of 325 MHz. It will deliver a 70 MeV beam at a current limit of 70 mA with a repetition rate of 4 Hz for injection into the SIS 18. The main beam parameters are listed in Tab. 1.

Table 1: FAIR Proton Linac Parameters

Parameter	Value
Final energy	70 MeV
Pulse current	70 mA
Protons per pulse	7.10^{12}
Macro pulse length	30 to 100 µs
Repetition rate	4 Hz
Trans. beam emittance	4.2 µm (tot. norm.)
RF-frequency	325.224 MHz

The fourteen Beam Position Monitors (BPMs) will be installed along the Linac as shown Fig. 1.

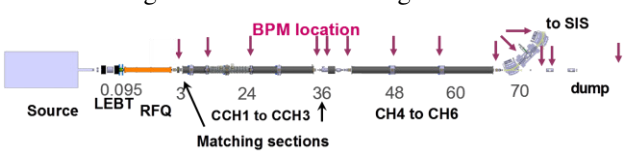

Figure 1: Distribution of Beam Position Monitors along the Linac.

#claire.simon@cea.fr

At nine locations the vacuum chamber aperture is 30 mm. Due to the different requirements, monitors installed in the transfer section, the dump and between the two dipoles will have a vacuum chamber aperture of 50 mm.

The same type of button electrode is foreseen along the Linac with an energy varying from 3 MeV to 70 MeV and a change of vacuum chamber geometry.

The main measurement is to determine the beam displacement, with a spatial resolution of 0.1 mm averaged on a macro pulse of 36 µs duration, by calculating the ratio of the difference over sum voltage between two opposite buttons. The sum signal from a BPM can be also used as a relative measurement for the beam current. An important application at a proton Linac comprising of novel CH-cavities is the determination of the beam energy after each DTL tank which can be calculated via the time of flight determination of a bunch between two BPMs. For this time measurement, an accuracy of 8.5 ps has to be achieved corresponding to a phase resolution of 1°.

The main parameters are summarized in Tab 2.

Table 2: FAIR Proton Linac BPM Parameters

Parameter	Value
Beam pipe diameter	30 mm intertank section, 50 mm transfer lines
Length	50 mm
Beam energy	From 3 MeV to 70 MeV
Bunch frequency	325.225 MHz
Beam pulse length	36 µs nominal
Bunch length	150 ps typical
Average current	35 mA nominal, max 70 mA
Position resolution (RMS)	100 µm averaged on a macro pulse of 36 µs
Operation range	± 5 mm
Phase resolution	1° averaged on a macro pulse of 36 µs

LAYOUT

Beam dynamics requirements and compactness of the beamline require that some BPMs (at four locations) will be an integral part of the inter-tank section between the CH cavities [2]. In this context and after having performed some preliminary simulations [3], a capacitive button type BPM with buttons of 14 mm diameter was chosen for its easy mechanical realization and short

ISBN 978-3-95450-141-0

PRODUCTION PROCESS FOR THE EUROPEAN XFEL RE-ENTRANT CAVITY BPM

C. Simon#, C. Boulch, P. Carbonnier, P. Contrepois, P. Daniel-Thomas, F. Eozenou, Y. Gasser, F. Gouit, O. Napoly, J. Novo, C. Servouin CEA-Saclay/DSM/Irfu, Gif sur Yvette, France
J. Kruse, D. Noelle, M. Schalwat, S. Vilcins- Czvitkovits, DESY, Hamburg, Germany
N. Rouvière, J.-P. Prestel, CNRS, IN2P3, Orsay, France

Abstract

As In-Kind contributor to the E-XFEL project, CEA is committed to the procurement of around one third (31) cold beam position monitors (BPM) of the re-entrant RF cavities type and to the assembly on the Saclay site of the 101 cryomodules of the superconducting linac. Each cryomodule is equipped with a beam position monitor connected to a quadrupole at the high-energy end of the cavity string. The industrial process of those BPMs, used in an ultra-clean environment at cryogenic temperature, includes several steps and involves a quality control in collaboration with industrial partners. This paper describes the different steps of the re-entrant cavity BPM fabrication process: machining, copper coating, thermal treatment, EB welding, cleaning and mounting in clean room on the quadrupole. Problems encountered and the lessons learnt will be also reported.

INTRODUCTION

The European XFEL [1] is an X-ray free electron laser user facility currently under construction in Hamburg, Germany. This accelerator has a superconducting 17.5 GeV main linac based on the TTF technology and is composed of 101 cryomodules including the injector module. Each module includes a string of eight 1.3 GHz RF cavities, followed by a BPM connected to a superconducting quadrupole. As In-Kind contributor to the E-XFEL project, CEA is committed to the integration on the Saclay site of the 101 cryomodules [2] as well as to the procurement of the magnetic shielding, superinsulation blankets and 31 cold re-entrant cavities beam position monitors (BPM). The others cold BPMs will be button BPMs and are not discussed here [3].

These re-entrant BPMs cavities have been studied and prototyped at CEA [4]. They are composed of two parts of stainless steel welded together to form a resonator. The production of the re-entrant cavities has been transmitted to a company named Gavard & Cie which is in charge of mechanical fabrication. Pickups and RF re-entrant BPM cavities are provided by the CEA/Saclay and sent to DESY to be mounted on the quadrupole inside an ISO4 cleanroom.

In this paper, the industrial process is reported with a description of different steps. In addition, difficulties met during production are discussed. Design and architecture of the re-entrant BPM electronics, developed by a collaboration of CEA/Saclay/Irfu, DESY and PSI, are not discussed here [5].

#claire.simon@cea.fr

GENERAL DESCRIPTION

In the XFEL accelerator modules, 31 cold re-entrant cavity BPMs will be installed. Independent of the type, all cold BPMs will have a common mechanical interface and the same specifications presented in Table 1.

Table 1: Cold BPM Parameters

Parameter	Value
Beam pipe diameter	78 mm
Length	170 mm
Single bunch resolution (RMS)	50 µm
Operation range for maximum resolution	± 3 mm
Transverse Alignment Tolerance (RMS)	300 µm

The re-entrant BPM will be connected to a cold quadrupole at the high-energy end of the cavity string as illustrated Fig. 1.

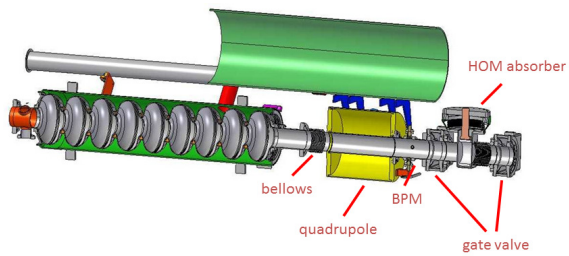

Figure 1: Layout of the XFEL cryomodule downstream end.

The length of this BPM is 170 mm to respect constraints imposed by the cryomodule and its aperture is 78 mm (see Fig. 2). It is composed of two parts, in stainless steel, welded together by electron beam welding (EB). Flanges are machined out of the same blocks to get the alignment tolerances. The alignment is done by dowel pins with respect to the cold magnet.

Each antenna, which is a combination of stainless steel, molybdenum and alumina Al2O3 ceramic brazed, is mounted on the cavity via a CF16 flange. They have to pass cryogenic shocks and to fulfil the conditions of Ultra High Vacuum (UHV). They have been manufactured by SCT (Société des Céramiques Techniques) [6]. Four copper-beryllium radio-frequency contacts are also welded in the inner cylinder of the cavity to ensure the electrical conduction between the feedthrough inner conductors and the cavity.

ISBN 978-3-95450-141-0

COMMISSIONING OF THE ELECTRONICS FOR HOM-BASED BEAM DIAGNOSTICS AT THE 3.9 GHz ACCELERATING MODULE AT FLASH*

N. Baboi#, O. Hensler, T. Wamsat, DESY, Hamburg, Germany
L. Shi, University of Manchester, Manchester, UK and DESY, Hamburg, Germany
N. Eddy, B. Fellenz, FNAL, Batavia, IL, USA
P. Zhang, CERN, Geneva, Switzerland

Abstract

Transverse Higher Order Modes (HOM) excited by electron beams in the 3.9 GHz accelerating cavities at FLASH may damage the beam quality. They can be reduced by extracting their energy through special couplers and by aligning the beam in the cavity. Electronics has been designed at FNAL for monitoring some of the potentially most damaging HOMs. This may be used for beam centering and therefore reducing the HOM effects. Moreover, the signals can be potentially calibrated into beam offset, so that they could be used as beam position monitors (HOM-BPM). The specifications of the monitors have been defined during an extensive study on the 4-cavity accelerating module installed at FLASH. Signals around 5.46 GHz have been chosen for higher precision measurements. However these signals propagate into the entire 1.2 m long module. Therefore in addition modes at about 9.06 GHz were selected for localized measurements in each cavity. The electronics has been recently installed at FLASH. The initial experience with this electronics is presented in this paper. The signals can already be used for centering. Some instability in the signals has been observed and the cause has to be further investigated.

INTRODUCTION

Higher Order Modes (HOM) excited by electron beams when traversing accelerating cavities can be used for beam alignment [1]. This is beneficial to the beam quality since in this way the transverse HOMs are reduced and therefore also their potentially damaging effect on the beam. HOMs can also be used as beam position monitors (BPM), similar to cavity BPMs. In particular dipole modes are very suitable due to the linear dependence of their strength on the beam offset.

The principle has been demonstrated in the past at the FLASH linac at DESY, Hamburg [1,2], using special HOM-BPM electronics built at SLAC and installed at forty 1.3 GHz cavities. One issue remains, namely that the calibration is instable [3]. However this affects only the functioning as a BPM, the raw HOM signals are used to align the beam.

Recently, electronics has been built at FNAL for the four 3.9 GHz cavities at FLASH. This paper presents the first beam experience with this electronics at FLASH. The challenges in comparison to the one for the 1.3 GHz cavities will be underlined.

*The work is part of EuCARD-2, partly funded by the European Commission, GA 312453.
#nicoleta.baboi@desy.de

The FLASH Injector

Figure 1 shows schematically the injector of the FLASH linac [2]. The electron bunches produced by the photo-gun pass the first accelerating module (ACC1), containing eight 1.3 GHz cavities, and then the third harmonic module (ACC39), containing four 3.9 GHz cavities, before going through the first bunch compressor. The 3.9 GHz cavities are used to linearize the energy spread along the bunch needed in the compression process. Magnets and beam monitors, such as charge, position and phase monitors are not shown.

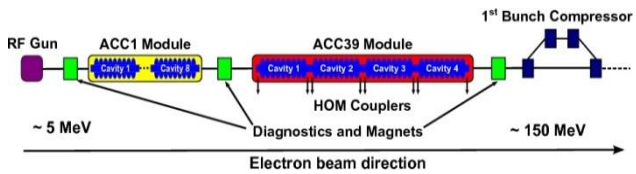

Figure 1: Layout of the FLASH injector. (The accelerating cavities are not to scale: the 3.9 GHz cavities are about 3 times smaller than the 1.3 GHz ones.)

The Third Harmonic Module

The arrangement of the 3.9 GHz cavities in ACC39 is shown in Figure 2. Each cavity has a power coupler and two couplers for HOM-damping. Two of the cavities, C1 and C3, are oriented with the power coupler downstream, the others have it upstream. The HOM-couplers are named with the cavity (C) and coupler (H) number, with H1 being on the power coupler side.

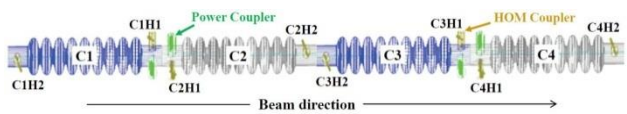

Figure 2: The arrangement of the 3.9 GHz cavities in the ACC39 cryo-module.

The HOMs in the 3.9 GHz cavities are much stronger than in the 1.3 GHz cavities due to the smaller aperture. This makes the need to align the beam in the cavities, and therefore avoid exciting transverse modes, more important. This is also the main reason why the beam pipes are larger than 1/3 of the beam pipes for 1.3 GHz cavities. This allows most modes to propagate along the entire module, and be damped by all couplers. On the

ISBN 978-3-95450-141-0

FLASH UNDULATOR BPM COMMISSIONING AND BEAM CHARACTERIZATION RESULTS

D. Lipka*, N. Baboi, D. Noelle, G. Petrosyan, S. Vilcins, DESY, Hamburg, Germany
R. Baldinger, R. Ditter, B. Keil, W. Koprek, R. Kramert, G. Marinkovic, M. Roggli, M. Stadler,
PSI, Villigen, Switzerland†

Abstract

Recently, the commissioning of FLASH2 has started, a new soft X-ray FEL undulator line at the DESY FLASH facility. In the FLASH2 undulator intersections, the beam positions are measured by 17 cavity beam position monitor (CBPM) pick-ups and electronics [1] developed for the European XFEL (E-XFEL). In addition four CBPMs are available at FLASH1 for test and development. The new CBPM system enables an unprecedented position and charge resolution at FLASH, thus allowing further analysis and optimization of the FLASH beam quality and overall accelerator performance. Results of first beam measurements as well as correlations with other FLASH diagnostics systems are reported.

INTRODUCTION

Beam position monitors (BPM) are an essential tool for the operation of a Free-electron laser (FEL). In the European X-FEL, cavity BPMs with sub-micron noise and drift are used for the alignment of the electron beam with the photon beam in the undulator area [2]; for a detailed description of a cavity BPM see [3, 4].

In addition to the undulator CBPMs with 10 mm aperture and 100 mm length, a second CBPM type with 40.5 mm aperture and 255 mm length will be installed in some locations in the warm beam transfer lines where the resolution of the standard button BPMs is not sufficient. A test area for the verification of the performance of both CBPM types has been installed at FLASH1 after the last undulator, see Fig. 1. The CBPM electronics, including its embedded FPGA firmware and software, is provided in an In-kind contribution from PSI, see Fig. 2. Both CBPM types have the same electronics because the BPM pickups have the same frequency of 3.3 GHz and similar loaded Q for their position and reference resonator.

In addition to FLASH1, a second undulator beamline FLASH2 [5] has been built to extend the capability of the FLASH soft X-ray FEL facility [6]. For the FLASH2 CBPMs, a pre-series for E-XFEL are used, with the BPM pickups provided by DESY and the electronics from PSI. In this report the results of CBPM measurements at FLASH1 and FLASH2 are reported, including comparisons with other monitors.

Figure 1: CBPM test-stand at FLASH1 with three undulator CBPMs (right) and one 40.5 mm beam pipe diameter CBPM (left). The beam passes the pickups from right to left. Each CBPM can be moved in both transverse directions with remote movers.

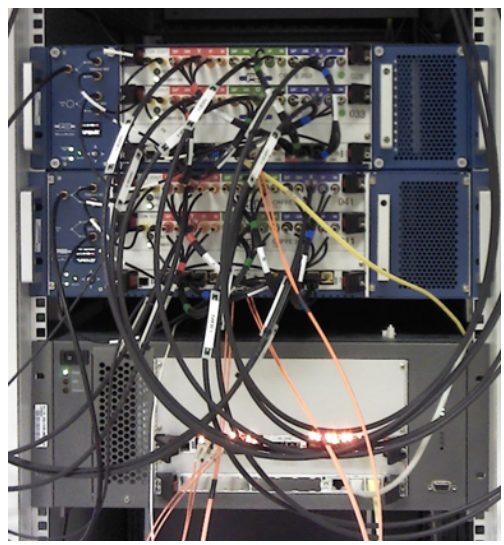

Figure 2: CBPM electronics provided by PSI for FLASH1 and FLASH2. For testing and verification purposes, the system was connected in parallel to the DOOCS based control system of FLASH, and also to EPICS based control system hardware provided by PSI for the commissioning of the systems.

CBPM AT FLASH1

The resulting position and charge values provided by the PSI electronics are transferred to the FLASH control system via an additional communication server. A rough calibra-

* dirk.lipka@desy.de
† This work was partially funded by the Swiss State Secretariat for Education, Research and Innovation SERI

ISBN 978-3-95450-141-0

DESIGN, DEVELOPMENT AND COMMISSIONING OF A MTCA-BASED BUTTON AND STRIP-LINE BPM SYSTEM FOR FLASH2

Bastian Lorbeer*, Frank Schmidt-Föhre, Nicoleta Baboi, Ludwig Petrosyan
DESY, Hamburg, Germany

Abstract

The FLASH (Free Electron Laser in Hamburg) facility at DESY (Deutsches Elektronen-Synchrotron) in Germany has been extended by a new undulator beam line called FLASH2 to provide twice as many experimental stations in the future [1]. After the acceleration of the electron bunch train up to 1.2 GeV, a part can be kicked into FLASH2, while the other is going to the old undulator beam line. In order to tune the wavelength of the SASE (Self Amplified Spontaneous Emission), the new line is equipped with variable gap undulators. The commissioning phase of FLASH2 started in early 2014 and continues mostly parasitically during user operation in FLASH1. One key point during first beam commissioning is the availability of standard diagnostic devices such as BPM (Beam Position Monitor) [2]. In this paper we present the design and first operational experience of a new BPM system for button and strip-line monitors based on MTCA.4 [3]. This is referred to as LCBPM (low charge BPM) in contrast to the old systems at FLASH initially designed for bunch charges of 1 nC and higher. We summarize the recent analog and digital hardware development progress [4, 5] and first commissioning experience of this new BPM system at FLASH2 and present a first estimation of its resolution in a large charge range from 1 nC down to 100pC and smaller.

INTRODUCTION

The demand for beam time at the user facility FLASH increased substantially in the past. In order to fulfill this need the FLASH facility has been extended by a new undulator beam line for SASE generation called FLASH2. The charge delivered to FLASH2 can be adjusted independently from the old FLASH facility with an independent laser. FLASH2 has been ready for electron beam commissioning in March 2014, has seen the first beam on 4th March and was able to deliver SASE for the first time on 20 August 2014 [6, 7]. This was done simultaneously during SASE delivery in the FLASH1 undulator beam line. The electron beam delivered to FLASH2 is accelerated within the same RF (Radio Frequency) pulse in the FLASH facility up to 1.2 GeV after approximately 150 m and is then kicked into the FLASH2 tunnel. One part of the diagnostics in FLASH2 are button and strip-line monitors at 16 locations in the machine utilizing new MTCA.4 electronics designed by us [4, 5]. Challenges in the development of this system are the resolution requirement of 50 µm, operation at charges well below 100 pC and a high bunch repetition rate of up to 4.5 MHz. This is compatible with the requirements for the European XFEL [8]. The hardware development status and operation experience with these new systems are summarized in this paper.

* bastian.lorbeer@desy.de

OVERVIEW

The new FLASH2 undulator beam line runs in parallel to the old FLASH1 undulator beam line which can be seen in Figure 1. It is divided into several sections namely EXTRACTION, SEED, SASE, BURN, and DUMP section with button and strip-line monitors in different locations. Most

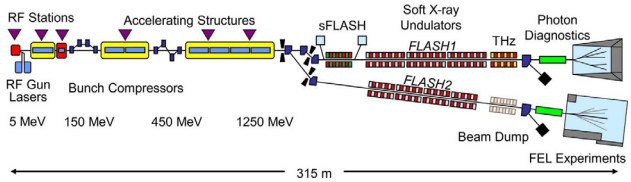

Figure 1: Section overview FLASH.

of the LCBPMs are distributed along the EXTRACTION section at the beginning of FLASH2 with nine BPMs and the rest of 4 BPMs are in the BURN/DUMP section. Due to space limitations in the SASE section three button BPMs have been installed here as well instead of using the more preferable cavity BPMs which offer the required resolution for orbit tuning in the SASE section [9, 10]. A variety of different beam pipe diameters for the button BPMs and a few refurbished strip-line BPMs with different RF cable lengths ranging from 35 to 58m installed in the machine required the development of a very robust but also flexible BPM electronics. The button type design is the same as for the European-XFEL that has been reported in [11]. Table 1 summarizes all types of BPMs for which the electronics are currently in operation. Electromagnetic field simulations [12] delivered the monitor constants. An overview of

Table 1: Types of Beam Position Monitors Installed in FLASH2 and Corresponding Monitor Constants

Type	amount	Diameter	Monitor constant
button	2	40 mm	10.6 mm
button	4	34 mm	9.06 mm
button	3	100 mm	23.84 mm
strip-line	4	44 mm	8.678 mm
in-air	1	100 mm	31.25 mm
button	3	10 mm	2.55 mm

the connections between the BPMs and readout electronics can be seen in Figure 2.

ISBN 978-3-95450-141-0

CALIBRATION OF OLYMPUS/DORIS BEAM POSITION MONITORS

U. Schneekloth, N. Görrissen, G. Kube, J. Neugebauer, R. Neumann, F. Schmidt-Föhre
DESY, Hamburg, Germany

Abstract

The goal of the OLYMPUS experiment is a precise measurement of the ratio of the positron-proton and electron-proton elastic scattering cross sections in order to quantify the effect of two-photon exchange. The experiment was performed using intense beams of electrons and positrons stored in the DORIS ring at Deutsches Elektronen Synchrotron in Hamburg, impinging on an un-polarized, internal, hydrogen gas target. An essential ingredient of the experiment is a precise determination of the luminosity, which requires a precise knowledge of the beam position of both beam species. During DORIS operation cylindrical button beam position monitors, read out by two independent electronics systems, were mounted up- and downstream of the target chamber. After the end of operation, the readout systems were cross-calibrated. The BPMs were then calibrated using a test-stand, consisting of a wire scanner assembly. The beam was simulated by applying an RF signal to the wire. This paper describes the calibration principles and test setup, together with the results compared to the expected BPM response.

INTRODUCTION

The OLYMPUS experiment at DESY [1] aims to determine this two-photon contribution by measuring the ratio of the positron-proton to electron-proton cross sections. The experiment was performed at the DORIS storage ring, with 2 GeV electron and positron beams impinging on an un-polarized, internal, hydrogen gas target. For the aimed-for precision of the experiment, the beam position was required to be known on the 0.1 mm level, since it directly affects the acceptance of the detector systems.

During DORIS operation the beam position at the OLYMPUS target chamber was measured by two beam position monitors (BPMs), mounted up- and downstream of the target chamber. The BPMs consisted of four cylindrical pickup buttons of 10.8 mm diameter in a cylindrical 60.3 mm diameter beam pipe. The BPMs were readout by two independent electronics: the standard DORIS electronics (so-called Neumann electronics) [2] and the commercially available Libera Brilliance+ readout system [3]. Both readout systems use the same measurement principle: the beam position is calculated as $X = k_x((V_a + V_d) - (V_b + V_c))/\Sigma - X_{offset}$ and similarly for Y, where V_i is the voltage at pickup electrode i, k_x a calibration constant and Σ the sum of the four voltages. However, the signal processing is quite different. The Neumann electronics does serial signal processing (Delay-line Multiplex Single Pass Technology). The four analog signals are passed through a delay line and are then sent to the same ADC. A gain/attenuation correction in done is steps of 1 dB. In constrast, the Libera electronics uses parallel signal processing, including RF channel switching, amplitude compensation, phase equalization and automatic gain control. Calibration constants k_x and k_y for the standard DORIS vacuum chamber profile were determined by measurements many years ago. For the present cylindrical BPMs the constants were calculated using a boundary element method as described in [4].

Data from both readout systems were stored in the DORIS accelerator archive. All of the Neumann data were stored in the OLYMPUS slow control data base, whereas the Libera data were only available for the last part of the data taking period.

The goal of the present studies was: calibrate the up- and downstream BPMs, i.e. determine the zero-positions and the response to the wire position, check whether there was a dependence on the beam current (wire input signal) and beam species (pulse polarity), and to transform the beam position (wire position) into the OLYMPUS coordinate system. In addition, the two different readout electronics were cross-calibrated, in order to get consistent beam position information for the complete running period.

SETUP OF BPM TEST STAND

The calibration of the OLYMPUS/DORIS BPMs was done on a vertical BPM test-stand, based on an original design by Paul-Scherrer-Institute (PSI), Villigen, Switzerland. The original test stand construction was comprised of a vertically oriented segment of the beam tube containing a single button-type BPM chamber, fixed by a flange on a holder-table at the lower end of the setup. A thin wire-antenna, stretched by an oil-damped steel-weight at its lower end, is fixed in a N-type RF-connector, that is placed at the outer end of a horizontal wire-holder plate attached to a x/y- micrometer-portal-guide (mover) on top of the C-shaped steel holder-frame of the test-stand. The wire-antenna is driven by an appropriate pulsed or cw RF-generator-signal via the N-connector. A solid RF-ground connection between the RF-connector and the fixed beam-tube enables an optimum conduction of the RF-signal, avoiding an instable transition of the characteristic impedance between signal source cable and antenna. The present setup incorporated a second button BPM chamber, located below the first one on the upper end of the structure. During the pre-tests, the signal originally driving the antenna by a tuned, typically 2 ns long button-type pulse-signal of 40 V, turned out to be too low for the Libera electronics. After changing the source generator setup to a sinusoidal 500 MHz-cw-signal and optimization

STABILITY STUDY OF THE HIGHER ORDER MODE BEAM POSITION MONITORS AT THE ACCELERATING CAVITIES AT FLASH*

L. Shi [a,b,#], N. Baboi [a], R.M.Jones [b]
[a] DESY, Hamburg, Germany, [b] The University of Manchester, UK

Abstract

When electron beams traverse an accelerating structure, higher order modes (HOMs) are excited. They can be used for beam diagnostic purposes. Both 1.3 GHz and 3.9 GHz superconducting accelerating cavities at FLASH linac, DESY, are equipped with electronics for beam position monitoring, which are based on HOM signals from special couplers. These monitors provide the beam position without additional vacuum components and at low cost. Moreover, they can be used to align the beam in the cavities to reduce the HOM effects on the beam. However, the HOMBPM (Higher Order Mode based Beam Position Monitor) shows an instability problem over time. In this paper, we will present the status of studies on this issue. Several methods are utilized to calibrate the HOMBPMs. These methods include DLR (Direct Linear Regression), and SVD (Singular Value Decomposition). We found that SVD generally is more suitable for HOMBPM calibration. We focus on the HOMBPMs at 1.3 GHz cavities. Techniques developed here are applicable to 3.9 GHz modules. The work will pave the way for HOMBPMs of the E-XFEL (European X-ray Free Electron Laser).

INTRODUCTION

FLASH (Free-electron-LASer in Hamburg) [1] is a FEL (Free Electron Laser) facility to generate XUV (Extreme Ultraviolet radiation) and soft X-ray by the so-called SASE (Self Amplified Spontaneous Emission) process from energetic electron beam bunches. The beam is accelerated by seven 1.3 GHz modules that each of them has eight TESLA cavities working at 1.3 GHz and one 3.9 GHz module with four 3.9 GHz cavities. Each cavity has two HOM (Higher Order Mode) couplers to minimise the effects from the beam excited HOMs. The HOMs are brought out of the module to room temperature via cables.

There are in total 78 channels of HOM signal. All channels are equipped with independent down converter electronics. For the 1.3 GHz modules, electronics are designed by SLAC. The electronics designed by Fermilab for the 3.9 GHz module are being commissioned.

HOMBPMs have been demonstrated good performance [2, 5]. They have a great potential to reduce the number of conventional BPMs which are relative expensive along the linac. This is especially desirable for facilities which have long linac such as ILC [3] etc.

*The work is part of EuCARD[2], partly funded by the European Commission, GA 312453
liangliang.shi@desy.de

However, we found in the past that the HOMBPM systems at FLASH are not stable. They perform good after immediate calibration but the results become inconsistent after some time, from several hours to days.

In this paper, we first briefly present the basic principle of a HOMBPM and procedures for its calibration. Then we move to the methods we used to calibrate them. The results are shown in the last section. Future work and final remarks conclude the paper.

PRINCIPLE OF HOMBPM

When an electron beam traverses a cavity, HOMs are excited. We can classify them by the azimuthal dependence into 'Monopole', 'Dipole' etc. [4].

Among these modes, dipole modes have linear dependence on the beam offset relative to the electrical centre of the cavity [5].

A dipole mode at around 1.7 GHz has been selected for such purpose in the TESLA cavity since it has strong coupling to the beam. Thus it provides high sensitivity to the beam position offset [5].

Figure 1 shows a block diagram of a HOMBPM system.

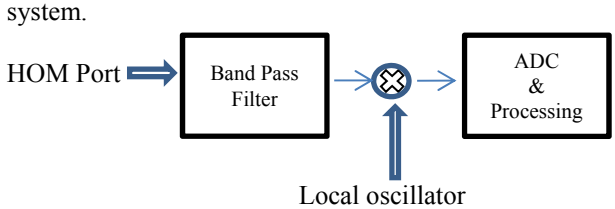

Figure 1: Block diagram of HOMBPM system.

The HOM signal is band filtered at around 1.7 GHz and down mixed with a signal from local oscillator. The signal is sampled and further transmitted to DOOCS (Distributed Object Oriented Control System) [6]. A user defined program was developed to perform data acquisition and post processing.

DATA DESCRIPTION AND MODEL OVERVIEW

Based on the HOMBPM system described above, the HOM data were gathered over half a year and are still under monitoring. The data was taken normally when FLASH operated in single bunch mode. The bunch repetition rate is 10 Hz. Most datasets were taken parasitically and we have four datasets that we moved the beam in a wide range. The data includes bunch charge from toroid readouts, the beam position from two cavity BPMs located upstream and downstream of the accelerating module and HOM signals from both HOM

ISBN 978-3-95450-141-0

MECHANICAL DESIGN OF CRYOGENIC VACUUM FEEDTHROUGHS FOR XFEL BUTTON BPMS

S. Vilcins, D. Lipka, DESY, Hamburg, Germany

Abstract

The European XFEL is a 4th generation synchrotron radiation source, currently under construction in Hamburg. Based on different Free-Electron Laser and spontaneous sources and driven by a superconducting accelerator, it will be able to provide several user stations with photons simultaneously.

Due to the superconducting technology in the accelerators modules many components have to operate at liquid helium temperature.

This poster will concentrate on high frequency ultra-high vacuum feedthroughs used for the beam position monitors of the cryogenic accelerator modules. Main emphasis will be put on the design of these feedthroughs, their material composition and the production process. The capability to be used under these very special conditions was investigated with FEM simulations, as well as with a test procedure. The results of these simulations will be presented; the tests and their results will be explained in detail.

INTRODUCTION

In particle accelerators like European XFEL (E-XFEL) many feedthroughs are used to monitor the electromagnetic field to determine and verify the actual beam position. At the European XFEL the Beam Position Monitors (BPM's) operate under two different ambient conditions, one under normal room temperature and the other one in a cryogenic environment, at ~4K. The cold button BPMs are installed close to the superconducting accelerator structures. Therefore they have to fulfil strict ultra-high vacuum and particle cleanliness requirements.

Many companies offer vacuum feedthroughs. Here the focus is on feedthroughs suitable for RF applications.

Such feedthroughs are coaxial structures, on one side with a pin, open conductor or button; on the other side a connector. In between there is a coaxial vacuum barrier, composed of inner and out conductor with dielectric material in between, providing the required leak tightness. Properties and geometry of the system has to be chosen such that they match to the required impedance of the coaxial system. The choice of isolation material is open to a wide field of materials. The usual technical ceramic materials are classified in three big groups, the oxide-ceramic (ZnO, LiO, SiO, Al_2O_3,), silicate ceramics (Stealit or porcelain) and non-oxide ceramics (Si_3N_4, BN or SiC).

The goal is to develop custom designed feedthroughs with well defined RF properties for accelerator applications at low temperatures and minimum particle emission. Therefore it is essential to understand the design principles and the mechanical characteristics of feedthroughs and BPM systems. Feedthrough prototypes installed on a test BPM at PSI, Fig. 1. The design of custom made feedthroughs requires, besides deep understanding of the RF requirements, other skills like knowledge in mechanical design and fabrication as well as some material science. Nowadays the extensive use of simulation tools help to speed up the design for the mechanical layout of a complete BPM [1], [2].

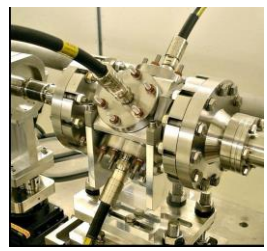

Figure 1: Cold button BPM mounted at SwissFEL test injector*.

R&D DESIGN PROPERTIES

The European XFEL is a 17.5 GeV superconducting linear accelerator with 71 button BPM's installed in superconducting cryostats next to the cold quadruple at temperatures about 4K. The beam pipe apertures of these BPMs is 78 mm, the length is 170 mm.

The BPM bodies, feedthroughs, cables have to deposit only negligible heat load into the cryogenic environment. High losses will increase the cryogenic cooling power and will raise the operation costs [3]. BPM body and button have to have high surface conductivity in order to minimize ohmic losses of high frequency HOM fields in the superconducting cavities. Therefore, all parts are copper plated or made from copper.

The nominal bunch charges of E-XFEL are between 0.1 and 1 nC. The BPMs must be able to measure position of single bunches with 220 ns spacing, in trains of up to 2700 bunches, and a repetition rate of 10 Hz. Train-by-train rms position resolution averaged over the bunch train was specified to be better than 10 µm, single bunch resolution should be better than 50 µm [4].

Mechanical robustness was the leading criterion. Vacuum tightness at 330 K and liquid helium temperature, as well as during cool down and warming up cycles and thermal-shock resistance are main design issues. Further requirements were implied due to the particle cleanliness requirements and the conformity to assembly procedures in the clean rooms. Therefore, the flange was designed for the so called diamond shaped aluminium gaskets, used for E-XFEL cavity string assembly. Due to the vicinity of the superconducting quadruple of the model as well as the cavities strict requirements on nonmagnetic materials had

*This photography is provided by Daniel Treyer, PSI, Swiss.

ISBN 978-3-95450-141-0

FIRST TESTS OF A MICRO-TCA-BASED DOWNCONVERTER ELECTRONIC FOR 5GHz HIGHER ORDER MODES IN THIRD HARMONIC ACCELERATING CAVITIES AT THE XFEL†

T. Wamsat*, N. Baboi, Deutsches Elektronen-Synchrotron DESY, Hamburg, Germany

Abstract

Beam excited higher order modes (HOM) in 3.9GHz accelerating cavities at the European XFEL are planned to be used for beam position monitoring. The specifications of the monitors have been defined during an extensive study on the 3.9GHz module at FLASH. Selected HOMs for precision measurement are located around 5440MHz and 9040MHz. An electronics developed by FNAL has been recently installed at FLASH and provides a basis for the XFEL electronics.

The paper will present the design and first test of the hardware for the MicroTCA standard used for the XFEL. The hardware consists of three different Rear Transition Modules (RTM), two four channel downconverter RTMs (5GHz and 9GHz) and a third RTM with two phase locked loop synthesizers on board for LO generation. Presently the 5GHz and the PLL RTMs are under construction. The first measurements with these cards will be presented.

INTRODUCTION

The European X-ray Free Electron Laser 3.9GHz accelerating cavities are located right after the 1.3GHz injector module before the first bunch compressor, as shown in Fig. 2 [1]. The module is similar to the ACC39 module built by FNAL for the Free Electron Laser Hamburg (FLASH) [2], containing four third harmonic cavities.

The XFEL 3.9GHz module consists of eight cavities each with two HOM couplers respectively as shown in Fig. 3. We want to equip four couplers, the respective outer two, with electronics for modes around 5440MHz and fourteen for modes at 9060MHz suitable for beam monitoring as obtained in tests at FLASH ACC39 [3].

System Overview

At the XFEL the MicroTCA.4 [4] standard will be used. Figure 1 shows the planned fully equipped MicroTCA crate, consisting of five four channel downconverter RTMs with its particular SIS8300 AMC card [5]at the other side (not visible), one for the 5.44GHz modes and four 9.06GHz boards. We also see the HOM-PLL (Higher Order Mode Phase Locked Loop) RTM with a DAMC2 [6] card on the other side (not visible) to generate the LO-frequency and the uLOG for LO amplification and distribution over the MicroTCA backplane. [7]

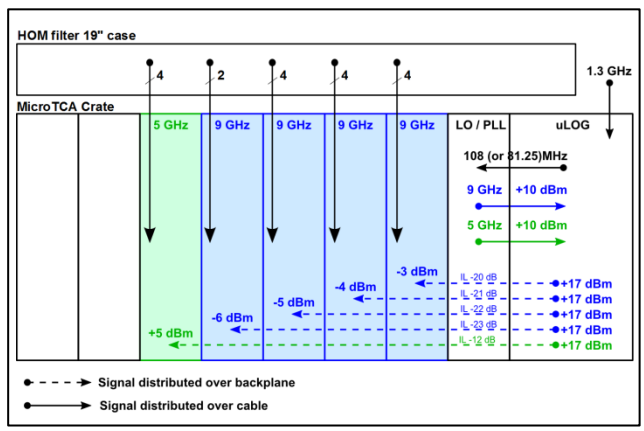

Figure 1: Overview over the complete system installation.

Above the crate there is a case which contains the HOM selecting bandpass filters for each channel. The outputs of the HOM coupler will be connected to the HOM filters.

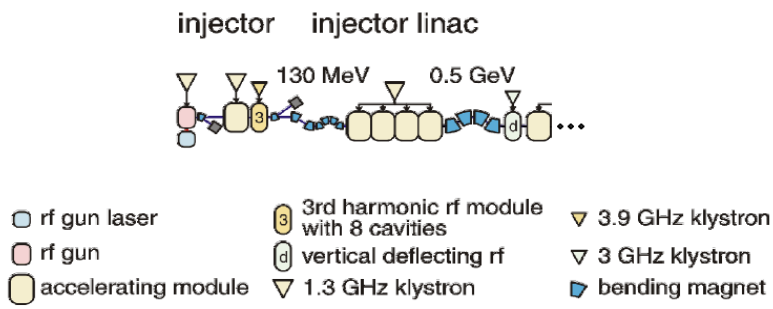

Figure 2: Schematic layout of the European XFEL injector [1].

†The work is part of EuCARD-2, partly funded by the European Commission, GA 312453

*thomas.wamsat@desy.de

ISBN 978-3-95450-141-0

DIAMOND-BASED PHOTON BPMS FOR FAST ELECTRON-BEAM DIAGNOSTICS IN SYNCHROTRON RADIATION SOURCES

M. Antonelli, G. Cautero, D. Giuressi, S. Lizzit, R. H. Menk,
Elettra – Sincrotrone Trieste S.C.p.A., Trieste, Italy
A. De Sio, E. Pace, Università degli Studi di Firenze, Firenze, Italy
M. Di Fraia, Università degli Studi di Trieste, Trieste, Italy

Abstract

Electron-beam stability is amongst the primary concerns in current Synchrotron Radiation (SR) sources; in particular, in third-generation SR facilities high-brightness beamlines using undulator radiation are extremely sensitive to electron-beam oscillations. Orbit stabilization has been intensively addressed in the past years and many SR machines have been equipped with a Fast Orbit Feedback (FOFB) based on electron Beam-Position Monitors (eBPMs).

On the other hand, photon Beam-Position Monitors (pBPMs), besides providing beamline users with crucial calibration data, are also a useful tool for keeping the electron beam under control, by monitoring position and intensity of the delivered radiation. The machine control system can take advantage of this information in order to improve the stability of the electron-beam.

A diagnostic beamline, utilizing a couple of fast pBPMs based on single-crystal CVD diamond detectors, has been built and inserted into the central dead-end outlet of one of Elettra's bending-magnets. Tests have been carried out both during normal machine operations and by deliberately moving the orbit during dedicated shifts. Owing to the outstanding properties of diamond in terms of speed and radiation hardness, the results show how the aforementioned system allows the beam position to be monitored with sub-micrometric precision at the demanding readout rates required by the FOFB. The radiation hardness of the sensors allows the operation over extended periods of time without special maintenance.

Therefore, this system is particularly suited for storage-ring sections lacking in electron-beam monitoring and the tested diagnostic line represents a demonstrator for future implementation of pBPMs at several bending-magnet front ends of Elettra.

INTRODUCTION

In modern SR facilities electron-beam monitoring and stabilization are amongst the primary concerns. In particular, the high-brightness beamlines using undulator radiation are the most sensitive to electron-beam oscillations occurring in 3rd-generation light sources [1]. Therefore, such machines are equipped with specific control systems, like the FOFB, based on the measurements of the eBPMs implemented along their storage rings [2].

Despite such stabilization measures and owing to a number of instability sources, the resulting photon beam can exhibit residual fluctuations in terms of both position and intensity. These phenomena can be detected by utilizing pBPMs, which are capable of simultaneously estimating the intensity and the position of the emitted beam passing through. Fast pBPMs inserted in beamlines are well-suited for either *a posteriori* data calibration or real-time adjustment in beamline experiments [3]. Nevertheless, the information provided by such detectors is useful for the electron-beam diagnostics and it can be integrated into the FOFB [4]. In particular, if pBPMs are installed upstream from the beamline optics, their measurements are directly related to the status of the electron beam as they are not affected by any instability imputable to optical elements (such as mirrors, monochromators, etc.).

Amongst the available technologies for the production of fast and semitransparent *in situ* pBPMs, diamond grown by Chemical Vapour Deposition (CVD) is one of the most suitable materials owing to its outstanding physical properties. Because of its high bond energy it can withstand the high dose rates occurring in 3rd- and 4th-generation SR sources and its low atomic number renders it semitransparent to X-rays. Besides, due to its high energy gap, intrinsic diamond is an insulator with low thermal noise at room temperature, while its high electron and hole mobility allows charge to be collected faster than in many other active materials [5, 6].

With the aim to provide Elettra's future FOFB with additional information stemming from state-of-the-art diamond pBPMs, a diagnostic beamline has been built at the central outlet of one of Elettra's bending magnets. The present document reports on the main features of the implemented line, its monitoring performances and its long-term reliability.

DIAGNOSTIC BEAMLINE

At Elettra, each bending magnet was originally designed with a three-way radiation pipe. The lateral outlets became then the anchoring points for the implemented user beamlines, while the central ones remained unused. The presented diagnostic line has been built at one of those central dead-end outlets in order to continuously monitor the photon beam without interfering with normal beamline operations. This prototype has been completely accommodated inside the shielding wall of the storage ring, between the pipes of the 10.1L and 10.1R beamlines, as shown in Fig. 1. This solution has imposed stringent space constraints, which have been met due to the compact size of the diamond pBPMs.

ISBN 978-3-95450-141-0

NEWLY DEVELOPED 6mm BUTTONS FOR THE BPMS IN THE ESRF LOW-EMITTANCE-RING

B.K. Scheidt, ESRF, Grenoble, France

Abstract

For the small beam pipe of the BPMs in the LE-ring a development of 6mm button-UHV-feedthroughs was launched and has resulted in the delivery of a total of 27 prototypes from both the Kyocera and the PMB-ALCEN companies. These buttons are flat, without skirt, with a central pin of Molybdenum ending in a male SMA connector. Among these prototype units are versions with Copper, Steel and Molybdenum material for the button itself, with the aim of assessing possible different heat-load issues. All design considerations, that are compatible with a further button reduction to 4mm, will be presented next to issues of costs, mechanical tolerances and feasibility.

DESIGN ASPECTS OF THE SMALL BPM BUTTONS-FEEDTHROUGHS

The European Synchrotron Radiation Facility has decided to replace its existing double-bend-achromat lattice for 7-bend-achromat lattice that aims to reduce the horizontal emittance from 4 to below 0.15nm·rad. [1]

In this new Ring a total of 288 BPM stations (9 in each of the 32 cells) are foreseen with beam-pipe diameters much reduced with respect to the dimensions in the present Ring. The Fig.1 shows the cross-section of two examples of the preliminary design.

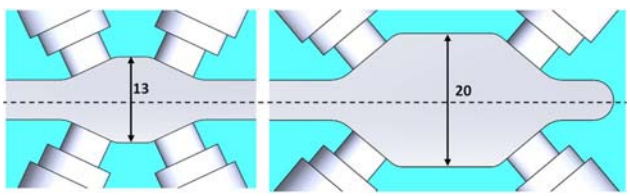

Figure 1: Cross sections of two different future BPMs.

In the existing Ring at total of nearly a thousand of buttons of 10mm diameter (but in BPM cross-sections of 70x34mm) have been successfully used for over 22 years for BPM purposes in a reliable way, i.e. without failures on the UHV aspects, or on the RF-signal pick-up aspects. This reliability issue was important to inspire the design of the new buttons.

For the new BPMs a diameter of 6mm for the button was decided and the study and the realisation of such button were pursued with two independent companies : Kyocera (Japan) and PMB-ALCEN (France). [2, 3]

The pictures in Figs.2 and 3 show the design of the entire button and feedthrough. The main characteristics can be resumed as follows :

- The button, the UHV feedthrough and the (male) SMA connector are all self-contained in one housing that can be (circularly) welded to its lodging hole of the BPM block. This design has successfully served the ESRF for its present ring and also avoids fully the use of vacuum flanges.
- The button (6mm diameter, 4mm height) is without skirt. It is brazed to the central pin and has a support ring (3mm) to the ceramic (but not brazed).
- The central conductor is of Molybdenum and forms the central pin of a standard SMA connector.
- The ceramic disk is of Alumina (Al2O3) and of 9mm diameter and 2.5mm height.
- The housing (13mm outer diameter) is of Stainless Steel.
- The concentricity specifications are at 50um between the button and the outside of the housing.

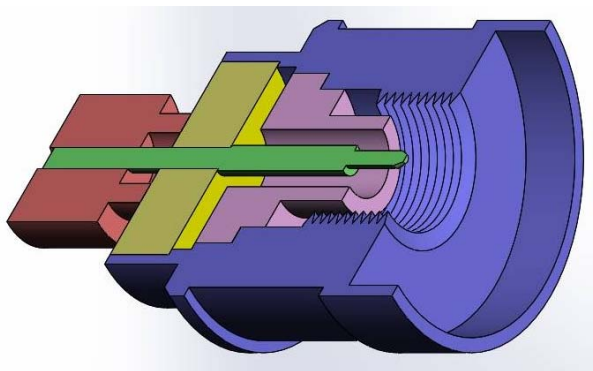

Figure 2: illustration of the button, central-pin-conductor, ceramic isolation, (male) SMA connector and housing.

All parts are prepared, assembled and then brazed according to the specific methods and technology of each of the two companies. The mechanical tolerances, and notably the concentricity, are accepted by each company as part of the final specifications at delivery.

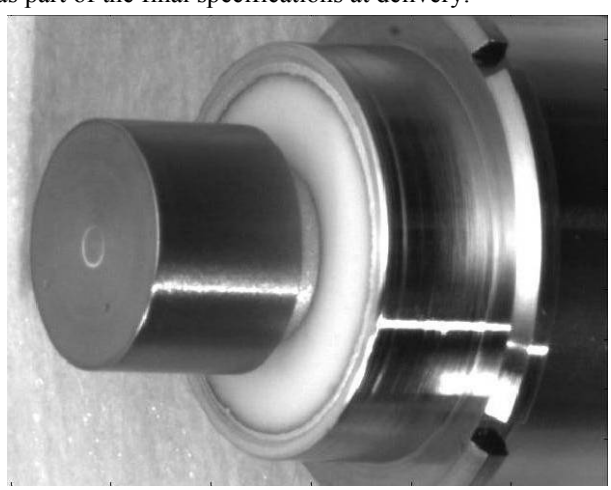

Figure 3: Photograph showing one unit with the 6x4mm button, its central pin welding and its support to the ceramic, and the UHV side of the housing.

FIRST RESULTS WITH THE PROTOTYPES OF NEW BPM ELECTRONICS FOR THE BOOSTER OF THE ESRF

B.K. Scheidt, ESRF, Grenoble, France

Abstract

The 25 year old BPM electronics of the ESRF's Booster (200MeV to 6GeV, 300m, 75 BPM stations) are in process of replacement with new modern acquisition electronics. The design and development of this acquisition system was done in collaboration with the Instrumentation Technologies company and has resulted in a commercial product under the name Libera-Spark. It contains RF filtering & amplification electronics in front of 14 bit & 125MHz ADCs for 4 channels, followed by a (Xilinx ZYNQ) System_on_Chip for all processing, that also includes the possibility of single bunch filtering directly on the ADC data. It is housed in a compact and robust module that is fully powered over the Ethernet connection and which facilitates its installation close to the BPM stations thereby avoiding long RF cabling. For simplicity and cost economic reasons this Spark is without PLL and adjustable RF attenuators since not needed for Booster BPM applications, but possible in elaborated versions for other applications. Two prototypes were fully tested with beam and the results in terms of resolution & stability were assessed since delivery in January.

THE ESRF BOOSTER RING AND MOTIVATION FOR NEW BPM SYSTEM

The European Synchrotron Radiation Facility operates a 200 MeV linear Pre-Injector and a full energy fast cycling Booster synchrotron that accelerates the electron beam to the 6GeV energy in an acceleration period of 50millisec before extraction to the 2nd transferline and subsequent injection into the Storage Ring. This Booster presently still uses the original power supplies for the magnets that function with a resonant "white-circuit" at 10Hz cycling frequency, producing biased sine wave currents in these magnets. That magnet's power supply system will be replaced in 2015 by ramping power converters, with a minimum cycling rate of 250ms (150ms ramping up and 100ms ramping down), followed by a partial re-commissioning of the Booster.

The Booster has a circumference of 300m and contains 75 BPM blocks with each 4 buttons of 10mm diameter in a circular chamber of 60mm internal diameter. The 4 buttons are angularly distributed with 4 equal 90deg angle shifts between them, but with a 45deg angle offset with respect to horizontal and vertical planes. The so-called K factor for this BPM geometry is 21.5mm when using the simple delta/sum algorithm for calculating the beam position from the 4 RF signal strengths measured at the buttons.

The RF signal amplitude, at the sma connector of the button feedthrough, is about 300uV rms for 1mA of Booster current. The RF frequency is 352.2MHz and the maximum nominal current 5mA in so-called long-pulse (from Linac) which produces a bunch-train of 352 bunches. However, the Booster also operates routinely in multi-single bunch configurations with only 1 to 5 bunches and typical currents between 0.1 and 0.5mA.

Motivation for the New BPM Electronics with Improved Functionality and Performance

The old electronics and acquisition system had no functionality for Turn-by-Turn measurements and could only perform 6 punctual measurements in the 50millisec acceleration cycle. These old electronics have an RF multiplexer in close vicinity to the BPM block (hence inside the Booster Tunnel) and the rest of the electronics in permanently accessible cabinets, but at RF cable lengths varying between 20 and 60meters. [1]

A few years ago 2 Libera-Brilliance units were installed to perform the signal acquisition of the RF signals from 2 BPM blocks and had been helpful to demonstrate the benefits of more performing BPM measurements, notably serving as a new Booster tune measurement system. However, the Libera system is specifically designed for Storage Ring BPM requirements with incorporated functionalities that have strictly no application in a Booster BPM system with only a beam duration of a fraction of a second.

The search for an alternative, but also more cost-effective, system for the acquisition of the 4 weak RF signals aimed at simplifying the concept to a strict minimum but yet achieving Turn-by-Turn measurement functionality even for (low current) single bunch fillings. A completely new hardware design that needs no maintenance (passive cooling, no disc, power over ethernet) was elaborated by the Instrumentation Technologies company and resulted in a new and now commercial, product, named as Libera Spark [2, 3].

FUNCTIONAL DESCRIPTION OF SPARK

The main features of the Spark device can be resumed as follows :

- 4 channels digitizer for weak RF signals.
- Adequate signal processing for the calculation of the 4 signal strengths, comprising I , Q and Sum values, the beam-position values, and this all for data-rates reduced to Turn-by-Turn rate and lower, and this also optimized for specific (single-bunch) filling patterns
- Efficient and straight-forward interface (SCPI commands) for the control & read-out via Ethernet.
- Suitable and compact chassis & housing, with Power-over-Ethernet (IEEE802.3af standard).

ISBN 978-3-95450-141-0

FRIB BEAM POSITION MONITOR PICK-UP DESIGN*

Oren Yair#, Jenna Crisp, Gerlind Kiupel, Steven Michael Lidia, Robert C. Webber, Facility for Rare Isotope Beams (FRIB), Michigan State University, East Lansing, MI 48824 USA

Abstract

The heavy ion linac under construction at Michigan State University as part of the Facility for Rare Isotope Beams requires a Beam Position Monitoring System with dual-plane pick-ups at 147 locations. Four different pick-up designs will be used with apertures of 40, 50, 100, and 150 mm. The 40 mm BPMs are designed to operate at cryogenic temperatures, as 39 are bolted to superconducting RF cavities and reside in the insulating vacuum of the cryomodule. The other designs serve only room temperature locations. Requirements, designs, analyses, tests, and status is reported

INTRODUCTION

The Facility for Rare Isotope Beams (FRIB) will be a new national user facility for nuclear science, funded by the Department of Energy Office of Science (DOE-SC), Michigan State University (MSU), and the State of Michigan. Under construction on campus and operated by MSU, FRIB will provide intense beams of heavy ions to produce rare isotopes. A heavy ion superconducting linac capable of accelerating ions up to Uranium with energies higher than 200 MeV/u and beam power up to 400 kilowatts will be used. The primary time structure for beam ranges from 50 μs pulses at 1 Hz to nearly CW beam with 100Hz 50 μs notches. The bunch rate will be 20.125, 40.25, or 80.5 MHz and the velocity will range from 3.3 to 50% the speed of light.

With 100 μA beam current, the required BPM system accuracy is ±0.4 mm and resolution is 0.1 mm. Accuracy includes survey errors with respect to the designed beam orbit, linearity and electrical center in the BPM, cable mismatch, amplifier impedance and gain, and receiver errors. Accuracy addresses the ability to thread the beam safely through the linac while preserving aperture. BPM stability reduces the frequency of beam based alignment and aperture scans used to identify and maintain optimum beam orbit.

Resolution is focused on the ability to measure changes while tuning. This allows measurement of the machine lattice and helps identify irregularities or failures in other accelerator components. The relevant time period for resolution is a day.

The BPM system will also be used to identify optimum accelerating cavity phase by measuring beam time of flight.[1] With 100 μA beam current, the required phase accuracy is ±2 degrees at 80.5MHz with 0.5 degree resolution.

Beam intensity will be measured with the BPM system as well. Sensitivity to position and bunch length is problematic. Accuracy of a few percent should be possible for reasonable beam conditions.[2][3]

BPM PICK-UP RESOLUTION

Split plate style BPMs are inherently more linear [4] than button or stripline BPMs. However, split plate and stripline designs require additional complexities to hold the electrodes in position. The single support point characteristic of button BPMs alleviates problems with differential expansion at cryogenic temperatures.

Button BPMs are both non-linear and dependent on the position in the orthogonal plane. A general rule of thumb is that the button width should be about 60° wide leaving a 30° gap between buttons. Buttons with a flat face rather than one that aligns with the inside surface of the BPM aperture are simpler and less expensive to make, yet, provide good response.

Position and resolution near the center of a button bpm of diameter D is estimated below. The D/π scale factor is only an approximation but is reasonably accurate over 1/3rd of the aperture.

$$Pos \approx \frac{D}{\pi}\frac{A-B}{A+B} \quad mm \qquad Pos_N \approx \frac{D}{\pi\sqrt{2}}\frac{V_N}{V_{button}} \quad mm$$

The voltage induced on a BPM electrode can be estimated from its geometry, beam current, and button impedance.[5] The image current has equal but opposite charge on the inside of the beam pipe and follows the beam. The image current flowing onto the button as the beam enters the BPM must come off of the button as the beam exits. The time difference is the combination of the beam flight time and the signal delay time across the button. The fraction of image current intercepted by a button is d/4D. The BPM output is nearly an ideal current source as the voltage induced on the button is not sufficient to change the beam current. For bunches reasonably short compared to the period of the frequency being measured, $I(\omega) \approx 2I_{avg.}$

*This material is based upon work supported by the U.S. Department of Energy Office of Science under Cooperative Agreement DE-SC0000661, the State of Michigan and Michigan State University. Michigan State University designs and establishes FRIB as a DOE Office of Science National User Facility in support of the mission of the Office of Nuclear Physics.

#yair@frib.msu.edu

ISBN 978-3-95450-141-0

DEVELOPMENT OF A BUTTON BPM FOR THE LCLS-II PROJECT*

A. Lunin#, T. Khabiboulline, N. Solyak, V. Yakovlev
FNAL, Batavia, IL 60510, USA

Abstract

A high sensitivity button BPM is under development for a linac section of the LCLS-II project. Since the LCLS-II linac will operate with bunch charge as low as 10 pC, we analyse various options for pickup button and feedthrough in order to maximize the BPM output signal at low charge regime. As a result the conceptual BPM design is proposed including an analytical estimation of the BPM performance as well as numerical simulation with CST Particle Studio and ANSYS HFSS. Both numerical methods show a good agreement of BPM output signals for various design parameters. Finally we describe the signal processing scheme and the electronics we are going to use.

INTRODUCTION

Achieving a low beam emittance is one of key factors for reliable operation of the LCLS-II project [1]. In order to preserve a low emittance during beam transportation through the superconducting linac, Beam Position Monitors (BPM) will be installed in every cryomodule with a quadrupole. These BPMs will be used to monitor the beam orbit and provide transverse beam position data for beam steering. Since the "cold" BPMs are the only beam instruments inside the cryogenic sections of the linac, therefore a high reliability of the BPM systems is essential. Some of the specific requirements of the cold BPMs are listed below:

• The space inside the cryomodule for installation is limited to ~180 mm length and ~200 mm transverse size (with feedthrough). The beam pipe aperture is circular, having 78 mm diameter.

• The BPM has to operate under ultra-high vacuum (UHV) conditions, and in a cryogenic environment at a temperature of ~2. 10 K.

• A cleanroom class 100 certification is required to prevent pollution of the nearby SC cavities.

The LCLS-II linac can operate in a variety of regimes with parameters of electron beam shown in Table 1. A single bunch (bunch-by-bunch) resolution of < 100 μm at 10 pC is required to preserve the low emittance by applying dispersion-free orbit correction methods during single short operation. The BPM ability to perform at low charge regimes also allows for troubleshooting and diagnostics during the linac commissioning procedure, but can be guaranteed only nearby (± 1...2 mm) the electrical center of the BPM pickup.

Based on the above requirements the choice of BPM is limited mostly to beam orbit monitoring with button BPM pickups due to its compactness, simple mechanical design and reliability. The large button cold BPM from the European XFEL is an existence proof of a design that has been successfully integrated into a cryomodule [2], which should be able to meet the resolution requirements here, but this has not been demonstrated at the low bunch charge expected and puts much more strenuous requirements on electronics processing scheme.

Table 1: Electron Beam Parameters of the LCLS-II Linac

Operation Mode	CW
Beam Energy	4 GeV
Bunch charge	10 ÷ 300 pC
Bunch length, rms	0.6 ÷ 53 μm
Emittance (at 100 pC, normalized)	~ 0.3 μm
Bunch rate	< 0.93 MHz

Thus, the design of the cold XFEL BPM with large 20 mm diameter buttons was chosen as a prototype pickup for beam diagnostic in the LCLS-II cryomodule [3]. According to the baseline scheme of a signal processing the frontend electronic will downmix the button signal in the pass band around 1 GHz comparing to 1.5 GHz ÷ 2.3 GHz frequency band used for the XFEL cold BPM [4]. Despite the simplicity of a processing scheme at low frequencies there are pro and contra arguments of working around 1 GHz instead of 2 GHz: a) the pickup will produce fewer signals, b) the RF bandpass filters and pickup cables will have smaller losses, c) signal of L-band linac may leak into the BPM [5]. While items a) and b) may compensate each other depending on the actual pickup cable parameters, prevention of effect c) requires that the upper bandwidth should be reduced significantly below 1.3 GHz. This might directly compromise usable signal level and, thus, the position noise. Because the exact relation of position noise versus bandwidth remains to be determined we don't limit ourselves with a design of low frequency button pickup only and propose the optimal geometry of a button and feedthrough assembly for 2 GHz also as a backup option.

GENERAL ASPECTS OF THE BUTTON TYPE PICKUP EM DESIGN

Relativistic charged particles moving inside a hollow metal beam pipe is followed by a pancake like electromagnetic field with longitudinal extension of the bunch size itself. The field on the inner wall of a beam pipe is diffracted on the button gap and induces wakefield travelling in the beam pipe and rf signal radiating through

* Operated by Fermi Research Alliance, LLC under Contract No. De-AC02-07CH11359 with the United States Department of Energy.
#lunin@fnal.gov

ISBN 978-3-95450-141-0

BEAM POSITION MONITOR ELECTRONICS UPGRADE FOR FERMILAB SWITCHYARD*

P.Stabile#, J. S. Diamond, J.A. Fitzgerald, N. Liu, D. K. Morris, P. S. Prieto, J. P. Seraphin
FERMILAB, Batavia, IL, 60510, USA

Abstract

The beam position monitor (BPM) system for Fermilab Switchyard (SY) provides the position, intensity and integrated intensity of the 53.10348MHz RF bunched resonant extracted beam from the Main Injector over 4 seconds of spill. The total beam intensity varies from $1x10^{11}$ to $1x10^{13}$ protons.

The spill is measured by stripline beam postion monitors and resonant circuit. The BPMs have an external resonant circuit tuned to 53.10348MHz.

The corresponding voltage signal out of the BPM has been estimated to be between -110dBm and -80dBm.

INTRODUCTION

During current operation the Main Injector accelerates beam to 120Gev and extracted to the Switchyard (SY). Beam is extracted at the MI52 area, transported through P1, P2 and P3 beam lines, and then steered to the original Switchyard beam line where it traverses Enclosures B, C and the F-manholes, finally arriving to the Target [1].

Extraction is implemented by the half-resonant integer mode and is regulated by a quadrupole circuit (QXR) to resonantly extract beam over 4 seconds.

The typical spill intensities vary from $1x10^{11}$ protons to $1x10^{13}$ protons per machine cycle with the protons distributed into 486 of the 588 53.10348MHz RF buckets that make up the machine's circumference. Extracting $1x10^{13}$ protons over 4 sec accounts for $2.5x10^{12}$ protons per second (pps). With a revolution frequency of the machine equal to 90.312KHz (53.10348MHz/588), a total of $27.68x10^{6}$ protons are extracted per turn ($2.5x10^{12}$pps/90.312KHz). Dividing the number of protons per turn by the number of buckets a total of $56.95x10^{3}$ protons per bunch can be estimated. Extracting $1x10^{12}$, using the same calculations, accounts for $5.695x10^{3}$ protons per bunch

SYSTEM DESCRIPTION

The stripline BPMs have a pair of detector plates, facing each other inside the beam pipe.

The plate capacitances are equal to 65pF and the plate-to-plate capacitance is 8pF.

In order to resonate at the desired extraction frequency three inductors were added to the circuit (Figure 1) [2].

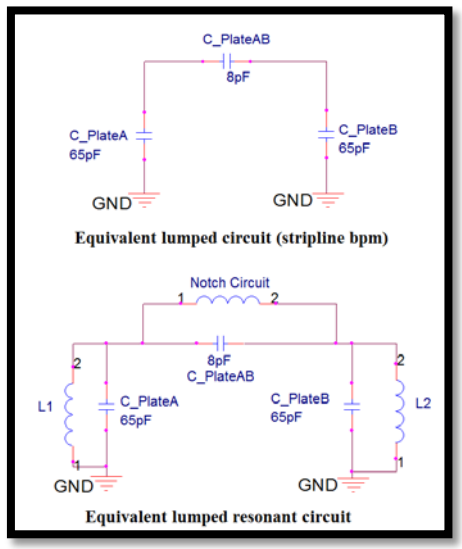

Figure 1: Equivalent circuit for resonant BPM.

During extraction the particle beam can be considered as a current generator at 53.10348MHz (flat top extraction frequency). The signal power detected by the position detector can therefore be increased by raising the detector shunt impedance for the Fourier components of beam current that are chosen (for simplicity the detector is tuned for the n=1 Fourier component).

The detectors are tuned to resonate at the RF frequency of 53.10348 MHz, with a resulting increase of detector shunt impedance from 50Ω to 9.5 KΩ and a Q of around 190.

The original beam position monitor system for the SY was first designed in 1985 [3] and then installed in 1986.

The new designed electronic system consists of:

1. Detectors (Resonant BPMs).
2. RF Transition Board (Analog Front-End).
3. Digitizer (Digital Acquisition and Processing).
4. MVME 5500 Single Board Computer (Software interface).

Figure 2 shows a block diagram of the SY electronic system.

* This work was supported by the U.S. Department of Energy under contract No. DE-AC02-07CH11359.

stabile@fnal.gov

ISBN 978-3-95450-141-0

NSLS2 VISIBLE SYNCHROTRON LIGHT MONITOR DIAGNOSTIC BEAMLINE COMMISSIONING*

W. Cheng#, B. Bacha, H. Xu, Y. Hu, O. Singh
NSLS-II, Brookhaven National Laboratory, Upton, NY 11973

Abstract

Visible Synchrotron Light Monitor (SLM) beamline has been designed and constructed at NSLS2 storage ring, to characterize the electron beam profile at various machine conditions. Due to careful alignment, SLM beamline was able to see the first light even before beam circulating the ring. Besides a normal CCD camera to monitor the beam profile, streak camera and gated camera are used to measure the longitudinal and transverse profile to understand the beam dynamics. Measurement results from these cameras will be present in this paper.

INTRODUCTION

NSLS2 is a third generation light source at Brookhaven National Laboratory. The 3GeV low emittance storage ring has been commissioned with beam recently. Average current of 50mA beam was able to be stored in the ring with superconducting RF cavity [1]. While electrons pass through the bending magnet, broadband synchrotron radiation will be generated. This can be used to measure the transverse and longitudinal profile.

Visible synchrotron light monitor (SLM) diagnostic beamline utilizes the radiation from C30 BM-B, which is the second dipole after injection straight. Nominal source point is ~2.75mrad into the dipole. The beamline has acceptance of +/-1.5mrad horizontal and +/-3.5mrad vertical. Visible light from the dipole synchrotron radiation will be reflected by in-vacuum mirror. The visible light is guided into SLM hutch located on the C30 experimental floor. There are various optics setups on the 4'x10' optical table, currently there are three branches setups: CCD camera branch; fast gated camera branch and streak camera branch. Visible light can be guided to different cameras. More information on the diagnostic beamline design can be found at [2].

Figure 1 shows the installed beamline and optical table setups. Radiations from the dipole pass through the fixed aperture, which defines the source point and horizontal/vertical apertures. Upstream of the fixed mask are vacuum gate valve (GV) and bending magnet photon shutter (BMPS). These two components are standard for NSLS2 beamlines which can be used to shut down the photon whenever needed. Most high energy photons are blocked by the thin absorber called "cold finger". The cold finger has vertical aperture of +/-0.5 mrad. Most of the power will be blocked by the cold finger so that downstream first mirror sees less than 1W of power at 500mA. The cold finger is controlled through a linear motor and stage. It can be fully retracted or tracking the electron beam position with 10um resolution. In vacuum first mirror reflect the visible (and near infrared) light 90 degree out of the vacuum window. The mirror was made from Glidcop with Aluminum coating. Both first mirror and vacuum window have flatness better than 50nm, which is about 1/10 of interesting wavelength. Visible light is then reflected by three 6'' diameter in air mirrors on to the experiment floor, where a dark room and 4'x10' optical table are located. Synchrotron light first gets focused on the optical table with 6'' achromatic lens. Focal length of the lens is 2.25 m. Light is then guided to different cameras using beam splitter and reflection mirrors.

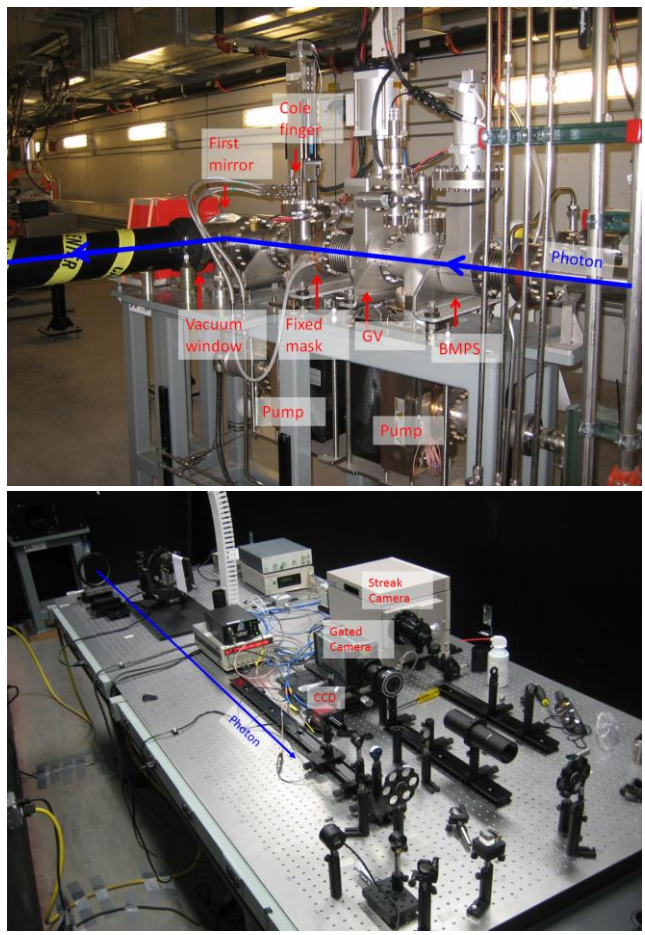

Figure 1: (top) Installed visible synchrotron light monitor (SLM) beamline components inside the NSLS2 storage ring tunnel; (bottom) Optical table setup in the SLM hutch.

* This material is based upon work supported by the U.S. Department of Energy, Office of Science, Brookhaven National Laboratory under Contract No. DE-AC02-98CH10886.
#chengwx@bnl.gov

ISBN 978-3-95450-141-0

BEAM SIZE MEASUREMENTS USING SYNCHROTRON RADIATION INTERFEROMETRY AT ALBA

L. Torino, U. Iriso, ALBA-CELLS, Cerdanyola, Spain
T. Mitsuhashi, KEK, Tsukuba, Japan

Abstract

First tests to measure the transverse beam size using interferometry at ALBA showed that the measurement reliability was limited by the inhomogeneous light wavefront arriving at the double slit system. For this reason, the optical components guiding the synchrotron radiation have been exchanged, and detailed quality checks have been carried out using techniques like the Fizeau interferometry or Hartmann mask tests. We report the results of the analysis of the optical elements installed in the beamline, and the beam size measurements performed using double slit interferometry in both horizontal and vertical planes.

INTRODUCTION

ALBA is a 3 GeV third generation synchrotron light source operative for users since 2012 [1].

Due to the machine small emittance it is not possible to measure the beam size by using a simple imaging system because of the diffraction limit. Measurements of the beam size are nowadays routinely performed using a x-ray pinhole camera [2]. In order to have a second reliable measurement of this parameter the double slit synchrotron radiation interferometry technique (SR interferometer) [3] has been proposed and is still under development. Preliminary tests were performed at the diagnostic beamline Xanadu using the already existing optical components which quality was not good enough to provide the best results [4].

In this report we describe the improvement of the beamline optical components and the tests performed to ensure their quality. We also report some results of the interferometry measurements.

THE SR INTERFEROMETER

The main parameters of the ALBA lattice that determine the transverse beam size at the source point are listed in Table 1.

Table 1: ALBA Lattice Parameters

	x	y
β	0.299 m	25.08 m
Dispersion	0.04 m	0 m
Energy spread	0.001 01	—
Emittance	4.6 nm	0.023 nm
Beam size	53.6 µm	23.9 µm

One of the most common techniques to measure beam sizes in this range is the SR interferometer. Using a double slit interferometer the degree of spatial coherence of the synchrotron radiation produced by the beam is measured, from where the beam size can be inferred. A sketch is presented in Fig. 1.

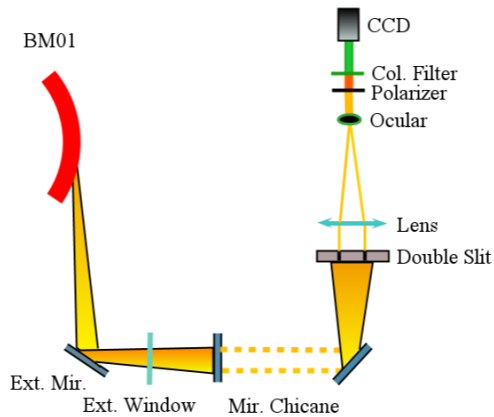

Figure 1: Sketch of the SR interferometer setup at ALBA. The optical path is composed by 6 mirrors in atmospheric pressure. The extraction mirror is set in the vacuum.

The visible part of the radiation produced by the electron beam passing through a bending magnet (BM01) is extracted by an in-vacuum mirror located at 8.635 m from the source and at $\simeq$ 6 mm from the beam orbit plane. In this way the extraction mirror is not in contact with hard x-rays that may compromise its characteristics. Only the radiation produced with a positive angle with respect to the beam orbit plane is collected, for this reason the mirror is said to be an "half-mirror". The light is extracted through a window and guided out from the tunnel up to the optical table in the beamline by 6 mirrors. The interferometer system is composed by a double slit aperture that produces the interferogram. The width of the slits is 1 mm and the height is chosen depending on the quantity of light needed. The separation between the two slits is variable from 8 mm to 22 mm. Immediately after the double slit an apochromat (BORG ED500) lens with focal length of 500 mm and flatness $\frac{\lambda}{10}$ is located. After the focal point an ocular (Takahashi MC LE 18 mm) is introduced to magnify the image. A polarizer and a 540 nm narrow bandpass color filter (width 10 nm) both from Thorlabs are used to select the σ radiation polarization and energy. Finally the interferogram is captured by a CCD camera whose pixel size is 3.75 µm × 3.75 µm.

WAVEFRONT ERROR

In order to obtain good measurements the wavefront error due to the quality of the optical components has to be

ISBN 978-3-95450-141-0

CHARACTERIZATION OF THE LASER BEAM FOR HHG SEEDING

S. Ackermann*, B. Faatz, DESY, Hamburg, Germany
V. Miltchev, University of Hamburg, Hamburg, Germany

Abstract

Recently free-electron laser (FEL) facilities around the world have shown that the direct seeding approach can enhance the spectral, temporal and coherence properties of the emitted radiation as well as reducing the fluctuations in arrival time and output energy. To achieve this, a photon pulse of the desired wavelength ("seed") is overlapped transversely and temporally with the electrons in the undulator to start up the FEL process from a defined radiation pulse rather than from noise. To benefit from the advantages of this technique, the energy of the seed has to exceed the energy of the spontaneous emission. The ratio between these two energies is strongly influenced by the seed beam properties. In this contribution, we will present simulations on the achieveable power contrast in dependence on the beam quality of the seed, and compare the results to the experimental data of the seeded FEL experiment ("sFLASH") at DESY, Hamburg. Additionally we show a way of creating FEL seed pulses for simulation purposes from Hermite-Gaussian generating functions.

INTRODUCTION

In order to benefit from the advantages of the high-harmonic generation ('HHG') direct seeding approach one has to ensure good quality of the external photon pulse ('Seed') as the energy transfer between the electrons and the electromagnetic field is strongly depending on the photon pulse wave front properties [7], which is in principle accessible through measurement, for example using a Shack-Hartmann wavefront sensor [9]. In an FEL the direct measurement of the wavefront distortions in the vicinity of the undulator is challenging due to limited space, or even excluded, e.g. if the beam pipe is small [2]. The M^2 -value [1] can be easily measured by focus scan technique [11] in the laser lab. In this contribution, we present simulations showing the importance of the M^2 -value onto the FEL output power as well as a method for the estimation of the M^2 -value using modal decomposition of single transverse intensity profiles similar to [5]

NUMERICAL SIMULATION SETUP

These studies have been carried out using the time-dependent 3D FEL code "GENESIS 1.3, v2" [14]. The electron beam line considered in the simulations is similar to the FLASH2 beam line of the FEL facility FLASH at DESY, Hamburg, Germany [6], [8]. Table 1 contains all important simulation parameters.

Table 1: Simulation Parameters and Ranges used in the Numerical Simulation

Electron beam		
Peak current	I_{max}	2.5 kA
Beam size	σ_{x}	100 μm
	σ_{y}	49 μm
Bunch Length (rms)	σ_{z}	30 μm
Energy	E	700 MeV
Energy spread	σ_{E}	500 keV
Normalized emittance	$\epsilon_{\mathrm{x,n}}$	1.4 mm · mrad
	$\epsilon_{\mathrm{y,n}}$	1.4 mm · mrad
HHG pulse		
Temporal shape		Gaussian
Wavelength	λ_{HHG}	37.6 nm
Pulse energy	E_{HHG}	70 pJ
Peak power	$P_{\mathrm{max,HHG}}$	2.5 kW
Duration (rms)	τ_{HHG}	12 fs
Undulators		
Lattice		FODO
Number of undulators		3
Undulator period	λ_{u}	31.4 mm
Periods per undulator	$_{\mathrm{periods}}$	76
Undulator intersection	L_{drift}	91.36 cm
Max. K parameter (rms)	K_{rms}	2.0

The goal of these simulations is to show the FEL output power at the end of the beam line as a function of the seed laser pulse quality in terms of M^2 . It has been assumed that the waist of the incoming seed pulse is located at the entrance of the first undulator module. For all simulations the waist size has been set to the value yielding the maximum FEL output power with an M^2 =1, namely 55 μm. Field distribution files containing seeds with different M^2 -values have been generated by superposition of different Hermite-Gaussian modes. The direct-search numerical algorithm [13] has been used to find amplitude and phase of the contributing modes to fullfill the following boundary conditions:

- The waist size has to be 55 μm.
- The total seed power equals 2.5 kW, see Table 1.
- M^2 is equal to the desired M^2 -value for **both** planes.
- In order to keep the axial symmetry of the multimode seed field, only TEM$_{mn}$ modes with even *n,m* are considered.

A large number of sets of Hermite-Gaussian modes exist fulfilling the aforementioned boundary conditions - we

* sven.ackermann@desy.de

ISBN 978-3-95450-141-0

LINEAR FOCAL CHERENKOV-RING CAMERA FOR SINGLE SHOT OBSERVATION OF LONGITUDINAL PHASE SPACE DISTRIBUTION FOR NON-RELATIVISTIC ELECTRON BEAM *

K. Nanbu#, K. Kashiwagi, H. Hinode, Y. Shibasaki, T. Muto, I. Nagasawa, S. Nagasawa,
K. Takahashi, C. Tokoku, A. Lueangaramwong, H. Hama,
Electron Light Science Centre, Tohoku University, Sendai, Japan

Abstract

Test accelerator as a coherent Terahertz (THz) source (t-ACTS) has been constructed at Tohoku University, in which generation of intense coherent THz radiation from sub-picosecond electron bunches will be demonstrated. Since final electron bunch length of accelerated beam is mostly dictated by the longitudinal phase space distribution at the exit of electron-gun, Measurement of initial electron distribution in the longitudinal phase space is indispensable for stable production of very short electron bunches. A novel method for measurement of electron kinetic energy applying a velocity dependence of the opening angle of Cherenkov light from a radiator medium has been proposed for relatively lower energy electrons. Combined use of a streak camera and a "turtle-back" mirror designed specifically that confines the Cherenkov light onto a linear focal line may allow us to observe the longitudinal phase space distribution directly. In this report, we describe the concept and designing of the linear focal Cherenkov-ring (LFC) camera system, as well as the current status of the system development.

t-ACTS PROJECT

In the t-ACTS project, the intense coherent THz radiation will be generated from an undulator and an isochronous accumulator ring via producing sub-picosecond bunches [1, 2, 3]. The t-ACTS consists of a thermionic cathode rf gun, an alpha magnet and a 3-meter-long accelerating structure, and velocity bunching scheme in the accelerating structure is being used for generate the sub-picosecond electron bunches. The thermionic rf gun composed of two independent cavities is capable of manipulating the beam longitudinal phase space, named an Independently-Tunable Cells (ITC) RF gun [4]. Employing a scheme of velocity bunching in the travelling-wave accelerating structure, the bunch compression will be performed [5]. The longitudinal phase space distribution at the exit of the rf-gun governs the final bunch length of electron beam after the bunch compression process, so that production of proper initial electron distribution in the longitudinal phase space is crucial to achieve very short electron bunch length of hundreds femtosecond.

*Work supported by JSPS KAKENHI Grant Numbers 24651096, 25790078.
#nanbu@lns.tohoku.ac.jp

LINEAR FOCAL CHERENKOV-RING CAMERA

Concept and Principle

In order to confirm directly whether the proper longitudinal phase space of the beam created by the ITC-RF gun for bunch compression, the LFC camera has been developed [6, 7].

The Cherenkov light is widely used for beam diagnostics and particle counters in high energy physics experiments. It is well known that the Cherenkov angle θ_c is inversely proportional to the particle velocity β (= v/c) as

$$\cos\theta_c = \frac{1}{n(\omega)\beta}, \qquad (1)$$

where n(ω) is the refractive index of the Cherenkov radiator medium at a radiation frequency. Since the Cherenkov angle contains information of the charged particle velocity, the photons having the same Cherenkov angle has to be focused onto an identical focal position of a detector in order to identify the particle momentum. If the focal points of different Cherenkov angles can be placed on a straight line, the momentum distribution of the beam will be observed at once. Furthermore, if information on relative arrival times onto the Cherenkov

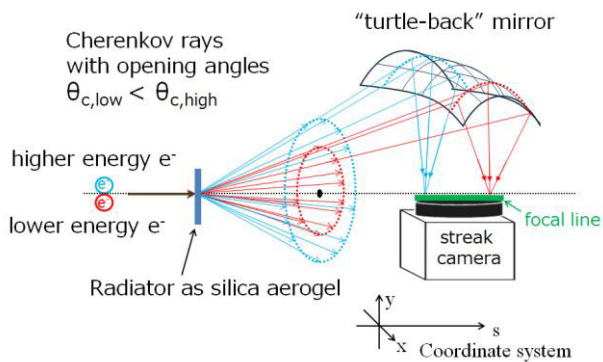

Figure 1: Conceptual drawing of the LFC camera. Electron emits the Cherenkov light when through the radiator made by silica aerogel. The turtle-back mirror is used to resolve the Cherenkov rays with the different opening angles with specific focal positions along a focal line. The streak camera can detect the relative arrival time of the rays with sub-picosecond time resolution.

ISBN 978-3-95450-141-0

OPTICAL SYSTEM FOR ESS TARGET PROTECTION

M. Donna, T. Grandsaert, M. Göhran, R. Linander,
Thomas Shea, Cyrille Thomas*, ESS, Lund, Sweden

Abstract

One specificity of the ESS accelerator and target is that a high power and ultra low emittance proton beam is sent straight onto a Tungsten target. The high power density proton beam from the ESS linac will damage any material it meets. Thus a strategy to protect the target and the target area has to be deployed: the proton beam on target will be defocused and swept, distributing homogeneously the power density on an area 10^4 times larger than its non defocused area. On its way towards the target, the beam goes through two windows: the proton beam window (PBW) separating the high vacuum of the accelerator to the 1-bar He filled area of the target monolith; and the target window (TW) marking the entrance area of the target wheel. In this paper, we present the PBW imaging system, one of the proton beam diagnostics to be developed for imaging the proton beam current density deposited in the PBW. We will describe the expected performance of the imaging system in order to satisfy the PBW protection requirement. We will also describe the radiative processes which could be used as the source of the imaging system. Finally, we will describe the necessary condition and hardware for the implementation of a protection system for both the PBW and TW.

INTRODUCTION

The ESS Linac is designed to deliver a proton beam on a tungsten target for the production of neutrons. The emittance of the beam is 0.7 mm.mrad and its average power is 5 MW [1]. As a result, the natural beam size at the end of the linac, thus on target, is expected to be 2-3 mm, and would damage the target instantaneously. The strategy chosen to prevent this is twofold: the beam is defocused and swept linearly across a large area on the target [2]. The results is a dilution of the proton current density on the PBW and target by a factor 10^4, bringing the density bellow the damaging threshold (0.110 mA/cm^2 on PBW). However, each proton beam macro-pulse, a train of one million proton bunches, 2.86 ms long with more than 10^{15} protons in total, can potentially damage the PBW and TW if the defocusing and rastering condition are not fulfilled. In order to monitor the proton beam current density distribution of each macro-pulse, we will implement redundant diagnostics [2]. One of these will be to perform an image of the beam passing through the PBW. Each image will show the current density distribution which can be recorded, analysed in such a way that not only the degradation state of the PBW can be monitored and anticipated, but also any fault of the rastering system can be detected and beam abort before the next macro-pulse. In the following, we will present the imaging system performance required for PBW protection, together with the constraints from the high radiation environment of the target. We will also mention the possible sources to be used, emerging from the interaction of the protons with the surface of the PBW. Finally, we will draw the necessary condition for the PBW protection to occur, and present the possible hardware and software to implement such a protection system.

* cyrille.thomas@esss.se

IMAGING SYSTEM EXPECTED PERFORMANCE

The imaging system for the PBW has to meet performance for protection of the PBW, but also, to overcome the constraints due to the hard radiation environment. The PBW is large, with $250 \times 110\,\mathrm{mm}^2$. The first optical element of the imaging system can be placed at 2.65 m from the PBW, 65 mm above or bellow the proton beam axis. The optical system has to go through a 4 m high plug, the Proton Beam Instrumentation Plug (PBIP), in order to exit the high radiation area of the target; then the optical path has to run another 7 m toward a radiation safe environment for camera and people. In total the distance from the PBW to the image sensor is close to 15 m. The size of the sensor imposes magnification less than $m = 0.2$. The resolution is specified to be of the order of 1 mm or less. The transmission must be optimised not only to permit single shot macro-pulse imaging, but also reliable analysis on the images. The distortion of the image must also be minimised to render image fidelity and avoid additional image processing prior analysis of the current density distribution. Finally, because the first optical elements are in radiation environment, the optical path goes through the radiation shield and thus its integrity must remain. In addition, the first optical elements must be remote handled during installation and removal after been degraded by long exposure to the hadronic shower. The expected performances described above translate into optical characteristics, which in turn, can be summarised with a reduced number of these characteristics. The position of the PBIB and the necessary small aperture to maintain the shield integrity define the maximum numerical aperture (NA) of the optical system. The first mirror aperture can be of the order of 100 mm, which define NA ≈ 0.19. The optimum resolution (R), without aberration of the optical system, is also determined by NA, by means of the well-known formula: $R = \frac{\lambda}{2NA}$, with λ the wavelength at which the object is imaged. So taking into account the requirements of 1 mm resolution or less, at $\lambda = 550\,\mathrm{nm}$, NA $> 3 \cdot 10^{-4}$. For the power transmission (T), NA also plays a role. In our case, the first mirror of the system is the defining aperture, so the best expected power transmission, without accounting for the reflectance of the mirrors, is simply given by the solid angle under which the first mirror sees the object. For a cir-

ISBN 978-3-95450-141-0

DISTINCT TRANSVERSE EMITTANCE MEASUREMENTS OF THE PXIE LEBT*

R. D'Arcy†, B. Hanna, L. Prost, V. Scarpine, A. Shemyakin, J. Steimel
Fermilab, Batavia, IL 60510, USA

Abstract

PXIE is the front-end test stand of the proposed PIP-II initiative i.e. the first step towards a CW-compatible, pulsed H- superconducting RF linac upgrade to Fermilab's injection complex. The test stand for this machine will be built step-wise; the Ion Source and Low-Energy Beam Transport (LEBT) are currently in place, with the RFQ and MEBT due for installation 2015.

The initial LEBT configuration under investigation in this paper is comprised of a D-Pace Filament-driven H- source and a single downstream solenoid, accompanied by a number of beam-diagnostic tools. The emittance studies expounded are performed via two methods: a position-angle phase-space sweep using an Allison-type emittance scanner; a solenoid corrector-induced transverse beam shift, impinging the bunch on an isolated, biased diaphragm. A detailed comparison of the two results is outlined.

INTRODUCTION

The proposed plan to upgrade Fermilab's injection complex consists of designing and building a CW SRF H- Linac. At its initial stage this is known as the Proton Improvement Plan II (PIP-II), to be used in pulsed mode. Front end components crucial for CW operation will be tested at an accelerator called, for historical reasons, PXIE [1], composed of a D-Pace [2] filament-driven H- ion source; a Low Energy Beam Transport (LEBT) section; a CW 2.1 MeV RFQ; a Medium Energy Beam Transport (MEBT) section; two SRF cryomodules (HWR and a SSR1); a High Energy Beam Transport (HEBT); and a beam dump. Figure 1 shows a schematic of the proposed beamline. The content of this paper will concern itself with the initial beam diagnostic results of the LEBT, namely the emittance measurements with two methods: Allison scanner and solenoid scans at the same beam conditions of, in part, a current of 2 mA. For a more detailed outline of the experiment, and its current status, please refer to [3].

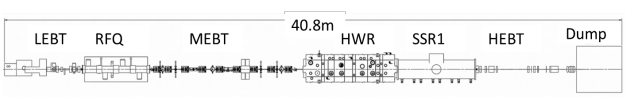

Figure 1: The proposed PXIE beamline.

LOW ENERGY BEAM TRANSPORT

The LEBT section of PXIE began with installation of the 30 keV H- ion source, producing beam in either pulsed (0.001 − 16 ms at 10 Hz) or CW mode with a beam current of 0.1 − 10 mA. Since then the beamline has been installed incrementally with the addition of a first solenoid, along with beam diagnostic tools, at the start of 2014. Once this initial layout was commissioned, the addition of two further downstream solenoids was completed in mid-2014. The data taking and results included in this paper are for the initial one-solenoid layout previously described, displayed in more detail in Fig. 2.

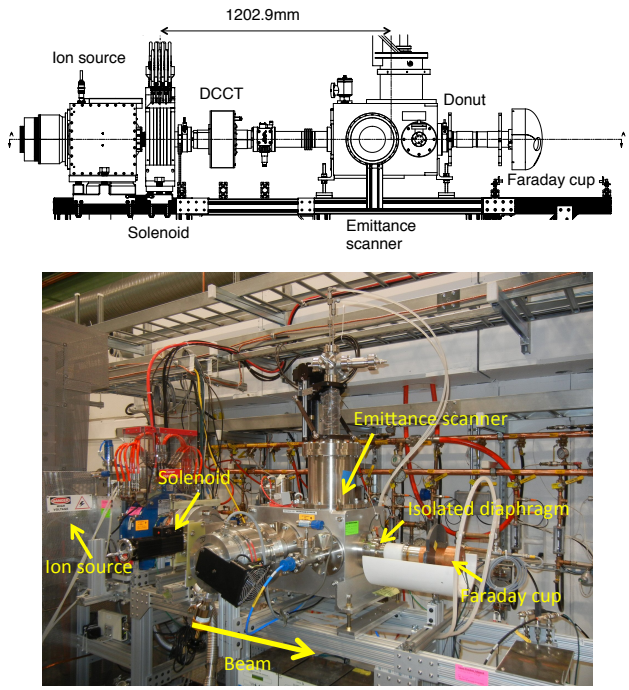

Figure 2: A schematic and photograph of the LEBT section constructed at the time of data taking for this paper.

ALLISON EMITTANCE SCANNER

The main tool to measure the beam emittance in the layout shown in Fig. 2 is the Allison Emittance Scanner. The Allison scanner was designed and built in collaboration with SNS and is based upon the original proposal in 1983 by P. Allison et al. [4]. The pictorial representation of the scanner, copied from [5], is shown in Fig. 3. The scanner measures the phase portrait of the beam in one dimension (vertical in the reported case). The scanner assembly consists of two slits, a Faraday cup with a suppressor electrode, and two de-

* Operated by Fermi Research Alliance, LLC, under Contract DE-AC02-07CH11359 with the U.S. DOE.
† rtpdarcy@fnal.gov

ISBN 978-3-95450-141-0

ELECTRON BEAM PROFILER FOR THE FERMILAB MAIN INJECTOR*

R. Thurman-Keup#, M. Alvarez, J. Fitzgerald, C. Lundberg, P. Prieto,
FNAL, Batavia, IL 60510, USA
W. Blokland, ORNL, Oak Ridge, TN 37831, USA

Abstract

The long range plan for Fermilab calls for large proton beam intensities in excess of 2 MW for use in the neutrino program. Measuring the transverse profiles of these high intensity beams is challenging and generally relies on non-invasive techniques. One such technique involves measuring the deflection of a beam of electrons with a trajectory perpendicular to the proton beam. A device such as this is already in use at the Spallation Neutron Source at ORNL and a similar device will be installed shortly in the Fermilab Main Injector. The Main Injector device is discussed in detail and some test results and simulations are shown.

INTRODUCTION

Traditional techniques for measuring the transverse profile of proton beams typically involve the insertion of a physical object into the path of the proton beam. Flying wires for instance in the case of circulating beams, or secondary emission devices for single pass beamlines. With increasing intensities, these techniques become difficult, if not impossible. A number of alternatives exist including ionization profile monitors, gas fluorescence monitors, and the subject of this paper, electron beam profile monitors.

The use of a probe beam of charged particles to determine a charge distribution has been around since at least the early 1970's [1-3]. In those examples, the charge distribution was a plasma, and the probe beam was electrons. Later, the concept was applied to ion beams at a number of facilities [4-6]. At CERN a version using a probe beam of ions was used to average over the bunch structure of the proton beam in the SPS [7]. A variation on the technique was the use of an electron probe beam to measure the longitudinal charge distribution in an electron injector at BINP [8]. The most recent incarnation of this technique is a profile monitor in the accumulator ring at SNS [9,10].

An Electron Beam Profiler (EBP) has been constructed at Fermilab and will be installed shortly in the Main Injector. The Main Injector is a proton synchrotron that can accelerate protons from 8 GeV to 120 GeV for use by a number of neutrino experiments, and eventually several muon-based experiments. The protons are bunched at 53 MHz for a typical rms bunch length of 1-2 ns. In this paper we discuss the design of the EBP and present some studies of the electron beam.

THEORY

The principle behind the EBP is just electromagnetic deflection of the probe beam by the target beam under study (Fig. 1).

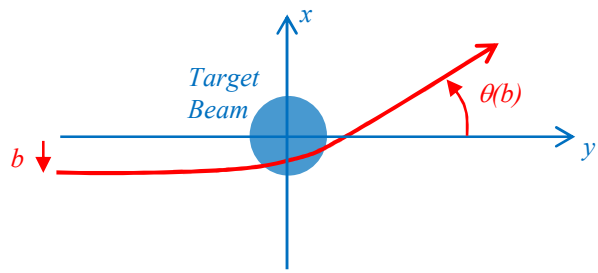

Figure 1: Probe beam deflection (red) for some impact parameter b.

If one assumes a target beam with $\gamma \gg 1$, no magnetic field, and $\rho \neq f(z)$, then the force on a probe particle is

$$\vec{F}(\vec{r}) \propto \int d^2\vec{r}'\rho(\vec{r}')\frac{(\vec{r}-\vec{r}')}{|\vec{r}-\vec{r}'|^2}$$

and the change in momentum is

$$\Delta\vec{p} = \int_{-\infty}^{\infty} dt\ \vec{F}\big(\vec{r}(t)\big)$$

For small deflections, $\vec{r} \approx \{b, vt\}$, and the change in momentum is

$$\Delta\vec{p} \propto \int_{-\infty}^{\infty} dx' \int_{-\infty}^{\infty} dy'\ \rho(x',y') \cdot \int_{-\infty}^{\infty} dt\ \frac{\{b-x', vt-y'\}}{(b-x')^2+(vt-y')^2}$$

where {} indicates a vector. For small deflections, $\vec{p} \approx \{0, p\}$ and $\theta \approx \frac{|\Delta\vec{p}|}{|\vec{p}|}$. The integral over time can be written as $\mathrm{sgn}(b - x')$ leading to an equation for the deflection

$$\theta(b) \propto \int_{-\infty}^{\infty} dx' \int_{-\infty}^{\infty} dy'\,\rho(x',y')\,\mathrm{sgn}(b-x')$$

If one takes the derivative of $\theta(b)$ with respect to b, the sgn function becomes $\delta(b - x')$ leading to

$$\frac{d\theta(b)}{db} \propto \int_{-\infty}^{\infty} dy'\,\rho(b,y')$$

which is the profile of the charge distribution of the beam. Thus for a Gaussian beam, this would be a Gaussian distribution and the original deflection angle would be the error function, $\mathrm{erf}(b)$. This of course is true only to the extent that the above assumptions are valid.

*Operated by Fermi Research Alliance, LLC under Contract No. De-AC02-07CH11359 with the United States Department of Energy.
#keup@fnal.gov

TERAHERTZ AND OPTICAL MEASUREMENT APPARATUS FOR THE FERMILAB ASTA INJECTOR*

R. Thurman-Keup#, A.H. Lumpkin, J. Thangaraj, FNAL, Batavia, IL 60510, USA

Abstract

ASTA is a facility at Fermilab that, once completed, will consist of a photoinjector with two superconducting capture cavities, at least one superconducting ILC-style cryomodule, and a small ring for studying non-linear, integrable beam optics. This paper discusses the layout for the optical transport system that will provide THz radiation to a Martin-Puplett interferometer for bunch length measurements as well as optical radiation to an externally located streak camera, also for bunch length measurements. It will be able to accept radiation from two synchrotron radiation ports in the bunch compressor, a diffraction/transition radiation screen downstream of the compressor, and a transition radiation screen after the spectrometer magnet for measurements of energy-time correlations.

INTRODUCTION

The Advanced Superconducting Test Accelerator (ASTA) is a facility that has been constructed at Fermilab for advanced accelerator research [1-3]. It consists of a photoinjector followed by an ILC-type cryomodule and a small ring called IOTA (Integrable Optics Test Accelerator) for studying non-linear optics. Recently, the initial photoinjector beamline was completed and rf tests of the cryomodule reached the ILC design goal in 7 of the 8 cavities, with one cavity just short of it. The plan for the photoinjector is to run it at 20-25 MeV while the beamline from the cryomodule to IOTA, and the corresponding accelerator enclosure are completed. At some point in time, the photoinjector will receive a second capture cavity (currently being repaired) which will increase the energy to around 50 MeV The photoinjector will support a number of small user experiments, some of which are already planned. When the full beamline to IOTA has been completed, the photoinjector will provide beam to IOTA to map out the optics of the ring. In support of photoinjector operations and experiments, there will be an optical / THz transport system with a number of instruments including a Martin-Puplett interferometer, and a Hamamatsu streak camera. This paper will describe the plan for this system.

ASTA

The ASTA injector (Fig. 1) starts with a 1.3 GHz normal-conducting rf photocathode gun with a Cs_2Te coated cathode. The photoelectrons are generated by a YLF laser at 263 nm that can provide several μJ per pulse [4]. Following the gun are two superconducting 1.3 GHz capture cavities that accelerate the beam to its design energy of around 50 MeV. Initially only the second capture cavity will be in place giving an energy of 20-25 MeV. After acceleration there is a section for doing round to flat beam transforms, followed by a magnetic

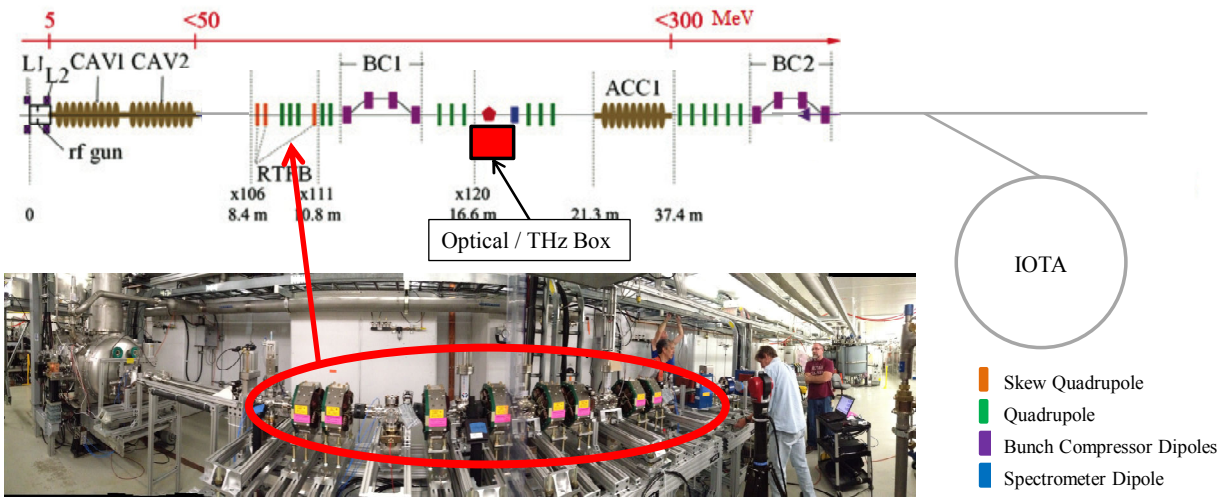

Figure 1: ASTA beamline layout. L1 and L2 are the gun solenoids. CAV1 and CAV2 are the capture cavities. Presently only CAV2 is installed. The section titled RTFB is the round-to-flat beam transform section which is followed by the magnetic bunch compressor BC1. The next section contains space for user experiments and is the location of the optical / THz system. ACC1 is the ILC-type cryomodule.

*Operated by Fermi Research Alliance, LLC under Contract No. De-AC02-07CH11359 with the United States Department of Energy.
#keup@fnal.gov

ISBN 978-3-95450-141-0

THIRD GENERATION RESIDUAL GAS IONIZATION PROFILE MONITORS AT FERMILAB*

J.R. Zagel#, M. Alvarez, B. Fellenz, C. Jensen, C. Lundberg, E. McCrory, D. Slimmer, R. Thurman-Keup, D. Tinsley, FNAL, Batavia, IL 60510, USA

Abstract

The latest generation of IPM's installed in the Fermilab Main Injector and Recycler incorporate a 1 kG permanent magnet, a newly designed high-gain, rad-tolerant preamp, and a control grid to moderate the charge that is allowed to arrive on the anode pick-up strips. The control grid is intended to select a single Booster batch measurement per turn. Initially it is being used to allow for a faster turn-on of a single, high-intensity cycle in either machine. The expectation is that this will extend the Micro Channel Plate lifetime, which is the high-cost consumable in the measurement system. We discuss the new design and data acquired with this system.

INTRODUCTION

Previous generations of residual gas ionization profile monitor's (IPM's) have been in operation, both at Fermilab and other laboratories, for many years [1-3]. The second-generation system applied a fixed permanent magnetic field, and polarity change to collect electrons to reduce space charge effects in the measurement [4]. Its field quality, while sufficient to improve the measurements, was not quite 1 kG, and required 4 feet of beam line to accommodate the magnetic unit. Two primary issues that arise have been the Micro Channel Plate (MCP) lifetime, and saturation effects of too much charge required from them. The third generation is designed to improve on these deficiencies, Fig. 1.

MEASUREMENT TIMING

The new system uses a timing module that combines the function of our Universal Clock Decoder (UCD), and the VME RF Timing module (VRFT). This module decodes the lab-wide timing 10 MHz clock (TCLK), the machine specific, beam synchronous clock (BSYNC), and a Machine Data (MDAT) Reference System, and outputs a clock trigger. Utilizing this board, we can generate a trigger on a specific machine state, and a particular machine clock cycle that then enables the beam synchronous clock pulses to gate our ADC's. The resolution of this trigger is one 53 MHz bunch. One sample per turn is generally acquired for a range of turns specified in the measurement specification. Multiple samples per turn is also a supported mode of operation.

* Operated by Fermi Research Alliance, LLC under Contract No. De-AC02-07CH11359 with the United States Department of Energy.
# zagel@fnal.gov

WHAT'S NEW

The new system incorporates the improvements added to the Fermilab Tevatron IPM [5] along with a few new features. Three new installations have been accomplished

New Magnet Design

The new magnet is designed using $SmCo_5$ permanent magnets. This material was chosen to give the highest residual magnetic field (Br) with the lowest variation in temperature dependence, at a reasonable cost and availability. A standard brick is 1" by 2" by 1/2". The magnet was intended to provide 1 kG in the detector area, with the return flux half upstream and half downstream, and shimmed, such that the beam sees a total integrated field of zero. The magnet is 31.5"L x 14"D with a minimum aperture of 4.25" to allow for a 4" diameter beam pipe suitable to both horizontal and vertical planes in the Main Injector and Recycler. Magnet design, modeling, and measurement details have been presented in [6].

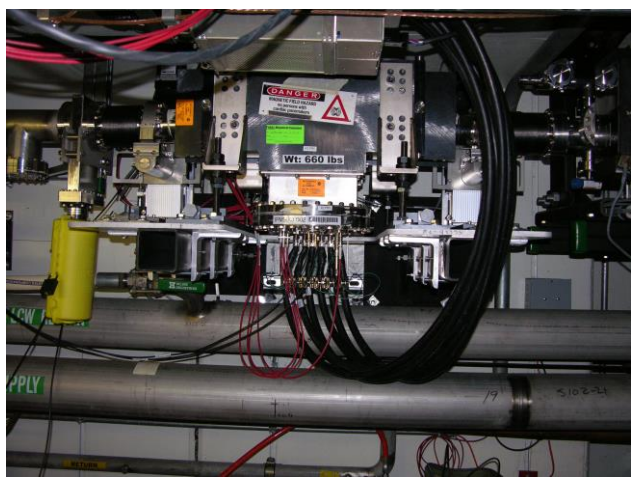

Figure 1: Recycler Vertical Installation.

Anode Strip Board

The anode strip pick-up board for both Main Injector and Recycler is a ceramic circuit board with 120 copper strips spaced at 0.5mm. The copper occupies 80% of that pitch with 20% space between strips. All signals are connected via 20 pin, ceramic mounted, quick release connectors. A multilayer flexible circuit delivers these signals to 6 front flange feed through connectors. A "Flash Test" strip has been added to the bottom of the

OPTIMIZATION OF BEAM INDUCED FLUORESCENCE MONITORS FOR PROFILE MEASUREMENTS OF HIGH CURRENT HEAVY ION BEAMS AT GSI

C. Andre, P. Forck, R. Haseitl, A. Reiter, R. Singh, B. Walasek-Hoehne,
GSI Helmholtzzentrum für Schwerionenforschung GmbH, Germany

Abstract

To cope with the demands of the Facility for Antiproton and Ion Research (FAIR) for high current operation at the GSI Heavy Ion Linear Accelerator UNILAC non intercepting methods for transverse beam profile measurement are required. In addition to intercepting diagnostics like Secondary Electron Emission Grid (SEM-Grid) or scintillating screens, the Beam Induced Fluorescence (BIF) Monitor, an optical measurement device based on the observation of fluorescent light emitted by excited nitrogen molecules, was brought to routine operation. Starting with the first installations in 2008 and consequent improvements, successively six monitors were set up in the UNILAC and in the transfer line (TK) towards the synchrotron SIS18. BIF is used as a standard diagnostic tool to observe the ion beam at kinetic energies between 1.4 and 11.4 MeV/u. Beside the standard operation mode where the gas pressure is varied, further detailed investigations were conducted. The BIF setups were tested with various beam parameters. Different settings of camera, optics and image intensification were applied to improve the image quality for data analysis. In parallel, the light yield from different setups was compared for various ions, charge states, beam energies and particle numbers.

INSTALLATIONS

Along GSI linear accelerator UNILAC and transfer line, six BIF monitors are installed. Each monitor consists of two perpendicularly mounted image intensified camera systems to measure transversal beam profiles in horizontal and vertical plane simultaneously (see Figure 1 and Table 1). The monitors are placed to observe changes of the beam due to stripping or acceleration. Profiles and positions of a single linac pulse can be observed at all positions without beam distortions.

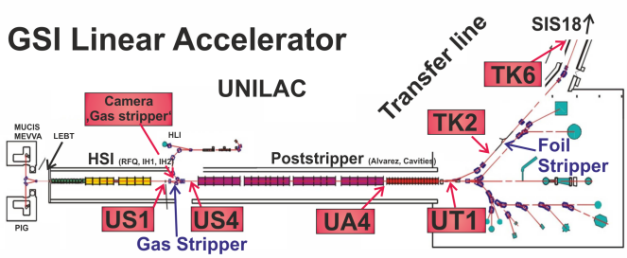

Figure 1: Locations of BIF monitors along GSI Linear Accelerator.

In addition, a regular CCD camera observes beam induced fluorescence at the gas stripper to control the gas flux. Here, different charge states of the same beam can be observed within one image.

Table 1: BIF Installations and Typical Beam Parameters

BIF		US1	US4	UA4	UT1	TK2	TK6
CCD coupling	H	T	R	T	R	T	T
	V	T	R	T	R	T	R
Energy [MeV/u]		1.4	1.4	11.4	11.4	11.4	11.4
Typical charge states :							
Argon		1+	11+	11+	11+	11+	18+
Nickel		2+	14+	14+	14+	14+	26+
Tantalum		4+	24+	24+	24+	24+	62+
Uranium		4+	28+	28+	28+	28+	73+

DETECTOR SETUP

The BIF principle and the detailed setup (hardware, optics, readout and control) of the system is described in [1]. To observe the fluorescence of the ion beam interaction with the nitrogen gas molecules at lowest gas pressures, image intensified camera systems (ICCD) are required, preferably with a 2-stage multichannel plate (MCP) to enable single photon counting. ProxiVision® developed two custom designed camera types; a fiber-taper coupled CCD (T) where the CCD chip is glued to the taper and a relay-lens coupled CCD (R) with c-mount standard (Figure 2, Table 1).

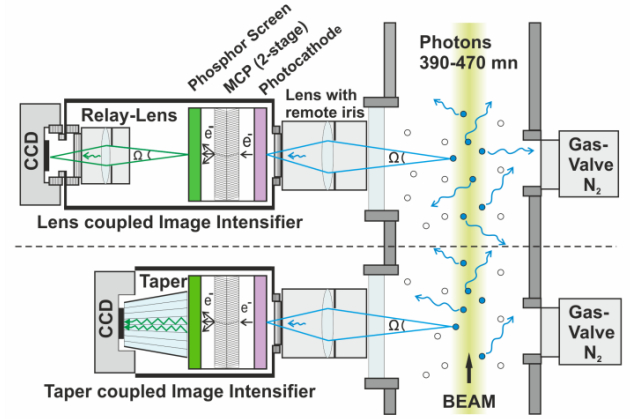

Figure 2: Types of Image Intensified Camera Systems.

CUPID: NEW SYSTEM FOR SCINTILLATING SCREEN BASED DIAGNOSTICS

B. Walasek-Höhne, C. Andre, H. Bräuning, A. Bräuning-Demian, R. Haseitl,
T. Hoffmann, R. Lonsing, A. Reiter, C. Schmidt, M. Schwickert
GSI Helmholtzzentrum für Schwerionenforschung GmbH, Darmstadt, Germany

Abstract

The Facility for Antiproton and Ion Research (FAIR) with its wide range of beam parameters poses new challenges for standard beam instrumentation like precise beam imaging. To cover the various foreseen applications for standard scintillating screen based diagnostics, a new technical solution was required.

CUPID (Control Unit for Profile and Image Data) is a new system for scintillating screen imaging, which is based on the data acquisition framework for FAIR. It includes digital image acquisition, remote control of the optical system (focus and iris; camera setup and power) and a graphical user interface (GUI). CUPID is also designed to work with different imaging devices like GigE cameras or video cameras using frame grabber cards. In this paper we report on the first results with this novel system during routine beam operation.

For imaging applications in the high radiation environment of the heavy ion synchrotrons radiation-hard cameras are required. One possible candidate for such cameras at FAIR is the CCIR MegaRAD3 from Thermo Fischer Scientific. We describe here our first results with this camera, which has been installed at the SIS18 extraction point, where a high radiation level is present.

CUPID SYSTEM

CUPID is a new, fully FAIR-conformal system for standard scintillating screen based beam diagnostics including pneumatic drive, data acquisition, slow control of parameters like focus and iris and graphical user interface. The new system, installed and commissioned at several GSI High Energy Beam Transport Lines (see Figure 1) in the beginning of this year, is now used in standard accelerator operation.

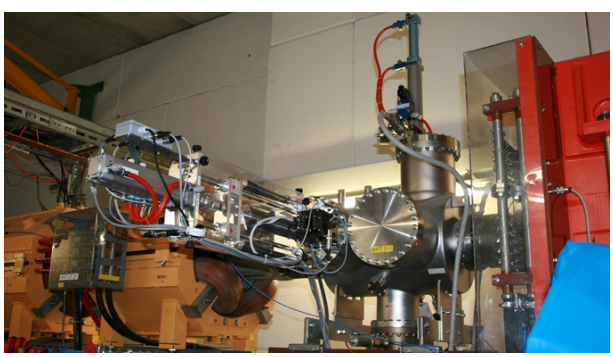

Figure 1: Scintillating Screen installation at High Energy Beam Transport Lines.

The scintillating screens with typically 120 mm diameter, made of Chromox or phosphor P43, are mounted on a pneumatic drive in vacuum. Special markers on the screen holder are used to calibrate the image and convert pixels into beam position and size in millimeters. The scintillating screens are typically (but not exclusively) mounted under 45° with respect to the beam axis and the optical axis of the camera. The camera is operated outside the vacuum chamber and views the screen through a UV-glass flange.

A LED can illuminate the scintillating screen for diagnostic purposes or recalibration of the optical system.

With the exception of the pneumatic drives, the direct hardware access (camera readout, lens control etc.) is based on FESA, the CERN Front-End Software Architecture [1]. Image acquisition, lens control and camera power are implemented as different FESA classes. Because CUPID is designed to work with different imaging hardware, a dedicated image acquisition FESA class is written for each imaging system supported. Using the inheritance mechanism in FESA a new imaging device can be easily incorporated in the system. The imaging base class contains all common code, like image manipulation (rotation, mirroring) and computations (profiles, intensity histogram, moments of the intensity distribution). It also provides the code to save raw images to disk (local or via network) as standard bitmap files. In addition, it enforces the common interface between the imaging FESA class and the CUPID GUI. The derived FESA class for the specific imaging device only implements the specific code to set up the device and acquire the images.

The decision to implement image acquisition, lens control and camera power as separate FESA classes (and thus devices) has the advantage, that single components can easily be exchanged or even removed. It is currently the responsibility of the GUI, to connect to the different FESA classes and hide this diversity from the operator. In the future FAIR control system, the paradigm proposed by the accelerator control system department is to treat all components as a single device and access it via a single FESA class. This is not contradictory to the approach used currently in the CUPID system. Using the 'association' feature of FESA, the single device paradigm can be implemented by creating a simple wrapper FESA class acting as a middle tier between the separate FESA classes now in use and the future control system.

The standard camera installed is the IDS uEye UI-5240SE-M [2], which is a digital GigE camera equipped with the radiation tested e2v CMOS sensor [3] with 1280 by 1024 pixel. A camera internal area-of-interest limits the image to

ISBN 978-3-95450-141-0

PERFORMANCE DEMONSTRATION OF THE NON-INVASIVE BUNCH SHAPE MONITOR AT GSI HIGH CURRENT LINAC*

B. Zwicker, C. Dorn, P. Forck, O. Kester, P. Kowina, T. Sieber, GSI, Darmstadt, Germany

Abstract

At the heavy ion LINAC at GSI, a novel scheme of a non-invasive Bunch Shape Monitor has been tested with several different ion beams at 11.4 MeV/u and beam currents in the range from 80 to 1000 µA. Caused by the beam impact on the residual gas, secondary electrons are liberated. These electrons are accelerated by an electrostatic field, transported via a sophisticated electrostatic energy analyzer and an rf-deflector, acting as a time-to-space converter. Finally a MCP amplifies the electrons and the electron distribution is detected by a CCD camera. For the applied beam settings this Bunch Shape Monitor is able to obtain longitudinal profiles down to 250 ps RMS width with a resolution of 34 ps, corresponding to 0.5° of the 36 MHz accelerating frequency. Systematic parameter studies for the device were performed to demonstrate the applicability and to determine the achievable resolution. The background contributions, as originated by x-rays, are investigated.

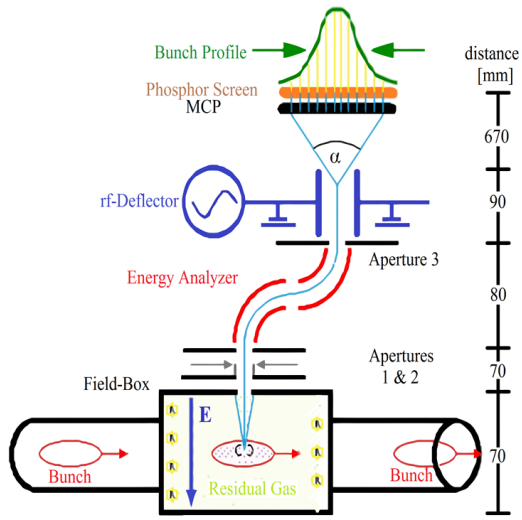

Figure 1: Schematic illustration of the non-invasive BSM

MOTIVATION

Within the FAIR-Project [1] a proton LINAC [2] is scheduled as a new injector for the SIS18 synchrotron at GSI. The p-LINAC will provide 70 MeV and 70 mA current in addition to a compact construction. Due to the high energy deposition for conventional intersecting Bunch Shape Monitors [3, 4] a novel design is foreseen. The new detector for the longitudinal bunch structure with a phase resolution of 1°, with respect to the 325 MHz acceleration frequency, is intended to ensure proper longitudinal matching of the accelerating structures. The presented device is a recommissioning of the non-intercepting Bunch Shape Monitor presented in [5].

WORKING PRINCIPLE

The non-invasive Bunch Shape Monitor (BSM) prototype is based on secondary electrons, which are freed by the interaction of beam ions and the residual gas. Figure 1 provides a schematic illustration. These electrons are accelerated towards an aperture by an external homogeneous electrostatic field of 4.2 kV/mm. Using side strips parallel to the electrodes the electric field is leveled. To further reduce the divergence of the secondary electrons (SEs) two apertures with a distance of 70 mm are used. The aperture width can be remotely adjusted between 0.1 mm and 2 mm. After passing these apertures the electrons are filtered by two 90° cylindrical electrostatic energy analyzers with a bending radius of 30 mm. Two similar analyzers are used to bend the SE beam back in original direction for mechanical reasons. The applied voltages are ±5.5 kV for the opposite cylinder segments. A third aperture is placed 10 mm away from the edge of the second analyzer to enable a point-to-point focusing from the entrance to the exit slit. After a drift of 90 mm the SEs reach a radio frequency (rf) driven deflector coupled to the accelerating frequency. The rf-deflector works as a time-to-spatial converter. Each electron is deflected in dependence to its time of arrival. Two deflectors with different resonance frequencies are available. One is operating at a frequency of 36 MHz for long bunches and the other one for short bunches at the third harmonic at 108 MHz. Both deflectors are 800 mm long parallel wires corresponding to $\lambda/4$ for high field strength. The maximum power applicable is 100 W at 36 MHz and 50 W at 108 MHz in pulses of 6 ms duration. The deflected SEs, after a 670 mm flight, are spatially detected by a Chevron MCP (Hamamatsu F2226-24P) with an effective diameter of 77 mm and finally monitored by a P20 phosphor screen. The illuminated spots on the phosphor screen are observed by a CCD camera (PCO 12 Bit SensiCam, CCD chip of 640×480 pixel). In addition, the deflector has a second function as a focusing electrostatic einzel-lens by a common DC-voltage of maximal 6000 V on the deflector's plates. Between the rf-deflector and the MCP a 1 cm thick stainless steel plate is inserted as a x-ray shield for the MCP detector.

COMPENSATION OF THE BEAM DEFLECTION

While operating the BSM the applied E-Field affects the ion beam. For an 11.4 MeV U^{28+} beam with an applied voltage of -31 kV (resulting in a field strength of 420 V/mm) the

* Supported by EU-Project CRISP, WP3 T1 Non-intercepting bunch shape monitors

ISBN 978-3-95450-141-0

YAG:Ce SCREEN MONITOR USING A GATED CCD CAMERA

Takashi Naito#, Toshiyuki Mitsuhashi
KEK, 1-1 Oho, Tsukuba, Ibaraki 305-0801, Japan

Abstract

Due to its good spatial resolution, the YAG:Ce screen monitor is often used for small beam profile measurement in the Linac and beam transport line. We constructed a high-resolution YAG:Ce screen monitor at KEK-ATF2 for the observation of small size beam. We tested two types of screen, one is ceramic (sintered alumina powder) YAG:Ce and the other is single crystal YAG:Ce. Both screens have 50μm thickness. To escape from the Synchrotron radiation(SR) from the upstream and the Coherent Optical radiation(COTR), we applied delayed timing of the gate for the CCD camera. A microscope having a spatial resolution of 4.3μm is set outside of vacuum chamber to observe the scintillation light from the YAG:Ce screen. The results of the difference between the two screens, the camera performance with delayed gate and the optical performance of microscope will be presented in this paper.

INTRODUCTION

The low emittance beams using the state-of-the-art technology are generated and accelerated in recent electron accelerators for the FELs and the collider machines. The beam monitors are required to have a high resolution to measure the small beam size. Screen monitor is often used to measure the transvers profile at the linac and the beam transport. Usually, a chromium doped Alumina (AF995R, Desmaruquest Co.) fluorescent plate is used for the screen material. Recently, the other materials are tested and used to improve the resolution. We developed a high resolution screen monitor using YAG:Ce for the momentum spread measurement at KEK-ATF2 beam line.

ATF2 is a test beam line to develop the final focus system for the International Linear Collider. The beam test is carried out to realize 37nm of the vertical beam size [1]. The ultra-low emittance beam is supplied from the damping ring(DR). The energy is 1.3GeV and the design emittances for horizontal and vertical are 1.3nm and 10pm, respectively. The momentum spread is one of the key parameters of the beam. In the DR, the intra-scattering effect increases the momentum spread, which is a function of the beam emittance and the bunch charge. The momentum spread is calculated from the horizontal beam size at the large dispersion location,

$$X = \sqrt{\left(\sqrt{\varepsilon_x \bullet \beta}\right)^2 + \left(\eta \frac{\Delta p}{p}\right)^2} \ .$$

where, X is the horizontal beam size, ε_x is the horizontal emittance, β is the beta function, η is the dispersion function and Δp/p is the momentum spread. The first parentheses can be ignored in the case of the large dispersion. The dispersion function can be measured by the horizontal beam position change when the RF is changed. At the ATF2, the dispersion function at the screen monitor location is about 0.5m. When the momentum spread is assumed at 6 x 10^{-4}, the horizontal beam size is estimated to be 300μm. However, the fluorescent screen does not have enough resolution to measure the beam size. OTR monitors are used at the downstream of the ATF2, however, OTR does not have enough light yield at the low bunch charge. We decided to employee YAG:Ce screen. YAG:Ce has a good scintillation property at 550nm wavelength. We tested two types of screen, one is ceramic (sintered alumina powder) YAG:Ce [2] and the other is single crystal YAG:Ce [3]. Both screens have 50μm thickness.

The hardware design and the beam test results are described in the following sections.

HARDWARE

Fig. 1 shows the schematic layout of the YAG:Ce screen monitor(YSC). The screen is inserted into the beam orbit at a 45-degree horizontal direction by the air actuator. The CCD observes the scintillation light of the screen from a perpendicular direction. The screen has an oblique angle (45 degrees) for the beam and the horizontal beam image is magnified by $\sqrt{2}$. The benefit of using the oblique angle is that, 1) the optical system can fully focus on the screen when the beam position moved, 2) the reflection of the synchrotron radiation (SR) and coherent optical radiation (COTR) can mostly be avoided, which are reflected to a 90-degree direction. Avoiding the COTR is a significant problem for the FEL application [4]. In the case of the ATF2, the CTOR is negligible small.

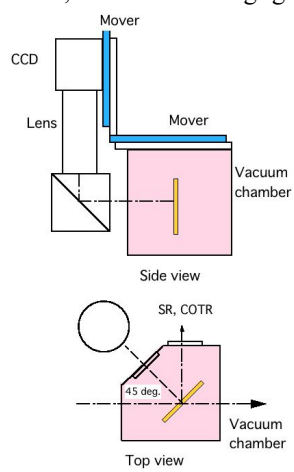

Figure 1: Schematic layout of YSM.

takashi.naito@kek.jp

VACUUM IMPROVEMENT OF BUNCH SHAPE MONITOR FOR J-PARC LINAC*

A. Miura#, Y. Kawane, N. Ouchi,
J-PARC Center, Japan Atomic Energy Agency, Tokai, Ibaraki, 319-1195, JAPAN
T. Miyao, J-PARC Center, High Energy Accelerator Research Organization, KEK, Tsukuba, Ibaraki, 305-0801, JAPAN

Abstract

Bunch shape monitors (BSMs) have been developed and installed in the summer of 2012 at the upstream part of new Annular-ring Coupled Structure Linac (ACS) section. Because a problem of the vacuum degradation was found during the BSM operations, BSMs were once dismounted from the beam line and the off-line baking operations with outgas analysis had been performed to reduce the vacuum pressure of BSM surrounding. The impacts of the bias voltage to the target wire and static lens, and the RF power to the deflector were examined in the vacuum test. Finally, we propose the additional vacuum system arrangement for the installation of BSM to the beam line. This paper describes the vacuum test results of BSMs and the additional vacuum system arrangement for the BSM installation.

INTRODUCTION

In the upgrade project in J-PARC to establish the 1 MW at the experimental laboratories connected to the upstream Linac and Rapid Cycling Synchrotron, we have two big projects as the energy upgrade from 181-MeV Linac to 400-MeV Linac and the front end improvement using new RF ion source and replacing of the upgraded Radio Frequency Quadrupole Linac (RFQ) cavity. To meet with the 400 MeV, 21 ACS cavities have been developed and installed in the beam line, and to meet with this installation, we have developed the beam monitors for the ACS cavity tuning. Because the acceleration frequency of ACS cavities is 972 MHz which is three-fold higher than that of upstream RF cavities, we need to take longitudinal matching at the upstream part of new ACS beam line.

We started the development of BSM for the J-PARC Linac in corroboration with the Institute of Nuclear Research, Russian Academy of Science (INR, RAS). After three years since the project started, three BSMs were completed to be fabricated. In the summer of 2012, prior to the installation of ACS cavities, we installed all three BSMs at the upstream of the new ACS section in order to conduct some test measurement using 181-MeV beams. During the BSM measurements, a problem of the degradation in vacuum conditions was found. One reason for this problem is the dark current resulting in desorption of absorbed gas molecules. And another reason is outgas released from materials when the high voltage and RF power were supplied for the electro-static lens and RF deflector, respectively. In order to evaluate and mitigate this problem, BSMs were once dismounted from the beam line and the off-line baking operations with outgas analysis had been performed to avoid the degradation of the vacuum in the summer of 2013. The impacts of the bias voltage to the target wire and static lens, and the RF power to the deflector were examined in the vacuum test.

Finally the improved arrangement of the vacuum system to install the BSM is also proposed. We will install a BSM in at the upstream of the ACS again in the summer of 2014 with additional vacuum arrangement. This paper describes the vacuum degradation of the BSMs, results of the vacuum test, and the proposed arrangement of vacuum system.

VACUUM DEGRADATION AT BEAM LINE

Longitudinal pulse width measurements were done with the beam energy of 181 MeV, the beam pulse current of 15 mA, the pulse duration of 100 μs, and the pulse repetition rate of 1 Hz [1]. During the measurement, several problems connected with the influence on the vacuum have been found. Before the BSM installation, vacuum pressure at the upstream part of ACS section is around 1.0e-6 Pa.

The first one was connected with too big excitation power of BSM power amplifier. It was observed that the vacuum degraded over 1.0e-4 Pa which is the machine protection level in J-PARC Linac immediately after supplying RF power to the deflector. Decreasing of the magnitude of the input RF signal immediately removed the influence on the vacuum.

The second problem was a vacuum degradation in the case of multipactoring in the RF deflector at the operating mode. This discharge occurred when the high voltage potential was not supplied to the deflector electrodes. The software had been modified to suppress this degradation. RF is switched on only during the measurements.

The third effect is an influence of a dark electron current from the target. The electrons are accelerated and bombard the surfaces resulting in desorption of the absorbed gas molecules. The effect was observed immediately after supplying high voltage potential. After conditioning for several days the effect almost decreased and it became possible to make measurement with the potential of -10 kV. After installation and beam line tuning, beam line pressure didn't recover the previous level because of the malfunction of the closest ion pump.

Above influences had been met at the beam line. We have examined the vacuum test for BSMs with additional pumps.

#akihiko.miura@j-parc.jp

ISBN 978-3-95450-141-0

AN ULTRAFAST LINEAR ARRAY DETECTOR FOR SINGLE-SHOT ELECTRO-OPTICAL BUNCH PROFILE MEASUREMENTS

L. Rota, M. Caselle, N. Hiller, A.-S. Müller, M. Weber,
Karlsruhe Institute of Technology (KIT), Karlsruhe, Germany

Abstract

A new spectrometer system has been developed at ANKA for near-field single-shot Electro-Optical (EO) bunch profile measurements with a frame rate of 5 Mfps. The frame rate of commercial line detectors is limited to several tens of kHz, unsuitable for measuring fast dynamic changes of the bunch conditions. The new system aims to realize continuous data acquisition and over long observation periods without dead time. InGaAs or Si linear array pixel sensors are used to detect the near IR and visible spectrum radiation. The detector signals are fed via wire-bonding connections to the GOTTHARD ASIC, a charge-sensitive amplifier with analog outputs. The front-end board is also equipped with an array of fast ADCs. The digital samples are then acquired by an FPGA-based readout card and transmitted to an external DAQ system via a high-speed PCI-Express data link. The DAQ system uses high-end Graphics Processors Units (GPUs) to perform a real-time analysis of the beam conditions. In this paper we present the concept, the first prototype and the low-noise layout techniques used for fast linear detectors.

INTRODUCTION

During the low-α_c-operation at the ANKA storage ring at the Karlsruhe Institute of Technology, the momentum compaction factor α_c is reduced to compress the bunches longitudinally and thus generate Coherent Synchrotron Radiation (CSR) in the THz range [1]. The emitted CSR exhibits a bursting behavior [2–4], which is caused by dynamic changes of the longitudinal bunch shape (e. g., microbunching). To study these dynamic changes, single-shot measurements with a sub-ps resolution are required.

The method of Electro-Optical Spectral Decoding (EOSD) offers the possibility to measure the longitudinal bunch profile and its arrival time relative to the revolution clock with a sub-ps time resolution without averaging. For EOSD, the field induced Pockels effect inside an electro-optical crystal is used to modulate the temporal profile of the electron bunch onto a laser pulse. Subsequently this laser pulse is detected with a commercial InGaAs line array inside an optical spectrometer and from the spectral modulation the bunch profile can be extracted.

First single-shot measurements with the EOSD setup at ANKA have indicated the formation of substructures on the compressed bunches [5, 6]. In principle, EOSD, offers the possibility to measure the longitudinal bunch profile on a turn-by-turn basis (f_{rev} = 2.7 MHz at ANKA) because the laser can easily be adjusted to the ANKA revolution frequency. The laser system at ANKA operates at 1050 nm, so an InGaAs based line array is required. The acquisition rate of the commercial InGaAs line arrays, however, is limited to the low kHz range [7] thus it is not possible to monitor fast dynamic changes of the longitudinal bunch profile. For this reason a fast spectrometer is being developed at KIT and the target frame rate has been set to 5×10^6 frames per second (Mfps) to make it also applicable to other facilities such as XFEL and ELBE for which the repetition rates are higher. The final system must also be able to perform some on-line analysis of the bunch conditions in order to be used as a real-time and non-destructive diagnostic tool.

DESIGN CONCEPT

The architecture of the new spectrometer system is shown in Fig.1. The system consists of a mezzanine card where the detector (a), the front-end electronics (b) and the ADCs (c) are mounted, an FPGA-based high-throughput readout board (d) and an external DAQ system (e).

Two different detectors technologies can be used to detect the modulated spectral response over different frequency ranges: an InGaAs linear array for the near IR and an uncoated Si linear array for visible light. The final version of the system will be based on a 1D detector with 512 pixels and a pitch of 50 μm.

The detector's output signals are fed via high density fine-pitch wire-bonding connections to the front-end electronics. A low temperature fine pitch wire-bonding technology is required. Therefore, an ultrasonic wedge-to-wedge alluminium wire with a diameter of 25 μm has been choosen.

Eight GOTTHARD ASICs [8] developed by PSI are used as charge-sensitive pre-amplifiers. Although the GOTTHARD has been developed for a Si microstrip detector, it can also be used with different detectors thanks to its automatic and adaptive gain selection stage. The current version of the GOTTHARD (v1.4) has 128 inputs and 4 outputs. A group of 32 inputs is connected to one output through a distributed multiplexer, clocked at 32 MHz. Therefore, a maximum frame rate of 1 Mfps can be achieved. A new GOTTHARD version (v1.6) with 8 analog outputs and an operating maximum frequency of 50 MHz is currently being submitted to the foundry. The new version allows to achieve a maximum frame rate of 3.1 Mfps. In order to meet the requirement of 5 Mfps with a linear array of 512 pixels, a special routing is required: each GOTTHARD chip will be connected to the detector in interleaving mode, and only 64 inputs of each chip will be used. In this way each output serves 8 pixels. With a reset after 8 clock cycles, a frame rate of up to 6.25 Mfps can be realized.

ISBN 978-3-95450-141-0

LANSCE 1L HARP DATA ACQUISITION SYSTEM UPGRADE*

J. Sedillo, J. Nguyen, J.D. Gilpatrick, M. Gruchalla, LANL, Los Alamos, NM 87545, USA

Abstract

The 1L Harp is the last beam diagnostic preceding LANSCE's 1L Target, the neutron source of LANSCE's Lujan Center, and consists of two orthogonal planes of stationary sense wires for monitoring the beam distribution prior to its arrival at the target. A new data acquisition system has been developed for the 1L Harp that features a National Instruments compactRIO contained within a BiRIO chassis hosting electronic circuits for signal conditioning and a new feature for sense wire integrity monitoring. Hardware design, software architecture, and preliminary data acquisition results will be described.

INTRODUCTION

The 1L harp is a fixed-position, beam diagnostic sensor for measurement of the beam's transverse profiles immediately prior to impingement on the 1L target. The sensor is composed of three planes of silicon-carbide (SiC) fibers; two sense planes for measuring horizontal and vertical beam profiles, and a bias plane for attraction of secondary electrons. Each sense plane is composed of seventeen, 0.079-mm diameter sense fibers spaced at 6-mm intervals. All fibers connect to individual 10 pF capacitors at one end and a cable plant at the other end for signal transmission to the data acquisition system [1] as shown in Fig. 1.

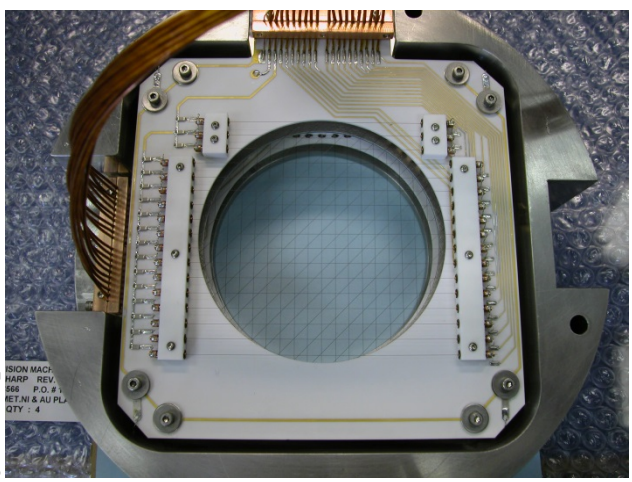

Figure 1: 1L Harp Sensor [1].

PRINCIPLE OF OPERATION

The 1L harp operates on the principle of secondary electron emission resulting from the interaction of the particle beam with the harp's sense wires. As the high-energy (800 MeV) H+ particle beam passes through the fiber's SiC material, electrons are forcefully removed from the fiber's surface into free space, leaving a positive charge gain within the fiber. The positive voltage resulting from the fiber's loss of electrons attracts a flow of electron current from the signal conditioning circuit to the sense wire, neutralizing the charge difference. This current and its associated net charge are transformed by the signal conditioning circuitry into a voltage signal proportionally related to the charge. Since the particle beam's transverse particle density is generally Gaussian, each fiber in the plane receives a different concentration of beam flux. This beam flux translates into secondary electron emission differences resulting in charge differences at the signal conditioning circuitry and finally a voltage difference at the ADC dedicated to each sense wire. Plotting the resulting voltages as a function of the fiber's relative position creates a Gaussian profile corresponding to the beam's transverse particle density.

Beam parameters at the 1L Harp are listed in Table 1. From the properties of the beam and the SiC fiber; application of the Bethe-Bloch formula described by Loveland in [2], with a ionization potential of 180 eV for SiC [3], and applying the Sternglass theory across the surface of a SiC fiber at beam center yields an expected negative charge loss of 484 picocoulombs.

Table 1: 1L Harp Beam Properties

Beam Property	Value
Beam species	H+
Beam energy	800 MeV
Longitudinal current profile	Triangular
Pulse duration	300 ns
Peak current	33.3 A
Transverse RMS	12.5 mm
Bunch charge	5 μCoulombs

SYSTEM HARDWARE

Data Acquisition System/ EPICS IOC

The data acquisition hardware consists of a National Instruments compactRIO with interfaces to three AFE (Analog Front End) boards and one integrity board housed within a BiRIO chassis as shown in Fig. 2. Logic signals for beam synchronization and AFE control connect to the compactRIO through a single NI-9401

*Work supported by the U.S. Department of Energy under contract DE-AC52-06NA25396.

DEVELOPMENT OF NON-INVASIVE ELECTRON BEAM POSITION MONITOR BASED ON COHERENT DIFFRACTION RADIATION FROM A SLIT*

Y. Taira#, R. Kuroda, M. Tanaka, H. Toyokawa, AIST, Tsukuba, Japan
K. Sakaue, Waseda Univ., Tokyo, Japan
H. Tomizawa, RIKEN Harima Institute, Japan

Abstract

Diffraction radiation is emitted when a charged particle passes through in the vicinity of a boundary between two media with different dielectric constants. An aperture, a slit, and an edge are used for diffraction radiation target. It is theoretically suggested that an asymmetry of a spatial distribution of diffraction radiation appears by changing the beam trajectory with respect to the center of a rectangular slit. We have developed the beam position monitor using the coherent diffraction radiation generated when a sub-picosecond electron beam passes through the rectangular slit. A theoretical background of the diffraction radiation emitted from the slit and experimental results will be reported.

INTRODUCTION

Generation of an ultra-short pulsed electron beam with a bunch length of few hundreds of femtoseconds and below 100 fs is key technique of accelerator science; that are generation of intense terahertz radiation [1] and x-ray free electron lasers (X-ray FEL) [2]. Many techniques for beam diagnostic have been developed so far.

Diffraction radiation (DR) is used as a non-invasive beam diagnostic and can be used to measure beam energy, transverse size, divergence, and position [3]. DR is generated when a charged particle moves in the vicinity of a boundary between two media with different dielectric constants with a condition of $d < \gamma\lambda/2\pi$, where d is the distance between the edge of the medium and the electron, γ is the Lorentz factor of the electron beam, and λ is the observed wavelength of DR [4]. An aperture, a slit, and an edge can be used as DR devices.

Recently, three-dimensional electron bunch charge distribution (3D-BCD) monitor has been proposed for the X-ray FEL by H. Tomizawa [5-6]. It is based on Electro-Optical (EO) multiple sampling (multiplexing) with a manner of spectral decoding. Here, three hollow EO detectors surround the electron beam axis azimuthally and are installed at three detection points on the beam axis. To simplify the monitor system of the 3D-BCD, the basic concept of the DR beam position monitor was proposed [5]. The electron bunch's center of mass and incident angle at the central EO detector of 3D-BCD is defined by the EO detectors of both ends. We investigated the feasibility of the concept of this novel monitor.

Our facility, S-band compact electron linac at the National Institute of Advanced Industrial Science and Technology (AIST) [7] is the beam energy of 40 MeV. If we observe an optical diffraction radiation with the wavelength of 500 nm, the distance d must be smaller than 6 μm. This value will be much smaller than the beam size. Therefore it is necessary to observe the longer wavelength of DR for realistic measurements.

Coherent radiation emits when the wavelength of the radiation is comparable to or longer than the electron bunch length. The frequency spectrum of coherent radiation is mainly depended on a bunch form factor described as

$$f(\omega) = \left| \int_{-\infty}^{\infty} \rho(t) \exp(i\omega t) \mathrm{d}t \right|^2, \quad (1)$$

where ω is the angular frequency of coherent radiation, $\rho(t)$ is the particle distribution, and t is time. If $\rho(t)$ is assumed to a Gaussian particle distribution of bunch length σ (rms), the form factor is expressed as

$$f(\omega) = \exp\left(-\sigma^2\omega^2\right). \quad (2)$$

Consequently, the frequency spectrum of coherent radiation is strongly depended on the bunch length σ. For example, if the bunch length is 200 fs, coherent radiation up to the frequency of 2 THz (wavelength of 150 μm) is coherently enhanced. If we observe the wavelength of 150 μm of the CDR, the distance d must be less than 2 mm. This condition is useful for the CDR measurement. Therefore, CDR can be used to measure electron bunch length, energy, transverse size, divergence, and position.

In this paper, we focus on the measurement of the beam position using the CDR emitted from a rectangular slit. A theoretical background and experimental results will be reported. We have successfully detected the beam position by measuring the asymmetry of the spatial distribution of CDR.

DIFFRACTION RADIATION GENERATED FROM A RECTANGULAR SLIT

Theoretical equations concerning with the DR emitted from the rectangular slit are described in Ref. [4]. The DR field generated by a charged particle passing through a rectangular slit opening in a rectangular screen can be described as

$$E_{x,y}^{DR}(a_{out}, b_{out}) = E_{x,y}^{TR}(a_{out}, b_{out}) - E_{x,y}^{TR}(a_{in}, b_{in}). \quad (3)$$

where the indices x and y are the horizontal and vertical polarization components at the detector coordinates, a_{out}

*Work supported by JSPS KAKENHI Grant Number 26246046.
#yoshtiaka-taira@aist.go.jp

EXPERIENCE WITH AND STUDIES OF THE SNS* TARGET IMAGING SYSTEM

W. Blokland, ORNL, Oak Ridge, TN 37831, USA

Abstract

The Target Imaging System (TIS) shows the size and position of the proton beam by using a luminescent Cr:Al2O3 coating on the SNS target. The proton beam hitting the coating creates light, which is transferred through mirrors and optical fibers to a digital camera outside the high radiation area. The TIS is used during operations to verify that the beam is in the right location and does not exceed the maximum proton beam peak density. This paper describes our operational experience with the TIS and the results of studies on the linearity, uniformity, and luminescence decay of the coating. In the future, tubes with material samples might be placed in front of the target for irradiation studies. The simulations of placing tubes in the front of target coating and the effect on the beam width and position measurements are also discussed.

INTRODUCTION

Spallation Neutron Source

The Spallation Neutron Source (SNS) uses short and intense pulses of neutrons for materials research. These neutron pulses are created through a spallation process by hitting the mercury filled target with 1 GeV protons pulses. The SNS accelerator creates these proton pulses and must steer them to the target within ±4 mm vertically and ±6 mm horizontally of the target center and with a maximum size and peak density to prevent a premature end of life of the target.

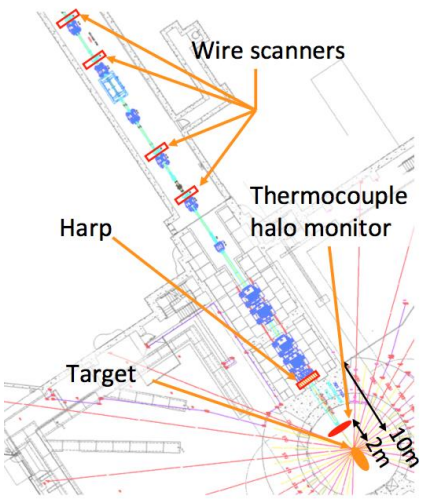

Figure 1: The locations of RTBT instrumentation.

*ORNL/SNS is managed by UT-Battelle, LLC, for the U.S. Department of Energy under contract DE-AC05-00OR22725

The Ring to Target Beam Transfer line (RTBT) Wizard program uses wire scanners and harp profiles to calculate the beam size and steering for the initial setup using low power beam. During neutron production with full beam power, the harp still provides profile data to verify the beam profiles but it is approximately 10 meters away and cannot, on its own, fully determine the location of the beam on the target. Thermocouples located at the Proton Beam Window (PBW), are only two meters away from the target, indicate only the halo of the beam. The beam halo is not necessarily symmetric and thus not a good measurement of the profile size or center position of the beam. Figure 1 shows the locations of the instrumentation. The Target Imaging System has been created to deal with these limitations.

Target Imaging System

The TIS measures the position and profile of the beam right on the target nose cone using a luminescent coating. The light produced by the protons hitting the coating is guided using mirrors, lenses, and a rad-hard fiber bundle to a camera outside of the high radiation area [1-5]. Figure 2 shows an example of the acquired image. The coating has fiducial markers that are measured before installation of the target and then used to calibrate the image obtained by the camera. Once calibrated, the TIS can determine the widths, peak density, and center of the beam on the target.

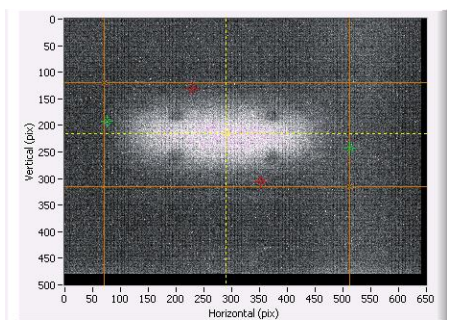

Figure 2: Image of beam on target.

OPERATION

Operators track the results of the TIS during the neutron production runs and adjust the beam trajectory if needed. Figure 3 shows the Target Errant Beam Control screen tracking the center of the beam on the target. The red circles are the individual measurements while the blue circles are the average positions. This shows a peak-to-peak noise of about 1 mm. The bottom part of the figure shows the magnets that can be adjusted to steer the beam if needed. This screen, created by the operators, is always visible in the control room and, in addition to being watched by the operators, also monitored by errant beam

ISBN 978-3-95450-141-0

DEVELOPMENT OF THE TRANSVERSE BEAM PROFILE MONITORS FOR THE PAL-XFEL*

I. Y. Kim†, J. Choi, H. Heo, C. Kim, G. Mun, B. Oh, S. Park, H. S. Kang,
Pohang Accelerator Laboratory (PAL), Pohang, 790-834, Republic of Korea

Abstract

The PAL-XFEL is an X-ray free electron laser under construction at the Pohang Accelerator Laboratory (PAL), Korea. In the PAL-XFEL, the electron beam can make coherent optical transition radiation (COTR) due to the microbunching instability in the compressed electron beam. In order to obtain transverse beam profiles without the COTR problem, we are developing scintillating screen monitors (with the geometric suppress method) and wire scanners. In this paper, we report test results at the test facility and progress in the development of the screen monitor and the wire scanner for the PAL-XFEL.

INTRODUCTION

Transverse beam profile diagnostics in electron linacs is widely based on optical transition radiation (OTR) as standard technique which is observed in backward direction when a charged particle cross the boundary between two media with different electrical properties. Unfortunately, microbunching instablities in high-brightness electron beam of modern linac-driven free-electron lasers (FELs) can lead to coherent effects in the emission of OTR. Because of this reason it is not possible to obtain a direct image of the particle beam. In order to allow the beam profile measurements in the presence of microbunching instabilites, there are solutions has been studied. First is to use scintillation screens instead of transition radiation and another is wire scanner [1, 2].

To successful commissioning, the transverse beam profile monitors which is not affected by COTR effect are necessary. In this reason we are studying scintillating beam profile monitors and wire scanners.

In this article, we report test results with transverse profile monitor installed at the injection test facility (ITF) and the new profile monitors design for PAL-XFEL.

MEASUREMENTS

The screen monitors and wire scanner which is used to acquire beam profie installed at the ITF. The screen monitor is operating for beam diagnostics. The Fig. 1 shows screen montor and wire scanner installed at the end of beamline.

ITF Screen Monitor

The RadiaBeam Technologies's Integrated Beam Imaging System II (IBIS-II) was installed at the ITF. This screen target is 100 μm thick YAG:Ce scintillator which is installed normal to the beam direction and 200 nm aluminized silicon wafer for mirror was installed 45 deg with respect to the beam axis. The BAUMER GigE cameras with 5M pixels and a 2/3 inch CCD sensor are used to obtain electron beam image. The electron beam image with this screen is shown in Fig. 2. The beam size was obtained with σ_x = 0.57 ± 0.03 mm and σ_y = 1.00 ± 0.05 mm.

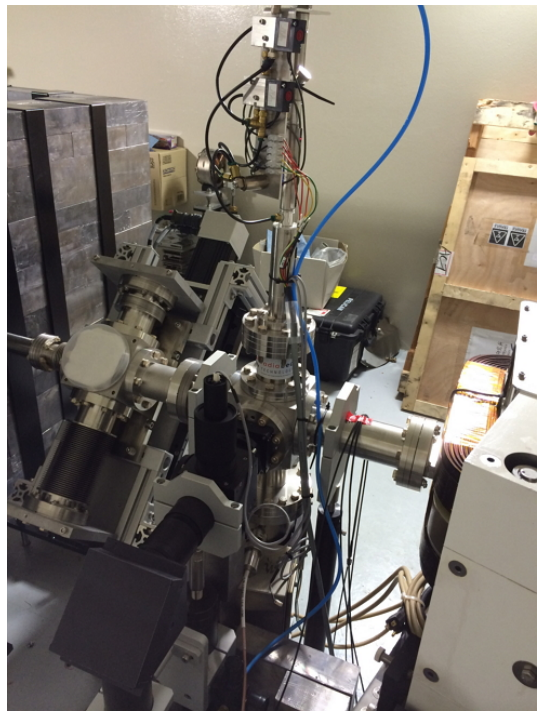

Figure 1: The wire scanner (Left) and screen monitor (Right) station.

ITF Wire Scanner

A wire scanner measures the average, projected beam profile in one plane over several successive beam pulses. The wire scanner was installed at the diagnostic section which was manufactured by RadiaBeam Technologies. This is consist of a wire card with three 25 μm thick tungsten wires and a ball-screw linear stage [3]. And the radiation intensity of the beam at a wire position determined by silica optical fiber with Photomultiplier (PMT). The schematic layout of measurement system are shown in Fig 3. The electron beam loss signal (shown Fig. 4) is pulse width is about 5 μsec.

Beam profile measurement and analysis were performed. Because of the motor controller is not yet integrated with timing system, it takes a few minutes to get a set of beam profile. The electron beam operation condition which is

* Work supported by MSIP, Korea
† ilyoukim@postech.ac.kr

AC COUPLING STUDIES AND CIRCUIT MODEL FOR LOSS MONITOR RING*

Zhengzheng Liu#, Jenna Crisp, Steven Lidia, Facility for Rare Isotope Beams (FRIB),
Michigan State University, East Lansing, MI 48824, USA

Abstract

As a follow-up study to the initial design of FRIB Loss Monitor Ring (previously named Halo Monitor Ring [1]), we present recent results of coupling studies between the FRIB CW beam and the Loss Monitor Ring (LMR). While a ~33 kHz low-pass filter was proposed to attenuate high-frequency AC-coupled signals [1,2], the LMR current signal may still contain low frequency signals induced by the un-intercepted beam, for example, by the 50μs beam notch that repeats every 10ms. We use CST Microwave Studio to simulate the AC response of a Gaussian source signal and benchmarked it to analytical model. A circuit model for beam-notch-induced AC signal is deduced and should put a ~33pA (peak) bipolar pulse on the LMR at 100Hz repetition rate. Although its amplitude falls into our tolerable region, we could consider an extended background integration to eliminate this effect.

INTRODUCTION

Loss Monitor Ring (LMR), or previously called Halo Monitor Ring, is described in Ref [1, 2] as a metal ring with carefully specified aperture designed to intercept ions that are likely to be lost further downstream. While the to-be-lost particles hit and stop in the ring, most of the beam passes through it. Therefore three dominating signals are generated: primary current by the impacting ions, secondary emission current by the escaped electrons, and AC-coupled current induced by the beam. The former two signals are low frequency signals, which we want to measure as beam losses [2]. Therefore we need to eliminate the AC-coupled signal and ensure it is insignificant in our data acquision.

Considering FRIB CW beam structure, it can be generally layered as mini pulses and macro bunches: The mini pulses have a 100 Hz repetition rate and 50μs pulse spacing, which is required by the AC beam current monitor; the macro bunches, inside the mini pulse, have a repetition rate of 80.5 MHz with variable pulse spacing. To attenuate the macro-bunch induced signal that is in MHz range, we can use a ~33 kHz low pass filter to attenuate it [2]. However, the 50μs notch of mini pulse could induce some fake data in low frequency range that we want to estimate and find solutions.

Since the CST computation of μsec excitation is extreme long, we first simulated a nano-seconds Gaussian pulse in CST Microwave Studio and benchmarked the result with our analytical models. The validated model will then be applied to calculate the 50μs notch induced signal. According to the estimation, the induced signal is not critical but could put some fake background samples. Integration for an extended time period might help and we are investigating other schemes to release the concern.

* This material is based upon work supported by the U.S. Department of Energy, Office of Science, Facility for Rare Isotope Beams under Cooperative Agreement No. DE-SC0000661

liuz@frib.msu.edu

EM SIMULATION FOR AC-COUPLING

There are generally two ways to simulate the AC-coupled signal: CST Microwave analysis that simulates an excitation signal through the capacitive pick-up; or Particle Studio that simulates a Gaussian bunch through the ring. Since we are interested in low frequency response rather than MHz range, nonrelativistic bunch is not our concern. Therefore we use CST Microwave Studio to help build the circuit model for LMR.

Geometry Modelling of LMR

Figure 1 shows an example of the basic LMR design [2]. The niobium ring, which intercepts lost particles, is sandwiched by two copper plates, one for electric field shielding and the other one attached on the wall to remove heat. The mounting and shielding rings are electrically connected to the chamber. Ceramic or sapphire washes are used to electrically isolate the Niobium ring while thermally connecting it to the chamber through the mounting ring.

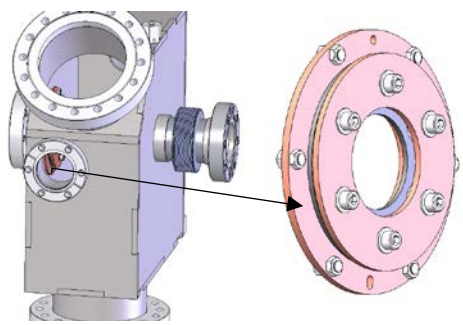

Figure 1: Basic mechanical design of LMR.

We modeled the basic LMR geometry in CST, as shown in Figure 2. The diagnostics box was simplified to a rectangular box and the bolts were smaller than the holes on niobium ring for electric isolation. Ceramic washers were attached on both sides of the niobium ring, as good dielectric material with reasonable thermal conductivity. A wire was set across the box with 220Ω approximate characteristic impedances at both ends.

EM Simulation

To measure the induced AC signal, we located a discrete ports (50Ω) from niobium intercept to grounded

ISBN 978-3-95450-141-0

BEAM LOSS MONITOR AT SUPERKEKB

Hitomi Ikeda*, Mitsuhiro Arinaga, John Walter Flanagan, Hitoshi Fukuma and Makoto Tobiyama,
KEK, High Energy Accelerator Research Organization, Ibaraki 305-0801, Japan

Abstract

We will use beam loss monitors for protection of the hardware of SuperKEKB against unexpected sudden beam losses. The sensors are ion chambers and PIN photo-diodes. The loss monitor system provides an important trigger to the beam abort system. We can optimize the threshold of the abort trigger by checking the beam information at each abort event. This paper explains the overall system of the SuperKEKB beam loss monitors including the damping ring (DR).

INTRODUCTION

The KEKB collider is being upgraded to SuperKEKB in order to get higher luminosity. The beam energy of the Low Energy Ring (LER) is 4 GeV for positrons, and that of the High Energy Ring is 7 GeV for electrons. The beam currents are 2.6 A in HER and 3.6A in LER. LER injection system includes a 1.1 GeV DR [1, 2]. The machine parameters of SuperKEKB are shown in Table 1. In order to get 40 times higher luminosity than that of KEKB, the beam currents will be increased 2 times higher than at KEKB and the beam size at the interaction point will be further squeezed with a large crossing angle. The first beam is expected in FY 2015.

Table 1: Machine Parameters of SuperKEKB

Parameter	LER	HER	DR	unit
Energy	4.0	7.0	1.1	GeV
Max. bunch charge	14.4	10.4	8	nC
No. of bunches	2500		4	
Circumference	3016		135.5	m
Max. stored current	3.6	2.6	0.07	A
Horizontal damping time	58	29	10.9	ms
x-y coupling	0.27	0.28	5	%
Emittance (h)	3.2	4.6	42.5	nm
Emittance (v)	8.64	12.9	3150	pm
Bunch length	6.0	5.0	6.53	mm
βx*/βy*	32/0.27	25/0.30		mm
Crossing angle	83			mrad
Luminosity	$8x10^{35}$			$cm^{-2}s^{-1}$
RF frequency	509			MHz

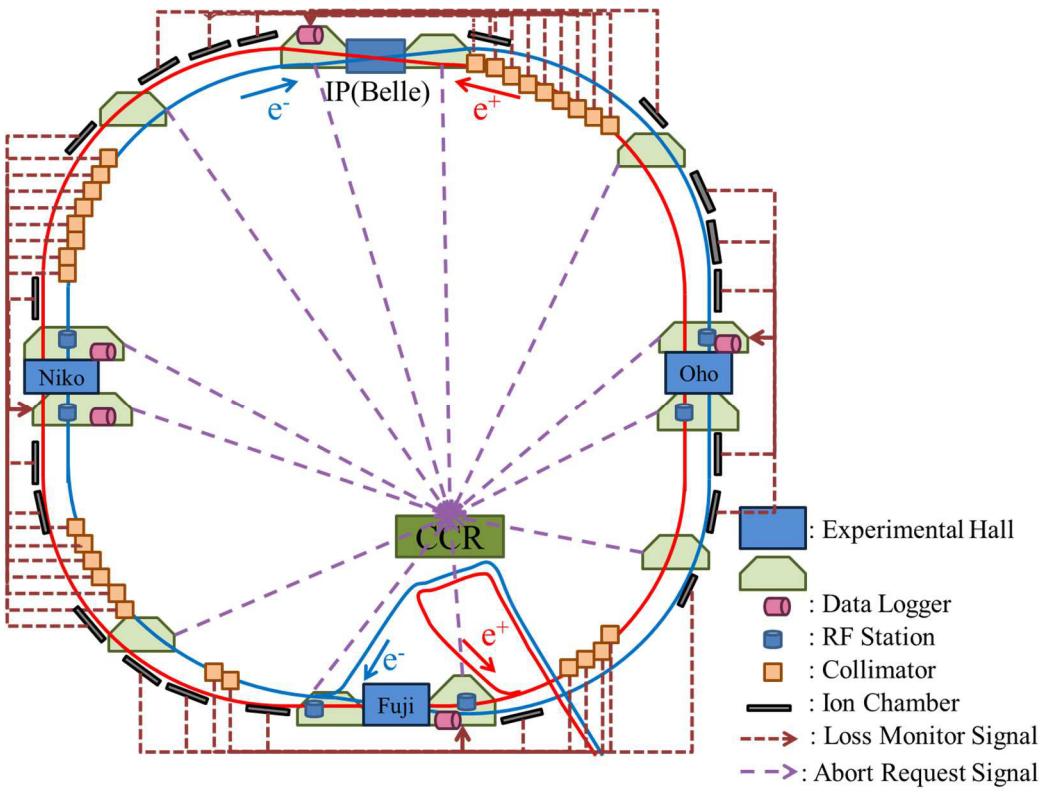

Figure 1: The overall system of the SuperKEKB beam loss monitor.

*hitomi.ikeda@kek.jp

ISBN 978-3-95450-141-0

REAL-TIME DISPLAY SYSTEM FOR THE OPTICAL FIBER BEAM LOSS MONITOR FOR THE PHIL AND THOMX FACILITIES

I. Chaikovska*, N. Delerue, A. Variola,
Laboratoire de l'Accélérateur Linéaire, CNRS-IN2P3, Université Paris-Sud XI, Orsay, France

Abstract

Fiber monitors are an attractive beam loss diagnostics tool. They are based on the detection of the electromagnetic shower produced by the beam losses. Cherenkov radiation is produced by the electromagnetic shower charged particles within the multimode fibers attached to the vacuum chamber. This radiation is consequently converted to an electrical signal containing the information about the position and intensity of the beam losses. Therefore, a system based on fibers installed alongside the whole accelerator together with a signal detection system forms a continuous, real-time Fiber Beam Loss Monitor (FBLM). In this context, the FBLM is a very useful tool for the commissioning and beam alignment. In this article we report on the development of the real-time display system for the FBLM at PHIL (PHotoInjector at LAL, Orsay, France) as a prototype of the beam loss monitor for the ThomX project, the compact Compton based X-ray source under construction in Orsay

INTRODUCTION

ThomX is a project proposed by a colaboration of French institutions and one company to build an accelerator based compact X-ray source in Orsay (France) [1]. The main goal of the project is to deliver a stable and a high energy X-ray beam (up to 90 keV) with a flux of the orders of 10^{11} – 10^{13} photons per second generated by the Compton backscattering process. At present, the ThomX machine is under construction.

The ThomX accelerator facility is composed by the linac driven by 2998 MHz RF gun, a transfer line and a compact storage ring where the collisions between laser pulses and relativistic electron bunches result in the production of the X-rays. Low energy, compactness and lack of the operation experience make such type of the machine very difficult to operate and, especially, to commission. In this context, a reliable beam loss monitor able to locate the losses will be indispensable for the commissioning (tuning of the linac and the transfer line to optimize the injection, setting-up of the ring working point) and further operation of the machine.

Nowadays, the beam loss monitor technology based on the optical fibers is established. Hereafter, we will describe the FBLM installed at PHIL facility as a prototype for the ThomX machine. PHIL is a photoinjector driven by the 2998 MHz RF gun [2]. The beam line consists of the three solenoids, a pair of steerers and a dipole (see Figure 1). Among the diagnostics tools are the ICTs, YAG screens, Cherenkov radiation monitor and a Faraday cup. Some of the ThomX and PHIL machine parameters are listed in Table 1.

A real-time display system for the FBLM is being developed for the future commissioning and operation of the PHIL and ThomX machine. It presents an application having the convenient GUI to control the FBLM equipment and helping easily locate beam losses along the accelerator.

Table 1: PHIL and ThomX Electron Beam and Machine Parameters

Description	PHIL	ThomX	Units
Beam energy	5	50 – 70	MeV
Bunch charge	< 1.5	1	nC
Bunch length (rms)	> 3.5	3.7 (injector) 30 (ring)	ps ps
Beam energy spread (rms)	< 2 – 3	< 1	%
Repetition frequency	5	50	Hz
Machine length	~ 5	~ 5 (injector) ~ 13 (transfer line) ~ 18 (ring)	m m m

PRINCIPLE OF THE BEAM LOSS DETECTION

The detection principle of the beam losses is based on the production of Cherenkov radiation in the optical fiber attached to the vacuum chamber by the electromagnetic shower generated when the main beam hits the vacuum chamber or any obstacle. The secondary charged particles produce Cherenkov radiation provided that the velocity of that particles are greater than the phase velocity of light in the fiber core material. Consequently, the Cherenkov light is converted to an electrical signal containing the information about the position and intensity of the beam losses.

The Cherenkov light is emitted along a cone with an opening angle defined by the velocity of the particle and the refractive index of the fiber core. Light yield is proportional to $1/\lambda^2$, where λ is a wavelength of the Cherenkov radiation and depends on the direction at which the particle crosses the fiber. A detailed description of the Cherenkov radiation process including production, photon yield, probability for the photon to be captured and guided by the fiber, photon detection, etc. has been extensively worked out in the framework of the Cherenkov fiber calorimetry [3].

* chaikovs@lal.in2p3.fr

ISBN 978-3-95450-141-0

INSTALLATION OF A BEAM LOSS MONITORING SYSTEM AT THE S-DALINAC*

L. Jürgensen#, U. Bonnes, C. Burandt, M. Fischer, F. Hug, T. Kürzeder, N. Pietralla, R. Stegmann, M. Steinhorst, Technische Universität Darmstadt, Germany

Abstract

The S-DALINAC is the superconducting linear accelerator of the Institut für Kernphysik at Technische Universität Darmstadt (Germany). In order to get a short-time response about occurring beam losses and their locations a new system based on PIN-diodes was installed. The readout of the commercially available beam loss monitors is done via an in-house developed system compatible to our EPICS-based control system. The system and the results of the commissioning will be presented in this paper.

INTRODUCTION

Since 1987 the S-DALINAC serves nuclear- and astrophysical experiments at TU Darmstadt [1]. It is fed by either a thermionic gun or a photoemission gun which delivers a spin-polarized electron beam [2]. After pre-acceleration up to an energy of 10 MeV by the injector module the electron beam can either be used for experiments at the Darmstadt High Intensity Photon Setup (DHIPS) [3] or it is guided through a 180°-arc to enter the main linac. By passing the linac up to three times the maximum energy of about 130 MeV can be reached. The beam current can be adjusted from several pA up to 60 µA.

In order to improve the accelerator's performance and also to decrease the contamination of the surrounding by undetected beam losses, a beam loss monitoring system has been set up. Comparable machines are using several different monitors based on e.g. ionizing chambers, scintillators, glass fiber or semiconductor detectors. The requirements for an operation at the S-DALINAC are sensitiveness for (secondary) electrons, easy mounting and space-saving dimensions. In addition the detectors should provide a short-time readout in order to provide the operator with direct feedback for an improved beam tuning.

Beam Losses at the S-DALINAC

At the S-DALINAC beam losses typically occur because of small misalignments in the beam line or deviations in the magnetic fields. Therefore part of the beam is lost in the walls of the vacuum chamber. Depending on the electron's initial energy the produced secondary radiation can penetrate and activate the beam tube and surrounding equipment.

BEAM LOSS MONITORING SYSTEM

Originally designed and implemented at HERA [4] the chosen Beam Loss Monitor (BLM) is currently manufactured and distributed by Bergoz Instrumentation [5]. The beam loss detection is based on a coincidence setup of two PIN-photodiodes interacting with ionizing radiation. The coincidence reduces the zero counting rate caused by the dark currents of the photodiodes. The operating principle is shown in Fig. 1.

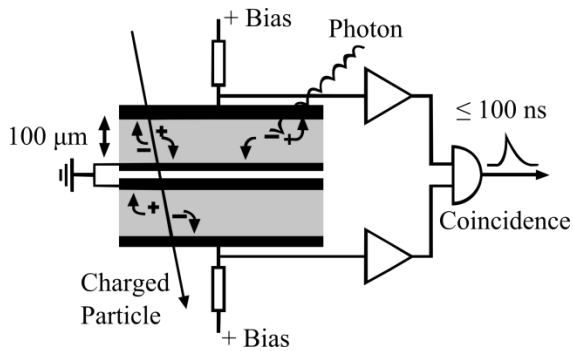

Figure 1: Operating principle of the Beam Loss Monitor [5].

Figure 2 shows the BLM circuit board with highlighted PIN-diodes of the BPW34 type. During operation the upper half is shielded from light and electromagnetic noise by a metal enclosure. The overall size is 69 x 34 x 18 mm³. To increase sensitivity, the original type of PIN-diodes can be exchanged by larger diodes.

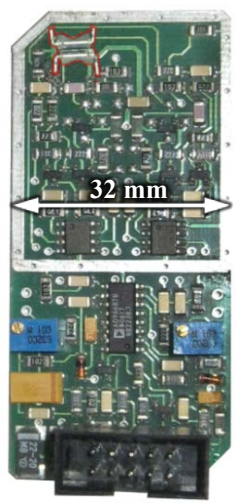

Figure 2: BLM circuit board with PIN-diodes at the upper left part.

*Work supported by BMBF through under contract No. 05K13RDA.
#ljuergensen@ikp.tu-darmstadt.de

ISBN 978-3-95450-141-0

CRYOGENIC BEAM LOSS MONITORS FOR THE SUPERCONDUCTING MAGNETS OF THE LHC*

M. R. Bartosik†, B. Dehning, M. Sapinski, CERN, Geneva, Switzerland
C. Kurfuerst, Technische Universität, Vienna, Austria
E. Griesmayer, CIVIDEC, Vienna, Austria
V. Eremin, E. Verbitskaya, IOFFE, St. Petersburg, Russian Federation

Abstract

The Beam Loss Monitor detectors close to the interaction points of the Large Hadron Collider are currently located outside the cryostat, far from the superconducting coils of the magnets. In addition to their sensitivity to lost beam particles, they also detect particles coming from the experimental collisions, which do not contribute significantly to the heat deposition in the superconducting coils. In the future, with beams of higher energy and brightness resulting in higher luminosity, distinguishing between these interaction products and dangerous quench-provoking beam losses from the primary proton beams will be challenging. The system can be optimised by locating beam loss monitors as close as possible to the superconducting coils, inside the cold mass in a superfluid helium environment, at 1.9 K. The dose then measured by such Cryogenic Beam Loss Monitors would more precisely correspond to the real dose deposited in the coil. The candidates under investigation for such detectors are based on p^+–n–n^+ silicon and single crystal Chemical Vapour Deposition diamond, of which several have now been mounted on the outside of cold mass of the superconducting coil in the cryostat of the Large Hadron Collider magnets. This contribution will present the mechanical and electrical designs of these systems, as well as the results of their qualification testing including results of a cryogenic irradiation test.

INTRODUCTION

Motivation

The magnets close to the LHC interaction points (IPs) are exposed to high irradiation from the collision debris. It has been shown in Fluka simulation [1] that with the present configuration of the installed Beam Loss Monitoring (BLM) in this region, the ability to measure the energy deposition in the coil is limited because of this debris, masking the real beam loss signal (see fig. 1).

The particle showers from beam loss measured by the present BLM configuration are partly shielded by the cryostat and the iron yoke of the magnets. The system can hence be optimised by locating beam loss monitors as close as possible to the elements that need protecting. This is what is foreseen for the High Luminosity LHC (HL-LHC) upgrade,

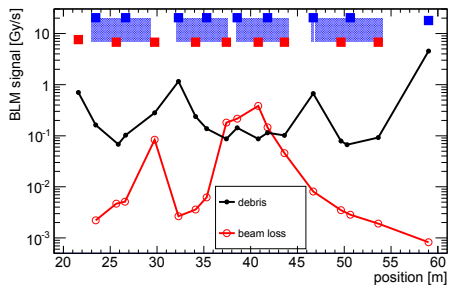

Figure 1: Doses in the coil and signal in the existing BLMs; black: BLM signal from collision debris (one point for each BLM); red: BLM signal from quench-provoking losses inside second central superconducting quadrupole magnet in the focusing triplet (Q2B).

where the BLM will be located near the superconducting coils inside the cold mass of the magnets in superfluid helium at a temperature of 1.9 K [2] (see fig. 2, courtesy of P. Ferracin)).

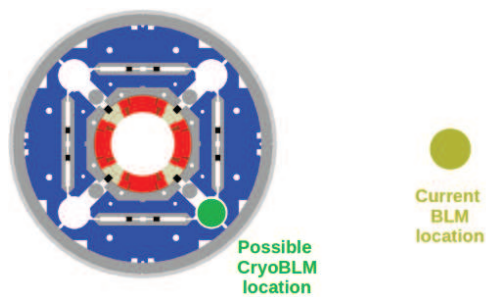

Figure 2: Cross section of a large aperture superconducting insertion magnet (MQXF) foreseen for HL-LHC with the current BLM placement and the future possible Cryogenic BLM location shown.

The advantage being that the dose measured by the Cryogenic BLM would more precisely correspond to the dose deposited in the superconducting coil [3].

Cryogenic BLM Requirements

From the mechanical point of view the main challenges of the Cryogenic BLM system is the low temperature of 1.9 K and 20 years, maintenance free operation [3]. Furthermore the Cryogenic BLM needs to work in a magnetic field of 2 T and at a pressure of 1.1 bar, and capable of withstanding a fast pressure rise up to 20 bar in case of a magnet quench.

* This research project has been supported by a Marie Curie Early Initial Training Network Fellowship of the European Community's Seventh Framework Programme under contract number (PITN-GA-2011-289485-OPAC).

† marcin.bartosik@cern.ch

ISBN 978-3-95450-141-0

LCLS BEAM DIAGNOSTICS*

H. Loos†, SLAC, Menlo Park, CA 94025, USA

Abstract

An extensive set of beam diagnostics has been one of the factors in the successful commissioning and operation of the Linac Coherent Light Source (LCLS) x-ray FEL over the last seven years. The originally developed and installed diagnostics were geared towards measuring the electron beam parameters of the LCLS design specifications. Since then, a number of improved and new diagnostics has been implemented to accommodate a much wider range of beam parameters and to overcome the challenges of diagnostics for a high brightness electron beam. Plans for the diagnostics of the high repetition rate LCLS-II project and ongoing developments will also be discussed.

INTRODUCTION

The Linac Coherent Light Source (LCLS) free electron laser facility is based on the last km of the existing SLAC linear accelerator using normal conducting copper accelerating structures providing a multi-GeV electron beam at a rate of up to 120 Hz feeding a 100 m long undulator system to generate soft and hard x-rays [1]. The facility has been operating since 2009 delivering up to about 5 mJ photon pulse energy to users during 9 user runs. A comparison of the LCLS baseline performance goals and the presently achieved operational parameters can be found in Table 1.

Over the past years the range of the available electron beam parameters has been significantly widened and new capabilities have been added to the FEL which poses enhanced demands on the existing diagnostics or made the development of new diagnostics necessary. As the baseline LCLS diagnostics has been extensively described in [2, 3], this paper will focus on recent developments. Among them, upgrades to BPM signal processing hardware and RF cavity BPM tests, improvements to the charge measurements, a new wire scanner design to significantly reduce emittance measurement durations and beam tuning time, a beam profile screen less susceptible to coherent radiation effects, and instrumentation to measure the shortest bunches single-shot using coherent radiation detection as well as an X-band deflecting cavity will be presented.

Recently, a new facility, LCLS-II [4], is being planned to enhance the existing LCLS capabilities by providing a MHz rate electron beam from a superconducting accelerator operating at 1.3 GHz feeding two undulator systems to simultaneously generate soft and hard x-ray beams and to generate shorter photon wavelengths using the existing LCLS-I linac, superseding the former LCLS-II project based on using an existing fraction of the normal-conducting (NC) SLAC 2-mile copper linac. The planned performance parameters can also be found in Table 1 where values in parentheses refer to the Cu-linac.

While the LCLS-II project design benefits from diagnostics improvements already underway, several key parameters of LCLS-II present new challenges to beam diagnostics [5]. The MW beam power greatly limits the use of intercepting diagnostics such as screens and wires which makes it necessary to incorporate low rate diagnostics beam lines into the machine design. Furthermore, the MHz beam rate requires very fast acquisition hardware and software to provide real-time beam pulse synchronized data for machine tuning and fast beam-based feedback systems. Diagnostics developments as they pertain to LCLS-II will be addressed throughout the paper.

BEAM CHARGE MEASUREMENT

The absolute charge measurement at LCLS is designed to be done with a number of toroids distributed at various locations from the injector through the undulator area which then serve as cross-calibration for all the BPM charge measurements. During the initial LCLS commissioning the readings were questionable and an existing toroid still installed from the SLC was used to provide the

Table 1: LCLS and LCLS-II Parameters

	LCLS		LCLS-II
	Baseline	**Operation**	**(Cu)**
RF frequency (GHz)	2.856		1.3
Repetition rate (Hz)	120	$1-120$	10^6
Beam energy (GeV)	$4.3-13.6$	$2.4-15.4$	4
Bunch charge (nC)	$0.200\ \&\ 1$	$0.02-0.25$	0.1
Bunch length rms (μm)	20	$<2-50$	8
Emittance norm. (μm)	1.2	$0.13-0.5$	0.4
X-ray energy (keV)	$0.83-8.3$	$0.25-10.5$	$0.2-5$ $(1-25)$
X-ray pulse energy (mJ)	<2	<4.7	<2.2
X-ray pulse length (fs)	230	$<5-500$	60

* Work supported by DOE contract DE-AC02-76SF00515
† loos@slac.stanford.edu

ISBN 978-3-95450-141-0

DIRECT (UNDER) SAMPLING VS. ANALOG DOWNCONVERSION FOR BPM ELECTRONCS*

M. Wendt#, CERN, Geneva, Switzerland

Abstract

Digital signal processing by means of undersampling the analog signal has become a popular method for acquiring beam position monitor signals. This presentation discusses the technique and its principle limitations, presents today's technical limits (e.g. in terms of performance of available ADCs), and provides an outlook for the future. It will also try to compare the technique with more tradition analog downmixing and signal processing methods

INTRODUCTION

Beam position monitors (BPM) are the workhorse of the beam diagnostics for every particle accelerator, linear, circular or transport lines, operating with leptons, hadrons or ions. A system of many, synchronized BPMs, distributed along the accelerator's beam-line allows the observation of the beam orbit, and, using well adapted read-out electronics, enables the extraction of a manifold of relevant information of the performance of the accelerator and it's beam quality. It is the optimization of BPM pickup, read-out electronics and data acquisition system, matched to the properties of accelerator and beam, which defines performance, quality and reproducibility of this important beam instrumentation system.

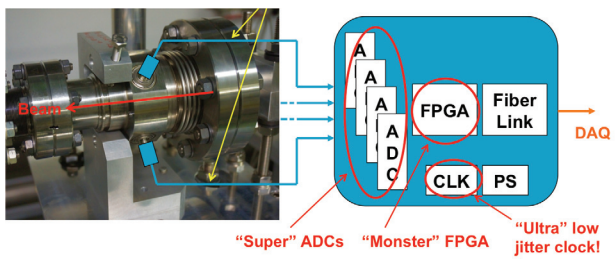

Figure 1: The ultimate digital BPM read-out electronics?

While the combination of both, the BPM pickup and the read-out electronics defines the ultimate performance in terms of resolution and long-term stability, most of the progress on these parameters have been made in recent years due to improvements in the read-out electronics, namely by adapting digital technologies, with profits taken from the commercial and military chip developments. Fig. 1 illustrates a provocative, "all digital" BPM electronics, using "super" ADCs and other equivalent components, hooked directly to the pickup electrodes.

Even with todays most advanced semiconductors, this idea is not feasible. Analog and RF components are still required in the signal path to guarantee the expected BPM performance, and to keep the costs reasonable, as the accelerator has to be equipped with many, sometimes more than 1000 beam position monitors, e.g. the LHC [1].

This work focuses on aspects of present technologies for BPM read-out electronics, trying to evaluate how much analog RF electronics is still necessary, and what can and should be accomplished digitally. A more general summary on trends and developments for BPM systems has been published some years ago [2].

BEAM SIGNALS

Understanding the beam properties, and the signals and characteristics of the BPM pickup is mandatory to specify and develop the optimal, best-suited read-out electronics.

Broadband BPM Pickups

A typical broadband BPM pickup consists out of symmetrically arranged RF antennas, typically "button" or stripline-like electrodes, which interact to the electromagnetic field of the passing beam.

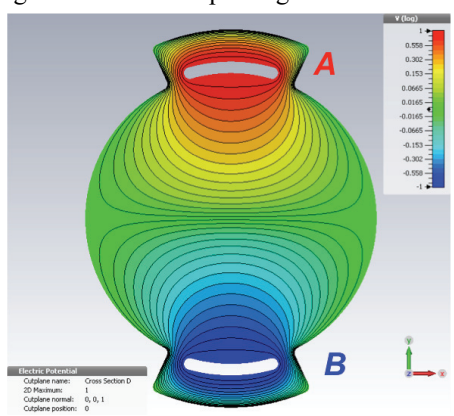

Figure 2: Equipotentials of a stripline BPM.

Figure 2 shows the cross-section of a stripline BPM with symmetrically arranged electrodes, for simplicity only the vertical ones. Plotted are the equipotentials for a potential difference between the electrodes, which indicate contour lines of beam positions giving constant signal amplitudes A and B. The beam displacement, or beam position is measured by detecting the asymmetry of these amplitudes, and normalizing them such that the beam position measurement is independent from the absolute signal level, as this varies with the beam intensity:

$$\text{norm. beam position} \propto \frac{A-B}{A+B}. \qquad (1)$$

The output signal of a BPM electrode or pickup is given by

#manfred.wendt@cern.ch

ISBN 978-3-95450-141-0

DEVELOPMENT OF A MODIFIED SIX-PORT DISCRIMINATOR FOR PRECISE BEAM POSITION MEASUREMENTS*

A. Penirschke†, T. Mahn, A. Angelovski, M. Hansli, R. Jakoby TU Darmstadt, Darmstadt, Germany

Abstract

For the European XFEL, new energy beam position monitors (EBPM) based on planar transmission lines where designed for energy measurements in the dispersive section of bunch compressor chicanes. The EBPM consists of transversely mounted stripline pickups in a rectangular beam pipe section and a signal detection scheme which measures the phases of the pulses at the ends of the pickup [1]. It allows simultaneous measurements of the beam energy and arrival-time. The EBPM needs a high dynamic range over the sensor length of 183 mm and high resolution of less than 20μm. Both, the dynamic range and the resolution depend on the operation frequency. Due to phase ambiguity, a low frequency is required for the high dynamic range whereas a high frequency is needed for the high resolution.

This paper presents the development of a RF readout electronic based on a modified six-port discriminator as a low-cost alternative to the readout electronics based on the MTCA.4 platform for the EBPM [2]. Based on the six-port, the beam position can be determined by means of the phase difference between the received signals from both ends of the transmission line pickup.

The six-port discriminator is a linear passive component, first developed in the 70's for accurate measurements of complex reflection coefficients in microwave network analysis [3]. It typically consists of two hybrid couplers and two power dividers or one Wilkinson power divider and three -3dB hybrid couplers. For the measurement of the difference of two signals excited from a single source one of the hybrid coupler can be omitted. The advantage of the six port is the fact that accurate phase measurements can be performed at microwave and millimeter wave frequencies only by amplitude measurements. This paper shows the principle of operation, developed prototype, and first test results.

INTRODUCTION

The rapid increase of computational power in the last decades made various possibilities of digital measurements available. As a result of this development well developed analog measurement techniques are only of minor importance today. For some applications, there is a more simple solution in the analog domain that is worth to be considered. This paper evaluates whether phase difference measurements are realizable using a analog six-port reflectometer circuit and determines the achievable phase resolution.

The six-port reflectometer, first mentioned in publications in the 1970's by Engen [3], never became commonly spread although many possible application fields exist. Application fields are amongst others measurement devices , communication receivers or sensors in automotive radar systems. This diversity comes from the relatively simple circuit design and the ability to scale the six-port circuit to almost any frequency [4]. The name already implies that the device has six connections whereof two are input ports and four are output ports. The superposition of the two input signals is internally phase shifted in the reflectometer. As a result four different powers at the outputs can be measured and further processed. Phase shifts can be realized by different types of couplers which makes the six-port reflectometer a relatively large but completely passive circuit structure.

One advantage of the six-port reflectometer is the direct application in the RF frequency range. Many applications like the MTCA.4 platform use signals in the RF range and down-convert them to an intermediate frequency for processing purposes [2]. In contrast the six-port reflectometer only needs one ADC for every output which is twice as many as a common receiver structure with I/Q-circuit has. A drawback using a reflectometer is the necessity of narrow bandpass filters for the RF signals, that can be easier realized at intermediate frequencies.

COPLANAR WAVEGUIDE ENERGY BEAM POSITION MONITOR

The operation of the European XFEL will require multiple special diagnostic tools to study the properties of the electron bunch. For the longitudinal properties Energy Beam Position Monitors (EBPMs) are utilized at three different locations along the European XFEL LINAC. Here the EBPM consists of two transversely mounted striplines and signal detection system, which measures the phases of the pulses emerging from both ends of the pickup in the dispersive section of a bunch compressor chicane [5]. The bunch energy can be determined from the phase differences that are directly proportional to the beam position by the formalism of the bunch compressor [6]. The principle of operation is visualized in Fig. 1 that shows a realized EBPM utilized with transversely mounted open coaxial lines in FLASH. The phase difference between the measured phases on the left and right side is direct proportional to the bunch position. The measurement resolution is defined by the minimum detectable phase-difference between both pulses. The phase of the pulse is defined by the phase constant of the transmission line. Without any distortions on the transmission line the phase constant is directly proportional to the fre-

* The authors would like to thank the CST AG for providing the CST Software Package.

† penirschke@imp.tu-darmstadt.de

ISBN 978-3-95450-141-0

NSLS-II RF BEAM POSITION MONITOR COMMISSIONING UPDATE

Joseph Mead#, Anthony Caracappa, Weixing Cheng, Christopher Danneil, Joseph DeLong, Al DellaPenna, Kiman Ha, Bernard Kosciuk, Marshall Maggipinto, Danny Padrazo, Boris Podobedov, Om Singh, Yuke Tian, Kurt Vetter
NSLS-II, Brookhaven National Laboratory, Upton, NY 11973, USA

Abstract

The National Synchrotron Light Source II (NSLS-II) is a third generation light source currently in the commissioning stage at Brookhaven National Laboratory. The project includes a highly optimized, ultra-low emittance, 3GeV electron storage ring, linac pre-injector and full energy booster synchrotron. Successful commissioning of the booster began in November 2012, followed by the ongoing commissioning of the NSLS-II 3GeV electron storage ring which began in March 2014. With those particles first injected came a value realization of the in-house developed RF Beam Position Monitor (RF BPM). The RF BPM system was envisioned and undertaken to meet or exceed the demanding applications of a third generation light source. This internal R&D project has since matured to become a fully realized diagnostic system with over 250 modules currently operational. Initial BPM performance and applications will be discussed.

INTRODUCTION

NSLS-II, a 3 GeV ultra-low emittance third generation light source, currently in the commissioning stage of construction at Brookhaven National Laboratory [1,2]. It includes a 200MeV LINAC, LINAC to Booster (LtB) transfer line, 200MeV to 3GeV Booster, Booster to storage ring (BtS) transfer line and 3GeV storage ring [3,4]. Injector commissioning was conducted from Nov 2013 to Feb 2014 and 3GeV ramped beam was established in the booster at the end of 2013. Storage ring commissioning began in March 2014 and 25mA of stored beam was achieved by May 2014. After a 2 month shutdown to install the super-conducting RF cavity, commissioning resumed at the end of Jun 2014 for a few weeks and the goal of 50mA of stored beam was achieved by mid July 2014. Commissioning is expected to resume in October of 2014. The NSLS-II storage ring is equipped with 180 RF BPMs (2 per each multipole girder, 3 multipole girders per ring cell) plus a number of "specialized" BPMs, 4 in injection straight, and (eventually) two or more per every ID straight.

BPM ELECTRONICS OVERVIEW

The NSLS-II RF BPMs incorporate the latest technology available in the RF, Digital, and Software domains. A single design has been achieved that strives to meet all NSLS-II operational requirements for all the injection components as well as the storage ring. During the linac and then booster commissioning BPMs performed very well, easily meeting the corresponding specifications. However, it is the storage ring performance specs, especially the resolution and long term drift that impose the strictest requirements [5]. The architecture of the rf bpm electronics has been carefully conceived to provide robust design with substantial flexibility to serve as a platform for other systems.

The rf bpm electronics system consist of 1) a chassis, housing an analog front-end (AFE), digital front-end (DFE) & power supply (PS) modules, shown in Fig. 1; and 2) a pilot tone combiner (PTC) module mounted in the tunnel near rf buttons, shown in Fig. 2.

Figure 1: NSLS-II RF bpm electronics chassis.

The AFE topology is based on band-pass sampling architecture which subsamples the 500MHz impulse response of the SAW band-pass filter at ~117MHz. The response of the filter produced for a single bunch results in an impulse of approximately 30 samples or ~300ns in length. Coherent timing is derived from an external 378 KHz revolution clock via differential CML. An analog phase-locked loop is used to synchronize VCXO ADC clock synthesizer [7,8]. The received revolution clock is transmitted to the DFE to serve as a time reference for the DSP engine.

The DFE is responsible for all DSP of the button signals and communication of the results with the control system. The DFE is based on a Xilinx Virtex-6 Field Programmable Gate Array (FPGA). The fixed-point DSP engine calculates TbT position based on a single-bin DFT algorithm. The FOFB 10KHz data and 10Hz slow acquisition data are derived directly from the TbT calculation.

The bpm system is parametrically configured for single-pass, booster or storage ring. The digital signal processing (DSP) architecture is also generic; all three operational modes use the same firmware.

*Work supported by DOE contract No: DE-AC02-98CH10886.
#mead@bnl.gov

ISBN 978-3-95450-141-0

STATUS OF THE SIRIUS RF BPM ELECTRONICS

S. R. Marques#, R. A. Baron, G. B. M. Bruno, F. H. Cardoso, L. A. Martins, J. L. Brito Neto, L. M. Russo, D. O. Tavares, LNLS, Campinas, SP, Brazil

Abstract

A modular and open-source RF BPM electronics based on the PICMG® MicroTCA.4 and ANSI/VITA 57.1 FMC standards is being developed to be used at Sirius, a 3 GeV low emittance synchrotron light source under construction in Brazil. This paper reports on the latest development advances focusing on bench tests of the second version of the RF front-end and evaluation of the electronics with beam at SPEAR3 (SSRL/SLAC). The interface of the BPM electronics with the orbit feedback system is also discussed.

INTRODUCTION

Sirius is a new 3 GeV synchrotron light source under construction in Brazil [1], targeting a 0.28 nm.rad natural emittance. Storage ring commissioning has been rescheduled and should occur in the 1st semester of 2018.

The Sirius RF BPM electronics is composed of a low noise RF front-end (RFFE) which process the signals coming from RF BPM pick-ups and a typical FPGA-based digital receiver employing direct RF sampling technique and further difference-over-sum algorithm to extract beam position information. The RFFE uses the "switching electrode" principle [2] to compensate for low frequency drifts originated in the RF chains. Instead of multiplexing the four BPM signals into one single RF chain or using a full four-by-four crossbar switching scheme [3], only diagonal BPM antenna signals are switched, as seen in [4].

The system is modular, based on proven industrial standards and is being developed as an open source project. Information on technical choices and hardware and software structures were detailed in the past [5, 6, 7].

During the last year, effort to consolidate the hardware has been done by the development team. Open questions about performance limitations were solved and a new spin of the RFFE and ADC boards was concluded.

Bench tests revealed the current BPM electronics performance status. In addition, beam tests performed at SPEAR3 (SSRL/SLAC) showed the operation of the electronics with realistic broadband BPM signals.

The MicroTCA.4-based digital platform, composed of CPU and FPGA boards for readouts and fast orbit feedback (FOFB) implementation, is currently being integrated and will be detailed in future work.

SYSTEM REQUIREMENTS

BPM electronics specification is mainly driven by beam orbit stability requirements. At Sirius, the most stringent electron beam stability requirement is given by the vertical beam size at the center of the longer straight sections, namely 1.94 µm. In order to achieve position stability better than 5% of this beam size within a 0.1 Hz to 1 kHz bandwidth, the corresponding vertical plane RMS orbit disturbance shall be lesser than 97 nm. By allocating half of this budget to orbit distortions exclusively caused by electronic and mechanical BPM noise, which is transferred to the beam through the fast orbit feedback loop, a 69 nm RMS orbit disturbance specification was derived for BPMs.

Simulations with the Sirius storage ring show that a factor of 0.72 translates uncorrelated RMS noise in all storage ring BPMs to an RMS orbit disturbance at each of the long straight sections. Hence the 69 nm orbit distortion specification derived above can be relaxed to 95 nm when translated to noise on the BPMs. From this resulting number, a 50 nm upper bound RMS BPM noise is reserved for mechanical vibration on the BPM stands, thus leaving 80 nm RMS noise (or resolution) budget for the BPM electronics itself.

Table 1 summarizes BPM electronics resolution specification alongside more general requirements for the Sirius's BPM system. The numbers have been reviewed since last publications [6].

Table 1: Requirements of Sirius RF BPM Electronics

Parameter	Value
Resolution (RMS) @ 0.1 Hz to 1 kHz	< 80 nm
Resolution (RMS) @ turn-by-turn full bandwidth	< 3 µm
1 hour position stability (RMS)	< 0.14 µm
1 week stability (RMS)	< 5 µm
Beam current dependence (decay mode)	< 1 µm
Beam current dependence (top-up mode)	< 0.14 µm
Filling pattern dependence	< 5 µm
First-turn resolution (RMS)	< 0.5 mm
Horizontal/Vertical plane coupling	< 1%

HARDWARE IMPROVEMENTS

The tests carried out in 2013 [6] were performed with the first versions of the RFFE and ADC boards, which has partially fulfilled specifications. The following sections describe the modifications made since then.

RF Front-End Board

The RFFE v1 board concept consisted of an analog front-end in which several calibration and compensation schemes (channels switching, pilot tone and temperature control) were available for comparative tests [8]. The RFFE v2 was designed as a cost-optimized board in

#sergio@lnls.br

ISBN 978-3-95450-141-0

A SQUID-BASED BEAM CURRENT MONITOR FOR FAIR / CRYRING*

R. Geithner #, Helmholtz-Institut Jena, Germany & Friedrich-Schiller-Universität Jena, Germany
T. Stöhlker, Helmholtz-Institut Jena, Germany & Friedrich-Schiller-Universität Jena, Germany &
Helmholtzzentrum für Schwerionenforschung, Darmstadt, Germany
R. Neubert, P. Seidel, Friedrich-Schiller-Universität Jena, Germany
F. Kurian, H. Reeg, M. Schwickert,
GSI Helmholtzzentrum für Schwerionenforschung, Darmstadt, Germany

Abstract

A SQUID-based beam current monitor was developed for the upcoming FAIR-Project, providing a non-destructive online monitoring of the beam currents in the nA-range. The Cryogenic Current Comparator (CCC) was optimized for lowest possible noise-limited current resolution together with a high system bandwidth. This CCC should be installed in the CRYRING facility, working as a test bench for FAIR. In this contribution we present results of the completed CCC for FAIR/CRYRING and also arrangements that have been done for the installation of the CCC at CRYRING, regarding the cryostat design.

INTRODUCTION

The high energy beam transport lines (HEBT) at FAIR require a non-intercepting, absolute and precise detection of high brightness, high intensity primary ion beams as well as low intensities of rare isotope beams. The expected beam currents in these beam lines are in the range of few nA up to several µA for continuous as well as bunched beams [1]. This requires a detector with a low detection threshold, a high resolution, and as well as high bandwidth from DC to several kHz.

A superconducting pick-up coil and SQUID system are the main components of a Cryogenic Current Comparator. Superconducting pick-up coils allow the detection of DC magnetic fields created by continuous beams without applying modulation techniques. A SQUID acting as current sensor for the pick-up coil enables the detection of lowest currents. Therewith the CCC optimally fulfils the requirements for the FAIR beam parameters.

DESIGN AND WORKING PRINCIPLE

The CCC [2, 3, 4] consists of a meander-shaped niobium shielding, a toroidal niobium pick-up coil with a ferromagnetic core, a toroidal matching transformer also including a ferromagnetic core and an LTS SQUID with the appropriate SQUID-electronics (see Fig. 1).

* Work supported by GSI Helmholtzzentrum für Schwerionenforschung, Darmstadt, Germany and Helmholtz-Institut Jena, Germany

rene.geithner@uni-jena.de

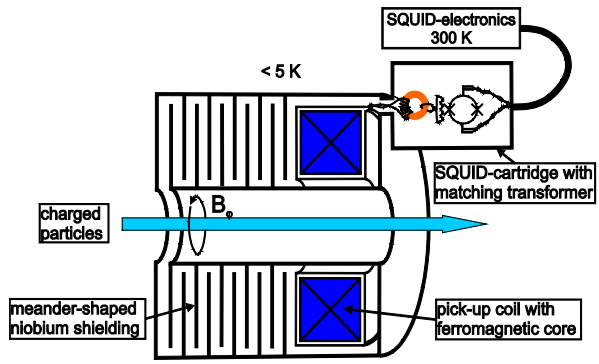

Figure 1: Circuit diagram of the CCC.

The azimuthal magnetic field of the particle beam passes the ceramic gap in the beam line and is guided to the pick-up coil by the meander-shaped shielding whereby all other external magnetic field components are strongly attenuated [3, 5].

Sensitivity Optimization

The total intrinsic noise of the entire CCC is composed by the intrinsic noise of the SQUID itself and its electronics, as well as the magnetization noise of the embedded coils. The spectral current density $\langle I^2 \rangle$ of a coil coupled to the input coil L_I of a SQUID at a temperature T can be calculated with the Fluctuation-Dissipation-Theorem (FDT) and the measured frequency-dependent serial inductance $L_S(\nu)$, respectively. With the serial resistance $R_S(\nu)$ in the equivalent circuit diagram of a real coil, $R_S(\nu)$ represents the total losses [6, 7]:

$$\langle I^2 \rangle = 4k_B T \int \frac{R_S(\nu)}{\left(2\pi\nu\left(L_I + L_S(\nu)\right)\right)^2 + \left(R_S(\nu)\right)^2} \qquad (1)$$

As one can see in Equation (1) the current noise decreases if $L_S(\nu)$ is as high as possible and, secondly, $R_S(\nu)$ remains low over the whole frequency range.

From preliminary investigations [5, 7] we found that the nanocrystalline ferromagnetic material Nanoperm [8] shows very satisfying results matching our requirements. A single-turn Niobium toroidal pick-up coil was electron-beam welded around a Nanoperm M764 core. This pick-up coil has an outer diameter 260 mm, an inner diameter of 205 mm and a width of 97 mm.

A possibility for optimization of the overall current sensitivity of the SQUID detector is the use of a matching transformer with optimized winding ratio and core material.

ISBN 978-3-95450-141-0

MEASUREMENT OF BEAM LOSSES AT THE AUSTRALIAN SYNCHROTRON

E. Nebot del Busto, M. Kastriotou, CERN, Geneva, Switzerland; University of Liverpool, Liverpool, UK,
M. J. Boland, ASCo, Clayton; The University of Melbourne,
P. D. Jackson, University of Adelaide, Adelaide,
R. P. Rasool, The University of Melbourne, Australia
E. B. Holzer. CERN, Geneva, Switzerland,
J. Schmidt, Albert-Ludwig Universitaet Freiburg, Freiburg, Germany
C. P. Welsch Cockcroft Institute, Warrington, Cheshire; University of Liverpool, Liverpool, UK

Abstract

The unprecedented requirements that new machines are setting on their diagnostic systems is leading to the development of new generation of devices with large dynamic range, sensitivity and time resolution. Beam loss detection is particularly challenging due to the large extension of new facilities that need to be covered with localized detector. Candidates to mitigate this problem consist of systems in which the sensitive part of the radiation detectors can be extended over long distance of beam lines. In this document we study the feasibility of a BLM system based on optical f ber as an active detector for an electron storage ring. The Australian Synchrotron (AS) comprises a 216 m ring that stores electrons up to 3 GeV. The Accelerator has recently claimed the world record ultra low transverse emittance (below pm rad) and its surroundings are rich in synchrotron radiation. Therefore, the AS provides beam conditions very similar to those expected in the CLIC/ILC damping rings. A qualitative benchmark of beam losses in a damping ring-like environment is presented here. A wide range of beam loss rates can be achieved by modifying three beam parameters strongly correlated to the beam lifetime: bunch charge (with a variation range between 1 uA and 10 mA), horizontal/vertical coupling and of dynamic aperture. The controlled beam losses are observed by means of the Cherenkov light produced in a 365 $\mu\ m$ core Silica f ber. The output light is coupled to different type of photo sensors namely: Metal Semiconductor Metal (MSM), Multi Pixel Photon Counters (MPPCs), standard PhotoMulTiplier (PMT) tubes, Avalanche PhotoDiodes (APD) and PIN diodes. A detailed comparison of the sensitivities and time resolution obtained with the different read-outs are discussed in this contribution.

THE AUSTRALIAN SYNCHROTRON AS A DAMPING RING TEST FACILITY

The compact linear collider CLIC [1] foresees two 20 km main linacs accelerating electrons and positrons up to 3 TeV. In order to provide an instantaneous luminosity on the order of $5 \cdot 10^{+34}\ cm^{-2}\ s^{-1}$, the beam spot at the interaction point shall reach unprecedentedly low nanometer sizes. This is only achievable with ultra low emittance beams at the entrance of the linac that account for the large contribution coming from the particle sources, particularly the positron source, and the emittance growth budget up to the interaction point. The Damping Rings (DR) designed to cool down the CLIC beams [2] comprise a 412 m ring built of FODO cells in the long straight section and Theoretical Minimum Emittance (TME) in the arcs with the use of two half cells for dispersion suppression. Superconducting wigglers aim to decrease the damping times to the 2 ms level, values well below the 20 ms imposed by the 50 Hz CLIC repetition rate. This constrains the requirements on time response of beam instrumentation. Moreover, the low foreseen longitudinal emittances triggers a set of single bunch collective effects typically not observable in electron machines. Hence, the measurement of beam parameters on a bunch by bunch basis imposes a tighter requirement on the time resolution of the instrumentation systems.

The Australian Synchrotron (AS) [3] is a third generation light source consisting of a 100 MeV linac, a 100 MeV to 3 GeV Booster and a 3 GeV Storage Ring (SR). The SR comprises 14 Double Bend Achromat (DBA) cells where a 200 mA beam is circulated in pulses of approximately 600 ns when f lling 300 out of the 360 buckets. As it is shown in table 1, there are many similarities between the parameters of the AS and the CLIC damping rings. In particular, the AS has recently measured vertical normalized emittances comparable to those expected in CLIC. Moreover, the synchrotron provides good f exibility to modify some of its nominal parameters to approach those of the DR. For instance it is feasible to reduce the pulse length to CLIC like values by keeping nominal beam charge. Hence, this facility provides a great opportunity to test and develop instrumentation targeting requirements for the DR of the future collider.

OPTICAL FIBER BEAM LOSS MONITORS: THE EXPERIMENTAL SETUP

The use of optical f bers, once restricted to waveguides for the transport of information, is increasingly being adopted in the beam instrumentation f eld. The light generated inside an optical f ber due to the crossing of ionizing radiation may be used as a tool for Beam Loss Monitoring

ISBN 978-3-95450-141-0

A TOROID BASED BUNCH CHARGE MONITOR SYSTEM WITH MACHINE PROTECTION FEATURES FOR FLASH AND XFEL

M. Werner*, T. Lensch, J. Lund-Nielsen, R. Neumann, D. Noelle, N. Wentowski,
DESY, Hamburg, Germany

Abstract

For the superconducting linear accelerators FLASH and XFEL, a new toroid based charge measurement system has been designed as a standard diagnostic tool. It is also a sensor for the bunch charge stabilization feedback and for machine protection. The system is based on MTCA.4 technology and will offer a high dynamic range and high sensitivity. The machine protection features will cover recognition of poor transmission between adjacent toroid sensors, bunch pattern consistency checks, and protection of the beam dumps. The concept, an overview of the algorithms, and the implementation will be described. A summary of first operation experience at FLASH will be presented.

INTRODUCTION

In the FLASH accelerator, toroid based Beam Current Monitor (BCM) systems have been used from the beginning.

Other requirements came up when the beam current increased due to the increasing number of bunches per RF pulse and a redundancy for the beam loss monitors (BLMs) became mandatory. Namely, pairs of beam current signals had to be applied for transmission interlocks. At this time, a "Toroid Protection System" (TPS) was developed [1] to detect beam losses by analysing the amplitude differences within toroid pairs. The TPS used the existing analogue toroid signals as inputs, and in addition to the control system digitizers, separate ADC and FPGA based data processing chains were implemented in a dedicated box. Connections to the Control System were avoided so as to insure maximum safety against unintended changes.

When beam current stability became an issue, a beam current feedback system was developed [2], again with the analogue toroid signals as inputs. It was realized by still another FPGA based system, providing a fast digital fibre connection to the injector.

Another application of the toroid signals was the beam loading compensation for the cavities realized by the LLRF group [3].

For the new European XFEL [4], it was desired to implement all this functionality into a single system, creating even more requirements.

For the x-ray cameras in the experiments, a "veto" signal is required to disable data acquisition for improper bunches.

For the protection of sensitive components, it is necessary to check that the integrated bunch charge is below a certain limit and that the bunches are directed to the correct branches of the beamline.

Since the exchange of a damaged beam dump is a major issue, dedicated protection algorithms were desired for the different kinds of dumps (three main beam dumps and two diagnostic dumps at the XFEL).

Another important topic is the ability of the system to work (with some restrictions) if the control signals from the machine timing system (clock, trigger) are not available or corrupted. In this case, the system should still measure the bunch charge (with relaxed precision) and the safety must be maintained.

*Matthias.Werner@desy.de

HARDWARE SETUP

The hardware consists of the toroid device, the front-end device (signal combiner, filter, amplifier) and the MTCA backend (see Fig. 1). The front-end device will be contained in a box together with a test pulse generator close to the toroid, the backend will be composed of a dedicated Rear Transition Module (RTM) in combination with a commercial 10 channel 125 MSPS digitizer board (Struck SIS8300-L2), housed in an MTCA.4 crate. The digitizer board will communicate over the MTCA backplane with the CPU in the crate, and the CPU will be part of the control system within an Ethernet network. The digitizer modules offer an FPGA for fast data processing and direct communication over Gigabit links with a speed of up to 6.25 Gb/s with other modules.

High Dynamic Range Feature

For the possibility of extending the dynamic range to a value above the dynamic range of the ADC, a two-channel arrangement will be implemented with two amplifiers of different gains, see Fig. 1. The high gain amplifier will provide improved SNR for low signals [5]; the low gain amplifier is still in the linear range for high amplitudes.

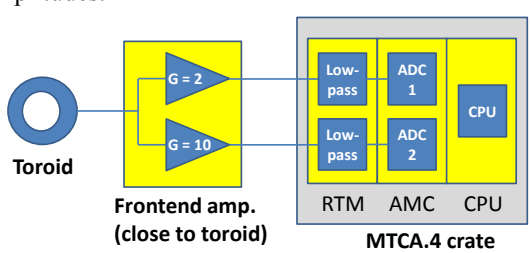

Figure 1: Hardware setup with high dynamic range feature (simplified).

OPERATION MODES

The system offers two basic operation modes: a self-triggered mode and a timing-triggered mode.

ISBN 978-3-95450-141-0

UPGRADE OF THE FAST BEAM INTENSITY MEASUREMENT SYSTEM FOR THE CERN PS COMPLEX

D. Belohrad*, J.C. Allica, M. Andersen, W. Andreazza, G. Favre,
N. Favre, L. Jensen, F. Lenardon, W. Vollenberg, CERN, Geneva, Switzerland

Abstract

The CERN Proton Synchrotron complex (CPS) has been operational for over 50 years. During this time the Fast Beam Current Transformers (FBCTs) have only been repaired when they ceased to function, or individually modified to cope with new requests. This strategy resulted in a large variation of designs, making their maintenance difficult and limiting the precision with which comparisons could be made between transformers for the measurement of beam intensity transmission. During the first long shutdown of the CERN LHC and its injectors (LS1) these systems have undergone a major consolidation, with detectors and acquisition electronics upgraded to provide a uniform measurement system throughout the PS complex. This paper discusses the solutions used and analyses the first beam measurement results.

INTRODUCTION

The CERN PS complex is a chain of accelerators producing accelerated beams for the Super Proton Synchrotron (SPS), and subsequently for the Large Hadron Collider (LHC). In addition it delivers a wide range of particle beams to the secondary experimental areas.

The complex (Fig. 2) is comprised of the proton and the heavy ion linear accelerators ($LINAC_{II}$, $LINAC_{III}$), the Proton Synchrotron Booster (PSB) and the Proton Synchrotron (PS). Transfer lines transport the beams from the CPS accelerators to the appropriate targets (e.g. the On-Line Isotope Mass Separator ISOLDE), to the experimental areas (e.g. the Antiproton Decelerator AD), and for further acceleration to the SPS.

The transfer of particle beams nearly always involves some beam loss which has to be minimised. The beam transfer efficiency is calculated from the measured beam intensities at various locations in the accelerator complex. The beam intensity measurement in the CPS transfer lines is provided by the FBCTs, as shown in Fig. 2.

The FBCTs were installed during the construction of the accelerator chain and they were only repaired or modified when they ceased to function, or to cope with new requests. This resulted in a large variety of FBCTs designs, acquisition techniques and calibration methods. This state of affairs limited the accuracy of the transfer efficiency estimate to no better than 5%.

In 2010 the CPS FBCTs were equipped with new acquisition systems. The originally used analogue integrators were replaced by digital signal processing [1]. This improved the calculation accuracy of the transfer efficiency to ≈ 2%. A further improvement could be only achieved by upgrading the FBCTs and their calibration methods.

During LS1, a major upgrade of the FBCTs for the PS complex was therefore performed. Twelve out of 21 old FBCTs measuring the bunched beams at the PSB extraction were replaced (the red boxes in Fig 2), with the remaining FBCTs foreseen to be upgraded during LS2 in 2018.

MECHANICAL CONSTRUCTION

The FBCT Toroid

The major issue associated with the design of the new FBCT for the PS complex was the choice of the measurement toroid. From past experience, it was known that the currently used toroids provided a beam position dependent signal which adversely affected the absolute accuracy of the intensity measurement. A collaboration was set up with Bergoz Instrumentation to design a toroid mitigating this problem. An iterative design process resulted in the fabrication of a new type of large-aperture toroid (210 mm) having an imperceptible beam position dependence. To achieve this the toroid's measurement bandwidth had to be lowered from the usual GHz range to 120 MHz. This 120 MHz bandwidth is sufficient to provide the bunch to bunch transfer line beam intensity measurements (droop ≈0.25%/μs) for the beams with bunch spacing greater than 100 ns. Using this toroid to measure the beams with bunch spacing of 25 ns (the LHC beams) requires further signal treatment

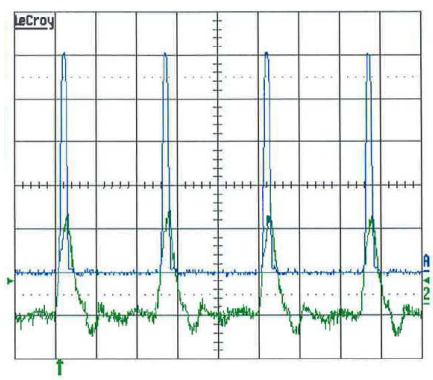

Figure 1: The impulse response of the 1:40 FBCT toroid. The blue trace shows the input signal fed through an antenna. The green trace shows the toroid output signal. The time scale is 10 ns/div.

* david.belohrad@cern.ch

ISBN 978-3-95450-141-0

A CRYOGENIC CURRENT COMPARATOR FOR THE LOW ENERGY ANTIPROTON FACILITIES AT CERN

M. Fernandes*, The University of Liverpool, U.K. & CERN, Geneva, Switzerland
J. Tan, CERN, Geneva, Switzerland,
C.P. Welsch, Cockcroft Institute & The University of Liverpool, Liverpool, U.K.

Abstract

Several laboratories have shown the potential of using Superconducting QUantum Interference Device (SQUID) magnetometers together with superconductor magnetic shields to measure beam current intensities in the sub-micro-Ampere regime. CERN, in collaboration with GSI, Jena university and Helmholtz Institute Jena, is currently working on developing an improved version of such a current monitor for the Antiproton Decelerator (AD) and Extra Low ENergy Antiproton (ELENA) rings at CERN, aiming for better current resolution and overall system availability. This contribution will present the current design, including theoretical estimation of the current resolution; stability limits of SQUID systems and adaptation of the coupling circuit to the AD beam parameters; the analysis of thermal and mechanical cryostat modes.

LOW-INTENSITY BEAMS CURRENT MEASUREMENT

Low-intensity charged particle beams present a considerable challenge for existing beam current diagnostics [1], this is particularly significant for coasting beams with average current below 1 μA which is the minimum resolution of DC Current Transformers. Other monitors, such as AC Current Transformers or Schottky monitors are able to measure low-intensity beam currents, but neither can simultaneously provide an absolute measurement, with a high current and time resolution, which is at the same time independent of the beam profile, trajectory and energy.

At CERN's low-energy antiproton decelerators, the AD and the ELENA (currently under construction) rings, circulate both bunched and coasting beams of antiprotons with average currents ranging from 300 nA to 12 μA [2]. Having a current measurement with the above mentioned characteristics would benefit the machine operation and optimization.

To meet these requirements, a low-temperature SQUID-based Cryogenic Current Comparator (CCC) is currently under development. Similar devices have already been developed for electrical metrology [3], and later for beam current measurements in particle accelerator [4]. The current, a collaboration between CERN, GSI, Jena University and Helmholtz Institute Jena aims to make this a fully operational device, with a prototype foreseen to be tested in the AD machine at CERN in 2015.

*Funded by the European Unions Seventh Framework Programme for research, technological development and demonstration under grant agreement no 289485.

The main design specifications for the monitor are: beam current resolution < 10 nA; and measurement bandwidth > 1 kHz.

Overview of the Functioning Principle of the CCC

The CCC (see Fig. 1) works by measuring the magnetic field induced by the particle beam current. This field is concentrated in a high-permeability ferromagnetic pickup core, from which it is coupled into a Superconducting QUantum Interference Device (SQUID). These are highly sensitive magnetic flux sensors that permit sensing the weak fields created by the beam. A superconducting magnetic shield structure around the pickup-core, as described in [4, 5], renders the coupled magnetic field nearly independent of the beam position and makes the system practically immune to external magnetic field perturbations.

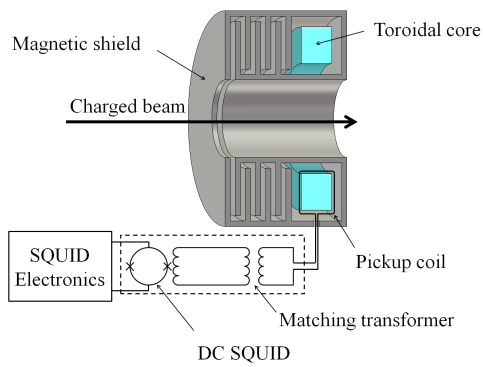

Figure 1: Schematic of the CCC.

CCC MONITOR DIMENSIONING

The AD CCC will in a first phase use a superconducting shield and pickup core developed by Jena University and Helmholtz Institute Jena. This core has a single turn inductance $L_P = 104\,\mu$H, while the SQUID device [1] has the following parameters, input coil self-inductance $L_i = 1\,\mu$H and mutual inductance $M_i = 3.3\,\phi_0/\mu$A [2].

Coupling Circuit and Resolution

The circuit such as the one depicted in Fig. 2 will be used to couple the beam current signal into the SQUID. The transfer function of this circuit, defined as the change

[1] Manufactured by Magnicon GmbH.

[2] $\phi_0 = 2.0678 \times 10^{-15}$ Wb is the magnetic flux quantum which is the unit commonly used for magnetic flux when dealing with SQUID systems.

ISBN 978-3-95450-141-0

SIMULATION OF THE BEAM DUMP FOR A HIGH INTENSITY ELECTRON GUN

A. Jeff , CERN, Geneva, Switzerland & University of Liverpool, U.K.
S. Doebert, T. Lefèvre, CERN, Geneva, Switzerland
K. Pepitone, CEA, Le Barp, France

Abstract

The CLIC Drive Beam is a high-intensity pulsed electron beam. A test facility for the Drive Beam electron gun will soon be commissioned at CERN. In this contribution we outline the design of a beam dump / Faraday cup capable of resisting the beam's thermal load.

The test facility will operate initially up to 140 keV. At such low energies, the electrons are absorbed very close to the surface of the dump, leading to a large energy deposition density in this thin layer. In order not to damage the dump, the beam must be spread over a large surface. For this reason, a small-angled cone has been chosen. Simulations using geant4 have been performed to estimate the distribution of energy deposition in the dump. The heat transport both within the electron pulse and between pulses has been modelled using finite element methods to check the resistance of the dump at high repetition rates. In addition, the possibility of using a moveable dump to measure the beam profile and emittance is discussed.

INTRODUCTION

The Compact Linear Collider (CLIC) will use a novel two-beam acceleration scheme to collide electrons and positrons at up to 3TeV [1]. Energy is extracted from a very intense, lower energy Drive Beam (DB) using specially designed RF structures, and transferred to the less intense, high energy colliding beams.

In order to prove the feasibility of generating such an intense electron beam, a new test stand will be installed at CERN during 2015. Only the electron gun is to be tested, so the beam will remain unbunched and at low energy. Some relevant parameters are shown in table 1.

Table 1: Relevant Parameters for the CLIC Drive Beam Test Stand

Beam Energy	100 – 140 keV
Beam Current	4.2 A
Pulse Length	150 μs
Pulse Population	4 x 10^{15} e^-
Pulse Energy	88 J
Repetition Frequency	1 - 50 Hz
Beam Emittance	12 mm mrad
Beam size at dump	σ=2.5mm

The high beam current means that stopping the beam is not trivial. Low energy electron beams are stopped very quickly in almost all materials, so the density of energy deposition close to the surface is extremely high. Thus, a beam dump must be designed to safely absorb the beam by distributing the heat load over as large a surface as possible.

In addition, the test stand aims to demonstrate the stability of the electron gun. Both the current flatness during a pulse and the charge variation between pulses should be below 0.1%. Thus, the beam current must be measured with a resolution at least at this level.

BEAM DUMP DESIGN

The depth profiles for energy deposition by the electron gun beam in various materials are shown in figure 1, assuming that the beam is incident normal to the surface. Since the energy is deposited in a very thin layer, the energy deposition density, and therefore the temperature rise, will be very large. The integrated peak energy deposition during the pulse is shown in figure 2 for the most promising materials. It can be seen that for the nominal current, no material can survive the full pulse. Thus, the beam must be incident at a shallow angle in order to dilute the beam.

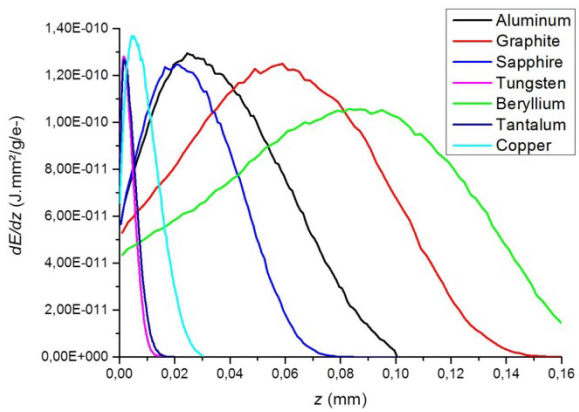

Figure 1: Energy deposition profiles for a 140 keV electron beam incident normal to the surface, for various materials, normalised to the material density.

ISBN 978-3-95450-141-0

A NEW INTEGRATING CURRENT TRANSFORMER FOR THE LHC

D. Belohrad, M. Krupa, P. Odier, L. Søby, CERN, Geneva, Switzerland
J. Bergoz, F. Stulle, Bergoz Instrumentation, Saint-Genis-Pouilly, France

Abstract

The existing Fast Beam Current Transformers of the LHC have been shown to exhibit both bunch length and bunch position dependency. A new Integrating Current Transformers (ICT) has therefore been developed in collaboration with Bergoz Instrumentation to address these issues. As goals a 0.1%/mm beam position dependency and 0.1% bunch length dependency were specified, along with a bandwidth of 100 MHz. This paper describes the principles of ICT operation and presents the laboratory measurement results obtained with the first prototypes at CERN.

INTRODUCTION

The present fast beam intensity measurements for the LHC rings are provided by four Fast Beam Current Transformers (FBCT), two per ring. They measure both bunch-by-bunch and total turn-by-turn beam intensities. The LHC proton bunch intensity varies from 5e9 to 1.3e11 charges with nominal bunch spacing of 25ns and up to 2808 bunches. While operational needs are covered by the present performance of the LHC FBCTs, the needs of the LHC experiments in terms of knowledge of the absolute bunch to bunch population during luminosity calibration puts more stringent demands on the intensity measurements accuracy. In addition to providing bunch by bunch intensity information, the FBCTs also send signals to the Machine Protection System (MPS), via the LHC Fast Beam Current Change Monitor (FBCCM). The FBCCM [1] calculates the magnitude of the beam intensity signal provided by the FBCT, looks for a change over specific time intervals, and triggers a beam dump interlock if losses exceed an energy-dependent threshold. The present FBCTs exhibit bunch-length and beam-position dependencies (Figure 1), which exceed the requirements for luminosity calibration and the LHC MPS. It was therefore decided to develop new intensity monitors with minimized bunch-length and beam-position dependency.

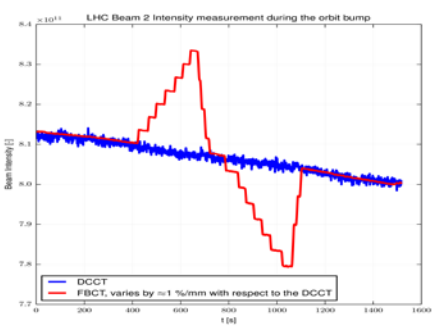

Figure 1: Beam position dependency in present LHC FBCTs with an orbit bump of ± 4mm.

PRINCIPLE OF OPERATION

The Integrating Current Transformer (ICT) and its respective read-out electronics are designed for accurate measurement of the bunch charge. To accomplish this, almost all information about the longitudinal bunch shape is sacrificed. Its working principle is based on the fact that the value of a pulse's time integral is contained in the lower end of its frequency spectrum. A precise bunch charge monitor may disregard information about the longitudinal bunch shape, which is contained in the high frequency part of the spectrum. That means, its bandwidth can be a lot narrower than the pulse spectrum.

This fundamental principle can be understood from the Fourier transform of a current pulse i(t), e.g. a particle bunch:

$$I(f) = \int_{-\infty}^{+\infty} i(t)\, e^{-i\,2\pi\, f\, t}\, dt \qquad (1)$$

For f = 0 we obtain:

$$I(0) = \int_{-\infty}^{+\infty} i(t)\, dt = q \qquad (2)$$

Eq. 2 proves that the value of the time integral of a current pulse i(t), i.e. its charge q, is carried by the DC component of the pulse spectrum. The ICT exploits exactly this principle, though reality is more complicated than this idealistic description.

A passive current transformer, including the ICT, can never transmit the DC component of the spectrum. In fact, any spectral content below the lower cut-off frequency is lost. The effect in time-domain is a droop, i.e. the signal amplitude drops with a certain time constant. To obtain a proper charge value, the integration time must be shorter than this time constant. Of course this implies that the output pulse length must be shorter than the time constant; speaking in frequency-domain terms the upper cut-off frequency must be sufficiently high.

A practical limit of the low frequency cut-off for the ICT has been chosen to be 500 Hz, which at LHC is sufficiently low for the Base Line Restitution (BLR) circuit to work correctly during batch injections of up to 288 bunches spaced by 25ns. The BLR corrects for any base line drifts before bunch integration.

Even though the information about the bunch charge is contained in the very low frequency components, the bandwidth of the ICT has to be wide enough to perform bunch-by-bunch measurements. In order to fulfil this requirement the ICT output pulse must settle at a steady baseline before the monitor is excited by the next bunch. The nominal bunch spacing in the LHC is 25 ns and a safe higher cut-off frequency of a bunch charge monitor was estimated to be in the order of 100 MHz.

ISBN 978-3-95450-141-0

OPTIMIZATION OF A SHORT FARADAY CUP FOR LOW-ENERGY IONS USING NUMERICAL SIMULATIONS*

A. Sosa†, E. Bravin, E. D. Cantero, CERN, Geneva, Switzerland
C. P. Welsch, Cockcroft Institute, Warrington, Cheshire,
The University of Liverpool, Liverpool, United Kingdom

Abstract

ISOLDE, the heavy-ion facility at CERN is undergoing a major upgrade with the installation of a superconducting LINAC that will allow post-acceleration of ion beams up to 10 MeV/u. In this framework, customized beam diagnostics are being developed in order to fulfil the design requirements as well as to fit in the compact diagnostic boxes foreseen. The main detector of this system is a compact Faraday cup that will measure beam intensities in the range of 1 pA to 1 nA. In this contribution, simulation results of electrostatic fields and particle tracking are detailed for different Faraday cup prototypes taking into account the energy spectrum and angle of emission of the ion-induced secondary electrons.

INTRODUCTION

The High Intensity and Energy (HIE) upgrade of the Isotope On-Line DEvice (ISOLDE) facility at CERN aims to increase the energy and intensity of the radioactive ion beams currently available on site. From the beam energy standpoint, an increase from the present 3 MeV/u to 10 MeV/u is foreseen for ions with a mass-to-charge ratio of A/Q≤4.5. The present room-temperature LINAC (known as REX) will be replaced with a superconducting LINAC with up to six cryomodules containing a total of 32 Nb-sputtered quarter-wave resonators [1]. All beam diagnostic devices will be installed in purpose-built diagnostic boxes, located in every inter-cryomodule region and along designated points in the High Energy Beam Transfer lines (HEBTs). A total of 15 diagnostic boxes (seven in the LINAC and eight in the HEBT) are required for the complete upgrade. The number and type of diagnostic devices in each box is different depending on the location in the accelerator. Beam intensity, transverse beam profile and beam position can be measured at each diagnostic box location. Other devices available in some boxes include a silicon detector, sets of collimators, beam attenuators and stripping foils.

COMPACT FARADAY CUP

Faraday cups are well known devices with a simple and reliable technique for measuring absolute beam intensities, but optimizing a Faraday cup for a specific set of beam parameters, especially with low-intensity ion beams remains challenging [2]. The Faraday cup used in the current REX-ISOLDE LINAC has been redesigned into a much shorter version in order to fit in the short (58 mm long) diagnostic boxes of HIE-ISOLDE. The Faraday cup to be used in HIE-ISOLDE should be 30 mm in diameter to cover the full beam aperture (max. beam sizes in HIE-ISOLDE are 1σ=5 mm). The initial prototype (Prototype 1), shown in Fig. 1(a), is just a rescale of the original design and has a repeller ring and ground ring measuring 1.5 mm in length, and a 2.5 mm thick collector electrode, the whole enclosed in a metallic housing. The collector electrode and repeller ring of the first prototype are made of stainless steel (AISI 316L [3]), the body is made of aluminium (6082) and the insulators are made of VESPEL© SP-1 [4].

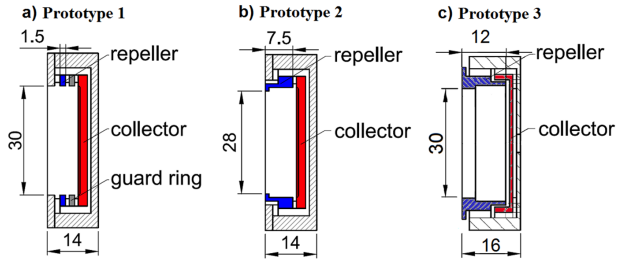

Figure 1: Schematic of the different Faraday cup prototypes developed for HIE-ISOLDE.

ELECTROSTATIC SIMULATIONS

Numerical simulations have been done in order to assess the design of the cups, analysing the electrostatic potential distribution and the secondary electron emission. CST Particle Studio [5] was used to study the electrostatic fields and track secondary electrons in these cups. When the repeller ring is biased at a given voltage, the electrostatic potential in the central axis of the Faraday cup varies according to the length and inner diameter of the repeller ring. The electrostatic potential is a maximum on the surface of the repeller ring and has a minimum value in the centre of the cup, corresponding to the beam axis.

In Fig. 2 the potential distribution for the initial HIE-ISOLDE Faraday cup prototype biased at -60 V is shown. The compact geometry of the FC results in only -5 V in the centre when the repeller ring is biased to a voltage of -60 V. As this repeller voltage is insufficient to contain

*This project has received funding from the European Union's Seventh Framework Programme for research, technological development and demonstration under grant agreement no 264330.

† alejandro.garcia.sosa@cern.ch

ISBN 978-3-95450-141-0

DOSIMETRY OF PULSED BEAMS IN PROTON THERAPY

J. Van de Walle, Y. Claereboudt, G. Krier, D. Prieels, IBA, Louvain-la-Neuve, Belgium
G. Boissonnat, J. Colin, J.-M. Fontbonne, LPC, Caen, France

Abstract

In the proton therapy system ProteusONE™ by Ion Beam Applications, the superconducting synchro-cyclotron provides intense proton pulses of 230 MeV in 10µs and with a repetition rate of 1 kHz. In these conditions, the large gap (few mm's) air-filled ionization chambers at the exit of the proton gantry suffer from recombination losses. Since these ionization chambers are crucial to control the dose delivered to the patient, these recombination losses have to quantified pulse-by-pulse. The concept of an "asymmetrical ionization chamber" has been introduced at the exit of the gantry to be able to do this.

INTRODUCTION

In order to reduce the cost of proton therapy systems, Ion Beam Applications has developed in recent years the ProteusONE™ system, which consists of a compact superconducting synchro-cyclotron (S2C2) [1] and a compact, iso-centric rotating gantry [2], which rotates 220 degrees around the patient. A layout of this gantry is shown in Figure 1. The S2C2 delivers a pulsed proton beam at 230 MeV with a repetition rate of 1kHz and a pulse duration of 10 µs. The concept of pulsed beam is ideally suited for Pencil Beam Scanning (PBS), a technique by which the tumor volume is scanned with a fixed size (typically 3 mm) proton beam with varying energy and intensity per irradiated voxel. The proton charge in each pulse in PBS treatments has to be measured with high precision.

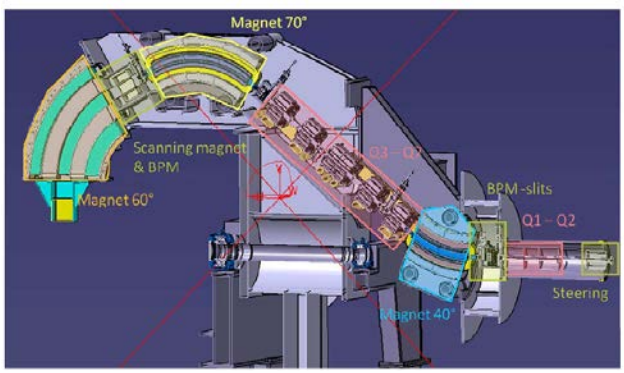

Figure 1 : Layout of the ProteusONE™ compact gantry. The ionization chambers are located at the exit of gantry, after the 60° magnet.

Air-filled ionization chambers (IC's) are used at the exit of the rotating gantry, with a typical surface area of 200x300 mm^2 and gap sizes of a few mm. This large surface area is needed to cover the full irradiation area. The charge collection times in these IC's is typically a few hundred µs, much more than the proton pulse of 10 µs. Recombination losses of the created electron-ion pairs in the air-filled IC's cannot be avoided with the pulse intensities needed to irradiate a tumor volume, which can go as high as 10 pC/pulse. To ensure an accurate measurement of the pulse intensity in PBS, these recombination losses have to be quantified on a pulse-by-pulse base. The concept of an "asymmetric ionization chamber" (AIC) has been introduced at the gantry exit to enable this.

THE ASYMMETRIC IONIZATION CHAMBER (AIC)

A schematic layout of the asymmetric ionization chamber (AIC) is shown in Figure 2. It consists of two ionization chambers with different gap sizes, d_1 and d_2. One such ionization chamber is in itself divided in two parts : the grounding foil is placed in between two high voltage foils and the detector signal is read from this grounding foil. For recombination calculations, only a distance d_1 has to be considered, the gain of ICi (i=1,2) in Figure 2 is given by :

$$G_i = \frac{2 d_i S \rho}{W}$$

where S is the stopping power of protons for a given energy, ρ is the density of air in the IC and W is the ionization potential of air. The measured charge in ICi ($Q_{det,i}$) is given by :

$$Q_{det,i} = G_i Q_{IN} \varepsilon_i$$

where Q_{IN} is the incident proton charge, which is the quantity of interest and ε_i is the efficiency of ICi, which is determined by recombination losses in the air-filled IC. The ratio of the two measured charges ($Q_{det,}$) is given by

$$R = \frac{Q_{det,1}}{Q_{det,2}} = \frac{d_1}{d_2}\frac{\varepsilon_1}{\varepsilon_2} = R_0 \frac{\varepsilon_1}{\varepsilon_2} \quad (1)$$

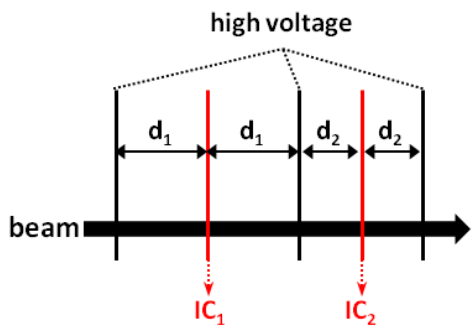

Figure 2 : Schematic layout of the asymmetric ionization chamber. It consists of two ionization chambers with different gap sizes (d1 and d2).

ISBN 978-3-95450-141-0

INTRODUCTION TO THE TEST RESULT OF TURBO-ICT IN PAL-ITF*

H. Choi†, M.S. Chae, S.-J. Park, H.-S. Kang
Department of Accelerator, PAL-XFEL, Pohang, Korea

Abstract

Pohang Accelerator Laboratory (PAL) built a PAL-ITF (Injector Test Facility) at the end of 2012 to successfully complete PAL-XFEL (X-ray Free Electron Laser) in 2015. The PAL-ITF is equipped with various kinds of diagnostic equipment to produce high-quality electron bunches. The three main parameters that an injection testing facility should measure are charge, energy and emittance. Although integrated current transformer (ICT) and Faraday Cup were installed to measure beam charge, the noise generated in a klystron modulator not only interrupted accurate measurement but prevented low charges under tens of pC from being measured. Due to the changes in the overall voltage level of ITF, integration of ICT measured value failed to maintain perfect accuracy in terms of methodology (measured value continuously changed by +/- 5pC). Accordingly, to solve the noise problems and accurately measure the quantity of electron beam charge, Turbo-ICT was installed. [1] This paper focuses on the processes and test result of electric bunch charge quantity measurements using Turbo-ICT.

PURPOSE OF BCM INSTALLATION

As shown in Figure 1, A charge generator or a device which accelerates or uses charge has its absolute amount of charge. In other words, knowing the amount of charge which a charge generator produces and a charge accelerator or a charge-based device uses would allow users to check where charge loss occurs and to decide the final amount of charge they will be supplied with. The coulomb (C) is a unit of electrical charge and is also the derived unit of International System (Système International d'unités, SI) of Unit. A bunch charge monitor (BCM) shall be installed after it is calibrated to measure the absolute amount of charge.

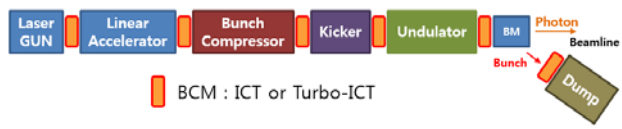

Figure 1: Locations where BCM installation is required.

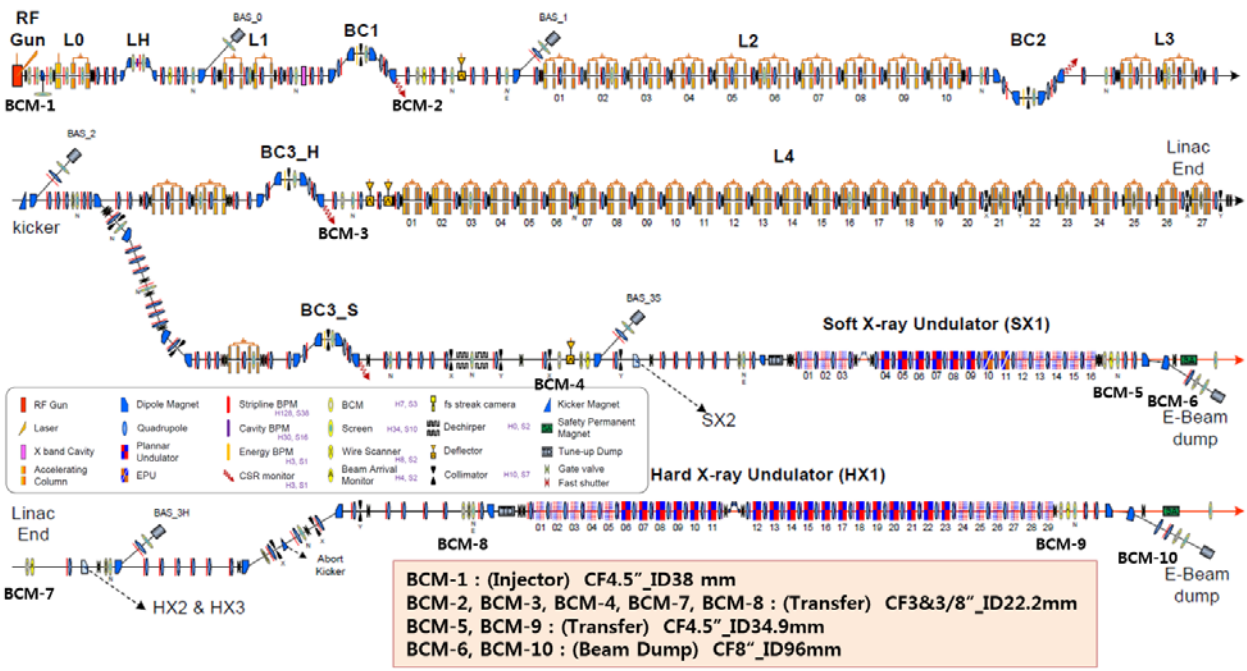

Figure 2: Locations of BCM installed on PAL-XFEL.

As shown in Figure 2, Ten BCMs are installed on PAL-XFEL: Laser gun generator, the rear part of a bunch compressor with the possibility of charge loss, Kicker-based bunch branch part, the end of a linear accelerator (Starting point of an undulator), the end of an undulator, and beam dump part. A BCM is a calibrated device for measuring the absolute amount of charge. Sometimes Stripline-BPM Sum Value and Cavity-BPM Reference Value are complementarily used to measure the amount

* Work supported by the Ministry of Science, ICT and Future Planning (MSIP) in Korea.
† choihyo@postech.ac.kr

ISBN 978-3-95450-141-0

RANGE VERIFICATION SYSTEM USING SCINTILLATOR AND CCD CAMERA SYSTEM

N. Saotome#, Y. Hara, K. Mizushima, R. Tansho, Y. Saraya, T. Furukawa, T. Shirai, and K. Noda,
National Institute of Radiological Sciences, Chiba, Japan

Abstract

For the daily QA of the energy scanning delivery, quick and easy range verification system is required. In this work, we have developed range verification system using scintillator and CCD (charge-coupled device) camera. From the comparison of the several methods, edge detection method is best for range detection. Accuracy of range detection for the system is within the 0.2 mm. Reproducibility of the range is within 0.1 mm. Our range check system has shown to be capable of quick and easy range verification with sufficient accuracy.

INTRODUCTION

At NIRS, three-dimensional irradiation with carbon-ion pencil-beam scanning has been performed from 2011 [1]. We have been commissioning the irradiation method that employs more than 200 multiple beam energies supplied by synchrotron instead of the energy degraders [2]. Since carbon ion deposits most of their energy in the last final millimeters of their trajectory, the accuracy of the beam energy/range is required for carbon ion treatment especially for using scanning method. ICRU78 recommend checking the range constancy for daily QA. Recommended relative accuracy of range measurements is less than 0.5 mm [3].

In the current daily QA at NIRS, Few-points depth dose measurement using ionization chamber is employed for range verification. It takes about 1 minute for a measurement of one energy beam. In order to apply the range check for multiple energy beams, quick and easy range verification system is required. The purpose of this work is to develop range verification system using scintillator and CCD camera and to estimate the accuracy of the range verification using the system.

MATERIALS AND METHODS

Experimental Setup

The scintillator and CCD system is shown in Fig. 1. The system is consisted of a scintillator block, CCD camera, and opaque (black) box. Light distribution is detected by CCD camera through a mirror. The optical path length between the scintillator and lens is 400 mm. The system was placed on the treatment couch. The center of the scintillator was placed at isocenter.

A EJ-200 plastic scintillator block was selected for pure tranceparent block, similar density with human body, and matching wavelength of maximum emission for CCD camera. The size of cylindrical scintillator block was 200 mm diameter ×100 mm thickness. For shading the light from the treatment room, the scintillator was wrapped by light blocking sheet. The CCD camera (Type BU-41L, 1360x1024 pixels, Bitran Corp., Japan) was installed on the light-shielding house. The spatial-resolution of the system is 0.2 mm/pixels.

Image Acquisition

All measurement was performed at fixed vertical beam line. Total 131 energy carbon beams with mini ridge filter that were in the range from 56 to 332 MeV/n were measured sequentially. The data acquisition of the CCD camera was synchronized with irradiation. We measured pencil-beam having intensities between 8×10^7 and 1.6×10^8 particles per second. Measurement time is 0.1 sec for all energy.

Image Processing

Measured two-dimensional images were processed by in-house program developed by c++. The workflow of image processing is shown in Fig. 2. After the background correction and median filter, projection on one-dimensional axis is performed.

Range Scaling Factor

The common reference point of range is distal 80% of the dose distribution. However the system measures the range not with the dose distribution but with the light distribution. Archambault *et al*. concluded that the distal 80% minimized discrepancies between expected and measured ranges for proton beam [4]. Fukushima *et al*. also use 80% and obtained great result [5]. To our knowledge, there is no published report of clinical carbon range measurement with scintillator. In order to select the best reference point on a light distribution, the authors compared two range detection methods using several parameters.

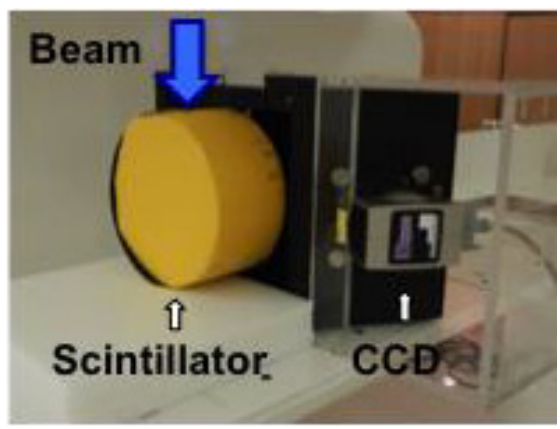

Figure 1: Layout of the scintillator and CCD system.

#naosao@nirs.go.jp

ISBN 978-3-95450-141-0

A DIAGNOSTICS OF ION BEAM FROM 28GHz ELECTRON CYCLOTRON RESONANCE ION SOURCE

Jung-Woo Ok# ,Byoung Seob Lee ,Seyong Choi ,JungBae Bahng, Jin Yong Park, Seong Jun Kim, Jonggi Hong, Chang Seouk Shin, Jang-Hee Yoon, Mi-Sook Won,
Korea Basic Science Institute(KBSI), Busan, Korea

Abstract

A neutron radiography facility utilizing a 28 GHz superconducting electron cyclotron resonance (ECR) ion source and a heavy ion accelerator is now under construction at Korea Basic Science Institute (KSBI). In order to generate a proper energy distribution of neutron, a lithium ion beam is considered. It will be accelerated up to the energy of 2.7 MeV/u by using a radio frequency quadrupole (RFQ) and drift tube linear (DTL) accelerator. The 28 GHz superconducting ECR ion source, which is the state of the art of an ion beam injector, has been built to produce the lithium ion beam. The ion beam of 12 keV/u would be extracted to low energy beam transport (LEBT) system, which is comprised of several types of electromagnets to focus and deliver the beam, effectively. After transporting an ion beam through LEBT, RFQ once accelerates the ion beam from 12 to 500 keV/u. Finally, we can achieve the final beam energy after accelerating at the DTL. Before the ion beam is delivered to accelerator, the requirements should be satisfied to confirm the status of beam. For this, we developed the instruments in the diagnostic chamber in the middle of LEBT system to observe the beam dynamics. An analyzing electromagnet, slits, wire scanners and faraday cup will be used to perform a diagnosis of ion beam characteristics. We will present and discuss the experimental results of ion beam profile and the current after selecting are required charge state.

INTRODUCTION

For the research facility based on accelerator technology at KBSI, a 28 GHz superconducting ECR ion source, a LEBT system, and linear accelerators are under development [1]. Recently, ECR plasma ignition was successfully implemented using 28 GHz superconducting ECR ion source [2]. Since then, a ion beam extraction from ECR ion source is scheduled to experiment. In the ion beam extraction test, the beam properties will be measured using various diagnostic technique. Figure 1 shows the layout of the KBSI Accelerator research facility. The first application to the KBSI accelerator research facility is neutron radiography. For the generation of neutron, the inverse kinematics technique is considered. In this method, a lithium beam accelerated up to 2.7 MeV/u will impact the hydrogen gas target, then the neutron will be generated. In order to accelerate lithium beam, radiofrequency quadrupole and drift tube linear accelerator will be used.

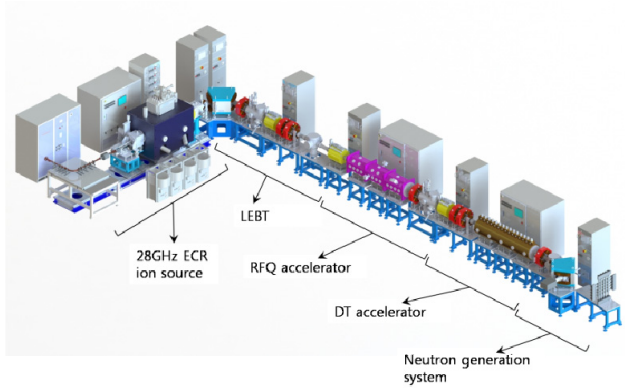

Figure 1: The layout of the KBSI accelerator research facility.

Also, for the beam transmission from ECR ion source to RFQ a LEBT system is designed. The schematic of LEBT system is showed in Figure 2.

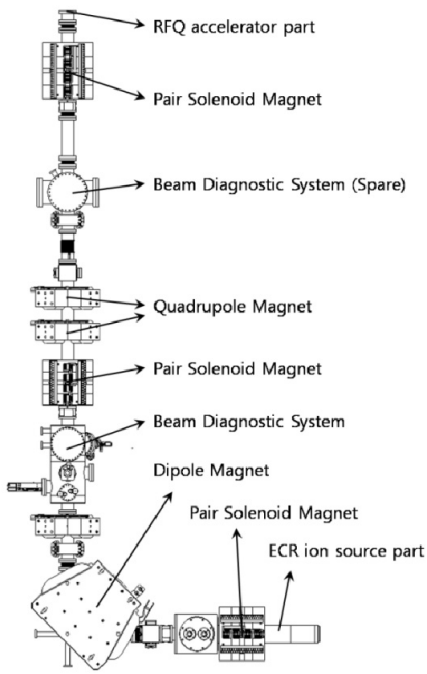

Figure 2: The schematic of LEBT system.

#jwo @kbsi.re.kr

ISBN 978-3-95450-141-0

THE STATUS OF BEAM DIAGNOSTICS FOR THE HIE-ISOLDE LINAC AT CERN*

E. D. Cantero†, W. Andreazza, E. Bravin, A. Sosa
CERN, Geneva, Switzerland

Abstract

The HIE-ISOLDE project aims at upgrading the CERN ISOLDE radioactive ion beam facility for higher beam intensities and higher beam energies. New beam diagnostic devices have to be developed as part of this upgrade, in particular for the measurement of intensity, energy, transverse and longitudinal profiles, and transverse emittance. The beam energy ranges from 300 keV/u to 10 MeV/u and beam intensities are between 1 pA and 1 nA. Faraday cups will be used for the measurement of the beam intensity while silicon detectors will be used for the energy and longitudinal profile measurements. The transverse profiles will be measured by moving a V-shaped slit in front of a Faraday cup and the beam position will be calculated from the profiles. The transverse emittance can be measured using the existing REX-ISOLDE slit and grid system, or by the combined use of two scanning slits and a Faraday cup. The final design of the mentioned devices will be presented in this contribution, including the results of the experimental validation tests performed on prototypes during the last two years.

INTRODUCTION

A major upgrade of the on-line isotope mass separator facility ISOLDE at CERN is taking place since 2010 under the HIE-ISOLDE project [1]. The technical challenges for beam diagnostics include the development of new instruments for low-intensity ion beams with energies up to 10 MeV/u. Moreover, in the inter-cryomodules regions of the superconducting LINAC, the longitudinal space available for beam instrumentation is very limited (58 mm) due to restrictions coming from the beam optics design. As a consequence all the devices need to be designed with a very compact geometry.

The diagnostic requirements of HIE-ISOLDE beams are [2]:

- Beam intensity measurements: an absolute accuracy of 1 %, for pilot beams of stable ions such as oxygen and neon, with intensities in the range of 10 pA to 1 nA.
- Transverse profile and position measurements: an accuracy of 10 % in the beam size measurement and of $\pm$ 0.1 mm in the beam position determination. Beam sizes are in the range of 1 to 5 mm (1 σ_{rms}).
- Longitudinal profile measurements: the energy spread and bunch length should be measured with resolutions of $<$1 % (2σ) and $<$100 ps respectively.
- Transverse emittance meter: a target accuracy of $\pm$ 20 % is expected, for beam currents up to 1 nA.

DIAGNOSTIC BOXES

The installation of stage 1 for the HIE-ISOLDE LINAC includes two cryomodules with five cavities each. It is scheduled to deliver the first beams for physics in October 2015. More cryomodules will be added at a later stage, increasing the beam quality and final energy per nucleon.

A total of five short Diagnostic Boxes (DBs) and eight long DBs will be required for the accelerator and its two transfer lines to the experiments. Their location is schematically presented in Fig. 1. The short DBs are located between the cryomodules and have a very compact design in the longitudinal direction compared to the long DBs. All DBs include a Faraday Cup (FC) and a scanning slit that will be used for the beam intensity and transverse profile measurements. All DBs are also equipped with circular and/or vertical collimators for beam cleaning purposes, with four DBs including carbon stripping foils to allow modification of the beam charge state. Two DBs will contain silicon (Si) detectors for longitudinal beam profile measurements.

In Fig. 2 a cutaway drawing of a short DB is presented. The modular, six port design of the box allows up to five instruments or devices to be attached, with one port reserved for the vacuum system. A FC, scanning slit and collimator blade with four circular collimators are shown, with the remaining extra ports available for the installation of a Si detector and a blade with stripping foils. The main tank is an octagonal-shaped box machined from a single block of 316L stainless steel, with a beam pipe aperture of 40 mm. Top and bottom faces are integrated with alignment and support devices respectively.

The position of the various devices is controlled by means of linear actuators driven by stepper motors. As the precision on the positioning of the scanning slit is critical for the accuracy of the transverse beam profiles measurements, a special mechanism was designed for that movement, which includes a robust guiding system with two rods. The plane of movement of the scanning slit, collimators and stripping foils is located slightly upstream of the plane of movement of the FC and the Si detector, al-

*The research leading to these results has received funding from the European Commission under the FP7-PEOPLE-2010-ITN project CATHI (Marie Curie Actions - ITN). Grant agreement No. PITN-GA-2010-264330.
† esteban.cantero@cern.ch

ISBN 978-3-95450-141-0

STATUS OF THE STANDARD DIAGNOSTIC SYSTEMS OF THE EUROPEAN XFEL

D. Nölle for the E-XFEL Diagnostic Team, DESY, Hamburg, Germany

Abstract

The European XFEL, an X-ray free-electron-laser user facility based on a 17.5 GeV superconducting linac, is currently under construction close to the DESY site at Hamburg. DESY is in charge of the construction of the accelerator. This contribution will report the status of the standard diagnostic systems of this facility. The design phase has finished for all main systems; most of the components are in production or are already produced. This paper will show details of the main systems, their installation issues and will report on the further time schedule. Furthermore, the preparation of the commissioning of the RF gun with beam will be presented.

INTRODUCTION

The European XFEL facility (E-XFEL) is currently under construction in Hamburg [1]. The facility is organized and will be operated as an international company with shares hold by the countries participating in the construction, either with cash or in-kind contributions. DESY acting for the German Ministry of Science and Education is the biggest shareholder of this company, and is taking the leadership of the Accelerator Construction Consortium, that is in charge to build and operate the accelerator.

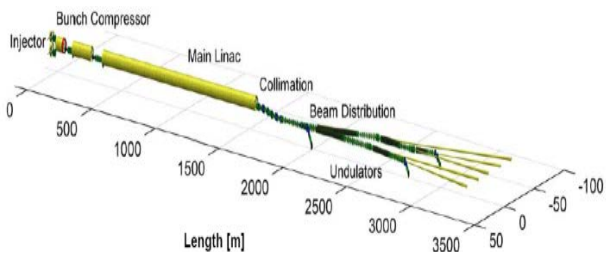

Figure 1: Layout of E-XFEL.

The core of the facility is the 17.5 GeV superconducting accelerator, able to supply up to 5 undulator systems with electrons simultaneously. The corresponding 5 photon beamlines transport the radiation into an experimental hall, with a distance of about 3.3 km to the gun (Fig.1). The overall facility will be installed in a tunnel system at an underground level between 28 and 7 m. Due to superconducting RF the machine is able to run long RF pulses at a repetition rate of 10 Hz each containing up to 2700 bunches. The beam distribution within the bunch train is enabled by a fast kicker septum system, capable to split the long bunch train into two sub-trains. Arbitrary bunch patterns out of this sub-trains are possible using a beam dump kicker to kick out bunches not requested by the users. This scheme was very recently successfully demonstrated at the FLASH facility with the first lasing of the FLASH2 beamline, simultaneously while FLASH was continuing to provide long bunch SASE delivery for users [2]. The electron beams are then send to X-ray SASE Undulator systems of up to 200 m length to produce intense photon pulses down to 0.5 Å at mJ level. One of the two main beamlines provides 2 SASE undulators for hard and soft X-ray production in a sequence, the other starts with only a hard X-ray system and has the option to be upgraded either with spontaneous radiation sources for hard X-rays or with soft X-ray laser sources. Due to the installation in a tunnel, all the electronics has to be installed close to the machine. Racks shielded by about 20 cm of heavy concrete will be used.

The project is now entering the installation phase [3]. All underground buildings are completed and the technical infrastructure is almost finished. The first of the 101 accelerator modules is installed in the tunnel. About 10 more are currently under test at the Accelerator Module Test Facility (AMTF) at DESY. Newly assembled modules are coming almost every week from the assembly facility at CEA, Saclay. Concerning the installation of the warm beamline, the assembly of the girder systems for the injector and bunch compressor sections has started.

The project time schedule foresees, to continue commissioning of the RF gun system this fall, to complete the injector and start commissioning in late spring 2015, the main accelerator should be completed about 1 year later, so that commissioning can start in summer 2016. The goal to get first photons is set to the end of 2016 and first lasing to spring 2017. First user operation with some relaxed operation parameters should be possible about 1 year after the start of the commissioning.

The work package of standard diagnostics is taking care of all systems needed as standard tools in bigger quantities, as described in Table 1. More special monitors, usually for longitudinal diagnostics are within the scope of the special diagnostics work package. In the standard diagnostics work package, the systems are either provided by DESY as the main contributor or as projects with in-kind contributions from PSI, CEA or IHEP Protvino. PSI, CEA and DESY are providing the BPM system as a collaborative effort [4], and IHEP has delivered the mechanical components of the BLM system [5]. In general the status of the different systems is advanced and within the current global time schedule. Therefore, also the diagnostics have entered the installation phase, details

ISBN 978-3-95450-141-0

ALGORITHM TO IMPROVE THE BETA-FUNCTION MEASUREMENT AND ITS EVALUATION IN STORAGE RINGS LATTICES

A.C. García B.*, Universidad Nacional de Colombia, Bogotá, Colombia

Abstract

In any beam-line, one of the basic measurements in the beam-diagnostics is the measurement of the Beta-Function. This can be achieved, in Storage Rings, by taking the tune change obtained when varying the intensity of quadrupoles, or by using the matrix response to fit the corresponding parameters, or by shaking the beam to obtain a betatron motion. In accelerators like the LHC, the Beta-Function measurement is done from the Phase Advance Measurement using the Transfer Matrix. In this paper, a study of a new algorithm or numerically approximation for this measurement is presented, as well as the results of simulations on LHC and CLIC lattices. The deduced and implemented algorithm takes into account a fraction of the both transverse planes measurements. A random (uniform) deviation of the MAD-X phase values is taken to obtain the measured values and then used to study the Beta Function measurement for a different amount of orbits. There are observed cases where the improvement is close to 30% and 50% compare to a traditional method.

INTRODUCTION

The measurement of the Beta Function in accelerators is an important task during the commissioning, because all the properties of the focusing structure are described and calculated using the Twiss functions or Courant-Snyder parameters. For any beam-line, in colliders and transport lines of high energy particles, the horizontal and vertical Beta functions determine the transverse beam sizes that change around the storage ring. During the beam-diagnostics, to know the twiss parameters implies, in general, to be able to determine all the dynamic beam parameters. [1],[2],[3].

One of the techniques used to measure the beta-function in colliders or storage rings, is by using the tune shift induced by quadrupole excitation, this consists in *to detect the shift in the betatron tune as the strength of an individual quadrupole magnet is varied*, pag. 17 on [4]. The theoretical expression is obtained from the trace of the corresponding transport matrix for the entire ring multiplied by the perturbation matrix, which represents the effect of the gradient change. In the simplified final expression, each transverse beta function depends on the tune change in the corresponding plane, the gradient change, and constants. A specific variation of this method, using two symmetric placed quadrupoles, allows measuring the beta-function at the interaction point in colliders [5].

* acgarciab@unal.edu.co,ac.garcia412@uniandes.edu.co

A second method is given by shaking the beam to obtain a betatron motion. The betatron oscillations are measured with multi-turn beam position monitors (BPMs) and *the beta function is calculated from the betatron phase advance between three adjacent BPMs*, pag. 21 on [4]. Theoretically, from the Transfer Matrix on element to element, one can obtain a set of two independent equations with the information of three BPMs. The final expression involves the matrix elements depending of the designed optics and the $\tan$ value of the measured phase advances. The α measure can also be obtained with this procedure.

Additionally, having a betatron motion in the beam-line allows measuring the Beta Function using an interpolation of the twiss functions between the BPMs. In this way, the matrix response is used to fit the corresponding parameters assuming that the magnetic gradients in the transfer line model between the monitors 1 and 3 are perfect. The theoretical expressions are similar of what was discussed for the previous method. Computers are used to calculate the fit, where the measured variables are normalized to create a symmetric covariance matrix to be solved by least squares. The final expression depends on the measured phase advances and Beta Function in the BPMs. [1], [5].

Another simple method is to measure the orbit change when a steering corrector magnet is excited at different values. This method use a BPM nearby the corrector, and it is where the beta function value is obtained. The theory involves the expression of the closed-orbit distortion in the presence of a single dipole kick. The final beta function measurement if obtained from the $\tan$ value of the tune, the closed-orbit distortion, the steering error value and constants. [4], [2].

For instance, in the LHC the measurement of the Beta Function for the relativistic beams is performed by using the second method described above, eq. (1) in [6].

THEORY

During the measurement of any optical quantity in an accelerator, it is expected to have a correspondence between the model scenario and what is measured at the machine. Using the transfer matrix for the beta function measurement, it is found that the following should be fullfilment

$$\cot \Delta\Phi_{1,2}^{ide} - \cot \Delta\Phi_{1,3}^{ide} = \cot \Delta\Phi_{1,2}^{meas} - \cot \Delta\Phi_{1,3}^{meas} \quad (1)$$

where, Φ are the phase advance in the transverse plane, at the three different longitudinal positions 1, 2 and 3; the labels *ide* and *meas* stand for the 'ideal' and 'measured' scenarios, respectively. The discrepancies among the model phase advances, or 'ideal' values, and the ob-

ISBN 978-3-95450-141-0

ERROR ANALYSIS FOR PEPPERPOT EMITTANCE MEASUREMENTS REDUX: CORRELATED PHASE SPACES*

S. Lidia[#†], K. Murphy[‡], Lawrence Berkeley National Laboratory, Berkeley, CA, USA

Abstract

Recently, Jolly *et al.* presented an analysis of the rms emittance measurement errors from a first principles approach [1]. Their approach demonstrated the propagation of errors in the single-plane rms emittance determination from several instrument and beam related sources. We have extended the analysis of error propagation and estimation to the fully correlated 4-D phase space emittances obtained from pepperpot measurements. We present the calculation of the variances using a Cholesky decomposition approach. Pepperpot data from recent experiments on the NDCX-II beamline are described, and estimates of the emittances and measurement errors for the 4-D as well as the projected rms emittances in this coupled system are presented.

INTRODUCTION

Jolly, *et al.* [1] recently published an analysis of the data acquisition and uncertainty estimation of beam emittances derived from pepperpot measurements. There, they presented a first principles methodology for propagating measurement errors into the nonlinear functions of position, angle and beamlet intensity that are typically used to calculate the horizontal or vertical root-mean-squared (rms) emittances. Estimates of measurement errors were discussed that stemmed from the practical implementation of the pepperpot measurement system. The dominant sources of measurement error were the spacing of holes in the pepperpot mask; the camera resolution and drift distance between mask and scintillation screen; and beam intensity variation and background intensity noise levels. Additional errors in the measurement system were not included, so that the estimates of uncertainty represent lower limits on the total error.

A pepperpot image and its correlations to the background mask can be utilized to estimate the complete 4-D phase space emittance by analyzing all 10 independent correlation terms in the 4-D beam matrix. In this paper we extend Jolly, *et al.*'s formalism to estimate the uncertainty of the 4-D emittance and related quantities that include the correlations between the horizontal and vertical phase spaces. The results of this analysis can be applied to coupled systems found in solenoidal or skew quadrupole transport lattices, and beams that carry significant canonical angular momentum.

*This work was supported by the Director, Office of Science, Office of Fusion Energy Sciences, of the U.S. Department of Energy under Contract No. DE-AC02-05CH11231.
#lidia@frib.msu.edu
†Presently at Facility for Rare Isotope Beams, Michigan State University.
‡Presently at Department of Physics, University of Chicago.

CORRELATED PHASE SPACES

The 4-D beam covariance matrix is constructed from the density-weighted, rms product averages of the beam distribution,

$$\Sigma_4 = \begin{pmatrix} \langle xx \rangle & \langle xx' \rangle & \langle xy \rangle & \langle xy' \rangle \\ \langle xx' \rangle & \langle x'x' \rangle & \langle x'y \rangle & \langle x'y' \rangle \\ \langle xy \rangle & \langle x'y \rangle & \langle yy \rangle & \langle yy' \rangle \\ \langle xy' \rangle & \langle x'y' \rangle & \langle yy' \rangle & \langle y'y' \rangle \end{pmatrix} \quad (1)$$

Here, the individual product terms are defined by

$$\langle fg \rangle = \frac{\sum_i \rho_i f_i g_i}{\sum_i \rho_i}, \quad (2)$$

where the index i labels the coordinates in the 4-D space of {x, x', y, y'} and ρ is the local beam density in that space. We assume that the 10 unique terms are linearly-independent of each other.

The 4-D beam matrix can be expressed in the symmetric, block form that reveals the separate, Cartesian sub-spaces as well as the correlation between them,

$$\Sigma_4 = \begin{pmatrix} \Sigma_x & C \\ C^T & \Sigma_y \end{pmatrix}. \quad (3)$$

We note that other representations [2,3] are also used.

The definitions of rms emittances follow from the determinants of the beam matrix. The determinant and emittance of the 2-D Cartesian (sub-)phase space has the well known definition:

$$\det \Sigma_x = |\Sigma_x| = \langle xx \rangle \langle x'x' \rangle - \langle xx' \rangle^2 = \tilde{\varepsilon}_x^2 . \quad (4)$$

We carry the definition to the 4-D space and 4-D emittance:

$$\tilde{\varepsilon}_4^2 = |\Sigma_4|. \quad (5)$$

To compare the equivalent beam quality defined by the 4-D emittance measure, we define an equivalent 2-D emittance

$$\tilde{\varepsilon}_2^2 = |\Sigma_2| = |\Sigma_4|^{1/2}. \quad (6)$$

For transversely uncoupled phase spaces, $\Sigma_4 = \begin{pmatrix} \Sigma_x & 0 \\ 0 & \Sigma_y \end{pmatrix}$, and $|\Sigma_2| = |\Sigma_x||\Sigma_y|$ so that $\tilde{\varepsilon}_2^2 = \tilde{\varepsilon}_x \tilde{\varepsilon}_y$.

We utilize the equivalent 2-D rms emittance measure, $\tilde{\varepsilon}_2$, as a basis of comparison with the single-plane rms

ISBN 978-3-95450-141-0

PRECISE DIGITAL INTEGRATION OF FAST ANALOGUE SIGNALS USING A 12-BIT OSCILLOSCOPE

M. Krupa*, M. Gasior, CERN, Geneva, Switzerland

Abstract

An accurate laboratory characterization of beam intensity monitors requires a reliable integration of analogue signals simulating beam pulses. This poses particular difficulties when a high integration resolution is necessary for short pulses. However, the recent availability of fast 12-bit oscilloscopes now makes it possible to perform precise digital integration of nanosecond pulses using such instruments. This paper describes the methods and results of laboratory charge measurements performed at CERN using a 12-bit oscilloscope with 1 GHz analogue bandwidth and 2.5 GS/s sampling.

INTRODUCTION

The study of using 12-bit oscilloscopes as a high resolution digitiser has been considered for a laboratory characterisation of new intensity monitors currently being developed for the LHC restart in 2015 [1]. These monitors, operating according to the current transformer principle, provide signals proportional to the beam current, which are then integrated to measure the charge of each bunch of the circulating beam. Precise laboratory characterisation of such monitors requires time domain integration of nanosecond pulses with a relative accuracy better than 1 %. This value is considered as the accuracy limit of the analogue integrators used operationally at the LHC. The analogue integrators will be soon replaced by a digital system being developed, however, which was not yet available for the laboratory measurements of the new intensity monitors.

The study and results presented in this paper are based on oscilloscope measurements of nanosecond pulses from a fast pulse generator. Therefore, they are believed to be applicable also in domains outside the beam intensity instrumentation, where measurements of precise integrals of short pulses are necessary.

SET-UP AND OSCILOSCOPE

The pulses simulating beam bunches in the measurements discussed in this paper were generated by a custom-made avalanche generator delivering pulses with the amplitude of about 25 V and 0.5 ns full-width-at-half-maximum (FWHM) [2]. The pulse rise and fall times are about 0.3 ns, resulting in the frequency spectrum with the high cut-off around 1 GHz. Longer pulses required in the measurements were obtained by stretching the 0.5 ns pulses using a few commercial low pass filters. This way the total integral of the pulses, simulating the charge of a circulating bunch, was kept constant while the shapes of the pulses varied significantly.

* michal.krupa@cern.ch

All data studied in this paper were acquired using a 12-bit oscilloscope with 1 GHz analogue bandwidth and running in the Random Interleaved Sampling (RIS) mode with the maximal equivalent sampling rate of 125 GS/s. In this mode, the final waveform is a result of many acquisitions performed with the sampling clock having a random phase with respect to a common stable trigger. The phase of the sampling clock is measured with respect to the trigger for each acquisition by a precise time-to-digital converter (TDC), with the time resolution defining the RIS equivalent sampling rate. Then all RIS records are aligned according to the precise sampling phase measurement obtained from the TDC. The RIS scheme requires that the sampled signal is repetitive and the trigger event is identical for every acquisition, both of which conditions were satisfied in the discussed measurements. The RIS mode allowed increasing the oscilloscope native time resolution of 400 ps by a factor of 50, which was very important for the presented studies.

Before using the oscilloscope for signal integration, the instrument itself was characterised. In order to check the oscilloscope channel symmetry, the same signal from the avalanche generator was successively injected into each of the four inputs and sampled in the same manner. The absence of RF signal splitters in the measurement setup removed sources of systematic errors introduced by the inevitable asymmetry of the splitters themselves, which is at the percent level even for precise devices.

Results of the symmetry measurement are shown in Fig. 1. The measurements were performed consecutively assuring stable measurement conditions. The acquired samples were manually aligned on the time axis to

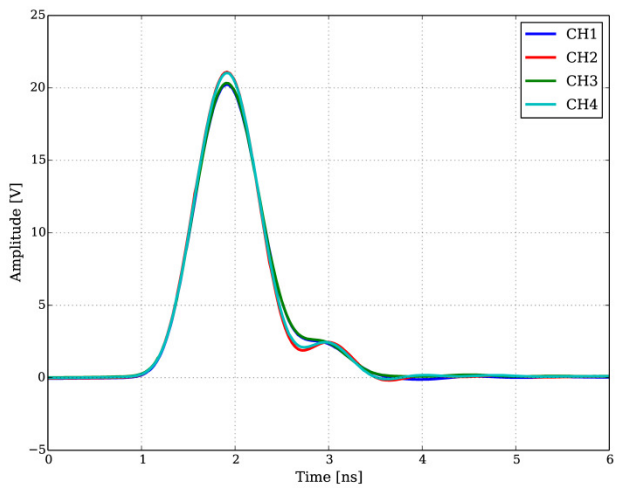

Figure 1: Measurement of the oscilloscope channel symmetry. Same input signal was acquired with consecutive channels.

ISBN 978-3-95450-141-0

FAST TRANSVERSE PHASE SPACE MEASUREMENT SYSTEM FOR GUNLAB – A COMPACT TEST FACILITY FOR SRF PHOTOINJECTORS

J. Völker*, T. Kamps, HZB, Berlin, Germany

Abstract

Superconducting radiofrequency photo electron injectors (SRF guns) are promising electron sources for the next generation of electron linear accelerators. The energy recovery linac (ERL) bERLinPro will employ a 1.5 cell 1.3 GHz SRF gun cavity with normal conducting high quantum efficiency photocathode to produce a 100mA CW electron beam with high brightness. We are currently working on a compact test beamline (GunLab) to investigate the phase space of the extracted electron beam and to optimize the drive laser as well RF parameters. The motivation for GunLab is to decouple the SRF gun development from the ERL development. The goal is to measure not only the complete 6 dimensional phase space of the extracted and accelerated bunches but also to investigate dark current and beam halo. In this paper we will discuss unique features of GunLab for the phase space measurements.

MOTIVATION

GunLab is an independent and optimized beamline to characterize electron guns and to investigate different phase space measurement systems for space charge dominated electron bunches at low energies up to 3.5 MeV. A schematic overview is shown in Fig. 1.

A pulsed drive laser extracts electron bunches from a normal conducting photocathode inside a superconducting RF cavity (SRF gun) which accelerates them up to 3.5MeV. A superconducting solenoid will be used to focus the divergent beam and for emittance compensation at a reference point. To investigate the phase space of the bunches as a function of SRF gun and drive laser settings and solenoid focusing strength we want to use a fast phase space measurement system. The longitudinal phase space will be measured by a combination of transverse deflecting cavity (TCAV) [1] and spectrometer dipole [2]. For measurements of the transverse phase space we want to use a combination of two opposite directed steerer magnets (the scanner magnet) and a slit mask. The scanner magnet moves the beam parallel to the beam axis over the slit.

In this paper specification and realization of the scanner system is discussed.

Parameters of GunLab

The expected beam parameters are determined by the injector setup.

A detailed report about the estimated beam parameter as a function of the injector parameters you can find here [3]. Table1 shows the range of the estimated beam parameter.

Table 1: SRF Gun Setup and Expected Beam Parameters

Parameter	Value
Drive laser pulse length	3. . .16 ps (FWHM)
Transversal laser shape	FlatTop
Drive laser repetition rate	1.3 GHz
Macro pulse repetition rate	10 Hz
SRF gun frequency	1.3 GHz
Electric peak field	30 MV/m
Bunch exit energy	1 . . . 3 MeV
Rel. energy spread	0.2%. . . 5%
Bunch charge	0 . . . 100 pC
Bunch length	2. . .10 ps (rms)
Max. Average current	4 μA
Normalized emittance	0.4. . . 10 mm mrad

TRANSVERSE PHASE SPACE MEASUREMENT

We want to observe the projected and the sliced transverse phase space of the electron bunches with dedicated techniques.

Projected Transverse Phase Space

A direct method to investigate the projected transverse phase space is a pepperpot or a slit mask. The slit samples narrow emittance dominated beamlets out of a space charge dominated beam. For a slit scan the scanner-magnet deflects the beam parallel to the beam axis and through a slit which has a stable position in the middle of the beam tube. The achievable frequency of such a measurement is limited by the power supply[1] for the magnets and the measurement system downstream, which can be a second slit-scanner with a Faraday-Cup (electronic measurement) or for small beam currents a view screen (optical measurement). For the optical measurement the CCD is the limiting factor for the measurement frequency.

Sliced Transverse Phase Space

As another technique to reconstruct the transverse phase space we will perform a slice emittance measurement. Therefore a TCAV together with two quadrupole magnets are installed in GunLab. The developed TCAV is an one cell cavity which can deflect the beam in two directions. For the slice emittance measurement the quadrupoles minimize the beam dimension in one direction on a screen downstream the TCAV. In a second step the TCAV streaks

* jens.voelker@helmholtz-berlin.de

[1] For magnets with low inductivities DC power supplies can achieve a frequency up to 1 kHz.

ISBN 978-3-95450-141-0

ELECTRON CLOUD DENSITY MEASUREMENTS USING RESONANT MICROWAVES AT CESRTA*

J.P. Sikora†, CLASSE, Ithaca, New York 14853 USA
S. De Santis, LBNL, Berkeley, California 94720 USA

Abstract

Hardware has recently been installed in the Cornell Electron Storage Ring (CESR) to extend the capability of resonant microwave measurement of electron cloud density. Two new detector locations include aluminum beam-pipe in a dipole magnet and copper beam-pipe in a field free region. Measurements with both positron and electron beams are presented with both beams showing saturation of the electron cloud density in the aluminum chamber. These measurements were made at CESR which has been reconfigured as a test accelerator (CESRTA) with positron or electron beam energies ranging from 2 GeV to 5 GeV.

INTRODUCTION

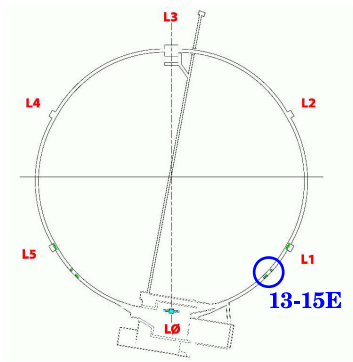

Figure 1: This sketch of the CESR storage ring shows the location of the 13-15E region where the the new measurement hardware is installed.

The Cornell Electron Storage Ring (CESR) has a circumference of 768 m and supports positron or electron beams with bunch populations of up to 1.6×10^{11} particles/bunch (10 mA/bunch) with total beam populations of 3.8×10^{12} particles/beam. Beam energies range from roughly 2 GeV to 5 GeV. The CESR test accelerator program (CESRTA) includes the study of the build-up and decay of electron cloud (EC) density [1], which in this storage ring is dominated by the photo-electrons that are produced by synchrotron radiation. A number of techniques have been used to measure EC density at different locations in CESR [2], including microwave measurements.

To use microwaves for EC density measurements, the microwaves are coupled into and out of the beam-pipe as described in Ref. [3] and shown in Fig. 2, typically using electrodes designed for the beam position monitor (BPM) system. If the response of the beam-pipe is resonant, the presence of the electron cloud will shift the resonant frequency slightly as given in Eq. 1 where n_e is the local EC density and E the local electric field of the microwaves, ϵ_0 is the vacuum permittivity, e is the charge and m_e the mass of an electron. The integral is taken over the resonant volume V of the section of beam-pipe. If the beam-pipe is excited at a fixed frequency near resonance and the electron cloud is periodic, as with a train of bunches in a storage ring, the result is modulation sidebands above and below the excitation frequency. The EC density can be calculated from the amplitude of the sidebands as described in Ref. [3]. This technique is also referred to as the resonant TE wave method [4, 5, 6].

$$\frac{\Delta\omega}{\omega_0} \approx \frac{e^2}{2\varepsilon_0 m_e \omega_0^2} \frac{\int_V n_e E_0^2 dV}{\int_V E_0^2 dV} \quad (1)$$

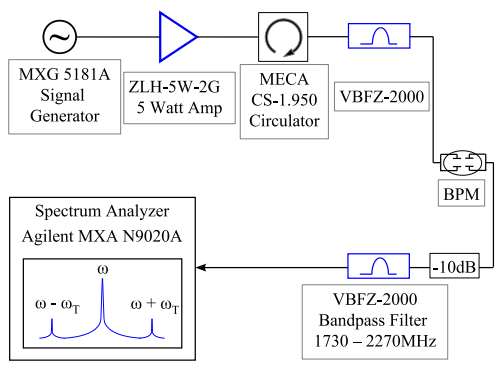

Figure 2: The hardware provides a drive signal to excite the beam-pipe at near a resonant frequency. The response will be phase modulated by the periodic EC density.

HARDWARE

The instrumentation needed to make the measurement is a signal generator and a 5 W amplifier to provide the drive and a spectrum analyzer to measure the sideband amplitudes. Filters and a circulator are also used to protect the instruments from the signal produced by the beam. We have recently added a set of high bandwidth relays that will allow the remote selection of three locations for connection to the drive and receive instruments during accelerator operation. Similar connections have already been made in other parts of the storage ring [7].

* This work is supported by the US National Science Foundation PHY-0734867, PHY-1002467 and the US Department of Energy DE-FC02-08ER41538, DE-SC0006505.

† jps13@cornell.edu

ISBN 978-3-95450-141-0

DOSIMETRIC VERIFICATION OF LATERAL PROFILE WITH A UNIQUE IONIZATION CHAMBER IN THERAPEUTIC ION BEAMS

Y. Hara#, T. Furukawa, K. Mizushima, R. Tansho, N. Saotome, Y. Saraya, T. Shirai and K. Noda,
National Institute of Radiological Sciences, Chiba, JAPAN

Abstract

It is essential to consider large-angle scattered particles in dose calculation models for therapeutic ion beams. However, it is difficult to measure the small dose contribution from large-angle scattered particles. Therefore, we developed a parallel-plate ionization chamber consisting of concentric electrodes (ICCE) to efficiently and easily detect small contributions. The ICCE consists of two successive ICs with a common HV plate. The former is a large plane-parallel IC to measure dose distribution integrated over the whole plane, the latter is a 24-channel parallel-plate IC with concentric electrodes to derive the characteristic parameters describing the lateral beam spread. The aim of this study is to evaluate the performance of the ICCE. By taking advantage of the characteristic of ICCE, we studied the recombination associated with lateral beam profile. Also, we measured a carbon pencil beam in several different media by using ICCE. As a result, we confirmed the ICCE could be used as a useful tool to determine the characterization of the therapeutic ion beams.

INTRODUCTION

The application of charged particles such as proton and carbon-ion beams for radiotherapy has been increased interest around the world. One solution to make optimal use of therapeutic ion beams and to provide flexible dose delivery is three-dimensional (3D) pencil-beam scanning technique [1-3]. It has been utilized since 2011 at the Heavy Ion Medical Accelerator in Chiba (HIMAC), operated by the National Institute of Radiological Sciences (NIRS) [4]. In the scanning irradiation method, since the 3D dose distribution is achieved by superimposing doses of individually weighted pencil beams determined in the treatment planning, the dose calculation must be more accurate.

In dose calculation, the lateral beam spread due to multiple scattering that elemental pencil beams undergo in matter is generally assumed by a single-Gaussian model. However, the dose contributions from large-angle scattered (LAS) particles are not properly modeled in the single Gaussian. When the field size is too small for scattered particle equilibrium, it has been reported that the single-Gaussian model cannot express the reduction of the doses at the center of the field [5-7]. Therefore, several studies have proposed the expression for pencil beams of the sum of two or three Gaussians [8-11]. The parameterization of LAS particles by the multi-Gaussian model works very well. Generally, it is necessary to measure the small dose contributions from the LAS particles to derive the parameters. To efficiently and easily measure the small dose contributions, we developed a unique parallel-plate ionization chamber with concentric electrodes (ICCE) [12]. Since the sensitive volume of each channel is increased linearly with radial distance, it is possible to efficiently and easily detect small contributions from the LAS particles.

In this paper, both the measurement using the ICCE and the validity of simplified parameterization of LAS particles are described.

#y-hara@nirs.go.jp

MATERIALS AND METHODS

Specification of the ionization chamber with the concentric electrodes

The detailed design of the ICCE was reported previously [12]. Only a simplified explanation is given here. The ICCE consists of two successive ICs with a common HV plate: a large plane-parallel IC to measure dose distribution integrated over the whole plane and a 24-channel parallel-plate IC with concentric electrodes to derive the characteristic parameters describing the lateral beam spread. Figure 1 shows a schematic of measurement system with concentric electrodes. The design of the concentric electrodes is based on the Rayleigh distribution transformed by the bivariate circular Gaussian distribution into polar coordinates. To increase the output at the large off-axis position, we increased the width of the electrode from 0.2 mm to 5.3 mm as a function of radius.

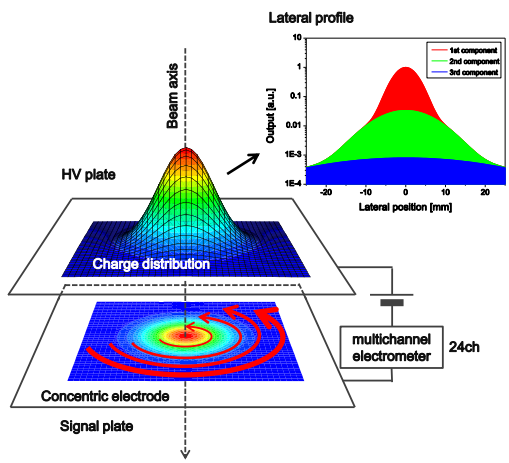

Figure 1: Schematic of the ICCE and lateral profile of carbon-ion expressed by the three-Gaussian model.

The large plane IC should have enough effective area to intercept all particles scattered. The diameter of the chamber is 150 mm. The gap between the HV plate and

ISBN 978-3-95450-141-0

DEVELOPMENT OF THREE-DIMENSIONAL DOSE VERIFICATION SYSTEM USING A FLUORSCENT SCREEN IN ION BEAM THERAPY

Y. Hara#, T. Furukawa, K. Mizushima, N. Saotome, Y. Saraya, R. Tansho, T. Shirai, K. Noda,
National Institute of Radiological Sciences, Chiba, JAPAN
E. Takeshita, Kanagawa Cancer Center, Kanagawa, JAPAN

Abstract

For quality assurance (QA) of therapeutic ion beams, QA tool having high spatial resolution and quick verification is required. The imaging system with a fluorescent screen is suitable for QA procedure. We developed a quick verification system (NQA-SCN) using a fluorescent screen with a charge-coupled device (CCD) camera for the sake of two dimensional dosimetry. The NQA-SCN is compact size to attach to irradiation port and water column. Several types of corrections were applied to the raw image obtained by the NQA-SCN. Our goal is to use the NQA-SCN for three-dimensional dose verification. In carbon-ion therapy, the fluorescent light is decreased by suffering from quenching effect due to the increased linear energy transfer (LET) in the Bragg peak. For the use of three-dimensional dose verification, as a first approach, we investigated the quenching effect of carbon-ion beam in water. Also, to evaluate the performance of NQA-SCN, we carried out experiments concerning QA procedures.

INTRODUCTION

Recently, to make the best use of physical and biological characteristics of therapeutic ion beam, three-dimensional (3D) pencil-beam scanning technique [1-3] has been implemented at some facilities. It has been utilized since 2011 at the Heavy Ion Medical Accelerator in Chiba (HIMAC), in the National Institute of Radiological Sciences (NIRS) [4]. In the scanning irradiation method, since the 3D dose distribution is achieved by superimposing doses of individually weighted pencil beams, any change in the scanned beams will cause a significant impact on the irradiation dose. Therefore, quality assurance (QA) procedures and tools for making refined measurements to verify the characteristics of the pencil beams (e.g. size and position) must be developed. For this purpose, we developed a verification system using a fluorescent screen with a charge-coupled device (CCD) camera, which we called the QA-SCN [5, 6], originally proposed by Boon et al [7, 8]. The QA-SCN is a very useful tool for QA of scanned ion beam because of a high spatial resolution and a quick verification at many points in the irradiation field.

On the other hands, in NIRS, the rotating gantry has developed to improve the dose conformity and less sensitivity to range uncertainties [9]. While the rotating gantry can be rotated 360 degrees, there are small errors due to gantry angle dependence of beam. Thus, a verification system which can be attached on the gantry nozzle is necessary for the commissioning of the rotating gantry and its QA. However, the QA-SCN is large to cover wide viewing field and heavy to maintain rigid. Additionally, the fluorescent light is decreased by suffering from quenching effect due to the increased linear energy transfer (LET) in the Bragg peak. It is difficult to use the QA-SCN for verification of 3D dose distribution in water. To overcome these problems, we developed the NQA-SCN. The NQA-SCN is very compact size. As a first approach, we investigated the response of the NQA-SCN to carbon-ion for various doses, dose rate and different linear energy transfer (LET) values. In this paper, the results of the QA measurements obtained by using the NQA-SCN are described.

#y-hara@nirs.go.jp

MATERIALS AND METHODS

Design of NQA-SCN

A schematic of NQA-SCN system was shown in Fig. 1. The NQA-SCN consists of a fluorescent intensifying screen, a CCD camera, a mirror, camera controllers and a dark box to protect against surrounding light. The mirror is located at 60 degrees relative to the beam axis. The distribution of fluorescent light is reflected by a mirror and is observed by a CCD camera, which is installed at -60 degrees relative to the beam axis. The path length to the CCD camera from the fluorescent screen is about 400 mm. The CCD camera installed in the NQA-SCN is the type BU-41L (Bitran Corp., Japan). The CCD resolution is 1360 × 1024 pixels and the pixel size of the CCD is 6.45 μm × 6.45 μm. The CCD camera allows for the measurements of a 2D light output with a large dynamic range by digitizing optical signals at 14 bits. To decrease thermal noise, the CCD chip is cooled to -1°C by the Peltier cooling unit. A focal length of a lens (V. S. Technology Corp., Japan) is 12 mm. To block direct fluorescent light from the screen, the light shield is placed near the lens. The viewing field and the aperture of the dark box cover an irradiation field of 220 × 220 mm^2. A fluorescent intensify screen, which the phosphor (ZnS: (Ag, Al)) with thickness of about 40 μm is coated on FR-4 board with thickness of 500 μm, is mounted at the entrance face. To verify a light yield difference for different screen positions depending on the coating thickness, we also used the two different types of screen for the flat field correction described later.

ISBN 978-3-95450-141-0

A FAST QUADRUPOLE MAGNET FOR MACHINE STUDIES AT DIAMOND

A. F. D. Morgan, G. Rehm, Diamond Light Source, Oxfordshire, UK

INTRODUCTION

Fast quadrupolar magnets (FQM) have been demonstrated in various schemes for increasing the coupled bunch instability thresholds [1] [3] [8], and for measuring the tune shift of transverse quadrupolar oscillation [5] [6], thus probing the transverse quadrupolar impedance [7]. Operationally they have been used to suppress quadrupole mode instabilities on injection at several machines [2] [4].

Due to machine upgrades, a ceramic vessel installed in the Diamond storage ring has become temporarily available for use. We decided to take advantage of this situation by designing and installing a simple air core quadrupole magnet which can operate at the fundamental quadrupolar frequencies for the horizontal (217kHz) and for the vertical plane (384kHz), as well as at the revolution frequency of the machine (533kHz).

Using this magnet we hope to be able to probe hitherto unexplored behaviours of the Diamond machine with the aim of improving our understanding of non centre of mass motions of the beam.

DESIGN AND REALISATION

After assessing several different coil geometries in a 2D EM simulation program a simple solution of two flat coils, on the top and on the bottom of the ceramic vessel was chosen. By driving the current in opposite directions in the two coils a quadrupolar field can be generated. Figure 1 shows the expected field distribution.

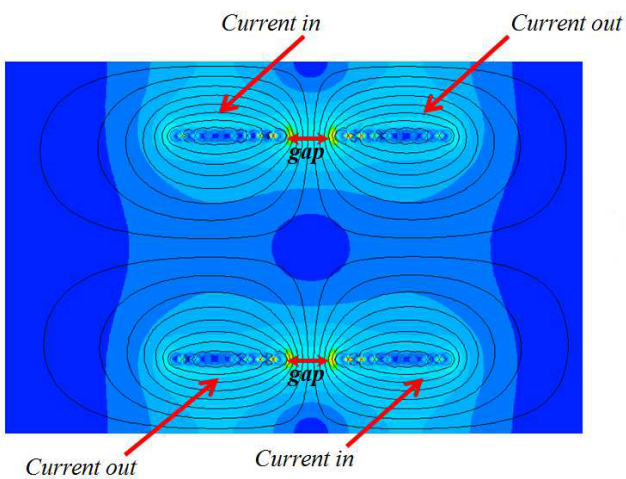

Figure 1: Simulated geometry of the magnet showing the expected quadrupolar field distribution.

The simulations showed that there should be as may turns as possible in order to increase the magnetic field, and also there should be as small a gap along the centre as possible in order to have a high field gradient. The number of turns on each coil was limited by the available space, and the wire radius set practical limits on the centre gap. The final magnet ended up being a pair of 14 turn coils with an 8mm centre gap, made of 2mm diameter enamelled copper wire.

Using these parameters to inform the model we calculated the horizontal and vertical field gradients as being 61mT/m and 64mT/m respectively (Fig.2). These field gradients are sufficient to drive growth and overcome radiation damping.

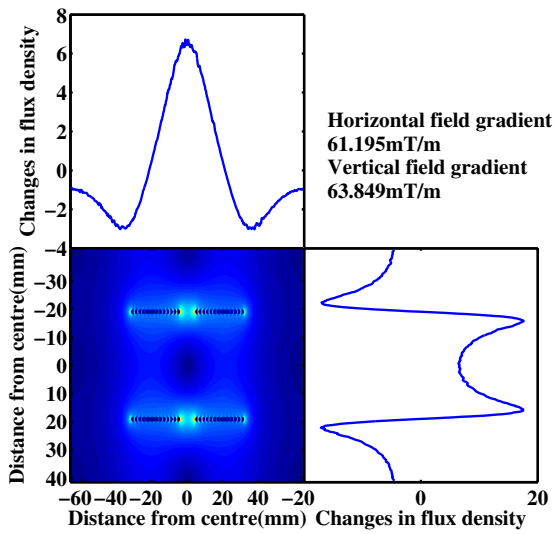

Figure 2: Simulated field gradients of the final magnet.

The coils were bonded in place on non-conductive boards. Using a simple frame, the boards were mounted around the ceramic vessel, as shown in Fig.3.

We planned to use an RF 50Ω amplifier as the power source. In order to match it well to the coils and so maximise the current flowing we decided to drive the coils as part of a resonator circuit. However this also has the effect that the system becomes narrow band and needs to be tuned to a frequency of interest. There are currently 3 operating modes, being tuned to either the vertical or horizontal quadrupole resonance frequencies to enable studies of tune shifts, or tuned to the revolution frequency in order to investigate transverse multibunch instability thresholds. In order to switch modes we change resonant circuits.

ISBN 978-3-95450-141-0

THE BROOKHAVEN LINAC ISOTOPE PRODUCTION FACILITY (BLIP) RASTER SCANNING UPGRADE*

R. Michnoff#, Z. Altinbas, P. Cerniglia, R. Connolly, C. Cullen, C. Degen, D. Gassner, R. Hulsart, R. Lambiase, L. Mausner, D. Raparia, P. Thieberger, M. Wilinski,
Brookhaven National Laboratory, Upton, NY, USA

Abstract

Brookhaven National Laboratory's BLIP facility produces radioisotopes for the nuclear medicine community and industry, and performs research to develop new radioisotopes desired by nuclear medicine investigators. A raster scanning system is being installed to provide a better distribution of the H^- beam on the targets, allow higher beam intensities to be used, and ultimately increase production yield of the isotopes. The upgrade consists of horizontal and vertical dipole magnets sinusoidally driven at 5 kHz with 90 deg phase separation to produce a circular raster pattern, and a suite of new instrumentation devices to measure beam characteristics and allow adequate machine protection. The instrumentation systems include multi-wire profile monitors, a laser profile monitor, beam current transformers, and a beam position monitor. An overview of the upgrade and project status will be presented.

INTRODUCTION

The purpose of the raster system currently under development at BNL's BLIP facility is to "paint" the H^- beam on the target in a circular pattern in order to provide a more even distribution of beam on the target material. At present, with a Gaussian beam profile, targets such as RbCl melt only in the region of highest beam intensity. This causes a large local density reduction leading to reduced and erratic production yield. The improved rastered beam distribution is expected to result in higher yield of the produced isotopes, especially the critical isotope Sr-82.

The BLIP H^- beam parameters are shown in table 1.

Table 1: BNL LINAC H^- Beam Parameters at BLIP

Energy options:	66, 116, 139, 181, 200 MeV
Repetition rate:	6.67 Hz
Pulse width:	450 microseconds
Peak beam current:	50 milliAmps
Max integrated current:	135 microAmps

The plan is to raster the beam in a circular pattern on the target at 5 kHz, which corresponds to 2.25 revolutions per 450 microsecond beam pulse. A repeating pattern as follows will be generated: 3 consecutive beam pulses at a radius of 19.5 mm, then 1 pulse at a 6.5 mm radius (ref. Fig. 1). Flexibility will be provided to vary the radius value and the number of beam pulses for each radius. In this manner near uniform deposition on the target can be achieved.

The concept of the BLIP raster system is based on the system that has been in operation at the Los Alamos National Laboratory Isotope Production Facility (IPF) [1]. However, several differences exist between the facilities, including increased magnet power requirements at BLIP due to a larger kick angle (3.3 milliRadians for BLIP, 1.5 milliRadians for IPF), and rastering with 2 different radii at BLIP for improved beam distribution.

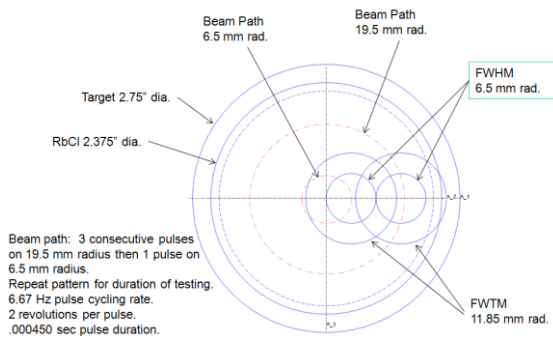

Figure 1: Diagram of circular raster pattern on target.

VACUUM COMPONENTS

The layout of the new BLIP beamline section is shown in Fig. 2. To the extent possible, aluminum components are used instead of stainless steel because aluminum has a shorter half-life and will present fewer activation issues in this high radiation area. The high radiation is primarily caused by back-scattering off the beryllium window that is used to isolate the upstream higher vacuum section from the downstream lower vacuum section.

Most the beam-line pipe is 8" OD. A 6.5" ID graphite collimator will be installed just upstream of the raster magnet to protect the magnet from being damaged by mis-steered particles, and a 4.5" ID graphite collimator just upstream of the multi-wire/LPM crosspiece to protect the beam current transformers. The BPM pipe is 8" OD with 4.5" ID pickups. Graphite is installed between the BPM pickups and the inner pipe wall to help shield the beam current transformers from backscattered particles from the beryllium window. Three aluminium bellows will be installed to facilitate assembly and alignment. A viewport section is in place for thermal imaging of the beryllium window in the future. Included in the viewport section is an electron suppressor ring that will prevent backscattered electrons from interfering with the BPM and current transformer measurements.

* Work supported by Brookhaven Science Associates, LLC under Contract No. DE-AC02-98CH10886 with the U.S. Dept. of Energy
#michnoff@bnl.gov

ISBN 978-3-95450-141-0

FAILURE MODE AND EFFECTS ANALYSIS OF THE BEAM INTENSITY CONTROL FOR THE SPIRAL2 ACCELERATOR

C. Jamet #, S. Leloir, T. André, B. Ducoudret, G. Ledu, S. Loret, C. Potier de Courcy,
GANIL, Caen, France

Abstract

The first phase of the SPIRAL2 project includes a driver and its associated new experimental areas (S3 and NFS caves). The accelerator, located in Caen (France), is based on a linear solution composed of a normal conducting RFQ and a superconducting linac. Intense primary stable beams (deuterons, protons, light and heavy ions) will be accelerated at various energies for nuclear physics.

The beam intensity monitoring is a part of the control of the operating range. A high level of requirements is imposed on the intensity control system. In 2013, a Failure Mode and Effects Analysis (FMEA) was performed by a specialized company helped by the GANIL's Electronic Group. This paper presents the analysis and evolutions of the electronic chain of measurement and control.

INTRODUCTION

In the first phase, the SPIRAL2 driver will be able to accelerate and deliver beams of protons, deuterons and ions with q/A=1/3 to NFS (Neutron for Science) and S3 (Super Separator Spectrometer) experimental rooms. Table 1 shows the main beam characteristics.

Table 1: Beam Specifications

Beam	P	D+	Ions (1/3)
Max. Intensity	5 mA	5mA	1 mA
Max. Energy	33 MeV	20 MeV/A	14.5 MeV/A
Max. Power	165 kW	200 kW	43.5 kW

Beam diagnostics are installed along the accelerator in order to measure and control continuously beam parameters and transmission losses [1],[3]. Beam intensity and transmission levels are measured by non-interceptive transformers ACCT and DCCT.

To obtain the commissioning authorization, the SPIRAL 2 project has to demonstrate and prove to the French Safety Authority that these devices which monitor the operating range of the facility are built in respect of the quality assurance rules.

To respond to this request, a FMEA (Failure Mode and Effects Analysis) of the intensity and transmission monitors was performed in 2013 by a French company, Ligeron®, specialized in the safety system developments.

Results, conclusions of this FMEA and the uncertainties of the measurement chains are presented in this paper.

REQUIREMENTS

Global Functions

The functions of the non-interceptive intensity measurements are:

- ✓ Tune the beam,
- ✓ Control and monitor the beam intensity at the LINAC exit,
- ✓ Control and monitor the intensity between several points of the accelerator (transmissions),
- ✓ Control the intensity quantity sent to the Beam Dump Linac over 24 hours.

Tuning Requirements

The initial operating ranges for beam intensity were:

- ✓ for proton and neutron beams: from 0,15 to 5 mA
- ✓ for heavy ions (Q/A=1/3) : from 0,15 to 1 mA

"Voltmeter" function: Measure the beam intensity average
"Oscilloscope" function: Visualize the beam intensity in time. Time resolution: few µs

MPS Requirements

The SPIRAL2 Machine Protection System is based on three technical subsystems [2], [4]:

- ✓ One dedicated to thermal protection (TPS), which requires a fast electronic protection system,
- ✓ One dedicated to enlarged protection (EPS), based on robust technologies consisting of a PLC associated with a redundant hard-wired system. It controls the operation domain of the facility from the safety point of view (beam intensities and energies)
- ✓ One dedicated to classified protection (CPS), which protects the vacuum safety valves of the facility.

Enlarged Protection System Requirements

Beam intensity control at the linac output:

- ✓ Intensity levels: 5 mA on the Linac Beam Dump, 1 mA in the S3 experimental room, 50 µA in the NFS experimental room
- ✓ Response time: 1 s

Beam intensity transmission:

- ✓ Level: 250 µA (maximum losses to limit the radiologic level outside the accelerator area)
- ✓ Response time: 1 s

Intensity at the linac output for the activation control of the Linac Beam Dump:

- ✓ Intensity levels: from 11 µA to 5 mA
- ✓ Response time: 10 s

ISBN 978-3-95450-141-0

PROGRESS ON THE BEAM ENERGY MONITOR FOR THE SPIRAL2 ACCELERATOR

W. Le Coz#, C. Jamet, G. Ledu, S. Loret, C. Potier de Courcy, D. Touchard, GANIL, Caen, France
Y. Lussignol, IRFU, Saclay, France

Abstract

The first part of the SPIRAL2 project entered last year in the end of the construction phase at GANIL in France. The facility will be composed of an ion source, a deuteron/proton source, a RFQ and a superconducting linear accelerator. The driver is planned to accelerate high intensities, 40 MeV deuterons up to 5 mA and heavy ions up to 1 mA.

A monitoring system was built to measure the beam energy on the BTI line (Bench of Intermediate Test) at the exit of the RFQ. As part of the MEBT commissioning, the beam energy will be measured on the BTI with an Epics monitoring application.

At the exit of the LINAC in the HEBT, another system should measure and control the beam energy. The control consists in ensuring that the beam energy stays under a limit by taking account of the measurement uncertainty. The energy is measured by a method of time of flight; the signal is captured by non-intercepting capacitive pick-ups.

This paper describes the BTI monitor interface and presents the system evolution following the design review of the HEBT monitor.

INTRODUCTION

The beam energy will be measured on BTI which is directly placed at the RFQ exit to qualify the beam properties in front of the LINAC. The beam energy at the LINAC exit in the HEBT will be also measured for the beam tuning and the energy control. The energy is monitored in order to ensure the respect of the accelerator operating range and the thermal protection of the machine. The energy is measured by a method of time of flight (TOF) [1].

Beam time structure may vary by using a slow chopper or a single bunch selector. The duty cycle of the slow chopper is included between 1/10000 and 1/1 with a frequency of 1 Hz and 5 Hz. The intensity beam will range from a few 10 µA to 5 mA.

As the energy control is part of the safety functions, Failure Modes and Effects Analysis (FMEA) and the measurement uncertainty are required on this control device.

BEAM ENERGY MEASUREMENTS

The energy monitor is composed by three electrodes installed along the beam line, the energy is calculated by a time of flight method (TOF).

In 2014, before the final installation, the BTI was assembled at the IPHC laboratory (Fig. 1) for mechanical verifications.

#lecoz@ganil.fr

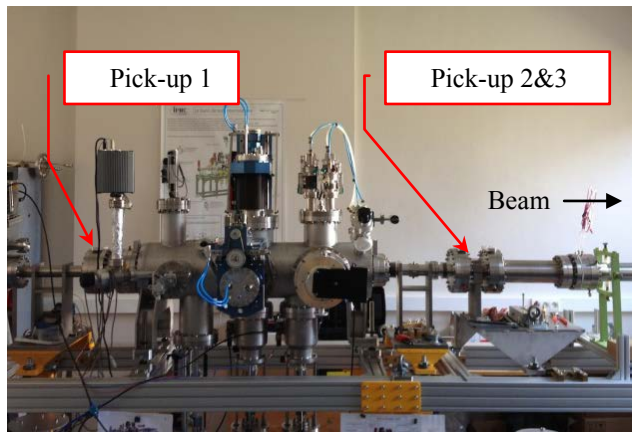

Figure 1: Electrodes along the BTI.

The first unit includes the Pick-up1 and the second unit is composed by the Pick-up2 and 3 (Fig. 2). The pick-up3 is designed to determine the number of bunches between the two first pick-ups. The length between the second and the third pick-up is calculated to be smaller than the distance between two bunches.

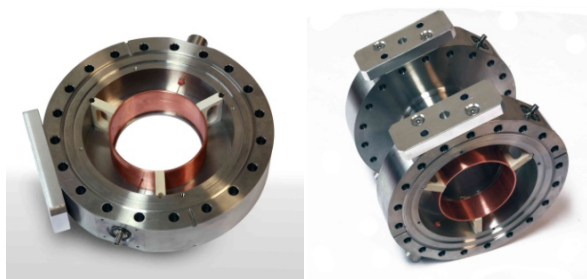

Figure 2: Pick-up1, Pick-up2&3.

The HEBT required performances are the following:
- Intensity range: from 10 µA to 5 mA
- Energy range: from 2 MeV/A to 33 MeV/A
- Response time: 1 s
- Required accuracy:
  +/-1 per mille for the beam tuning
  +/-1 per cent for the beam control

ELECTRONIC DESCRIPTION

The phase measurement of the TOF is based on an electronic system which realizes the lock-in amplifier function [2]. The signals come from three pick-up electrodes. The phase of the first harmonic is measured by the TOF device.

ISBN 978-3-95450-141-0

STUDY OF GENERAL ION RECOMBINATION FOR BEAM MONITOR USED IN PARTICLE RADIOTHERAPY

R. Tansho#, T. Furukawa, Y. Hara, K. Mizushima, N. Saotome, Y. Saraya, T. Shirai and K. Noda
National Institute of Radiological Sciences, Chiba, Japan

Abstract

For particle radiotherapy, accurate dose measurement using a beam monitor of an ionization chamber (IC) is essential to control prescribed dose to a tumor. General ion recombination is one of the most impact factors on the accurate dose measurement. The Boag theory predicts the general ion recombination effect on ionization current under the condition that ions are uniformly generated throughout the gas volume. For the particle radiotherapy using a pencil beam scanning system, however, the ions generated by the pencil beam is not uniform. We have developed a calculation code for accurate prediction of the general ion recombination effect for the pencil beam scanning system. The calculation code is called as division calculation method. The division calculation method takes into account the different ionized charge density in the beam irradiation area by dividing the ionization distribution into many sub-elements. The general ion recombination effect in each sub-element is calculated by the Boag theory. The calculation accuracy was verified by comparison of the saturation curve, which is the curve of applied voltage versus measured current, between measurements and calculation results. We measured the saturation curves by using a parallel plate IC and a cylindrical IC. We confirmed that the calculated saturation curves were good agreement with the measured curves. The division calculation method is effective tool to accurately predict the saturation curve for the pencil beam scanning system.

INTRODUCTION

Carbon ion radiotherapy has been attracted for a cancer treatment due to the characteristic depth-dose distribution with Bragg peak. Dose localization at the Bragg peak is utilized for concentrated irradiation to a tumor. To optimize dose distribution in the tumor, a 3D pencil beam scanning system [1, 2] has been developed at the new treatment research facility in National Institute of Radiological Sciences (NIRS) [3]. The pencil beam scanning system scans the pencil beam laterally by two scanning magnets and longitudinally by variable energy changes and using range shifters. Main and sub flux monitors of an ionization chamber (IC) are also used to control prescribed dose to the tumor. Since the discrepancy between the prescribed dose and the irradiated dose leads to the worse treatment results, accurate dose measurement in the flux monitors is essential.

General ion recombination is one of the most impact factors on the accurate dose measurement. The saturation curve, which is the curve of applied voltage versus measured current, represents the reduction rate of the collected ions with reducing the applied voltage due to the general ion recombination. Accurate prediction of the saturation curve is important to design the proper specifications of the IC such as applied voltage, gap length and kind of gas to obtain the saturation current.

We can predict the saturation curve by Boag theory [4-6]. The Boag theory assumed that ions are uniformly generated throughout the gas volume in the IC. However, the ionized charge distribution generated by the pencil beam is not uniform and the distribution is modeled by the 2-dimensional Gaussian form.

In this paper, we present a calculation method giving the accurate saturation curve for ions generated by the pencil beam.

MATERIALS AND METHODS

Calculation Methods

For a parallel plate IC, the Boag theory gives an ion collection efficiency f at an applied voltage V [V] by following formulae:

$$f = \frac{1}{1+\frac{\xi^2}{6}} \tag{1}$$

$$\xi = 2.01 \times 10^7 \left(\frac{d^2 \sqrt{q}}{V} \right) \tag{2}$$

where d [m] is the gap length between the electrodes of the IC and q [C m^{-3} s^{-1}] is ionized charge density per a unit of time. Since the ion collection efficiency f depends on the ionized charge density q, accurate estimation of the

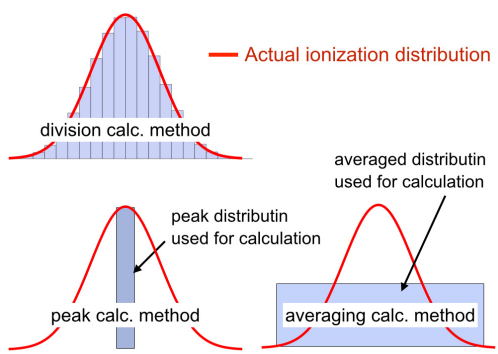

Figure 1: The different calculation methods to estimate the ionized charge distribution generated by the pencil beam irradiation.

ISBN 978-3-95450-141-0

SENSOR STUDIES FOR DC CURRENT TRANSFORMER APPLICATION

E. Soliman, K. Hofmann, Technische Universität Darmstadt, Darmstadt, Germany
H. Reeg, M. Schwickert, GSI Helmholtzzentrum für Schwerionenforschung GmbH, Darmstadt, Germany

Abstract

DC Current Transformers (DCCTs) are known since decades as non-intercepting standard tools for online beam current measurement in synchrotrons and storage rings. In general, the measurement principle of commonly used DCCTs is to introduce a modulating AC signal for a pair of ferromagnetic toroid. A passing DC ion beam leads to an asymmetric shift of the hysteresis curves of the toroid pair. However, a drawback for this measurement principle is found at certain revolution frequencies in ring accelerators, when interference caused by the modulating frequency and its harmonics leads to inaccurate readings by the DCCT. Recent developments of magnetic field sensors allow for new approaches towards a DCCT design without using the modulation principle. This paper shows a review of different kinds of usable magnetic sensors, their characteristics and how they could be used in novel DCCT instruments.

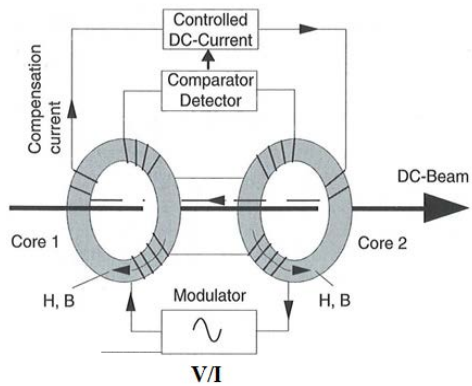

Figure 1: Conventional DCCT Block diagram [2].

INTRODUCTION

Commonly, DCCTs are the main tool in synchrotrons and storage rings for online monitoring of DC beam currents. The SIS100 heavy ion synchrotron will be the central machine of the FAIR (Facility for Antiproton and Ion Research) accelerator complex currently under construction at GSI. Beam operation at SIS100 requires a novel DCCT device with large dynamic range and high accuracy [1]. Currently a Novel DCCT (NDCCT) based on modern magnetic field sensors is under development at GSI. Main motivation for this research project is to investigate different commercially available magnetic field sensors with regard to their applicability for reliable beam current measurements with the goal to simplify the device as compared to the conventional DCCT setup.

Figure 1 presents the schematic of a conventional DCCT sensor, consisting of two symmetrical toroid and modulator/demodulator circuit. In this setup the modulator circuit drives the two cores to magnetic saturation with a 180º phase shift. In case a DC current passes through the two cores the magnetic flux density generated in the cores is shifted asymmetrically. The sum of the total magnetic flux of the two cores is proportional to the DC current amplitude. A feedback circuit is used to compensate the change in the magnetic flux inside the cores to reach zero flux. The output current signal of the feedback circuit is a direct measure for the DC current passing the DCCT [3].

Besides many quality characteristics, a major disadvantage of this design is the fact that for precise beam current measurements the magnetic properties of the two ring cores must be perfectly matched, which requires an intricate manufacturing process. A second drawback of this setup, especially for the usage at SIS100, is the fact that the modulation frequency is 20 kHz; when the beam's basic revolution frequency or harmonics are the same as the even harmonics of the modulating frequency interference occurs. Therefore, the current measurement of a conventional DCCT becomes erroneous without notification to the user.

Thus, the requirement for a simpler DCCT assembly with a single core and without using the modulation technique came up. The principle for current sensing in the NDCCT is using commercially available integrated circuit magnetic field sensors. The sensitivity of modern sensors is sufficient to directly measure the magnetic field as generated by the DC ion beam current, without the need of using the modulation technique.

In Fig.2 a schematic view of an open loop NDCCT is depicted. The NDCCT consists of a high permeability slotted flux concentrator which allows for easy installation of the setup around the ceramic gap without breaking the vacuum. The magnetic sensor is placed inside the air gap of the flux concentrator.

*Work supported by BMBF; Project. No.: 05P12RDRBG between GSI and TU Darmstadt

ISBN 978-3-95450-141-0

OBSERVATIONS OF THE QUADRUPOLAR OSCILLATIONS AT GSI SIS-18

R. Singh, P. Forck, P. Kowina, GSI, Darmstadt, Germany
W.F.O. Müller, J.A. Tsemo Kamga, T. Weiland, TEMF, Technische Universität Darmstadt, Germany
M. Gasior, CERN, Geneva, Switzerland

Abstract

Quadrupolar or beam envelope oscillations give valuable information about the injection matching and the incoherent space charge tune shift. An asymmetric capacitive pick-up was installed at GSI SIS-18 to measure these oscillations. In this contribution, we present the simulations performed to estimate the sensitivity of the quadrupolar pick-up to the beam quadrupolar moment and compare it with respect to other pick-up types installed at SIS-18. Further, dedicated beam measurements are performed to interpret the quadrupolar signal under high intensity conditions.

INTRODUCTION

A symmetric pick-up is shown in Fig. 1 along with a Gaussian beam with centroid at $\bar{x}$, $\bar{y}$ and rms dimensions $\bar{\sigma}_x$, $\bar{\sigma}_y$. The image current induced by the beam at the pick-up (PU) electrodes is derived in [1] and reproduced here,

$$J_{\text{image}}(a,\theta) = \frac{I_{beam}}{2\pi a}\left\{1 + 2\left[\frac{\bar{x}}{a}\cos\theta + \frac{\bar{y}}{a}\sin\theta\right] + 2\left[\left(\frac{\bar{\sigma}_x^2 - \bar{\sigma}_y^2}{a^2} + \frac{\bar{x}^2 - \bar{y}^2}{a^2}\right)\cos 2\theta + 2\frac{\bar{x}\bar{y}}{a^2}\sin 2\theta\right] + \text{higher order terms}\right\} \quad (1)$$

On a symmetric pick-up, the four plate signals are obtained for $\theta = 0$, $\pi/2$, π and $3\pi/2$ radians. The second order component that contains beam width information is referred to as the "quadrupole moment" and is given by,

$$\kappa = \bar{\sigma}_x^2 - \bar{\sigma}_y^2 + \bar{x}^2 - \bar{y}^2 \quad (2)$$

To extract the quadrupole moment from the pick-up electrode signals (denoted by U referring to the voltages induced), the electrodes are connected in the following "quadrupolar" configuration,

$$\Xi_q = (U_r + U_l) - (U_t + U_b) \quad (3)$$
$$= Z \cdot I_{beam}\left(\frac{\bar{\sigma}_x^2 - \bar{\sigma}_y^2 + \bar{x}^2 - \bar{y}^2}{a^2} + \text{higher order terms}\right)$$
$$\Xi_s = (U_r + U_l + U_t + U_b) \quad (4)$$
$$= Z \cdot I_{beam}$$

where Z is the transfer impedance of the pick-up and Ξ_q is the quadrupolar signal and when Ξ_q is normalized to the sum signal of all electrodes Ξ_s, it is referred to as the normalized quadrupolar signal.

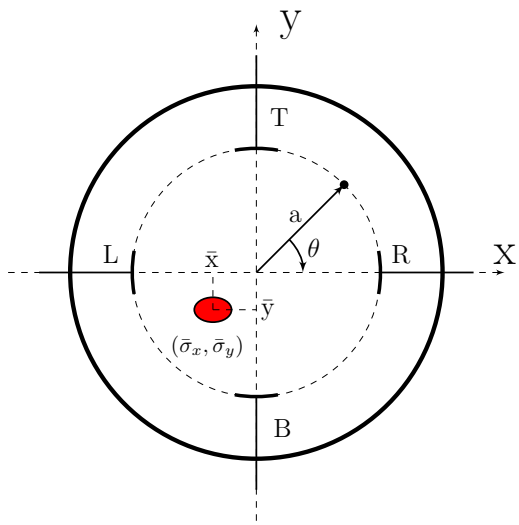

Figure 1: Symmetric pick-up for the analytical calculations.

Quadrupole signal monitors were first suggested as non-invasive emittance monitors at SLAC [1]. In synchrotrons, the quadrupole monitors were initially used to detect the injection mismatch causing envelope oscillations. It was also used to estimate the space charge dependent detuning [2] based on theoretical and numerical works [3,4]. Special pick-up designs and signal processing schemes were developed at CERN-PS to use quadrupolar pick-ups as regular emittance monitors [5].

At GSI SIS-18, quadrupolar beam transfer function (BTF) measurements were performed to get a direct measure of incoherent tune shift [6]. Due to unavailability of appropriate non-linear pick-ups int those studies, a new asymmetric pick-up was developed for SIS-18 [7]. There were recent studies which focussed on the signal processing methods to suppress the dipole contributions in the quadrupolar signal [8].

The first section of this paper summarizes the simulations performed to compare the sensitivities of various pick-up types installed at SIS-18 to the quadrupolar moment. The second section details the present installation of the quadrupolar pick-up, its data acquisition and the signal processing. The final section presents the beam experiments and results.

ISBN 978-3-95450-141-0

CONCEPTUAL DESIGN OF ELLIPTICAL CAVITY BEAM POSITION MONITORS FOR HEAVY ION STORAGE RINGS

M. S. Sanjari*, X. Chen, P. Hülsmann, Yu. A. Litvinov, F. Nolden, J. Piotrowski, M. Steck, Th. Stöhlker, GSI Darmstadt, 64291, Darmstadt, Germany

Abstract

Over 50 years in the history of accelerator physics, RF cavities have been used as beam position and intensity monitors. Their structure has been extensively discussed across numerous papers reporting their successful operation (a review can be found in [1]).

The application of RF cavities as pickups has recently been extended to include radioactive ion beam (RIB) facilities and heavy ion storage rings. These pickups allow very sensitive, accurate, and quick characterisation of ion beams and turn out to be indispensable tools in nuclear as well as atomic physics experiments. A notable example is the resonant pickup in the ESR at GSI Darmstadt [2] where single ion detection was achieved for lifetime measurements of radioactive nuclides [3]. A similar cavity pickup was installed in CSRe in IMP Lanzhou [4].

Usually, cavity pick-ups in dipole mode are used to accomplish position sensitive measurements. These achieve high sensitivities for small aperture machines (see e.g. [5] and [6]). In this work, we describe a novel conceptual approach that utilizes RF cavities with an elliptical geometry. While allowing a high precision determination of the position and intensity of particle beams, it has to cope with design restriction at heavy-ion storage rings such as large beam pipe apertures. The latter becomes inevitable at facilities aiming at storing large-emittance beams as e.g. planned in the future Collector Ring (CR) of the FAIR project at GSI Darmstadt.

THEORY OF OPERATION

Schottky Noise Analysis

Schottky noise analysis is meanwhile a well established method in beam diagnostics in storage rings, providing valuable information on beam characteristics. While transversal Schottky noise signals contain information on tune and chromaticity, longitudinal signals can be used for the determination of the revolution frequency and momentum spread of the beam. In an in-ring experimental scenario, longitudinal Schottky signals can be used to identify different nuclear species circulating in the storage ring. Using the fundamental relation of mass to charge ratio and the frequency resolution in storage rings [7], one can measure different nuclear masses by comparing the frequency difference with known reference nuclides. Using time resolved Fourier analysis, it is possible to monitor an unstable isotope in order to determine its lifetime. A more detailed account on mass and lifetime measurement in storage rings using the Schottky signal analysis can be found in [7].

Schottky noise signals are random processes. The power spectral densities show frequency bands around multiples of the beam revolution frequency [8]. These bands contain the same amount of power, and although increasing frequency affects their width and height, they essentially carry the same information about the beam. So provided that the recorded Schottky signal is mixed down into base band, an experimental event which causes a frequency change Δf (a decay event, isomeric states, determination of mass, beam cooling, jitter, etc.) is better resolved at higher harmonics for a given recording time Δt. In other words, for a required frequency resolving power, one needs a shorter recording time.

RF Cavities as Schottky Pick-Ups

Microwave cavities possess a set of eigenmodes, each oscillating at their corresponding eigenfrequency. Each of these modes ν can be thought of as an electrical resonator containing an ideal RLC element [9], each of which can be described by its frequency f_ν, Q value Q_ν and shunt impedance $R_{sh,\nu}$:

$$P_{diss,\nu} = \frac{U_\nu^2}{R_{sh,\nu}} = \frac{1}{2}\frac{U_\nu^2}{R_\nu} \tag{1}$$

where U_ν is the induced voltage after the passage of the particle, and $P_{diss,\nu}$ is the dissipated power to that mode and R_ν is the resistor in the equivalent RLC circuit. For the Q value we have

$$Q_\nu = \frac{\omega_{0\nu} W_\nu}{P_{diss,\nu}} \tag{2}$$

where $\omega_{0,\nu}$ is the angular eigenfrequency and W_ν is the energy stored in the mode. Instead of the shunt impedance, it is often useful to use a material independent version of it which is normalized to the Q value. It is often called *R/Q*, the *characteristic impedance* or *geometric factor* in units of ohms

$$\left(\frac{R_{sh}}{Q}\right)_\nu = \left(\frac{\widehat{R_{sh}}}{Q}\right)_\nu \Lambda_\nu(\beta)^2 \tag{3}$$

where $\Lambda_\nu(\beta)$ is the so called *transit time factor* as a function of the relativistic β of the beam. The hat shows the ideal characteristic impedance for a cavity with zero length and a beam travelling with the speed of light.

The signals from a beam of particles can be used to excite a microwave cavity . The resulting standing waves can

* s.sanjari@gsi.de

HIGH POSITION RESOLUTION AND HIGH DYNAMIC RANGE STRIPLINE BEAM POSITION MONITOR (BPM) READOUT SYSTEM FOR THE KEKB INJECTOR LINAC TOWARDS THE SuperKEKB

R. Ichimiya#, T. Suwada, M. Satoh, F. Miyahara, K. Furukawa, KEK, Tsukuba, Japan

Abstract

The SuperKEKB accelerator is now being upgraded to bring the world highest luminosity ($L=8x10^{35}/cm^2/s$). Hence, the KEKB injector linac has to produce low emittance and high charge electron (20 mm mrad, 7 GeV/c^2, 5 nC) and positron (20 mm mrad, 4 GeV/c^2, 4 nC) beam, respectively. In order to achieve these criteria, the accelerator structure has to be aligned within 0.1 mm position error. Since BPMs are essential instruments for beam based alignment (BBA), it is required to have one magnitude better position resolution to get enough alignment results. We have begun to develop high position resolution BPM readout system with narrow bandpass filters (fc = 180 MHz) and 250 MSa/s 16-bit ADCs. It handles two bunches with 96 ns interval separately and has a dynamic range from 0.1 nC to 10 nC. To compensate circuit drift, two calibration (x-direction and y-direction) pulses are output to the BPM electrodes between beam cycles (20 ms). Since it needs to achieve not only high position resolution but also good position accuracy, overall nonlinearity within ±0.02 dB is required and the system has to have more than ±5 mm accurate position range. We confirmed the system performance with a 3-BPM resolution tests at KEK Injector Linac and it turned out that the system has 3 μm position resolution. We plan to install this system during 2015 summer shutdown.

INTRODUCTION

KEK Injector Linac is now being upgraded as a part of SuperKEKB accelerator complex [1] to achieve $L = 8x10^{35}$ /cm^2/s luminosity, both electron and positron beam emittance have to be 20 mm mrad. To perform the BBA stably, BPMs are required to have one magnitude better position resolution than the required alignment accuracy. To accomplish <10 μm position resolution, we have designed dedicated narrow bandpass filter (BPF) type readout circuitry with 250 MSa/s 16 bit pipeline ADC (AD9467-250 [2]). As the SuperKEKB injector injects electron / positron beams into four different energy rings (SuperKEKB HER/LER, PF and PF-AR) simultaneously, we employed electrical attenuators to keep enough dynamic range.*

BPM readout system has to have not only high position resolution (σ < 10 μm) but also good position accuracy. There are many sources of position error, especially input channel gain drift from each BPM electrode is one of dominant sources. To compensate this, calibration pulse generator [3] is implemented. A calibration pulse from one electrode is equally divided into adjacent electrodes with coupling capacitance (see Fig. 1). By calculating both channel output power, channel gain ratio can be monitored and compensated.

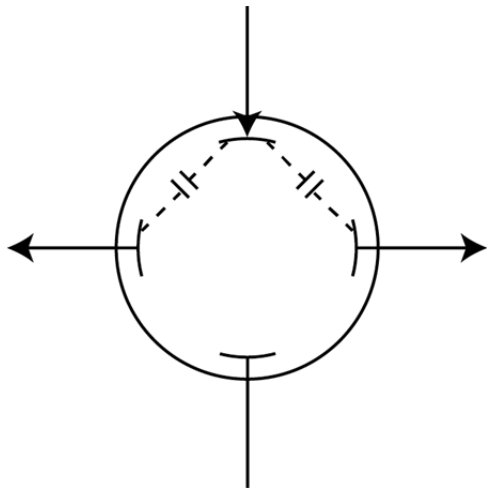

Figure 1: BPM calibration scheme is illustrated. Calibration tone is provided to the top electrode and induced pulses are generated on both adjacent electrodes with coupling capacitance.

HARDWARE IMPLEMENTATION

Baseline design of this BPM readout system has been reported at previous IBIC2013 conference [4]. Hence, we report updates from the last design here.

As discussed in previous section, we need to handle the signal with high linearity to achieve target position resolution (σ < 10 μm). It turned out that first prototype has following rooms to be improved:

At first, helical coils are needed to precise tuning, so it is not suitable for high linearity application. Therefore, we changed BPF centre frequency to 180 MHz so that we can use normal LC filters. Figure 2 shows the photograph of the prototype of the BPM readout board, Figure 3 shows block diagram of 2nd prototype BPF board. The latter BPF performs waveform shaping (burst length = 60 ns) and limits the bandwidth (22 MHz). The former BPF (BW=60 MHz) is for anti-aliasing at the ADC.

In addition, the latter amplifier is the critical device that limits the overall linearity. Therefore, we tested three RF amplifiers shown in Table 2. As shown in Fig. 4 an ADL5536 (Analog Devices (AD)), which have the highest output third-order intercept point (OIP3), has optimal (flat) linearity.

Figure 5 shows the BPF output waveform and ADC sampled data points. Waveform is stretched to about

* ryo@post.kek.jp

ISBN 978-3-95450-141-0

IMPROVEMENT OF DATA TRANSFER SPEED OF LARGE MEMORY MONITORS

M. Tobiyama*, KEK Accelerator Laboratory, 1-1 Oho, Tsukuba 305-0801, Japan, and
Graduate University for Advanced Studies (SOKENDAI), 1-1 Oho, Tsukuba 305-0801, Japan

Abstract

Beam monitors with long memories will be widely used in SuperKEKB accelerators. Since the slow data transfer time of such devices usually limits the operational performance, improvement of the transfer rate is required. Two kind of devices, VME-based modules and Ethernet-based modules have been developed. On the VME-based devices such as turn-by-turn position monitors for damping ring or long bunch oscillation monitors, MBLT and BLT transfer method have been implemented. For the Ethernet based system, such as the gated turn-by-turn monitors (TbT), SiTCP has been implemented on the FPGA and the EPICS device support for SiTCP has been developed. The improvement of the data transfer speed with the long-term reliability will be presented.

INTRODUCTION

With the rapid development of digital technology, it is much easier to implement large memory in the beam monitor system since late 1990's where we had designed the beam monitor devices for KEKB accelerators. As new accelerators with strongly improved performance such as SuperKEKB need much detailed information of the beam to achieve the design characteristics, the number and scale of the beam monitors with long memory becomes much larger than that of KEKB accelerators.

On the other hand, the environment of the beam instrumentation such as the selection of the field bus tends to be fairly conservative mainly due to saving of the design and construction efforts and costs. For example, in SuperKEKB beam instrumentations, though we newly introduce MTCAs and modules with direct Ethernet connection in some limited sections, we will still use the legacy bus such as VMEbus, VXIbus and GP-IB.

In the operational view, it is needless to emphasize the importance of the fast data acquisition and the fast data processing to minimize loss time of the operation. For example, during the operation of the KEKB collider, we have used the VMEbus based bunch oscillation recorders (BOR) with total 20 MB of memory which enables us to record the 4k turns of bunch oscillations for all the buckets in the ring [1]. We have also used the same recorders with limited address space of 5120 bytes for the bunch current monitors (BCMs). The BORs have been used for the post-mortem analysis of the beam abort and the machine developments such as the detailed analysis of the beam oscillation coming from intra-bunch oscillation due to electron cloud instabilities [2]. BCMs have been used to support the injection bucket selection systems to realize the equally filled bunch filling. As the EPICS system we had mainly used during the KEKB operation (R313) did not support larger array than 4k bytes, we needed to store the data to the remote disk directly from the IOC through the fairly slow Ethernet line (10base connection). Typical data transfer time from the BOR to the disk was 5 min to 10 min depending on the network traffic and the CPU usage of the host workstation with the remote disks. Of course that kind of waiting time was painful for all of us and had spoiled the efficiency of the machine operation.

For the SuperKEKB accelerators, we have developed the beam instruments with improved data transfer speed. Two kind of devices, the VMEbus based modules and direct Ethernet connection modules will be shown here. Table 1 shows the main parameters of SuperKEKB accelerators, main rings (LER and HER) and the positron damping ring (DR).

Table 1: Main Parameters of SuperKEKB Rings

	HER/LER	DR
Energy (GeV)	7/4	1.1
Circumference(m)	3016	135.5
Beam current (A)	2.6/3.6	0.07
Number of bunches	2500	4
Single bunch current (mA)	1.04/1.44	18
Bunch separation (ns)	4	>98
Bunch length (mm)	5/6	6
RF frequency (MHz)	508.887	
Harmonic number (h)	5120	230
T. rad. damping time (ms)	58/43	11
L. rad. damping time (ms)	29/22	5.4
Number of BPMs	466/444	83
Number of TbT monitors	135/135	83

VMEBUS BASED SYSTEM

Though the specifications and the expected performance of the VMEbus system might not be so modern [3], still the system have many strong points as:

- Board size fits most of our purpose as the beam instrumentation devices.

*makoto.tobiyama@kek.jp

EVALUATION OF LIBERA SINGLE PASS H FOR ESS LINAC*

M. Cargnelutti, M. Žnidarčič, Instrumentation Technologies, Solkan, Slovenia
H. Hassanzadegan, ESS AB, Lund, Sweden

Abstract

The Beam Position Monitor system of the ESS linac will include in total more than 140 BPM detectors of different sizes and types. The resolution and accuracy of the position measurement with the nominal 62.5 mA beam current and 2.86 ms pulse width need to be 20 μm and 100 μm respectively, and those of the phase measurement are 0.2 deg and 1 deg respectively. The BPM system also needs to work successfully under off-optimal conditions, ex. with a de-bunched beam, or with the current and pulse width being as low as 6 mA and 10 μs respectively. Options for the implementation of the ESS BPM electronics include: 1) a custom or commercial front-end card combined with a commercial digitizer with in-house developed firmware and 2) a fully commercial off the shelf system.

Libera Single Pass H is an instrument intended for phase, position and charge monitoring in hadron and heavy ion LINACs. The instrument was tested at the ESS laboratory, to prove the feasibility of operation with ESS beam conditions. To give a realistic picture of the device performance, different testing setups were evaluated, including all the signal and environment conditions foreseen for the final ESS linac operation. The results present resolution, precision and accuracy evaluations, as well as stressful long-term and stability tests. This paper presents the achieved results of the Libera Single Pass H for the ESS beam parameters.

INTRODUCTION

During the evaluation of Libera Single Pass H, every parameter that was supposed to influence the instrument performance was treated as a degree of freedom. The measurements were carried out at the ESS laboratories within a 6 weeks time-frame, and the complete report on which this article is based, can be found in [1].

To determine the operating conditions in which the instrument is required to work (input signal levels and dynamic range, temperature variations), the analysis of the ESS beam and BPM characteristics was particularly useful, and it is presented in the next section. The third session explains how parameters like *resolution*, *precision*, *accuracy* are calculated, and for each one a definition is provided. Later on, a basic test setup for the measurements is presented, introducing the role of the most significant components.

Finally the phase and position measurements results are discussed and compared with the ESS requirements.

*This project has received funding from the European Union's Seventh Framework Programme for research, technological development and demonstration under grant agreement no 289485

ESS BUTTON BPMS

The ESS linac will include BPM detectors of different sizes and types, and a detailed overview is given in [2]. However, most of the detectors will be of electrostatic button type and according with the beam pipe size they will be of two different diameters: 60 and 100 mm. Table 1 introduces some ESS significant parameters which are useful to understand the signal characteristics.

Table 1: ESS Beam and BPM Parameters

Parameter	Value	Unit
RF frequency	352.21 and 704.42	MHz
Bunch repetition rate	352.21	MHz
Pulse repetition rate	14	Hz
Pulse duration	0.01 - 2.86	ms
Pulse current	6.25 – 62.5	mA
BPM diameter	60 and 100	mm
Button diameter	24 and 40	mm
Button capacitance	5.2	pF
Beam max displacement (with ref. to beam pipe)	50	%

It is possible to notice that even if the RF frequency changes from 352.21 to 704.42 MHz passing from the spokes section to the super-conductive linac, the bunch repetition rate remains the same. In terms of the BPM signals, this means that the fundamental harmonic is always at 352.21 MHz, and the other components are multiples of it.

Considering the Libera SPH capabilities, the instrument processes the first and the second harmonic, providing phase and position measurements for both of them.

BPMs Signal Levels

To estimate the signal levels coming from the BPMs, an analytical model of the beam and detectors is used. The expected signal levels for both harmonics are calculated according with the value of the influential parameters. Most are listed in Table 1: geometrical properties, beam current and b-factor all influence the amplitude of the BPM outputs. Considering the extreme cases, with a beam in the centre of the pipe:

- First harmonic ranges from -3.55 to -27.98 dBm
- Second harmonic ranges from -1.13 to -25.56 dBm

On the base of the same model, if the beam is 50% off-centred the signal coming from the closest button gains 8.72 dB while the opposite one loses 8.72 dB.

ISBN 978-3-95450-141-0

BEAM JITTER SPECTRA MEASUREMENTS OF THE APEX PHOTOINJECTOR*

H. Qian#, J. Byrd, L. Doolittle, Q. Du, D. Filippetto, G. Huang, F. Sannibale, R. Wells, J. Yang,
LBNL, Berkeley, CA 94720, USA

Abstract

High repetition rate photoinjectors, such as APEX at LBNL, are one of the enabling technologies for the next generation MHz class XFELs. Due to the higher repetition rate, a wider bandwidth is available for feedback systems to achieve ultra-stable machine and beam performance. In a first step to improve APEX beam stability, the noise spectra of the APEX laser beam and electron beam are characterized in terms of amplitude and timing. Related feedback systems are also discussed.

INTRODUCTION

The Advanced Photo-injector Experiment (APEX) is for demonstration of MHz repetition rate high brightness electron beam injection for the next generation high repetition rate free electron lasers [1]. APEX is staged in 3 phases. In phase 0, the 186 MHz normal conducting (NC) RF gun was successfully conditioned to achieve CW operation at nominal beam energy (750 keV) with low vacuum pressure performance (10^{-11} – 10^{-9} Torr). In phase I, several high QE photocathodes are being tested to demonstrate 0.3 mA beam current, and 6D beam phase space will be characterized at gun energy. In phase II, beam brightness will be more reliably demonstrated after being compressed by a buncher and accelerated by a 30 MeV NC pulsed linac.

Due to CW RF operation and MHz beam rep. rate, a wider bandwidth (BW) is available for feedback system, so ultrastable operation of the next generation FELs is being pursued [2]. Since photoinjector is one of the main noise sources, a tighter stability requirement has been put on photoinjectors like APEX, as shown in Table 1. With Phase I installed and in operation, efforts to characterize and improve APEX RF, laser and electron beam stability have been initiated.

Table 1: LCLS-II Injector Stability Requirements [3]

Injector Stability Parameters	RMS Tolerance
Bunch charge	1%
Timing jitter at injector exit	25 *f*s
Electron beam energy	0.01%
$\Delta x/\sigma_x$ and $\Delta y/\sigma_y$	1%

GUN RF STABILITY

Compared with the high frequency NC RF guns, APEX gun is special in terms of RF dependence of electron beam stability. Due to a low resonant frequency of 186 MHz, 1 degree of RF phase corresponds to 15 ps, which makes the electron beam energy much less sensitive to laser-RF timing jitter. Due to relatively low energy of 750 keV and inverse square dependence of drift space R_{56} on beam energy, beam arrival jitter before the linac booster becomes much more sensitive to RF amplitude jitter. In this sense, APEX gun behaves more like a DC gun.

In order to achieve the 25 *f*s arrival jitter at injector exit, the gun RF amplitude jitter is at least 7×10^{-5} rms without considering other jitter sources. Two feedbacks are implemented on the APEX gun RF, one is a slow feedback based on the cavity frequency tuner to keep the gun frequency on tune, and the other is a fast feedback based on the low level RF (LLRF) drive to keep the gun RF amplitude and phase stable [4]. A close-loop measurement shows gun RF amplitude and phase jitters are reduced to 2×10^{-4} and 0.01 degree respectively, as shown in Fig. 1, and gun dark current energy jitter measurement shows consistent result. The closed-loop amplitude stability of 2×10^{-4} includes strong components from a few lines at 6667 Hz, 6690 Hz, and 9672 Hz, which are out of the feedback BW. These lines show up in forward power and cavity pickup measurements, open and closed loop. Work is ongoing to identify and then eliminate the source of these lines in order to get below 10^{-4} RF amplitude stability.

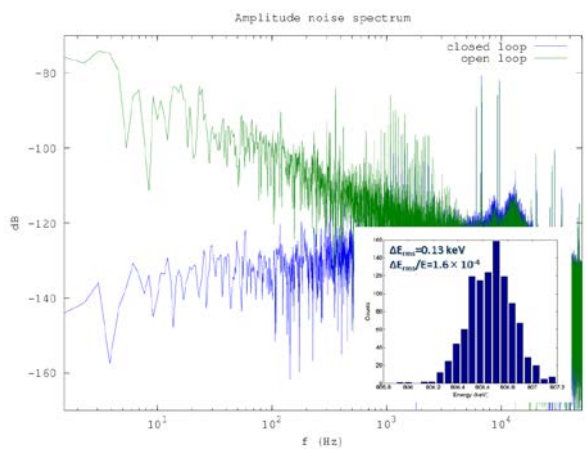

Figure 1: Gun RF amplitude jitter open and close loop (2×10^{-4}), insert shows consistent dark current energy jitter.

*This work was supported by the Director of the Office of Science of the US Department of Energy under Contract no. DEAC02-05CH11231
#hqian@lbl.gov

DEVELOPMENT OF A HIGH SPEED BEAM POSITION AND PHASE MONITORING SYSTEM FOR THE LANSCE LINAC*

H. Watkins#, J.D. Gilpatrick, R. McCrady, LANL, Los Alamos, NM 87544, USA

Abstract

The Los Alamos Neutron Science Center (LANSCE) is currently developing beam position and phase measurements (BPPMs) as part of the LANSCE risk mitigation project. BPPM sensors have been installed in the 805-MHz linac and development of the monitoring electronics is near completion. The system utilizes a high speed digitizer coupled with a field programmable gate array (FPGA) mounted in a VPX chassis to measure position, phase and bunched-beam current of a variety of beam structures. These systems will be deployed throughout the LANSCE facility. Details of the hardware selection and performance of the system for different timing structures are presented.

INTRODUCTION

Development efforts at LANSCE over the last year have been focused on creating a new electronics system to measure the beam position, bunched-beam current and phase of particles for the variety of time structures and species accelerated in the LANSCE 805-MHz side coupled linac. This system will replace the legacy ΔT system used during accelerator tune-up and also provide valuable transverse beam information during beam production which is not currently monitored.

ARCHITECTURE

The design of the system requires capturing signals from 4-electrodes of a beam position and phase monitor (BPPM) along with the accelerator reference signal. The signals are then conditioned to 201.25MHz RF waves. The five signals are then digitized and analyzed by a digital signal processor (DSP) to convert waveforms to position, phase and bunched-beam current. Processed data is provided to the end user through channel access managed by EPICS. [1] The system architecture is shown in Figure 1.

A high speed digitizer was selected to capture data at a 4-nanosecond time increments in order analyze beam position and phase variations that occur throughout the 1 millisecond pulse cycle. A field programmable gate array (FPGA) is being used for the DSP to analyze these signals in different timing modes such as long pulse (50 µsec), short pulse (150 nsec), and single shot (1 nsec).

A soft core processor, which resides in FPGA fabric, is used to store the results to the EPICS database for use by beam operators and other users.

Timing for synchronous measurements between BPPMs and beam specific information is provided by an event receiver connected to the master timer via optical links. The BPPM results are then stamped with the timing and beam species information prior to submission to the EPICS database. A real time operating system is used to collect data and match it with the correct timing information for each cycle of the beam.

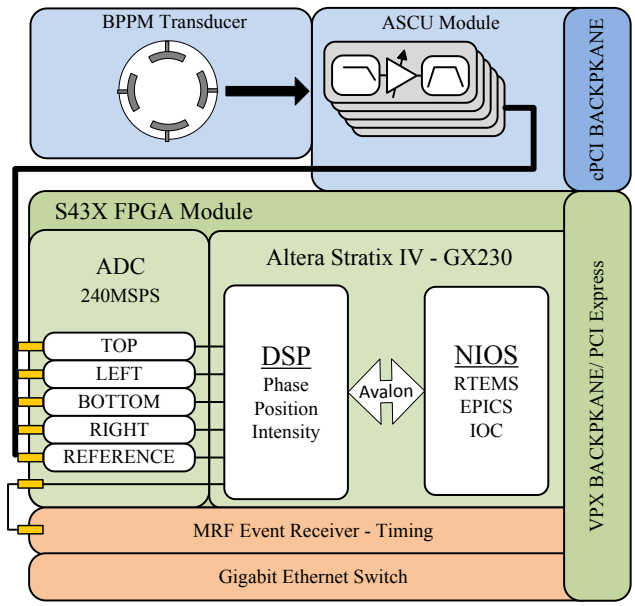

Figure 1: BPPM architecture.

REQUIREMENTS

The requirements for the BPPM system were broken up into two main regimes. The first regime is phase requirements that translate to time of flight (ToF) and energy measurements. These measurements are used to determine the phase set points for the acceleration modules. The second regime is position measurements that determine the transverse location of the beam centroid [2, 3].

*Work supported by the U.S. Department of Energy, Contract No. DE-AC52 06NA25396

hwatkins@lanl.gov

ISBN 978-3-95450-141-0

FRONT END CONCEPT FOR A WAKE FIELD MONITOR

M. Dehler, M. Leich, S. Hunziker, PSI, Villigen PSI, Switzerland

Abstract

Wake field monitors (WFMs) are used to directly measure the alignment between beam and RF accelerating structure via the transverse higher mode spectrum. As a sub task of the EuCARD^2 project, we are developing a front end for the monitors of the multipurpose X band structure installed at the SwissFEL Injector Test facility (SITF) at PSI. We plan to use electro optical technology offering strong advantages in the robustness to interference and radiation, and in the ease of signal transport. We present the concept of the device, discuss the theoretical performance in terms of noise. For a proof of principle, we built a basic system, which we tested together with the existing monitors with beam at SITF.

INTRODUCTION

Inside RF accelerating structures, the level of transverse wake fields responsible for emittance dilution is determined by the alignment between structure and beam. Wake field monitors (WFMs) are devices for the direct measurement of this effect by coupling to the transverse higher order modes (HOM) excited by the offset beam. This is specially of interest for X band structures used in low to medium energy accelerators like free electron lasers, where the beam degradation due to transverse single bunch wake fields is a much bigger concern.

For structure with HOM damping like those developed for the CLIC project, suitable signals can be extracted from the HOM couplers. More classical structures, like the multipurpose X band structures [1,2] developed in a collaboration between PSI, CERN and Sincrotrone Trieste, use special pickup geometries to couple to the internal wake fields inside the structure.

As part of the EuCARD^2 project [3]), we are in the process of developing front ends for these class of devices, to be used for the existing wake field monitors installed in SITF at PSI [4] and FERMI at Sincrotrone Trieste. Given the relatively high frequency and large bandwidth and the need to operate the front end in a radiation environment, we decided not to use a classical RF front end, but to use an electro-optical approach, which promises the following advantages:

- Technology already used in space communications, so there is considerable experience concerning the radiation hardness of the device.
- Use of optical fibers vs. hollow wave guides in classical RF, which are cheaper, more flexible to put, have much larger bandwidths, are ideal to carry signal over long distances and have virtually no problem with electromagnetic interference.
- Only minor amount of hardware exposed to the radiation in the tunnel, essentially only an optical modulator and a microwave limiter near the structure.
- Off the shelf components available for bandwidths up to 40 GHz (practically tested even up to 1.5 THz)
- Possible secondary applications for break down monitors, wide band wall current pickups etc.

Measurement Principle

Wake field monitors are not isolated devices, but integrated parts of RF acceleration structures, whose transverse wake fields they are measuring. Fig. 1 shows the inner volume of such a structure, which we are using as a signal source for the front end.

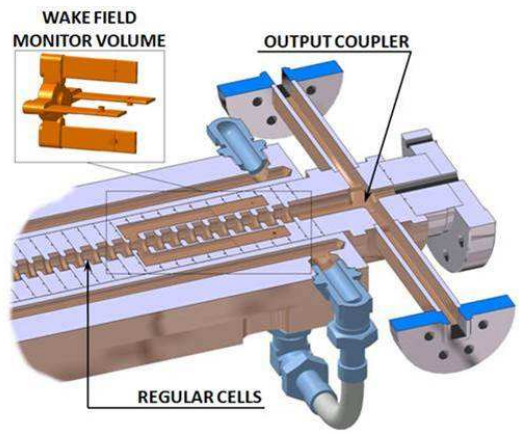

Figure 1: Wake field monitor inside a cutoff accelerating structure.

It is a 72 cell traveling wave structure working at the European X Band frequency of 11.9985 GHz. Its design employs a large iris, $5\pi/6$ phase advance geometry, which minimizes transverse wake field effects while still retaining a good efficiency. Its function in the FEL projects at PSI and Sincrotrone Trieste is actually not to accelerate the beam, but to compensate nonlinearities in the longitudinal phase space of the beam caused by prior acceleration stages [5].

One of the characteristics of its constant gradient structure design is the smooth variation of the cell dimensions along the structure, which compensates for internal losses and keeps the gradient of the fundamental mode constant. This leads to a spread of the synchronous frequency of the position dependent dipole modes over the 15-16 GHz region. Upstream, an offset beam will excite lower dipole mode frequencies than downstream. Also, the modes will not extend throughout the structure, but will be confined. To capture as much information as possible, two sets of monitors are used, one in the middle coupling to dipole modes in the upstream

ISBN 978-3-95450-141-0

BEAM-BASED CALIBRATION AND PERFORMANCE OPTIMIZATION OF CAVITY BPMS FOR SwissFEL, E-XFEL AND FLASH2*

B. Keil, G. Marinkovic, M. Stadler, Paul Scherrer Institute, Villigen, Switzerland
D. Lipka, DESY, Hamburg, Germany

Abstract

SwissFEL, the European XFEL (E-XFEL) and FLASH2 all use dual-resonator cavity beam position monitors (CBPMs) [1,2,3]. The CBPM electronics that is built by PSI has a larger number of calibration parameters that need to be determined in order to maximize the CBPM system performance. Beam measurements with the BPM electronics have been made in BPM test areas at the SwissFEL test injector and FLASH, as well as at FLASH2 where 17 E-XFEL type CBPMs have recently been installed in the undulator intersections. The CBPMs are pre-calibrated in the lab using an automated test and calibration system [4], and then the final calibration is done with beam. This report discusses beam-based methods to optimize the system performance by improving the pre-beam system calibration as well as the mechanical alignment of the BPM pickup position and angle.

PICKUPS

CBPM pickups with two resonators are the standard choice for measuring and stabilizing the beam orbit with highest resolution and lowest drift in the undulators of free electron lasers (FELs). The reference resonator measures the bunch charge, while the position resonator provides the product of bunch position and charge. The bunch position is thus obtained by normalizing position to reference resonator amplitude for the relevant monopole (reference) and dipole (position) modes, with a scaling factor that depends on the usually variable attenuation of the RF front-end (RFFE) input channels. All of the above mentioned FELs have CBPMs with cylindrical resonators and mode-selective couplers in the position resonator, where the frequencies of position and reference cavity modes are identical, thus minimizing the impact of frequency-dependent gain drift on the position readings.

Since the above mentioned FELs can also have several bunches with rather short bunch spacing (222ns for E-XFEL and FLASH, 28ns for SwissFEL), comparatively low loaded quality factors Q_L were chosen (see Table 1). This minimizes bunch-to-bunch crosstalk and keeps the effort and latency of the digital signal processing low, as required for the E-XFEL Intra Bunch Train Feedback (IBFB) [5]. Only in the SwissFEL undulators that have single bunches with 100Hz repetition rate, the CBPM pickups have a higher Q of ~1000 [6]. All E-XFEL CBPMs and the SwissFEL injector and linac CBPMs have stainless steel pickups with ~3.3GHz nominal frequency, which is safely below the cut-off frequency of the different beam pipe diameters. This allows using the same low-Q CBPM electronics for all machines [4,7]. In the following, the pickups will be named according to their beam pipe aperture, where e.g. CBPM16 is the 16mm aperture pickup of the SwissFEL linac.

Table 1: Overview of CBPM Pickups

	F [GHz]	Q_L	Aper-ture [mm]	Length [mm]
E-XFEL Transfer	3.300	70	40.5	255
E-XFEL/FLASH2 Undulators	3.300	70	10	100
SwissFEL Linac and Injector	3.284	40	38	255
	3.284	40	16	100
SwissFEL Undul.	4.855	1000	8	100

The E-XFEL CBPM10 and CBPM40 pickups developed by DESY have already been produced. First beam in the E-XFEL injector is expected spring 2015, first beam in the main linac end 2016. For the SwissFEL BPM pickups designed by PSI, the CBPM38 production is finished, while the CBPM16 pickups are ready for series production that will start shortly. Prototypes of the BPM8 pickup have recently been tested successfully with beam [6], where we have made a 3.3GHz stainless steel version with Q_L~200 and a 4.8GHz copper-steel hybrid version with Q_L~1000. Until recently the steel version had been the baseline since it is simpler and could have been operated with the standard 3.3GHz electronics with minor changes. However, after successful fabrication and test of the 4.8GHz pickup we made it the baseline version due to its higher expected resolution both at high charge (due to higher Q) and very low charge (due to higher sensitivity that improves with higher frequency). First beam in the SwissFEL injector is scheduled for end 2015, first main linac beam for end 2016.

Presently, three E-XFEL CBPM10 and three CBPM40 pickups are installed at the SwissFEL Injector Test Facility SITF at PSI, one more CBPM40 and three CBPM10 at FLASH1. At SITF, also one SwissFEL CBPM38, one CBPM16 and two CBPM8 (steel and copper version) are installed, see Figure 1. While these pickups are only intended for testing (with stripline and button BPMs used as "working horses" for normal machine operation), the recently installed 17 CBPM10 systems in the FLASH2 undulator intersections are needed for machine operation, but are also still part time

* This work has partially been funded by the Swiss State Secretariat for Education, Research and Innovation SERI.

ISBN 978-3-95450-141-0

LOW-Q CAVITY BPM ELECTRONICS FOR E-XFEL, FLASH-II AND SwissFEL*

M. Stadler#, R. Baldinger, R. Ditter, B. Keil, F. Marcellini, G. Marinkovic, M. Roggli, M. Rohrer
PSI, Villigen, Switzerland
D. Lipka, D. Nölle, S. Vilcins, DESY, Hamburg, Germany

Abstract

PSI has developed BPM electronics for low-Q cavity BPMs that will be used in the E-XFEL and FLASH2 undulators, as well as in SwissFEL injector, linac and transfer lines. After beam tests at the SwissFEL test injector (SFIT) and FLASH1, a pre-series of the electronics has been produced, tested and commissioned at FLASH2 [1]. The design, system features, signal processing techniques, lab-based test and calibration system as well as latest measurement results are reported.

INTRODUCTION

The European XFEL (E-XFEL) has a superconducting 17.5GeV main linac that will provide trains of up to 2700 bunches, with 0.1-1nC bunch charge range, 600µs train length, ≥222ns bunch spacing, and 10Hz train repetition rate. A kicker/septum scheme can distribute fractions of the bunch train to two main SASE undulator lines followed by "secondary undulators" for spontaneous or FEL radiation. The E-XFEL will provide SASE radiation down to below 0.1nm wavelength and supports arbitrary bunch patterns within a bunch train, with bunch spacing of n*111ns, where n is an integer >1.

The cavity BPM electronic system is being developed at PSI [2, 3, 4]. For detailed performance measurements of the E-XFEL undulator BPM system an array of 3 pickups have been installed both at the SwissFEL injector test facility [3] and FLASH1 [1]. 22 E-XFEL undulator BPM systems have recently been installed at the FLASH2 section [1].

CAVITY PICKUP

The 3.3 GHz cavity pickups used for FLASH2 and EXFEL undulator and transfer line sections were designed at DESY [5]. Sensitivity parameters are given in Table 1.

Table 1: EXFEL Cavity BPM Pickup Parameters (10mm Beam Pipe Aperture)

	position cavity (TM110 mode)	reference cavity (TM010 mode)
Resonant frequency	3300 MHz	3300 MHz
Sensitivity	2.8 mV/nC/µm	42 V/nC
Cavity loaded-Q	70	70
Aperture	10mm (undulator) and 40.5mm (transfer line)	

markus.stadler@psi.ch

* This work was partially funded by the Swiss State Secretariat for Education, Research and Innovation SERI

Due to the low bunch rate of only 28ns (double-bunch operation) the cavity pickup used in the SwissFEL linac and transfer line sections have a loaded-Q (Q_L) factor of 40. SwissFEL undulator BPMs use high-Q cavities with a Q_L of ~1000 and a frequency of 4.8 GHz.

Table 2: SwissFEL low-Q cavity pickup data

	BPM38	BPM16
Frequency (GHz)	3.284 GHz	3.284 GHz
Min. bunch separation (ns)	28 ns	28 ns
loaded-Q	40	40
aperture	38 mm	16 mm
Sensitivity (reference resonator in mV/nC/µm)	5.7	7
Sensitivity (position resonators in V/nC)	66	135

BPM ELECTRONICS

The present BPM electronics prototype consists of:

- The RF front-end electronics (RFFE): One I/Q downconverter for reference, x- and y-position signal channel, using a common LO synthesizer, and an ADC sampling clock synthesizer. Active local temperature stabilizer circuits are employed on the RFFE PCBs for drift reduction.
- 6-channel, 16-bit 160MS/s analog-to-digital converters for all RFFE I and Q baseband differential output signals.
- Digital signal processing hardware ("GPAC" board) for signal processing and interfacing to control, feedback, timing and machine protection systems.

Detailed description of the overall electronics is given in [2, 3, 5].

RF Frontend (RFFE)

The simplified block diagram of the RFFE electronics used is shown in Figure 1. The basic principle of the BPM electronics and cavity design is based on [3].

ISBN 978-3-95450-141-0

DEVELOPMENT OF THE SWISSFEL UNDULATOR BPM SYSTEM

M. Stadler#, R. Baldinger, R. Ditter, B. Keil, F. Marcellini, G. Marinkovic, M. Roggli, M. Rohrer
PSI, Villigen, Switzerland

Abstract

For SwissFEL, two types of cavity BPMs are used. In the linac, injector and transfer lines, low-Q dual-resonator cavity BPMs with a loaded-Q factors (Q_L) of ~40 and 3.3GHz mode frequency allow easy separation of the two adjacent bunches with 28ns bunch spacing. For the undulators that receive only single bunches from a beam distribution kicker with 100Hz repetition rate, dual-resonator BPM pickups with higher Q_L are used. The baseline version for the undulator BPMs is a stainless steel pickup with Q_L=200 and 3.3GHz frequency. In addition, an alternative version with copper resonators, Q_L=1000 and 4.8GHz frequency has been investigated. For all pickups, prototypes were built and tested. The status of pickup and electronics development as well as the latest prototype test results are reported.

INTRODUCTION

Due to different apertures in different parts of SwissFEL, three different BPM pickups are needed. While the injector and linac have BPM pickup apertures of 38mm ("BPM38") and 16mm ("BPM16), the undulator BPMs have 8mm ("BPM8").

Injector and Linac BPMs

The planned cavity BPM system for injector and linac is similar in architecture to that already developed by for E-XFEL and FLASH2 [1,2,3,4]. In order to independently measure position and charge of the two bunches with 28ns spacing (compared to 222ns for E-XFEL), the SwissFEL BPM38 and BPM16 pickups have a lower Q_L of ~40, compared to Q_L=70 for E-XFEL. The signal frequency is f_o=3.284 GHz for BPM38 and BPM16, which is still safely below the cut-off frequency of the larger (38mm aperture) beam pipe. Moreover, this frequency is an integer multiple of the machine reference clock frequency (142.8MHz), where the bunch spacing is four reference clock periods. As a result, both bunches have (nearly) the same IQ phase, which simplifies the algorithms for BPM signal processing and local oscillator phase feedback (see ref [3]). Finally, the choice of this frequency also allows direct reuse of large parts of the E-XFEL cavity BPM electronic system that also work at 3.3GHz (with a similar aperture of 40.5mm for the warm E-XFEL beam transfer lines), thus minimizing the development effort.

For Q_L=40 and f_o=3.284 GHz the resulting decay time $\tau=Q_L/(\pi \cdot f_o)$ of the BPM38 and BPM16 pickup signals is 3.9 ns. After 28ns, the cavity signal is decayed to <0.1% of the initial amplitude before the second bunch arrives, thus causing only negligible RF crosstalk between bunches. In order to be able to use the same 160MSPS ADCs like for E-XFEL, the RFFE shapes the output pulses for the two bunches such that enough samples for a sufficiently accurate computation of the beam position are available, using a simple algorithm in the BPM electronics FPGAs to eliminate any bunch-to-bunch crosstalk caused by the pulse shaper. Compared to pickups with high Q where overlapping pickup signals can have constructive or destructive interference, the low-Q RFFE output pulse shaper only causes small overlap of baseband amplitude signals, where a simple (scalar) subtraction of the overlapping signal pulses is sufficient to supress bunch-to-bunch crosstalk, without the necessity to use phase information.

The RMS noise requirements of the SwissFEL linac BPMs is <5µm for the 16mm aperture cavity and <10µm for the 38mm cavity (see Table 1) at 10-200pC bunch charge. Tests with a slightly modified E-XFEL BPM electronics have already demonstated sub-micron resolution for a BPM16 prototype pickup installed at the SwissFEL Injector Test Facility SITF [1].

Undulator BPMs

The BPMs in the SwissFEL undulator intersections have higher resolution and precision requirement than the linac and injector sections (see Table 1). From the experience gained with the E-XFEL and FLASH2 cavity BPM system we decided to use BPM pickups of the same basic structure, but with higher Q_L. The main reasons for this decision are:

1. In contrast to EXFEL, the SwissFEL undulators are operated in single bunch mode with 100Hz repetition rate, therefore we do not need a low Q_L to avoid bunch-to-bunch crosstalk of pickup output signals.
2. With higher Q_L, more data samples are available per bunch when using a similar ADC sampling rate. This reduces the impact of ADC noise on the BPM position noise and thus increases the ratio of measurement range to noise (for higher bunch charges), which is typically ~1000 for Q_L~40-70.
3. Direct digital quadrature downconversion from a finite IF frequency is able to eliminate systematic measurement errors due to phase and amplitude imbalance. Position and charge readings are thus less sensitive to sampling phase or bunch arrival fluctuations, increasing robustness and overall accuracy.

markus.stadler@psi.ch

ISBN 978-3-95450-141-0

COMMISSIONING RESULTS OF MICROTCA.4 STRIPLINE BPM SYSTEM*

C. Xu#, S. Allison, S. Hoobler, D. J. Martin, J. Olsen, T. Straumann, A. Young,
SLAC National Accelerator Laboratory, Menlo Park, CA 94025, USA
H. Kang, C. Kim, S. Lee, G. Mun
Pohang Accelerator Laboratory, Pohang, Kyungbuk, Korea

Abstract

SLAC National Accelerator Laboratory is a premier photon science laboratory. SLAC has a Free Electron Laser (FEL) facility that will produce 0.5 to 77 Angstroms X-rays and a synchrotron light source facility. In order to achieve this high level of performance, the beam position measurement system needs to be accurate so the electron beam bunch can be stable. We have designed a general-purpose stripline Beam Position Monitor (BPM) system that has a dynamic range of 10pC to 1nC bunch charge. The BPM system uses the MicroTCA (Micro Telecommunication Computing Architecture) for physics platform that consists of a 14bit 250MSPS ADC module (SIS8300 from Struck) that uses the Zone 3 A1.0 classification for the Rear Transition Module (RTM). This paper will discuss the commissioning result at SLAC LINAC Coherent Light Source (LCLS), SLAC Sanford Synchrotron Radiation Lightsource (SSRL), and Pohang Accelerator Laboratory (PAL) Injector Test Facility (IFT). The RTM architecture includes a band-pass filter at 300MHz with 30 MHz bandwidth, and an automated BPM calibration process. The RTM communicates with the AMC FPGA using a QSPI interface over the zone 3 connection.

NEW ELECTRONICS AND TEST SUITE

The test result presented at IBIC 2013 was conducted using a 16bit 125MSPS SIS8300 ADC module. After the conference, more tests were done using the 14bit 250MSPS ADC module on LCLS-I. In addition, more tests were moved to automate testing to decrease testing time and increase accuracy by eliminating operator error.

250MSPS ADC Module

With a 250MSPS ADC, the BPM electronic was able to capture two times the waveform data. With the faster ADC, a 30MHZ band-pass filter replaced the 15MHz band-pass filter used for the original electronic.

A narrower band-pass filter will produce a ringing signal with less amplitude comparing to a wider band-pass filter. By using a wider band-pass filter, it will increase the dynamic range of the BPM electronics by the square-root of the bandwidth factor (i.e., in our case $\sqrt{2}$). Figure 1 shows the comparison between 125MSPS system and 250MSPS resolution difference.

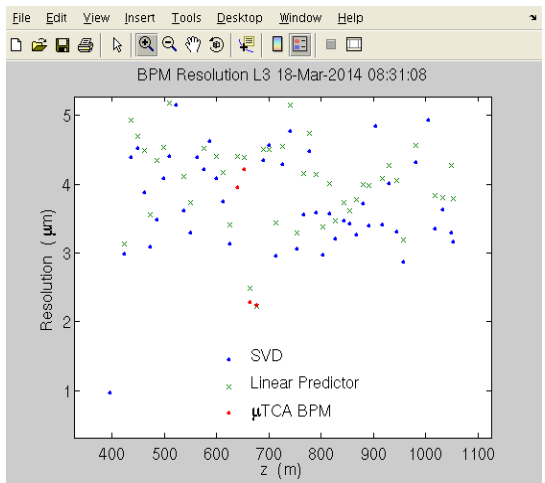

Figure 1: Resolution measurement with both 125Msa/s and 250Msa/s ADCs shown in red.

Automated Test Suite

To decrease the testing time for the eight BPM systems, an automated test suite was created using MATLAB and Python script. Each module was tested for signal to noise ratio (SNR), effective number of bits (ENOB), linearity test (IP3), attenuator linearity test, and simulated beam resolution. Two Agilent vector generators were controlled via SLAC intranet. The operator has the ability to choose between the full test and individual tests. Each test records the board serial number of the date the test is performed. Comparing to the original test duration, the test suite reduced the testing time by 75%. In addition, test results can be accessed later if needed.

POHANG ACCELERATOR LABORATORY – INJECTOR TEST FACILITY

In preparation for the new PAL FEL, PAL has constructed an injector test facility (ITF) to test instruments like TCAVs, modulators, BPMs, and other accelerator components. PAL asked SLAC to build seven BPM systems for the PAL ITF. The ITF is composed of two Kystrons and one TCAV for beam

*This work supported by the U.S. Department of Energy, Office of Science, SLAC National Accelerator Laboratory under Contract No. DE-AC02-76SF00515 and WFOA13-197.

#charliex@slac.stanford.edu

BPM DATA CORRECTION AT SOLEIL

N. Hubert, B. Béranger, L. S. Nadolski, Synchrotron SOLEIL, Gif-sur-Yvette, France

Abstract

In a synchrotron light source like SOLEIL, Beam Position Monitors (BPM) are optimized to have the highest sensitivity for an electron beam passing nearby their mechanical center. Nevertheless, this optimization is done to the detriment of the response linearity when the beam is off-centered for dedicated machine physic studies. To correct for the geometric non-linearity of the BPM, we have applied an algorithm using boundary element method. Moreover the BPM electronics is able to provide position data at a turn-by-turn rate. Unfortunately the filtering process in this electronics mixes the information from one turn to the neighboring turns. An additional demixing algorithm has been set-up to correct for this artefact. The paper reports on performance and limitations of those two algorithms that are used at SOLEIL to correct the BPM data.

INTRODUCTION

BPM Block Description

SOLEIL BPM blocks have been designed to optimize the position measurement resolution for a centred beam. Its geometry is the same as the one that is generally used in the other parts of the machine (all arcs) for impedance reasons. Aperture is 84 mm in horizontal and 25 mm in vertical. Electrodes are circular buttons of 10 mm diameter spaced by 16 mm in horizontal and 25 mm in vertical (Fig. 1).

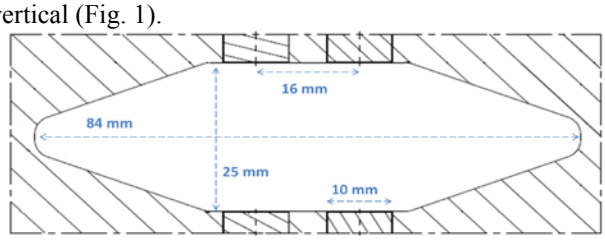

Figure 1: Cross section of a BPM. Design optimizes the resolution in the centre of the chamber.

Non Linear BPM Response

The beam position measurement is given by the usual "difference over sum" method:

$$X_{POS} = K_X \times \frac{(\Phi_A + \Phi_D) - (\Phi_B + \Phi_C)}{\Phi_A + \Phi_B + \Phi_C + \Phi_D} \quad (1)$$

$$Z_{POS} = K_Z \times \frac{(\Phi_A + \Phi_B) - (\Phi_C + \Phi_D)}{\Phi_A + \Phi_B + \Phi_C + \Phi_D} \quad (2)$$

With Φ_i the potential read on electrode (A, B, C and D), and K_X, K_Z the geometric factor for each transverse plane.

This commonly used formula is linear for a centred beam but becomes strongly nonlinear in the horizontal plane when the beam goes to large amplitudes, typically above ±2 mm (Fig. 2).

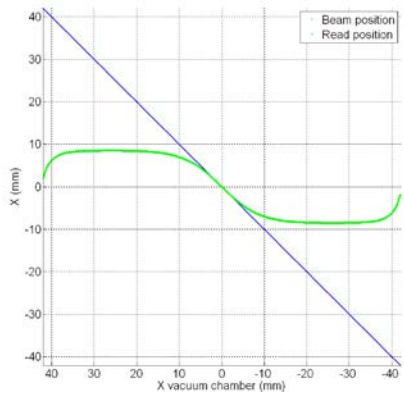

Figure 2: Read beam position (green) with respect to the real beam position (blue) in the horizontal plane for a centred beam in vertical plane. Linear region is limited to ± 2mm around the BPM centre.

CORRECTION OF THE NON LINEAR BPM RESPONSE

Theoretical Reconstruction

Beam position can also be reconstructed from the potential read on the four electrodes. The method used is based on a preliminary theoretical calculation of the BPM response [1, 2, 3]: knowing the theoretical beam position, potential on the four electrodes is calculated using the Poisson equation and the boundary element method. This step requires the definition of a mesh to slice the vacuum chamber wall into elementary parts. Then, in a second step the theoretical BPM response is inverted using the standard Newton method. This method gives a very good beam position reconstruction (Fig. 3) for a large area (~± 15 mm in H, ~±8 mm in V around the BPM centre), compared to the difference over sum method.

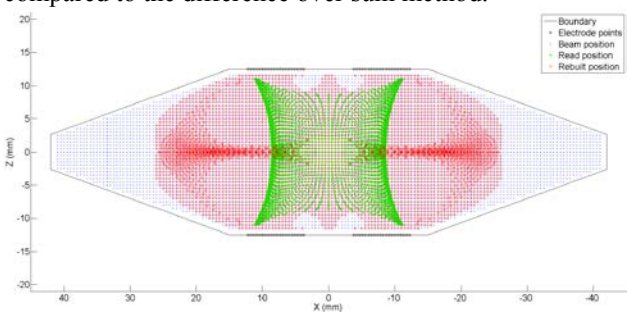

Figure 3: Reconstruction of the position of the beam (blue points) using the difference over sum method (green points) and the Newton inversion (red points).

ISBN 978-3-95450-141-0

DESIGN OF A NEW BLADE TYPE X-BPM

N. Hubert, N. Béchu, J. Dasilvacastro, L. Cassinari, J-C. Denard, M. Labat, J-L. Marlats, A. Mary,
Synchrotron SOLEIL, Gif-sur-Yvette, France
S. Marques, R. Neuenschwander, LNLS, Campinas, Brazil

Abstract

A new photon Beam Position Monitor (X-BPM) design has been developed in collaboration between the Brazilian Synchrotron Light Laboratory (LNLS) and SOLEIL Synchrotron [1]. This blade-type X-BPM has been carefully studied in order to minimize beam current dependence and temperature dependence. The main advantage of the design is a better stability compared to the standard X-BPMs initially installed at SOLEIL. This new design is used for the new X-BPMs installed at SOLEIL and is being considered for the bending magnet front-ends of the future SIRIUS [2] light source. A first "double" unit has been constructed by LNLS for the two canted Anatomix and Nanoscopium SOLEIL beamlines, and has been installed at SOLEIL in May 2014. Design and first results are presented.

INTRODUCTION

X-BPMs are used in synchrotron machines to monitor the photon beam position in the beamline frontend. They are composed of a stand and a head that supports four blades placed in the photon beam halo (Fig. 1).

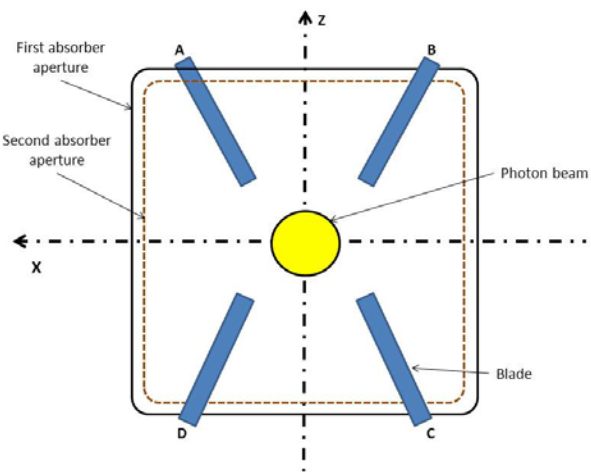

Figure 1: Layout of an X-BPM using blade signals for position measurements of a photon beam produced by an insertion device.

Taking benefit of the photoemission principle, the photon beam will create on each blade a current that vary with the distance between the beam and the blade. The centre of mass of the photon beam is then deduced using the classical difference over sum equation:

$$X_{POS} = K_X \times \frac{(I_A + I_D) - (I_B + I_C)}{I_A + I_B + I_C + I_D} \quad (1)$$

$$Z_{POS} = K_Z \times \frac{(I_A + I_B) - (I_C + I_D)}{I_A + I_B + I_C + I_D} \quad (2)$$

With I_i the current read on blade (A, B, C and D), and K_X, K_Z the horizontal and vertical geometric factors, for photon beams produced by an undulator. In the case of bending magnet or wiggler photon beams, only the vertical position is measured by two pairs of blades.

At SOLEIL, 21 X-BPMs are already installed on undulator beamline frontends, whereas 11 are installed on bending magnets/wiggler beamline frontends.

At LNLS, in total, four X-BPMs are installed, two X-BPMs in the U11 undulator front-end and other two in the bending magnet X-Ray diagnostics beamline.

STABILITY REQUIREMENTS

In its original design, the X-BPM was made of a head supported by a stand, both made of stainless steel (Fig. 2). This design was subject to mechanical deformation in case of temperature variations like tunnel air temperature drifts or changes in the heat load deposited on the X-BPM by the beam. As a consequence, photon beam position reading could be impacted by a few µm, in particular during the few tens of minutes following a reinjection (in case of beam loss).

For beamlines requiring a high stability, the stand has been made of INVAR to reduce its vertical expansion. This expansion was consequently reduced from 3 µm (stainless steel) to 0.3 µm (invar) for a 0.2 °C temperature variation.

Then it has also been decided to study a new X-BPM head to minimize the position dependence to the heat load variations. This work has been done in collaboration between SOLEIL and LNLS.

Since a 3rd generation light source is currently under construction at LNLS, the new concept of XBPM has been considered as candidate solution for all bending magnet beamline front-ends and possibly for some undulator beamlines.

MECHANICAL DESIGN

When designing the new X-BPM head, efforts have been focussed on an optimized power dissipation to minimize the effect on the position measurement.

Symmetrical Thermal Expansion

In its new design, the X-BPM head presents a (beam) axial symmetry, and is fixed to the stand by a cradle in the beam plane. The heat load deposited by the beam is supposed to be homogeneous around its axis which is true

ISBN 978-3-95450-141-0

COMMISSIONING OF THE ALBA FAST ORBIT FEEDBACK SYSTEM

A. Olmos, J. Moldes, R. Petrocelli, Z. Martí, D. Yepez, S. Blanch, X. Serra, G. Cuni, S. Rubio,
ALBA-CELLS, Barcelona, Spain

Abstract

The ALBA Fast Orbit FeedBack system (FOFB) started its commissioning phase in September 2013, when all the required hardware was installed and the development of different controls for the feedback started. This report shows our experience tuning the different parameters to setup the system, together with vibration and beam noise measurements at different conditions. Finally, the present results and future steps for this system are described.

FOFB DESCRIPTION

ALBA Synchrotron machine is an already running facility providing beam for users in decay mode (2 injections per day). Even though ALBA has been demonstrated to be a low noise machine, the near use of a Top-up injection mode [1] will demand a better and faster feedback than the current Slow Orbit FeedBack (SOFB). Description of the FOFB layout and the different devices of the system has been already presented on IBIC13 [2]. A description of what have been done during the commissioning and the bottlenecks we have found is reported here.

Correction Calculation and GUI

Most of the effort and time during the last year has been dedicated to the development of the correction code and all required controls associated infrastructure. Correction algorithm runs on the 16 distributed CPUs where the Beam Position Monitors (BPMs) data is transferred to and the new setpoints for the correctors power supplies are computed. Testing of different CPUs has been performed in order to find the ideal hardware to match the FOFB requirements. Performance of one and two cores CPUs has been demonstrated to be not sufficient, since some of the 100 us loops of the FOFB are lost when using these CPUs [3]. Final solution using 4 cores CPUs matches the requirements, especially after the distribution of the different processes to the different cores: one core to do BPMs position data reading, another to perform correction calculation and power supplies interfacing and the other cores to take care of interruptions, handling of operating system, …

Each CPU runs a C correction code that retrieves the position data from the PMC FPGA Board [2]. Correction computation is based on broadly used SVD algorithm and a PI loop controller. 16 TANGO device servers are running on the 16 cPCI crates hosting the CPUs, while a high level device server controls the whole system. A preliminary Graphical User Interface (GUI) has been developed for the commissioning phase of the FOFB, from where we can start/stop the feedback system and set the PI and RF frequency loops parameters (Fig. 1).

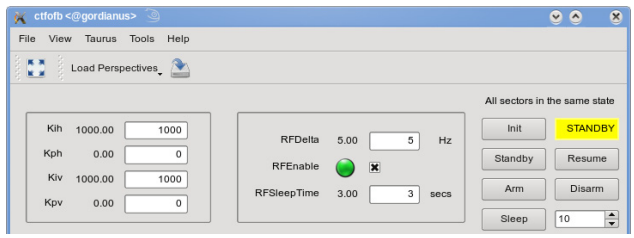

Figure 1: Commissioning FOFB GUI.

PI Controller

Different implementations of the PI loop after the SVD calculation have been tested, being the one showed on Fig. 2 the implementation that gave best results.

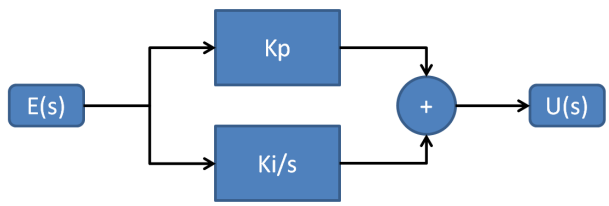

$$U(n) = U(n-1) + A0 * E(n) + A1 * E(n-1)$$

$$A0 = (Ki * Ts / 2) + Kp$$

$$A1 = (Ki * Ts / 2) - Kp$$

Figure 2: PI loop implementation.

Last version of the correction code has separated PI loops for horizontal and vertical plane, since the feedback requirements and beam noise are different depending on the plane.

RF Frequency Control

Our intention is to run just the FOFB during operation, without SOFB. That means that the control of the RF frequency has to be moved from the SOFB, running nowadays as a Matlab MiddleLayer routine, to the FOFB system. Decision has been taken to implement a routine on the high level FOFB device server that monitors the dispersive pattern on the correctors and changes RF frequency in case it is needed. Minimum frequency step and the correction periodicity will be modified from the main FOFB GUI.

System Limitations

Related with the RF frequency control, one of ALBA limitations is that we don't have fast and slow correctors, so the RF frequency cannot be handled in separate power supplies from the FOFB correction.

ISBN 978-3-95450-141-0

NEW FEATURES AND MEASUREMENTS USING THE UPGRADED TRANSVERSE MULTIBUNCH FEEDBACK AT DIAMOND

G. Rehm, M.G. Abbott, A.F.D. Morgan, Diamond Light Source, Oxfordshire, UK

Abstract

A Transverse Multi-Bunch Feedback has been used in the Diamond Storage Ring for the stabilization of instabilities since 2007. Following a recent upgrade of the FPGA code and EPICS layer, a set of new features is now available to support operation and machine development: Firstly, a bunch by bunch choice of feedback filter allows for better stabilization of a single high charge bunch in a hybrid fill pattern. Secondly, complex grow-damp experiments are now possible using a sequencer of internal states allowing precise measurements of the damping rates on a mode by mode basis. Thirdly, a phase locked loop excitation and detection has been implemented to allow both extremely fast (kHz update rates) and extremely precise tracking of the betatron tune frequencies. Finally, short FIR filters on the ADC input and DAC output enable a fine tuning of the impulse response to provide maximum bunch to bunch isolation, as for instance required for efficient bunch cleaning.

INTRODUCTION

At Diamond we stabilise transverse oscillations of the bunches with two FPGA based Transverse Multi-Bunch Feedback (TMBF) processors, one operating horizontally, one vertically. Each processor is a Libera Bunch-by-Bunch from Instrumentation Technologies [1], packaged as a 1U unit containing 4 14-bit ADCs running at 125 MHz, a Virtex-II Pro FPGA clocked at 125 MHz, a 14-bit DAC running at 500 MHz, and an embedded Single Board Computer (SBC) ARM microprocessor running Linux to provide the control system.

The system was delivered as a basic development platform with interfacing software on the Linux board and a layer of FPGA code for interfacing to the external signals and the processor board. The initial implementation of the Transverse Multi-Bunch Feedback (TMBF) processor was done at Diamond [2] based on work at the ESRF [3]. The Diamond implementation consists of FPGA code together with an EPICS driver running on the embedded processor board.

Diamond has been using transverse multibunch feedback since 2007 [4]. The firmware and software have continued to develop and include functionality beyond the pure feedback action required for suppression of multibunch instabilities, most importantly a numerically controlled oscillator (NCO), which can be used to excite bunches and detect their oscillation in phase with the excitation.

The developments described in this paper provide support for more detailed measurements, finer control, and more complex experiments. In particular, the following major functionality has been added in a recent upgrade of FPGA and EPICS firmware:

- Input (ADC) and Output (DAC) gain pre-emphasis using a 3 point FIR to compensate the frequency response of various system components.
- Program sequencing, allowing a sequence of different control parameters to be applied to the beam at the same time as data capture.
- Tune detection and fast following via a phase locked loop (PLL) excitation of either one or many bunches.
- Concurrent swept tune measurements on up to four individual bunches.
- Separate feedback parameters for individual bunches. For example, we can now use one feedback filter for the hybrid bunch and a different filter for the rest of the fill.

Details of the implementation have been previously published [5, 6]. This paper will present results from some of the new types of measurements and operational modes that are enabled by the new features of the TMBF.

FREQUENCY RESPONSE CORRECTION

If a TMBF is employed purely for stabilisation using a turn-by-turn FIR filter applied to each bunch individually, this may be understood as a time invariant linear response system (within the linearity limits of the hardware). As such, the only effect of the broadband frequency response from DC to half sampling frequency will be a variation of damping efficiency as a function of frequency or mode number.

However, once different filters or even excitations are applied to individual bunches, the system is no longer time invariant. In that case, it becomes important to ensure the frequency response is as flat as possible (impulse response as sharp as possible). It is also not sufficient to apply a round trip frequency response correction just in one place (for instance before the DAC), as this would compensate for all errors (also from the ADC) by applying a corrected impulse response to the bunches. Instead, there need to be separate corrections before the DAC (to compensate for the effects of the DAC, power amplifier and strip lines), and after the ADC (to compensate for the effects of the hybrids, low level RF and ADC). In this way maximum isolation between bunches both in acting on them and in reading back their position can be achieved.

We have shown previously how we optimised the impulse response (equivalent to optimising the frequency response)

ISBN 978-3-95450-141-0

UPGRADE DEVELOPMENT PROGRESS FOR THE CERN SPS HIGH BANDWIDTH TRANSVERSE FEEDBACK DEMONSTRATION PROCESSOR*

J. E. Dusatko, J. M. Cesaratto, J.D. Fox, C.H. Rivetta
SLAC National Accelerator Laboratory, Menlo Park, CA, USA
W. Hofle, CERN, Geneva, Switzerland
S. De Santis, LBL, Berkeley, CA, USA

Abstract

A high bandwidth feedback demonstrator system has been developed for proof of concept transverse intra-bunch closed loop feedback studies at the CERN SPS. The system contains a beam pickup, analog front end receiver, signal processor, back end driver, power amplifiers and kicker structure. The main signal processing function is performed digitally, using very fast (4 GS/s) data converters to bring the system signals into and out of the digital domain. The digital signal processing is itself implemented in an FPGA allowing for maximum speed and flexibility. The signal processor is a modular design consisting of commercial and custom components. This approach allowed for a rapidly-developed prototype to be delivered in a short time with limited resources. Initial beam studies at the SPS using the system prior to the CERN long shutdown one (LS1) have been very encouraging. Building on this success, we are planning several key upgrades to the system, including the signal processor. This paper describes these key upgrades and reports on their progress.

OVERVIEW AND UPGRADES TO THE DEMONSTRATION SYSTEM

The high-current operation of the SPS for HL-LHC injection will require mitigation of possible Ecloud and TMCI driven intability effects [1]. A single-bunch wideband digital feedback system (Fig. 1) was initially commissioned in November 2012 and used through the February 2013 SPS LS1 shutdown. During the CERN LS1 interval we are upgrading the Demonstration system to add functions necessary to validate a full-featured control system.

PHASE I UPGRADES

The Demo system [3] was rapidly developed in 2012 and the first operational version included a snapshot mode that captures 32000 turns of digitized bunch motion. This data can be processed offline to study beam motion in the frequency domain and see changes in the beam motion as the feedback parameters are varied. The original studies contained some hard to understand narrowband spectral features that were not from the beam, but instead from interactions with the SPS RF and timing systems, as well as some internal digital clocks which were visible roughly 8 - 10 dB above the digitizer noise floor. As part of the upgrade, the A/D boards were relocated within the system chassis, grounded to a common copper plate and the narrowband interferring signals are now neglible. Additional studies and development of the RF and sampling clock signals have also been completed and we anticipate the next round of measurements to be free of the spurious interferring signals.

The beam dynamics measurements use an excitation/response formalism with chirps applied to the beam while the response is recorded. In these first measurements the existing 4 GS/s excitation system [2] was used to excite the beam with an analog summation of the feedback signal into the power amplifier input. These measurements required careful synchronization and alignment of the excitation system, feedback system and beam signals. As an upgrade, we have integrated the excitation system function within the demo system, so that the same system clocks drive the excitation sequence and the DSP aquistion and filter functions, so the summation of the excitation signal and filter output is now a digital addition with controlled saturation and gain.

The second major improvement is a phase-locked loop for system clocks. The DAC device (Maxim Semi MAX19693) does not have a mechanism to resynchronze its 4:1 input data mux, for many frequency domain applicationsthis is not a concern. This arbitrary synchronization meant that the excitation sytem and DSP processing had to be manually timed for each set of measurements, or after any interruption of the system power or clocks. The upgraded system uses a phase lock technique to adjust the phase of the input clocks to the D/A so that the divided parallel data clock is always consistently syncronized to the beam. This important upgrade makes the system timing repeatable and consistent from measurement to measurement. It also provides a path for a future upgrade allowing energy ramping and compensation for vaiations in synchronous phase and system timing with acceleration. In conjunction with the new operating modes, the system operator's interface has been simplified and expanded.

WIDEBAND KICKER STRUCTURES AND POWER AMPLIFIERS

A kicker structure to apply correction fields to the beam is a critical system function. A July 2013 design report

* Work supported by the U.S. Department of Energy under contract # DE-AC02-76SF00515 and the US LHC Accelerator Research Program (LARP).

ISBN 978-3-95450-141-0

BUNCH-BY-BUNCH FEEDBACK SYSTEMS AT THE DELTA STORAGE RING USED FOR BEAM DIAGNOSTICS*

M. Höner†, S. Khan, M. Sommer
Center for Synchrotron Radiation (DELTA), TU Dortmund University, Dortmund, Germany

Abstract

At the 1.5-GeV electron storage ring DELTA operated by the TU Dortmund University, a bunch-by-bunch feedback system was installed in 2011. Since then, it is in operation for different beam diagnostic purposes. A fast analysis of bunch-position data allows a real-time multibunch mode analysis during machine operation. In addition, the data analysis can be triggered by external events, e.g. beam losses or the injection process. In this paper, a feedback-based method to measure the damping times of multi-bunch modes is presented. Furthermore, a chromaticity-dependent single-bunch instability is analyzed. Finally, the use of the feedback system in the presence of an RF-phase modulation is presented.

INTRODUCTION

In 2011, a digital bunch-by-bunch feedback system [1] was installed at the 1.5-GeV electron storage ring DELTA (Fig. 1, Table 1) for beam diagnostics purposes [2, 3] and to suppress longitudinal and transverse coupled-bunch instabilities. The system comprises processing units for the longitudinal, horizontal and vertical plane as well as a common frontend and backend. In user operation, ~144 out of 192 buckets are filled with a beam current up to 130 mA (3/4 filling pattern). Longitudinal coupled-bunch modes show up above a current threshold of ~75 mA, while transverse instabilities are rarely observed. A modulation of the RF phase is routinely applied [4, 5] to suppress longitudinal instabilities and to improve the beam lifetime by reducing the mean electron density and thus the rate of Touschek scattering.

Ultrashort radiation pulses in the VUV and THz regime are generated since 2011 by an interaction of femtosecond laser pulses with an electron bunch of enhanced current [6]. For this purpose, the storage ring is either filled with a single bunch during dedicated machine shifts or with a hybrid filling pattern (an additional bunch in the gap of the 3/4 filling pattern). One purpose of the longitudinal feedback system is to suppress longitudinal oscillations of the bunch interacting with the laser pulses.

In addition, the feedback system is used to provide post-mortem data on the bunch motion preceding beam losses [3] and to study the beam dynamics under various circumstances. One example is to record the bunch motion during the injection process [2, 3], other more recent examples are descibed below.

* Work supported by the BMBF (05K13PEC).
† markus.hoener@tu-dortmund.de

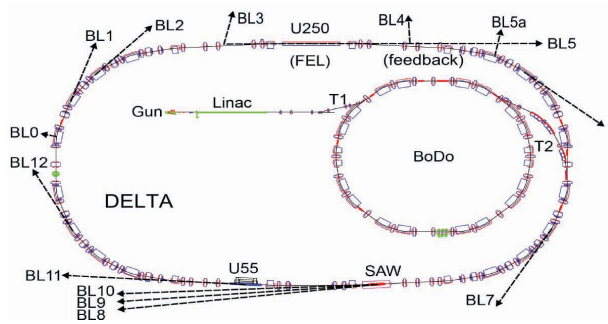

Figure 1: Overview of the DELTA facility including the storage ring and its booster synchrotron (BoDo).

Feedback Setup

To extract the horizontal, vertical and longitudinal position of every single bunch, the signals from a beam position monitor with four symmetrically arranged buttons are combined in a hybrid network to extract the horizontal and vertical differential signal as well as the sum signal. The three resulting signals are stretched using a two-cycle comb-filter in the feedback frontend and are mixed with a 1.5-GHz reference signal. The resulting signals are filtered by a low-pass filter. Using phase shifters and attenuators, the mixed signals can be adjusted to be either phase sensitive (longitudinal position) or amplitude sensitive (transverse position). Finally, the signals are digitized by 12-bit ADCs in the feedback processing units. By applying a 24-tap FIR filter on consecutive input data, the output signals are created, which are converted to analog signals driving the power amplifiers and the corresponding kicker structures [7]. In the longitudinal plane, the output signal is mixed up to 1.5 GHz in the feedback backend before being sent to the amplifier. In addition to an FIR-filter, the processing units include a frequency generator, which allows to send a dedicated RF signal to the beam, e.g. to excite specific multibunch modes, as shown in the next section.

Table 1: Storage Ring Parameters

parameter	value
revolution frequency	2.6 MHz
RF frequency	500 MHz
nominal RF power	25 kW
maximum beam current (multibunch)	130 mA
maximum beam current (single bunch)	20 mA
synchrotron frequency	15.7 kHz
fractional horizontal tune	0.10
fractional vertical tune	0.28

ISBN 978-3-95450-141-0

COMMISSIONING OF BUNCH-BY-BUNCH FEEDBACK SYSTEM FOR NSLS2 STORAGE RING*

W. Cheng#,1, B. Bacha[1], D. Teytelman[2], Y. Hu[1], H. Xu[1], O. Singh[1]
[1] NSLS-II, Brookhaven National Laboratory, Upton, NY 11973
[2] Dimtel Inc., San Jose, CA 95124

Abstract

Transverse bunch by bunch feedback system has been designed to cure the coupled bunch instabilities, caused by HOM, resistive wall or ions. The system has been constructed, tested and commissioned with beam. Preliminary studies show that the feedback system can suppress single bunch instability as well as coupled bunch instabilities. Mode analysis of the unstable coupled bunch motion reveals fast ion instability exist even at relative low current.

INTRODUCTION

As the newest third-generation light source, NSLS2 at Brookhaven National Laboratory has been constructed and commissioned recently. 50mA stored beam has been achieved without insertion devices [1]. Insertion devices commissioning and user operation will follow in the near future. NSLS2 storage ring will have < 1nm.rad horizontal emittance by using weak dipoles together with damping wigglers. For the storage ring of 792m circumference, geometric impedance, resistive wall impedance and ion effects are expected to be significant. A transverse bunch-by-bunch feedback system has been designed to suppress the coupled bunch instabilities. More information can be found in previous papers [2,3].

Pickup signals for transverse feedback system are coming from button BPMs. Broadband RF front end electronics detect the bunch to bunch positions separated by 2ns, which is then digitized and processed to get the correction signal. The correction signal can be precisely timed to act on the individual bunches come back in one turn. Dimtel's iGp12 digitizer [4] was selected for NSLS2 bunch by bunch feedback. It has EPICS driver and graphical operation panel integrated and other diagnostic features like bunch cleaning, transfer function measurement and others.

High power amplifiers from Amplifier Research are fully controlled through LAN/RS232 gateway remotely. Amplifier gain, forward power, reverse power and other status can be monitored/controlled from the CSS panel. There are temperature sensors installed on the stripline kicker feed-throughs and chambers. These RTD's temperature data will supply health information of the kicker, especially when the machine is running at high current.

*Work supported by DOE contract No: DE-AC02-98CH10886.
#chengwx@bnl.gov

KICKER PERFORMANCE

As the feedback actuator, stripline kicker was designed to have sufficient high shunt impedance and minimized beam impedance. The stripline kicker has two 30cm long plates housed in round chamber with inner radius ~ 39mm. The chamber inner surface and plates are copper coated. Each plate was fed by a 500W broadband amplifier though 1/2'' Heliax cables.

Figure 1 shows one assembled stripline kicker and its TDR measurement result. Between the cursors were the 30cm (1ns) plate. The plate was matched to 50 Ohm. The dip was coming from vacuum feedthrough ceramic seal.

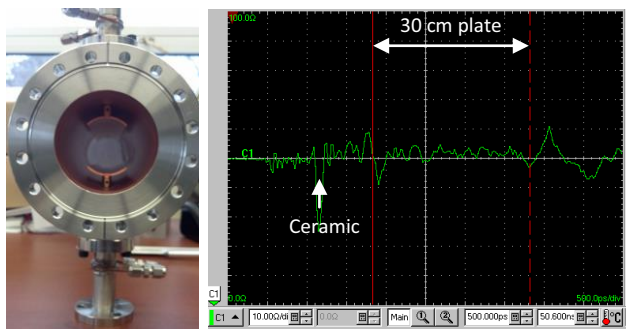

Figure 1: Assembled Stripline kicker (left) and TDR measurement response (right).

Installed stripline frequency response, together with high power amplifier, long Heliax cables and 500W attenuator, were measured using network analyzer, as shown in Fig. 2. In the working frequency range of 0-250 MHz, gain flatness is about 3dB. Phase response is less than 5 degrees difference in the range.

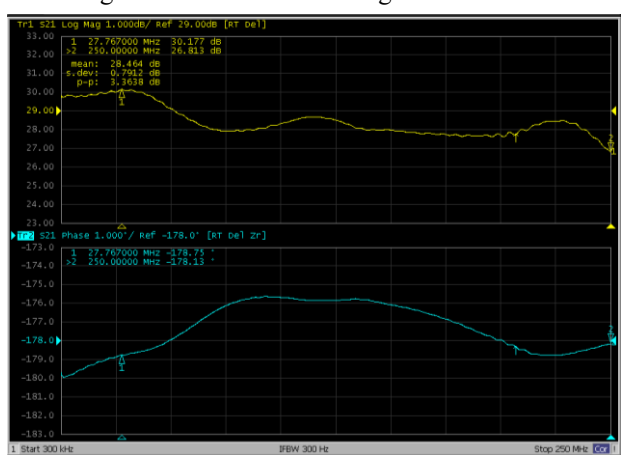

Figure 2: Network analyzer measured amplitude and phase response, including high power amplifier, stripline kicker, Heliax cables and attenuator.

ISBN 978-3-95450-141-0

COMMISSIONING OF THE FLASH2 ELECTRON BEAM DIAGNOSTICS IN RESPECT TO ITS USE AT THE EUROPEAN XFEL

N. Baboi# and D. Nölle, DESY, Hamburg, Germany,
for the electron beam diagnostics team

Abstract

This report presents the first operation experience of the electron beam diagnostics at FLASH2. FLASH2 is a new undulator line at the FLASH linac at DESY. Most electron beam diagnostics installed, like the beam loss monitors, cavity beam position monitors, toroids, beam halo monitors, have been designed for the European XFEL, and will provide operational experience beforehand. A few systems, as for example the button beam position monitors and the ionization chambers, have been developed for FLASH. The controls use the new MTCA.4 standard. Both linacs, FLASH and the European XFEL, require similar performance of the diagnostics systems. Many beam parameters are similar: bunch charge of 0.1 to 1 nC, pulse repetition frequency of 10 Hz, while others will be more critical at the XFEL than the ones currently used at FLASH, like the bunch frequency of up to 4.5 MHz. versus 1 MHz. The commissioning of FLASH2 and its diagnostics is ongoing. The beam monitors have accompanied the first beam through the linac, fine tuning for some systems is still to be done. The achieved performance will be presented in view of their use at the European XFEL.

INTRODUCTION

The FLASH linac at DESY, Hamburg has recently been upgraded with a second undulator beamline, FLASH2, in order to increase the number of user beamlines [1,2]. FLASH is a Free Electron Laser (FEL) based on Self Amplified Spontaneous Emission (SASE-FEL). It produces ultra-short, highly intense photon beams typically in the range from 45 down to 4.2 nm.

In order to make use of the synergies between the FLASH facility and the European X-ray Free Electron Laser (E-XFEL) [3], many of the diagnostics components installed in FLASH2 are the same or similar to the ones developed for the E-XFEL [4,5]. Some are similar to the old FLASH components, and others have been designed especially for FLASH2. This paper gives an overview of the diagnostics installed in FLASH2 and reports on the first operational experience.

Overview of the FLASH Linac

Figure 1 shows schematically the layout of FLASH. Two independent lasers are sent to the Cs_2Te cathode, placed on the back plane of the 1.5-cell RF-gun, to produce, within the same RF pulse, the beam for each of the two electron beamlines, FLASH1 and FLASH2. In the following FLASH will denote either the whole facility or the common, accelerating part.

The electron beam is accelerated to an energy of up to 1.25 GeV by 7 cryo-modules, each containing 8 TESLA cavities, operating at 1.3 GHz (in yellow in the figure). One third-harmonic cryo-module containing four 3.9 GHz cavities (in red), placed after the first 1.3 GHz module, is used to linearize the energy chirp. Two magnetic chicanes are used to compress the bunches, down to the order of 100 fs and below, in order to achieve the peak currents needed for the FEL process.

A kicker-septum system is used to extract part of the beam pulse into the FLASH2 line. The kicker rise time of ca. 30 µs determines the minimum gap between the beams for FLASH1 and FLASH2, which are within the same pulse. The electrons produce the FEL beam in FLASH1 within six 4.5 m long fixed-gap undulators. The photon wavelength is varied by changing the electron energy. A seeding experiment, sFLASH, is also placed in the FLASH1 beamline.

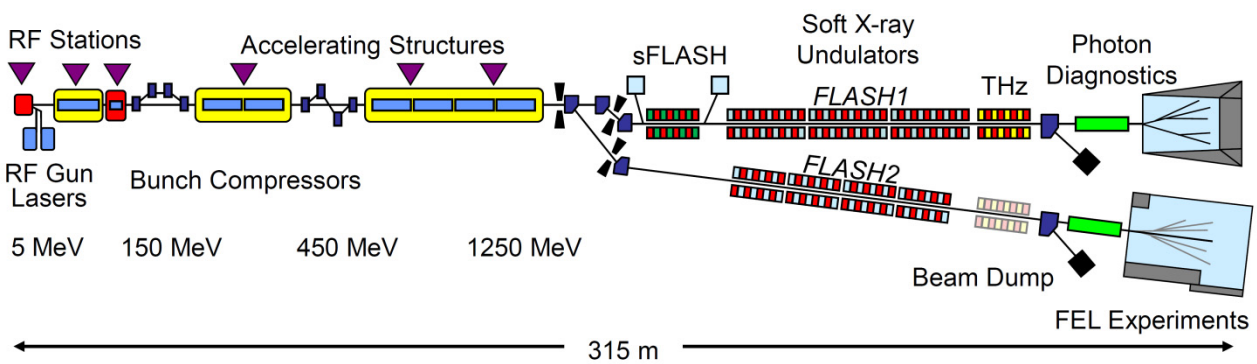

Figure 1: Schematic of the FLASH facility with the two undulator beamlines, FLASH1 and FLASH2 [1].

#nicoleta.baboi@desy.de

ISBN 978-3-95450-141-0

CROSS-CALIBRATION OF THREE ELECTRON CLOUD DENSITY DETECTORS AT CESRTA*

J.P. Sikora†, J.R. Calvey, J.A. Crittenden, CLASSE, Ithaca, New York, USA

Abstract

Measurements of electron cloud density using three detector types are compared under the same beam conditions at the same location in the Cornell Electron Storage Ring (CESR). Two of the detectors sample the flux of cloud electrons incident on the beam-pipe wall. The Retarding Field Analyzer (RFA) records the time-averaged charge flux and has a retarding grid that can be biased to select high energy electrons. The Shielded Button Electrode (SBE) samples the electron flux without a retarding grid, acquiring signals with sub-nanosecond resolution. The third detector uses resonant microwaves and measures the electron cloud density within the beam-pipe through the cloud-induced shift in resonant frequency. The analysis will include comparison of the output from POSINST and ECLOUD simulations of electron cloud buildup. These time-sliced particle-in-cell 2D modeling codes – simulating photoelectron production, secondary emission and cloud dynamics – have been expanded to include the electron acceptance of the RFA and SBE detectors in order to model the measured signals. The measurements were made at the CESR storage ring, which has been reconfigured as a test accelerator (CESRTA) providing electron or positron beams ranging in energy from 2 GeV to 5 GeV.

INTRODUCTION

The Cornell Electron Storage Ring (CESR) has a circumference of 768 m and supports positron or electron beams with energies from 2 GeV to 5 GeV. Bunch populations can be as high as 1.6×10^{11} particles/bunch (10 mA/bunch) with total beam populations of 3.8×10^{12} particles/beam.The storage ring has been used as part of a test accelerator program (CESRTA) that includes the measurement of electron cloud (EC) density and mitigation techniques. A number of devices have been installed for EC density measurements at the locations shown in Fig. 1.

The subject of this paper is a comparison of the measurements made with different devices at the same location. Section 15E, shown in Fig. 2, includes a retarding field analyzer (RFA), a shielded button electrode (SBE) and connections for resonant microwave measurements. The RFA and the SBE sample the flux of electrons onto the wall of the beam-pipe, while resonant microwaves are sensitive to the EC density within the beam-pipe volume.

* This work is supported by the US National Science Foundation PHY-0734867, PHY-1002467 and the US Department of Energy DE-FC02-08ER41538, DE-SC0006505.

† jps13@cornell.edu

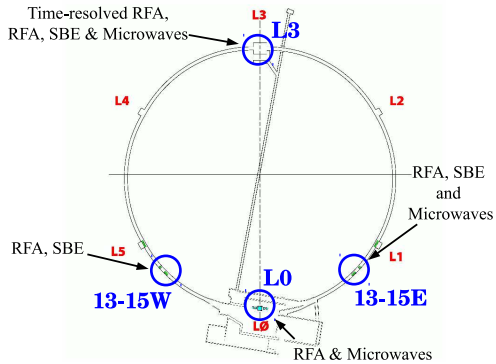

Figure 1: This sketch of the CESRTA storage ring shows the location of electron cloud detectors, including the group at 15E used in this study.

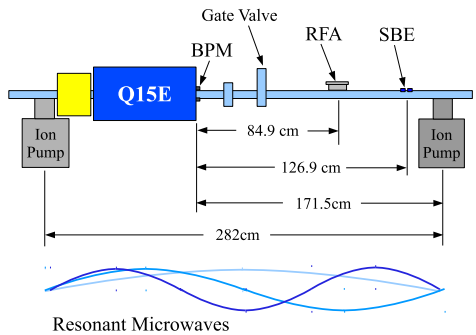

Figure 2: The 15E section of the CESR storage ring contains an SBE, an RFA and a resonant section of beam-pipe.

RETARDING FIELD ANALYZER

Figure 3 shows the conceptual layout of the RFA [1]. Cloud electrons can enter the detector through an array of small holes in the beam-pipe wall. Nine positively biased collectors are arranged horizontally. The current is time averaged to give a DC current measurement. There is a grid between the holes and the collectors which can be negatively biased to prevent lower energy electrons from impacting the collectors. In a typical measurement, the currents are measured as a function of the grid bias voltage in order to gain information about the energy distribution of the cloud electrons. A plot of such a measurement is given in Fig. 4 showing that most of the electrons are of relatively low energy, but there are some electrons at the central collectors with energies above 200 eV.

SHIELDED BUTTON ELECTRODE

The SBE also has a pattern of holes that allow electrons to enter the detector, shown in Fig. 5, but the collector provides

ISBN 978-3-95450-141-0

PERFORMANCE EVALUATION OF THE INTRA-BUNCH FEEDBACK SYSTEM AT J-PARC MAIN RING

K. Nakamura, Kyoto University, Kyoto, Japan
M. Tobiyama, T. Toyama, M. Okada, Y.H. Chin, T. Obina, T. Koseki, H. Kuboki
KEK, Ibaraki, Japan
Y. Shobuda, JAEA, Ibaraki, Japan

Abstract

An intra-bunch feedback system has been developed at J-PARC (Japan Proton Accelerator Complex) Main Ring (MR) for suppression of head-tail motions and reduction of particle losses. This system consists mainly of a BPM, a signal processing circuit (iGp12), power amplifiers, and stripline kickers. These components were fabricated and installed to MR in April of 2014. This system successfully suppressed internal bunch motion caused by injection kicker errors in the 3GeV constant-energy operation, It also achieved a shorter damping time than that by the bunch-by-bunch feedback system, which is currently used in the routine operation. Comparisons with simulations confirm that internal motion is actually suppressed by intra-bunch feedback system.

INTRODUCTION

The J-PARC is composed of three proton accelerators: the 400MeV linear accelerator (LINAC), the 3 GeV Rapid Cycling Synchrotron (RCS), and the Main Ring (MR) Synchrotron. The main parameters are listed in Table 1. At the J-PARC MR, transverse instabilities have been observed at the injection and during the acceleration. The present narrowband bunch-by-bunch feedback system (BxB FB) is effectively suppressing these transverse dipole oscillations [1]. But the BxB feedback system can damp only the whole bunches, and internal bunch oscillations have been still observed, which is causing additional particle losses [2]. To suppress intra-bunch oscillations, a more wideband and advanced feedback system (named the intra-bunch feedback system) has been developed.

Table 1: Main Parameters of J-PARC Main Ring

Circumference	1568m
Injection Energy	3GeV
Extraction Energy	30GeV
Repetition Period	2.48s
RF Frequency	1.67-1.72 MHz
Number of Bunches	8
Synchrotron Tune	0.002-0.0001
Betatron Tune (Hor./Ver.)	22.41/20.75

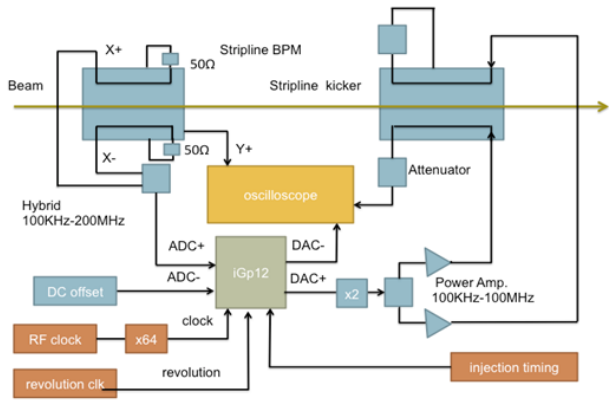

Figure 1: Schematic of the intra-bunch feedback system.

INTRA-BUNCH FEEDBACK SYSTEM

Figure 1 shows the schematic of the intra-bunch feedback system. It is composed mainly of three components: a BPM (Fig. 2), a signal processing circuit (iGp-12) and kickers (Fig. 3). The signal processing circuit detects betatron oscillation of bunches using signals from the BPM and calculates feedback signals. These feedback signals are sent to the kickers through the power amplifiers.

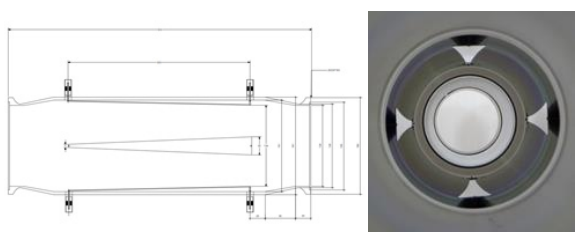

Figure 2: Side (left) and front (right) views of BPM.

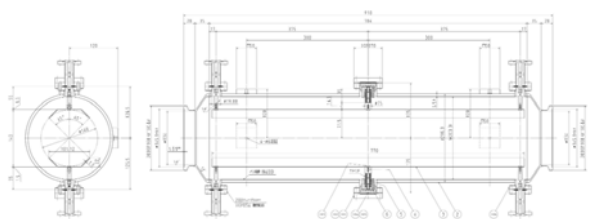

Figure 3: Kicker design.

ISBN 978-3-95450-141-0